Thèse n° 7231

Optimal retrofit and investment planning methodologies for improving industrial energy and resource efficiency

Présentée le 7 février 2020

à la Faculté des sciences et techniques de l'ingénieur
Groupe SCI STI FM
Programme doctoral en energie

pour l'obtention du grade de Docteur ès Sciences

par

Hür Ebuzer BÜTÜN

Acceptée sur proposition du jury

Dr P. Ott, président du jury
Prof. F. Maréchal, I. D. Kantor, directeurs de thèse
Prof. S. Harvey, rapporteur
Prof. Z. Kravanja, rapporteur
Prof. D. Kuhn, rapporteur

École
polytechnique
fédérale
de Lausanne

2020

To my family

"All we have to decide is what to do with the time that is given us."
J.R.R. Tolkien

Acknowledgments

Life is complex, like energy systems, with all the interactions between people. One can optimise energy systems (you will see that later in this thesis), but life? Perhaps not, though I feel like I got pretty close to it (local optima?) thanks to the people around me, who contributed to this PhD professionally and socially. I would like to pay my dues by naming them here, since "the palest ink is stronger than the sharpest memory".

I will keep the tradition and start with my supervisors, François and Ivan. François, thank you for giving me the opportunity to work in your group. Although your often triple-booked calendar was a challenge, all the ideas I have worked on in this thesis originated from intensive discussions we managed to fit in your schedule. I also appreciated the hierarchy-free environment you created in the lab, your friendly approach in our work related and social conversations as well as your effort to spend time with the group by organising ski weekends and Christmas dinners and last but not least your late-night electric guitar solos. You are and will most probably remain as the coolest boss I have ever had.

Ivan, thank you for being on my side (literally left side) for all my PhD, and a great person in general. When I was overdosed with François' ideas, you were always there to put bits and pieces together, to make things clear for me, to proceed - so to say - bring me back to life. You did my part of the work for EPOS many times, so that I can spend more time on my PhD. I am also grateful that you reviewed every single scientific content I have written. I am sorry that I haven't managed to figure out how to use punctuation (among many other things) in English in more than four years. It was simply and honestly a privilege to have you as my supervisor.

I would also like to thank my jury members, Prof. Harvey, Prof. Kravanja, Prof. Kuhn and the jury president Dr. Ott for their availability and feedback.

The environment in the lab was great, and I would like to express my gratitude to all the people who contributed to it. Thank you Stèphane for introducing me to IPESE and being a perfect example that doing a PhD can be cool; Dilan for the homie support and your effort for trying to integrate me in the Turkish community; Sophia for all the awkward moments from the first day in the office; Jean-Loup for the first and last IPESE party; Stefano for your sarcasm and co-organising the best Vivapoly stand (Energy Police) with Elfie; Alessio, Paul, Francesca and Luise for the companion in teaching; Rafael for your faith in EPFL Valais; Julia for sharing the pain and suffering at the gym; Victor for the name tag you gifted me, which didn't get me a free lunch but a bunch of "why do

you have his name tag?" questions; Maziar for your help in Lua and AMPL; Nils for protecting the silence in the open office; Ligang and Francesco for the football games; Shivom for your wisdom and availability to help whenever needed; Luc for your high-entropy life style (it was fun watching you running to the train station at least once a week); Alberto for always having a story to tell; Theodoros and Daniel for the fellowship of the conference travels; Sebastian and TiVi for the board games; Frederic for showing up whenever there is a fun event; Hanfei for being adorable; Sylvie for all the administrative work; Nicolas, Gillian, Cyrille, Michel and Cedric for the IT support.

I would like to extend my gratitude to the members of our sister lab, GEM, who participated in IPESE events more than us. Big thanks to Manuel and Priscilla for promoting the gym and the pool and organising events to bring everyone together and Gillaume for all the fun presentations.

Although secluded in Valais, I managed to keep contact with some friends mostly thanks to the mountains (i.e. ski resorts) around Sion. I would like to start with the Magic Winter group, Jean-François and Hassan. Jean-François, thank you for helping me find an apartment even before receiving my visa (this is impressive for anyone familiar with the Swiss real estate market), all the inaccurate Swiss information and your ability to handle (and of course deliver) offensive jokes. Hassan, thank you for being such a random person, it is impossible to be in a bad mood when you are around. Thank you both for all the magic winters we spent together. I would also like to thank my Greek friends; Angelos for annual meet ups, Konstantina for her remote support and Vera for the Greek wedding experience. Finally, many thanks to Cagri, for being the person who can relate to me the most, mainly because of having the same problems. I hope we will keep this understanding between us but with less troubles in life in the future.

I would like to thank the Beney family for being my Swiss contact, which everybody needs at some point in Switzerland, teaching me how to ski and most importantly treating me like one of them. Also many thanks to the Suciu family for receiving me well and their support throughout the end of this thesis.

My family has always been there for me both during my PhD and before to provide in any way they can. Mom, dad, thank you for encouraging and supporting me to study abroad even if it meant seeing you twice a year. Thank you Zeynep, my older sister, for being a pioneer in the family for many things, but kindly letting me become the first doctor and for all the UK travels, though I hate the UK visa application procedure! (I had to have it written somewhere). Thank you Sida Zeren, my sweet little sister, whose childhood I missed because of my BSc. and MSc. and teenagehood because of this PhD. I guess I ran out of education levels not to be a present big brother.

Last but foremost, Raluca, thank you for giving me the chance to make this thesis neither the only nor the greatest thing that came out of this PhD. You have been a supporting colleague, a good conference travel companion, an even better conference travel sponsor and a fantastic partner. I don't know how this PhD would turn out in your absence but surely know that I cannot picture a single moment of it without you. Thank you.

Once again, thank you all. It was fun while it lasted!

Sion, 06.01.2020

Abstract

A major shift in energy systems has started due to drastic changes in climate and air quality, depleting resources, as well as rising social awareness to all these changes. As a result international protocols, such as the Paris agreement, are signed setting ambitious targets on both energy consumption and CO_2 emissions. As industry is the responsible for a high share in energy consumption and environmental impact, such international treaties, combined with the regional and country based regulations put the industrial sector in the spotlight for energy and resource efficiency improvements.

This thesis explores the issues that have been overlooked in the domain of industrial energy and resource efficiency. The first two chapters look at the energy consumption at the plant level, while the remaining chapters also consider interactions between plants, in the context of an industrial cluster. Chapter 1 presents the concept of heat exchange interfaces to assess the cost of heat integration within industrial plants at early design stages. Switching from one interface to another is linked to modifying existing heat exchangers and to the cost of additional heat exchange area requirement. An optimisation method is developed to consider the trade-off between the cost of switching interfaces and the operational benefits due to better heat integration. Chapter 2 takes the retrofit analysis of heat exchanger networks one step further, by introducing the plant layout in a mathematical formulation and considering further retrofit actions, such as moving heat exchangers, repiping streams, adding new heat exchangers and adding area to existing heat exchangers. Chapter 3 expands the boundaries of the retrofit problem to industrial clusters, considering interactions between the plants, such as sharing heat and resources. A method is proposed to simultaneously optimise the energy conversion technologies to be installed on the plants and the piping infrastructure for inter-plant exchanges. The method takes into account the locations of the plants and their impact, by considering heat losses, temperature and pressure drops, as well as the cost of piping, to prioritise recovery within and nearby the plants. Chapter 4 addresses the complexity of industrial retrofit investment planning with an optimisation method considering long time horizons. The method determines the commissioning and decommissioning time of the retrofit investments under given budget constraints.

This thesis proposes a set of optimisation based methods to provide guidelines for the industries to reach short and long term energy and environmental targets. The results show that there is a large potential for energy and resource efficiency, protecting the economic interest of companies. Further

potentials can be unlocked by sharing excess heat and resources with neighbouring industries and districts.

Keywords:
energy and resource efficiency, industry, process integration, optimisation, mixed integer linear programming, investment planning, retrofit, industrial symbiosis.

Resumé

Aujourd'hui. un changement majeur dans les systèmes énergétiques a débuté en raison de la prise de conscience de la responsabilité des activités humaines sur le changement climatique, la qualité de l'air et de l'environnement en général ainsi que sur l'épuisement des ressources naturelles. En conséquence, des protocoles internationaux, tels que l'accord de Paris, ont été signés, fixant des objectifs ambitieux en matière de consommation d'énergie et de limitation d'émissions de CO_2. Ces traités internationaux, combinés aux réglementations régionales et nationales, mettent le secteur industriel au centre de l'attention en tant qu'acteur majeur pour une utilisation plus efficace de l'énergie en particulier renouvelable et des ressources naturelles.

Cette thèse explore l'utilisation de techniques d'optimisation en tant que méthode d'aide à la décision pour l'identification des solutions d'utilisation plus efficace et plus rationelle de l'énergie et des resources dans l'industrie. Les deux premiers chapitres portent sur la consommation d'énergie au niveau de l'usine, tandis que les chapitres suivants traitent des échanges entre plusieurs usines formant une grappe industrielle. Le chapitre 1 présente le concept d'interfaces d'échange de chaleur qui permet d'évaluer, dès les premières étapes de l'étude, le coût de la récupération de chaleur dans les installations industrielles . Le passage d'une interface à l'autre est lié à la modification des échangeurs de chaleur existants et au coût des surfaces d'échange supplémentaires nécessaires. La méthode d'optimisation mise au point tient compte du compromis entre le coût de changement d'interfaces et les gains obtenus grâce à une meilleure récupération de la chaleur. Cette approche permet de maximiser la récupération de chaleur tout en minimisant les modifications du système existant et ainsi cibler les modifications les plus importantes. Le chapitre 2 va encore plus loin dans l'analyse des possibilités de rénovation des réseaux d'échangeurs de chaleur en représentant l'agencement de l'usine sous forme mathématique et en envisageant d'autres actions, telles que le déplacement des échangeurs de chaleur, la modification de flux, l'ajout de nouveaux échangeurs de chaleur ou l'ajout de surfaces aux échangeurs de chaleur existants. Le chapitre 3 élargit les limites du problème de rétrofit aux grappes industrielles. Cela permet de prendre en compte les échanges possibles entre les usines, tels que le partage de chaleur et de ressources. La méthode proposée permet d'optimiser simultanément les technologies de conversion d'énergie à installer dans les usines, la récupération de chaleur et l'infrastructure de tuyauterie nécessaire pour réaliser les échanges entre les différentes usines. La méthode prend en compte l'emplacement des usines et leur impact. Elle considére les pertes de chaleur et les chutes de température associées ainsi que les pertes de charge et le coût des tuyaux, afin de prioriser la récupération à l'intérieur et à proximité

des usines. Le chapitre 4 traite quant à lui de la complexité de la planification des investissements industriels dans une situation de rétrot en proposant une formulation d'optimisation linéaire en nombre entier qui considère un horizon de planification sur le long terme. La méthode détermine, en fonction de contraintes budgétaires données, le moment optimal pour la réalisation et la mise en services des investissements ainsi que pour le démentellement des installations devenues obsolètes. Cette thèse propose anisi un ensemble de formulations mathématiques basées sur les techniques d'optimisation en nombre entier qui fournit aux ingénieurs les recommandations pour atteindre les objectifs énergétiques et environnementaux à court et long terme. Les résultats des applications montrent qu'il existe un grand potentiel d'amélioration de l'utilisation de l'énergie et des ressources dans l'industrie, sans pour autant péjorer les intérêts économiques des entreprises. Ce potentiel étant d'autant plus grand lorsqu'il est possible d'étendre les frontières du système et les échanges par le développement de symbioses industrielles.

Mots-clés :
Utilisation efficace des énergie et ressources, industrie, intégration des procédés, optimisation, programmation linéaire en nombres entiers, planification des investissements, rétrofit, symbiose industrielle.

Contents

List of figures

List of tables

Acronyms and abbreviations

CC	composite curve
CCC	Carnot composite curve
CHP	combined heat and power
DHN	district heating network
EI	energy integration
EoL	end of lifetime
GA	genetic algorithm
GCC	grand composite curve
GEP	generation expansion planning
HEN	heat exchanger network
HI	heat integration
HLD	heat load distribution
HP	heat pump
ICC	integrated composite curve
ICE	internal combustion engine
IEA	international energy agency
IP	integer programming
KPI	key performance indicator
LHV	lower heating value
LMTD	logarithmic mean temperature difference
LP	linear programming
MD	Manhattan distance
MER	maximum energy recovery
MILP	mixed integer linear programming
MINLP	mixed integer non-linear programming
MOO	multi objective optimisation
MP	mathematical programming
MVR	mechanical vapour recompression
NLP	non-linear programming
NPV	net present value

OECD	organisation for economic co-operation and development
PA	pinch analysis
PDM	pinch design method
PI	process integration
PIIP	process integration and long term investment planning
PV	photo-voltaic
TCF	trenching cost factor
TSA	total site analysis

List of symbols

Sets

AS	set of area segments
BU	set of base case units
CG	set of cold stream groups
CK	set of cold streams within temperature interval k
CS	set of cold streams
ES	set of electricity streams
EX	set of existing heat exchangers
H	set of heat streams
HG	set of hot stream groups
HI	set of inter-location heat streams
HK	set of hot streams within and above temperature interval k
HS	set hot of streams
I	set of initial stream matches
IE	set of initial stream and heat exchanger matches
IT	set of heat transfer interfaces
IU	set of investment units
K	set of temperature intervals
KB	set of bottom temperature intervals
KT	set of top temperature intervals
KZ	set of temperature intervals of zones
LC	set of locations
L	set of layers
MG	set of possible stream group matches
MS	set of possible stream matches
NU	set of new units
OL	set of other locations
P	set of periods
PS	set of standard piping sizes

PU	set of process units
$\mathbf{R^1}$	set of the first retrofit category: moving heat exchangers
$\mathbf{R^2}$	set of the second retrofit category: adding area to existing heat exchangers
$\mathbf{R^3}$	set of the third retrofit category: repiping
$\mathbf{R^4}$	set of the fourth retrofit category: adding new heat exchangers
RL	set of resource links
S	set of streams
SG	set of stream groups
SP	set of stream parents
SS	set of streams of stream groups
TR	set of transfer types
TT	set of times
UU	set of utility units
U	set of units
Z	set of resource streams
ZN	set of zones

Parameters (MILP)

ΔP	pressure drop	[Pa]
Δh	specific enthalpy difference	[kJ/kg]
Δt	operating time	[h]
ε	surface roughness	[mm]
λ	conductive heat transfer coefficient	[W/mK]
ν	kinematic viscosity	[m^2/s]
λ	density	[kg/m^3]
A	area	[m^2]
CEPCI	chemical engineering plant cost index	[-]
D	distance	[m]
F	factor	[-]
LI	unit file span	[years]
T	temperature	[C]
V	overall heat transfer coefficient	[kW/m^2K]
X	thermal resistance	[kW/mK]
bigM	big M	[-]
c	specific cost	[various]
d	diameter	[m]
$\dot{e}$	electricity flow	[kW]
ff	friction factor	[-]

h	convective heat transfer coefficient	[kW/m^{2}K]
i	interest rate	[-]
LMTD	log mean temperature difference	[K]
$\dot{m}$	reference resource flow rate	[various]
$\dot{m}c_P$	heat capacity	[kW/K]
$\dot{q}$	reference heat flow rate	[kW]
r	rate	[-]
Re	Reynold's number	[-]
u	velocity	[m/s]
x	thickness	[m]

Variables (MILP)

A	area	[m^2]
C	cost	[various]
$\dot{E}$	scaled electricity flow	[kW]
$\dot{M}$	scaled resource flow	[various]
NPV	net present value	[€]
$\dot{Q}$	scaled heat flow	[kW]
$\dot{R}$	residual heat flow	[kW]
a	resource stream splitting factor	[-]
b	stream parent splitting factor	[-]
ex	using existing heat exchanger for a stream match	[-]
f	unit sizing factor	[-]
f'	unit time dependent sizing factor	[-]
l	unit life	[years]
n	using a new heat exchanger for a stream match	[-]
s	stream sizing factor	[-]
y	unit scheduling variable / stream match existence	[-]
y'	unit time dependent scheduling variable	[-]
z	unit binary investment variable	[-]

Superscripts

add	additional
amb	ambient
an	annualisation
b	buying
bb	bought before
bm	bare module

cf	cash flow
comp	compressor
cond	condenser
cur	current
d	dying (EoL)
dep	depreciation
dv	dying (EoL) value
e	existence
en	engineering
evap	evaporator
extra	extra
fan	fan
fr	freight
gr	grass-roots
ground	ground
h	heat
hex	heat exchanger
in	inlet
init	initial
ins	insulation
int	interface
inv	investment
lb	lower bound
lr	labour
lt	life time
max	maximum
min	minimum
move	moving
mt	material
mut	mutual
new	new
nh	new heat exchanger
oh	overhead
op	operating
out	outlet
pc	cold stream piping
ph	hot stream piping
pipe	piping

pm	pumping
pr	resource stream piping
ps	piping size
r	resource
rad	radiation
ref	reference
rep	repiping
ret	return
rl	resource links
rv	remaining value
s	selling
sal	salvage
sc	scrap
slack	slack
sup	supply
sv	sold value
tc	trenching cost
ub	upper bound
water	water

Indexes

as	area segment
es	electricity stream
i	donor / hot stream
ig	hot stream group
it	interface
j	receiver / cold stream
jg	cold stream group
k	temperature interval
lc	location
ly	layer
o	other location
p	period
pp	previous period
ps	piping size
s	stream
sg	stream group
sp	stream parent

t	time step
tr	transfer type
u	unit
z	resource stream / zone

Introduction

"It's the job that's never started as takes longest to finish."
J.R.R. Tolkien

Overview

- Current energy situtation, its environmental impact and future perspectives;
- Industry's role in the current energy consumption and CO_2 emissions;
- Conceptual industrial cluster, what are the challenges?
- Process integration, what are the gaps in literature?
- Contributions and novelty of this thesis.

Energy has had vital importance for human beings since the discovery of starting and controlling fire. The modest energy needs for heating and cooking have grown immensely with the industrial revolution, which made exponential economic growth possible. As a result, people have higher comfort levels and quality of life in each next generation, which leads to increasing consumption of goods as well as energy.

The world population is expected to grow ~40% until 2100 and half of this increase will happen by 2040 [1]. Considering that the population growth is higher in the developing countries and that access to energy sources, transportation systems and consumer goods is increasing rapidly in those countries, the current increasing trend in the world energy demand is expected to continue. Currently more than 80% of the energy demand is supplied by fossil energy sources (i.e. oil, coal and natural gas) [2], which contributes significantly to the world CO_2 emissions. Figure 1 depicts the evolution of energy demand and CO_2 emissions between 1990 and 2017 as well as projections of the international energy agency (IEA) for 2040, corresponding to three scenarios. The increase in energy demand and CO_2 emissions is expected to continue linearly with the current policies. The sustainable development scenario is subject to a constant energy demand, however it requires drastic improvements in CO_2 emissions.

According to the IEA, a substantial shift in energy sector trends has started, driven by concerns about energy security, energy poverty, air quality, climate change and economic competitiveness. One successful example of an action taken against such concerns is Europe 2020, in which a ten

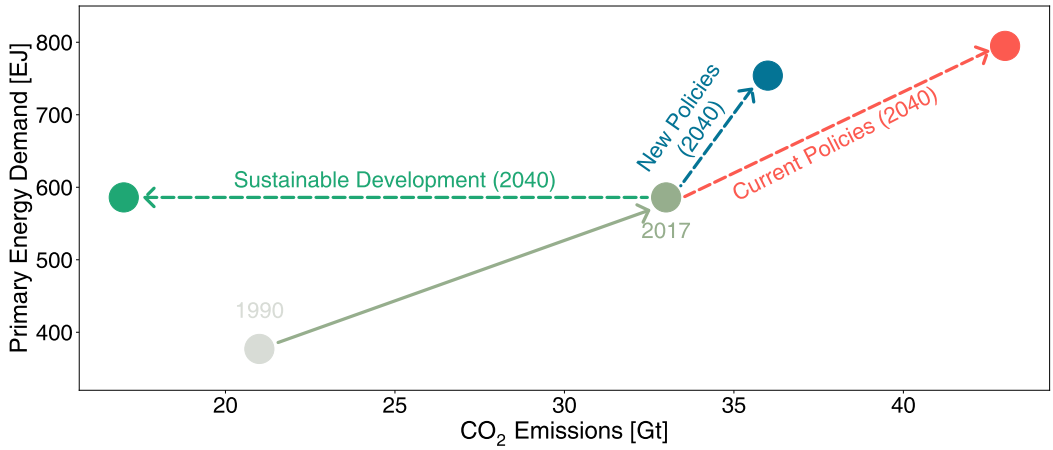

Figure 1 – World energy demand and CO_2 emissions by IEA scenarios [3].

year strategy is proposed, and gradually implemented in the European states to decrease green house gas emissions by 20%, increase energy efficiency by 20% compared to the 1990 levels and have a penetration of renewables in the energy mix of 20% [4]. In addition to national and regional regulations, international agreements have been signed by most of the countries in the world. The most recent one is the Paris agreement signed at the 21st Conference of the Parties (COP21), in which all participating countries pledged to keep the global temperature rise well below 2°C compared to the pre-industrial levels and to pursue further efforts to limit the increase to 1.5°C. Despite the policies that have been in effect, such as Europe 2020 and the ones that came in force after the Paris agreement, an increase of 2.7°C in the average global temperature is projected [3], which could be regarded as an improvement compared to the business as usual state before COP21, but is not enough to prevent dangerous changes in climate. Thus, in order to confine the rise in temperature below 2°C and reach the ambitious targets settled in the Paris agreement, a solid understanding and analysis of the energy intensive sectors and more aggressive energy efficiency improvement strategies are needed.

Industrial energy consumption and CO_2 emissions

Final energy use and direct CO_2 emissions in industry accounted for ~150 EJ and ~12 Gt in 2017, corresponding to 37% of global final energy consumption [2] and 34% of global CO_2 emissions [5], respectively (see Figure 2). The industrial sector is the largest coal and natural gas consumer, with 60% and 37% respectively, and the second largest oil consumer, with 8% [6]. Industrial final energy use has grown by 65% since 1971; following the same trend, CO_2 emissions are expected to increase 1.7 times by 2030 [7].

The 2°C target of the Paris agreement requires reducing CO_2 emissions to a net zero by 2100 and to stay well below 2°C, this CO_2 emissions target should be accomplished by 2060 [3]. Considering that

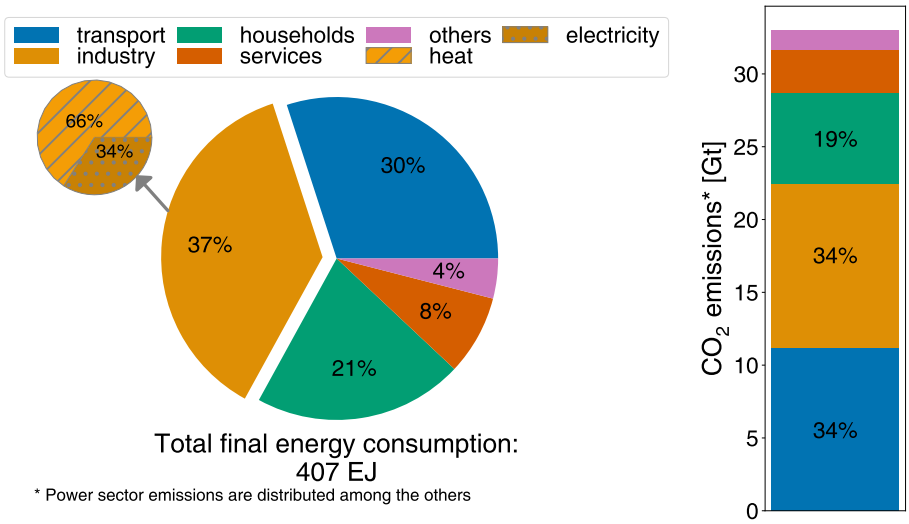

Figure 2 – World final energy consumption (left) [2] and CO_2 emissions (right) [5] by sector.

industry is one of the biggest contributors to both world energy consumption and CO_2 emissions, it has been inevitably in the spotlight of energy saving and environmental impact reduction strategies. In the past decades, the energy intensity of chemical processes decreased significantly, alternative fuels penetrated in cement production and steel manufacturing improved by recycling production gasses. Despite these efforts and improvements in energy intensity, population growth and rising income levels have led to an increase in industrial energy consumption and CO_2 emissions.

On a regional basis, in 2017 energy consumption increased by 2.7% in the Middle East, Africa and India and by 2% in Asia (excluding China) [3]. On the other hand, organisation for economic co-operation and development (OECD) countries and China experienced a slowdown of 0.1% and 0.7%, respectively. Similarly, CO_2 emissions increased in most regions, while OECD countries and China saw a decline of 1%.

In order to unlock industry's potential for further energy savings and reduction in CO_2 emissions and to achieve the long term goals set by the regulations and international agreements, contributions from all the industrial sectors are required. Low-energy intensity sectors, such as food, beverage and textile represent 70% of the improvements expected in the short term, while the industry overall has a potential to produce twice as much value per unit of energy consumed compared to the current state [8]. According to the IEA, deployment of best available techniques (BAT), implementation of process integration (PI) measures and co-operative frameworks, such as industrial symbiosis, and development of CO_2 capture systems are the main strategies for paving the way to net zero CO_2 emissions in industry [8]. However, given the diversity and complexity of industrial energy systems, it is a challenge to identify optimal investments for the plants.

Energy in industrial clusters

It is crucial to understand how energy is consumed in industrial plants, to be able to find ways to reduce it. Energy flows into industrial plants in the form of fuel and electricity. While electricity is directly used, fuel is typically combusted in boilers, combined heat and power (CHP) plants and furnaces, to convert its chemical energy into heat and electricity. The majority of the energy consumption on the sites occurs in the form of heat (see Figure 2). Industrial sites are typically located close to each other, forming an industrial cluster, to benefit from common resources (e.g. the natural gas grid, surrounding lakes) and economies of scale. An industrial cluster can consist of several sites from the same sector (e.g. chemical clusters) or sites from a combination of industrial sectors. Because of regulations, industrial clusters are generally not located in cities, however they are often not too far from districts. Figure 3 illustrates a fictitious industrial cluster neighbouring a district.

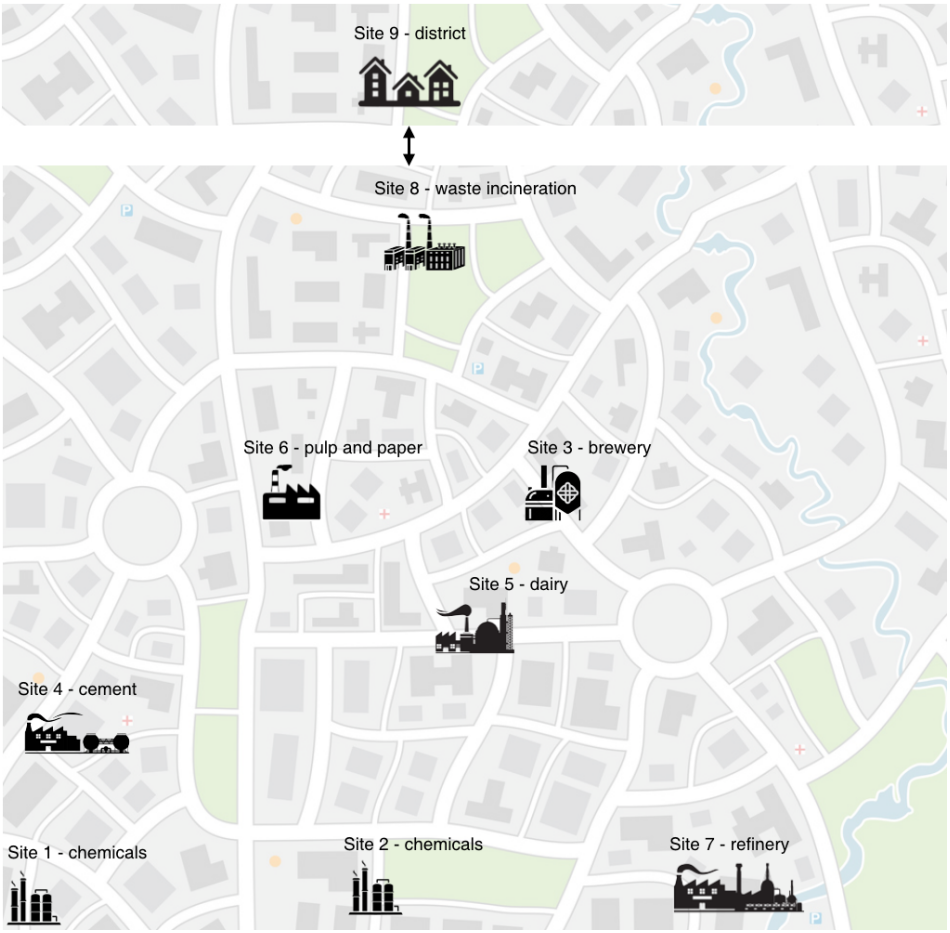

Figure 3 – An industrial cluster with plants from different sectors in the neighbourhood of a district.

An industrial plant typically comprises several process units. Energy requirements vary greatly, depending on the processes carried out (e.g. pre-heating, distillation, reaction) in the unit. While for

electricity only the magnitude matters, for heat also quality (i.e. temperature) plays an important role in the feasibility of its transfer, as it flows from high temperatures to lower ones. Considering that a unit has several processes requiring heating or cooling at a variety of temperatures and that a plant has several process units, analysing and improving heat consumption becomes very complex, already at the plant level. Excess heat from a process unit can be recovered in another unit, given that it is at a higher temperature than the heating requirement of the other unit. Typically there are numerous options for heat recovery within a unit which increases dramatically at the plant level. Moreover, plants often have complex utility systems providing electricity, heating and cooling. Heat can be generated from fuel using different energy conversion technologies, such as boilers and CHPs and can be distributed at several temperature levels using steam networks. Analysing industrial plants in the context of an industrial cluster adds another layer of complexity, since the excess heat or by-product of a plant can be used in another plant or in a neighbouring district.

In addition, in retrofit problems, existing plant infrastructures must be taken into account. For example, an energy conversion technology can replace an existing one only if its operational benefits over the existing system are higher than the capital cost of investment. The age of the existing installation is another important parameter to consider when deciding on investments. Such parameters can be accounted for only in long time horizons, which brings about challenges regarding the optimal time for investments.

A wide range of energy efficiency retrofit measures are available in industry, but due to financial and non-financial barriers, they remain unimplemented. Low budgets for investments targeting energy efficiency, costs exceeding company budgets, high payback times and low profitability are the main financial barriers, while non-financial barriers include the lack of know-how to identify and implement energy saving solutions, lack of time and short-term perspectives [9]. Thus, there is a clear need for retrofit methods targeting energy and resource efficiency both short and long term, to guide engineers and provide decision support for authorities in industry.

Process integration

PI is a domain in chemical engineering, which emerged due to the oil crisis in the 1970s and has been developed ever since, addressing environmental concerns, regulations and agreements. PI is based on mass and energy balances and aims to design more efficient processes, improve existing ones, decrease material and energy losses and reduce operating and investment costs, as well as environmental impact. The methods developed in the domain of PI can be considered in two main groups: graphical methods, based on pinch analysis (PA) and mathematical programming (MP) methods.

PA builds upon the principle of considering the processes as hot (i.e. heat source) and cold streams (i.e. heat sink) to model their cooling and heating requirements, respectively. The aim of PA is to

maximise the heat recovery between hot and cold streams and to minimise the cooling and heating requirements, which are satisfied by energy conversion systems consuming fuel and electricity available on the plants. PA was first developed by Linnhoff and Hindmarsh [10] for a single industrial process and afterwards extended to several production processes. Total site analysis (TSA) was derived from PA by using utility systems to transfer heat between industrial processes, in order to overcome the limitations of direct process heat exchange [11]. In order to reach the maximum heat recovery targets of PA, the heat exchanger network (HEN) of the plants should be designed accordingly. Pinch design method (PDM) is based on PA and used to design HENs following a set of heuristics. Although effective for small systems, large scale industrial applications of PDM are limited, due to difficulties of following heuristics and obtaining optimal solutions.

MP methods formulate PI as a set of mathematical constraints, mainly dealing with mass and energy balances and take advantage of well established solution algorithms and solvers. The main principle in such methods is setting the selection and sizing of utility systems variable and optimising those variables with the aim of minimising the total annual system cost [12]. This way, while the energy and resource consumption of the industrial processes is reduced, due to the contribution of the operation cost in the objective function, only economically viable solutions are selected, as the investment cost is also taken into account. Similar to PA based methods, the cost of heat recovery is studied with HEN design and retrofit methods in MP as well. Early work in this field divided the problem into three sub-problems. The first one is utility integration [12], which closes mass and energy balances in the system by optimal selection and sizing of utilities. The second step solves the heat load distribution (HLD) sub-problem [13], which determines the connections between the hot and cold streams and the amount of heat transferred. The final step determines the optimal design of HEN [14] by selecting the placement and area of the heat exchangers. Decomposing the problem, although it makes it easier to solve, may result in missing the global optimum. In order to overcome this issue, a simultaneous optimisation method was proposed by Yee and Grossmann [15] in 1990 and has been developed ever since.

Although PI methods are effective at identifying the maximum energy and resource recovery both for a single industrial site and for cluster, the methods available in the literature are more fit for designing new plants, rather than retrofitting existing ones. The domain of PI is mature in answering ‘how much energy/material can be saved?’ but ‘how should the plant layout be modified to implement energy/resource saving measures?’ and ’when is the best time for an investment?’ are questions often overlooked. Thus, energy saving scenarios identified by PI often remain as theoretical targets instead of practical solutions.

The research gaps are, therefore, 1) systematic methods to generate optimal retrofit solutions within industrial plants considering modifications in the plant layout; 2) taking into account interactions and retrofit options between industrial plants; 3) evaluating energy efficiency projects over long time horizons and determining the optimal time for investments. These gaps are addressed in this

thesis by 1) determining the trade-off between the additional heat exchanger area requirement and operational benefits, by introducing heat exchange interfaces in Chapter 1 and going deeper in HEN modifications by HLD retrofit in Chapter 2; 2) embodying location aspects in PI in Chapter 3 for better analysis of industrial clusters and interactions between plants; 3) consolidating PI by integrating investment planning, which allows retrofit over long periods and consequently deciding the optimal time for investments in Chapter 4.

Contributions and novelty

The main chapters of the thesis are presented, following four main research questions.

Chapter 1: Targeting retrofit at early design stages

"How do we take the cost of heat integration into account at early design stages?"

The cost of heat integration within industrial processes instead of using energy consuming utilities corresponds to modifications required in heat exchangers. In PI, this is either neglected or calculated using elaborate HEN methods, that are difficult to solve for large systems. This chapter introduces the concept of heat exchange interfaces and presents a method to estimate the cost of switching interfaces, which represents modifications in existing heat exchangers by adding heat exchanger area. A novel mixed integer linear programming (MILP) formulation is proposed to simultaneously determine the selection of energy conversion technologies and heat exchange interfaces for the processes, considering the trade-off between the cost of additional heat exchanger area and the decrease in operating cost. This way promising retrofit options are identified at early stages while fallacious ones are eliminated.

Chapter 2: Incorporating plant layout in heat exchanger network retrofit

"What is the impact of plant layout in heat exchanger network retrofit?"

Chapter 1 analyses retrofit in industrial plants focusing on additional heat exchanger area as a preliminary analysis. This chapter goes deeper into HEN retrofit by studying HLD. The retrofit actions considered include moving heat exchangers, adding heat exchanger area to the existing heat exchangers, adding completely new heat exchangers and re-piping streams. Locations of the streams are also included in the formulation which has an impact as re-piping cost is dependent on the distance. An MILP formulation is proposed embodying all the retrofit actions in the HEN. The method can be used to estimate the cost of the retrofit actions in the HEN. It also provides a good basis for HEN synthesis methods as it determines the matches between the hot and cold streams taking into account the existing plant layout.

Chapter 3: Retrofit considering inter-plant exchanges

"How do we determine the optimal interactions between industrial plants, taking their locations into account?"

PI methods available in the literature often ignore the locations of the plants and offer inconsequential solutions in which heat and materials are transferred between plants, over long distances. This chapter presents a PI method which considers the locations of the plants and their impact, embedding heat losses, temperature and pressure drop and piping cost, in an MILP framework. The method uses parametric optimisation, by applying ϵ-constraints on piping cost and systematically generating multiple options for retrofit, which also include the infrastructure between the plants. Industrial clusters are the main target of this method as it can identify cost-effective heat and resource sharing opportunities between industries to unravel recovery options that are not feasible within plants. The method is also suitable to consider investments from a third party (e.g. utility company) perspective which is illustrated with a case study.

Chapter 4: Planning investments in long time horizons

"What is the optimal time for energy efficiency investments?"

The methods presented in the previous chapters identify how industrial plants can be improved in terms of energy and resource efficiency, as well as the optimal infrastructure between the plants. However the optimal time for energy efficiency investments, remains yet to be determined. The timing of the investments is specifically important for the cases in which there are many competing energy efficiency solutions and there is an overall/yearly budget restriction. This chapter consolidates PI, by integrating it to a novel investment planning formulation. This allows considering long time horizons and other important aspects, such as the existing infrastructure, its age, the lifetime of the equipment and the yearly investment budget. The resulting problem is large, elaborate and difficult to solve. Thus, solution strategies are also proposed to obtain the optimal solution and generate multiple solutions for investment decision support. The method provides a holistic retrofit tool as it simultaneously identifies energy efficiency solutions and their investment timing as well as re-purchase of the existing equipment as they arrive to the end of their lifetime. It helps the decision makers in the industry by providing a set of optimal solutions from which the most suitable one can be chosen considering the practical constraints.

Retrofit at early design stages

1

Overview

- Definition of heat exchange interfaces and their relationship with the additional heat exchanger area;
- Trade-off between operating cost benefits and investment required to switch interfaces;
- A novel MILP formulation for simultaneous optimisation of heat exchange interfaces and utility system superstructure;
- Sensitivity analysis using energy prices from 25 OECD countries.

The content of this chapter is published in [16, 17].

Identifying retrofit opportunities in large industrial problems is extremely complex due to numerous interconnections and dependencies between process units, sub-units and utilities present on most industrial sites. Therefore, when attempting to identify promising retrofit opportunities, methods detecting early design decisions are crucial. This chapter proposes a methodology based on heat integration (HI) and mixed integer linear programming (MILP) to represent process energy requirements with different heat exchange interfaces. Switching from the current utility interface to an alternative one requires additional heat transfer area while it might bring operational benefits due to better system integration. The optimal combination of the processes with different interfaces is obtained by considering the trade-off between the cost of additional heat exchanger area required and decrease in the operating cost. The proposed method is applied to two industrial case studies which show the added value for HI and impact of the proposed method for reducing the problem size in heat exchanger network (HEN) design. In the first case study, the total cost of the system is reduced by 45% taking into account the cost of the modifications in the existing heat exchangers while in the second case study the computation time of heat load distribution (HLD) is reduced by 78% using the results of optimal interface selection. The proposed method provides early design decisions for retrofit solutions on industrial sites. Utilising this methodology provides a dual benefit of identifying the most promising options for retrofit applications while also eliminating inconsequential ones at an early stage of the analysis.

1.1 Introduction

This chapter develops and presents a novel methodology to define the heating and cooling demand of industrial processes with multiple heat exchange interfaces and to optimise interface selection which represents decisions for heat exchanger modifications. The methodology builds upon previous work in energy targeting and utility integration and provides additional unique insights by accounting for estimated heat exchanger modification costs within the HI problem; therefore, providing additional support for solving retrofit problems. Moreover, the method reduces the problem size of more complex analyses, such as HEN design. Both of these aspects are illustrated using industrial case studies to elucidate the relevance of the method. After this short introduction, the state of the art is covered in Section 1.2, the methodology is explained in Section 1.3, the details of the case studies and the utility systems are given in Section 1.3.4, results are presented in Section 1.4 and the conclusion is drawn in Section 1.5.

1.2 State of the art

HI is a specific domain of the broader process integration (PI) and is used to assess the heat recovery potential of several processes, process units, or complex industrial sites. HI is based on pinch analysis (PA), which was initially developed by Linnhoff and Hindmarsh [10] and extensively studied by other researchers [18–20]. The idea behind PA is to recover the maximum amount of heat between processes to minimise the provision of heat by utilities external to the process. The results of PA are represented in composite curves (CCs) and grand composite curves (GCCs). CCs present a combination of hot streams, respecting their associations to the relevant temperature intervals, which results in the hot composite curve while the same procedure is followed for the cold composite curve. The pinch point(s) and maximum energy recovery (MER) can be read from the CCs. The GCC is another representation of the CCs and is built from a summation of hot and cold streams in the same temperature intervals, which is more practical for determining the integration of utilities. Although PA yields promising results for individual processes, heat exchange between process streams is required to reach the identified energy targets. This process – process interaction is typically impossible on industrial sites for various practical reasons including shutdown, startup [21] and safety issues [22]. Total site analysis (TSA) is a method derived from PA initially by Dhole and Linhoff [11] and further developed by Raissi [23] to overcome the drawbacks of the process-process interaction. It includes indirect heat transfer between the processes meaning that the excess heat of one process can be recovered by a utility and then used as a heat source for another process.

Although graphical techniques are based on determination of MER, it is equally important to determine the optimal utility system that satisfies the MER. Utility system integration should be carried out with HI, as the utilities are a part of the plant. Maréchal and Kalitventzeff [24] proposed a mathematical programming (MP) methodology which addressed the optimal utility selection

for integration with the process. The method was extended to a multi-period formulation [25] to account for different operating modes of the process units in a production plant. Although utility integration has often been driven by economic objectives, exergy efficiency has also been considered either in the objective function [26] or post-optimisation analysis using Carnot composite curves (CCCs) [27, 28]. CCCs are constructed by exchanging the CCs temperature axis with the Carnot factor. As such, CCCs aid in determining the exergy losses in the heat transfer between utility systems and processes.

Creating the temperature – enthalpy profiles is a crucial step of HI, as they are used to determine the real process energy requirements [29]. The heating and cooling requirements of processes can be represented in different levels of detail. For example, Brown et al. [30] classified two representation levels, technological and thermodynamic. The technological representation defines the process according to the utilities that it consumes whereas the thermodynamic representation presents the real process requirements. For example, a cold process which is heated by steam can be represented by production of steam at the technological level, at the pressure level at which it is used or by temperature-enthalpy profile of the process as the thermodynamic representation. The two process representations correspond to the same energy (i.e. heating or cooling) demand, while the temperature levels differ. Pouransari et al. [31] included versions of these representations using the terms black-box and grey-box for technological and thermodynamic representations, respectively.

In industry, following the principles of TSA, it is common to use intermediate fluid circuits such as water or oil to transfer heat between a higher temperature heat source and a low temperature heat sink. Taking this into account, a triple representation was proposed by Muller [32]. An example of the triple representation can be seen in Figure 1.1, where a hot water cycle fed by steam delivers heat to a process. The representations are shown in both real temperature and Carnot factor scales where the temperatures are consistent with the Carnot factor while the non-horizontal elements reflect the Carnot factor scale. The results in Section 1.4 are visualised the same way.

Although the energy requirement of the process does not change with the chosen level of detail, the temperature profile differs, leading to alternative heat integration solutions. Pouransari et. al. [31] proposed a methodology which classifies the energy requirement into five levels of detail and uses a multi objective optimisation (MOO) based on genetic algorithm (GA) for selection of the optimal representation.

The method proposed by Pouransari [31] considered the trade-off between operating cost and the number of system modifications by changing the representation of the processes; however, utility integration was not considered. This chapter proposes a methodology to represent a process with different heat transfer interfaces to account for retrofitting opportunities. Interface changes imply modifications in the heat exchangers and instead of only taking into account the number of modifications as in [31], the estimation of the heat exchanger modification cost is added to

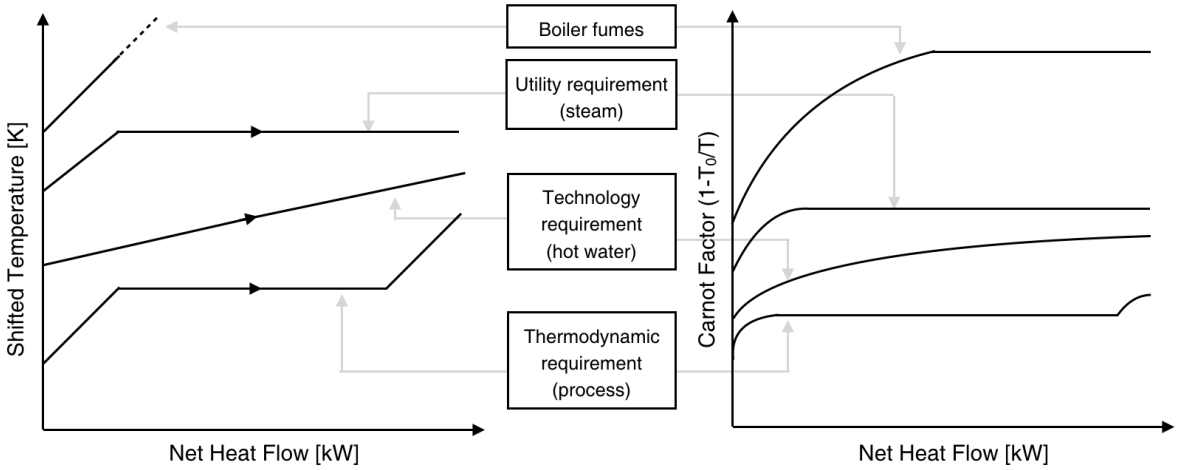

Figure 1.1 – Triple representation of the same process energy requirement (adapted from [32]).

provide the balance of cost/benefit for the modification. The decision of changing the interface depends if the operating cost benefits are higher than the cost of modification required. Since the operating cost is dependent on the utility system, interface and utility selection must be considered simultaneously which is a major contribution of this chapter. Compared to previous work which applied either an iterative approach [32] or GA [31] due to the complexity of the problem, the present work overcomes these difficulties with a novel MILP formulation which has the advantage of yielding a global optimum with fast convergence by deterministic optimisation. The proposed method can be used to make early retrofit decisions in the heat exchanger network with the utility systems currently in place or new utilities. In addition, the results of the proposed method can be used as a problem size reduction for HEN design.

1.3 Method

In this work, instead of restricting the representation of the processes into a defined number of levels, a more flexible heat exchange interface definition is used. The process interface corresponds to the thermodynamic representation (i.e. temperature - enthalpy profile) of the process. It allows the integration of the current utility, candidate utilities and other processes. The current utility interface represents the temperature - enthalpy profile of the utility that the process currently consumes. Usage of this interface implies that the process energy requirement will be supplied with the current utility and hence requires no modification of the heat exchanger. The candidate utility interface represents the temperature - enthalpy profile of a utility that can potentially supply the process. Processes can therefore have as many candidate utility interfaces as the number of utilities able to satisfy the process energy requirement. The usage of the process and the candidate utility interfaces imply modifications in the existing heat exchangers which satisfy the process requirements. The cost associated with these modifications and its contribution to energy targeting and utility integration

are explained in Section 1.3.1 and Section 1.3.2, respectively.

1.3.1 Calculation of interface cost

An example of a cold process can be seen in Figure 1.2. It is a process stream at the bottom of a distillation column that is re-boiled and returned to the column. Currently, the heating requirement is supplied by 24 bar superheated steam. As the process temperature is low, steam at other pressure levels that are available on the site could be used instead. Accounting for the process, current utility and candidate utilities, the process can be represented by six heat transfer interfaces.

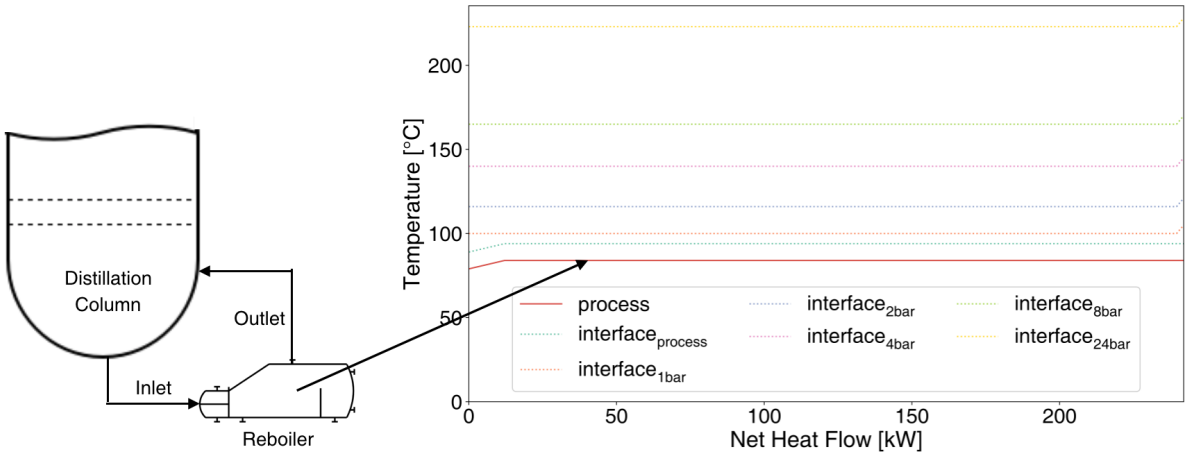

Figure 1.2 – Multiple heat exchange interfaces of a process unit operation.

Using a lower temperature utility (i.e. candidate utility) or a process stream requires additional heat exchanger area, since the logarithmic mean temperature difference (LMTD) decreases. The additional area is calculated by Equation 1.1.

$$A^{add} = \frac{\dot{q}^{hex}}{V^{new} \cdot LMTD^{new}} - \frac{\dot{q}^{hex}}{V^{cur} \cdot LMTD^{cur}} \tag{1.1}$$

The cost of the additional area is calculated by using the cost estimation Equations 1.2 and 1.3 for shell and tube heat exchangers [33, 34]. The cost of an interface is directly linked to the annualised investment cost of the additional heat exchanger area. The currently-used interface logically has zero cost, since no additional heat exchanger area is required. For all the other interfaces, the interface cost is calculated using Equation 1.4. Table 1.1 shows the description of the parameters used in the equations.

$$c^{b} = \frac{CEPCI^{t}}{CEPCI^{ref}} \cdot 10^{k1+k2 \cdot logA^{add}+k3 \cdot (logA^{add})^{2}} \tag{1.2}$$

Table 1.1 – Description of the parameters in the interface cost calculation.

Parameter	Description
A^{add}	Additional area requirement [m^2]
$\dot{q}^{hex}$	Heat load of the heat exchanger [kW]
V^{new}	Overall heat transfer coefficient of the new stream match [kW/m^2K]
V^{cur}	Overall heat transfer coefficient of the current stream match [kW/m^2K]
$LMTD^{new}$	Logarithmic mean temperature difference of the new stream match [K]
$LMTD^{cur}$	Logarithmic mean temperature difference of the current stream match [K]
$CEPCI^{t}$	Cost index at the time the project is realised [-]
$CEPCI^{ref}$	Cost index of the reference year [-]
k1, k2, k3	Cost estimation constants [-]
F^{bm}	Bare module factor [-]
F^{an}	annualisation factor [1/year]
c^{b}	Purchase cost [€]
c^{gr}	Grass-roots cost [€]
c^{int}	Cost of interface [€/year]

$$c^{gr} = F^{bm} \cdot c^{b} \tag{1.3}$$

$$c^{int} = F^{an} \cdot c^{gr} \tag{1.4}$$

As the heat exchange interfaces represent the same energy requirement, changing the interface of one process stream does not make a difference. However, at the unit or site level, where the integration of processes with each other and with the utilities is considered, the heat exchange interface could potentially have a large impact on the overall site heating and cooling demand.

1.3.2 Problem Formulation

A mathematical formulation based on Maréchal's optimal utility selection method [25] is developed. In the MILP formulation, the system is represented with a set of units ($u \in \mathbf{U}$), which contains the subsets of process units ($pu \in \mathbf{PU}$) and utility units ($uu \in \mathbf{UU}$), thus ($\mathbf{U} = \mathbf{PU} \cup \mathbf{UU}$). Process units are always added to the problem with fixed size, while utilities have variable sizes. For utility units, binary variables (y_u) and continuous variables (f_u) are defined to represent existence and size, respectively. The method is formulated as a multi-time problem for a fixed number of time steps ($t \in \mathbf{TT}$). Hence, to determine the existence and size of the units in each time segment, binary ($y'_{u,t}$) and continuous ($f'_{u,t}$) variables are also defined. [25] used an objective of the total cost of the system, accounting for both operating and investment cost. Since the purpose of the proposed method is to

consider the trade-off between operating cost benefits and interface cost, the objective function (see Equation 1.5) is modified accordingly, including the interface cost.

$$\min\left\{\sum_{u\in\mathbf{U}}\left[\sum_{t\in\mathbf{TT}}\left(\mathrm{c}_{u,t}^{\mathrm{op1}}\cdot y_{u,t}^{'}+\mathrm{c}_{u,t}^{\mathrm{op2}}\cdot f_{u,t}^{'}\right)\cdot \mathrm{t}_{t}^{\mathrm{op}}\right]+\mathrm{F}^{\mathrm{an}}\cdot\left(\mathrm{c}_{u}^{\mathrm{inv1}}\cdot y_{u}+\mathrm{c}_{u}^{\mathrm{inv2}}\cdot f_{u}\right)\right\}+\sum_{sp\in\mathbf{SP}}\sum_{it\in\mathbf{IT}}\mathrm{c}_{sp,it}^{\mathrm{int}}\cdot x_{sp,it} \tag{1.5}$$

In order to ensure that heat is transferred only from streams at higher temperature level to streams at the same or lower temperature level, heat cascade constraints Equations 1.6 and 1.7 are added. The sizing factor of the streams ($f_{s,t}$) in a unit ($s\in\mathbf{S}$) is set equal to that of the unit by Equation 1.8. By including the utilities in the problem, the energy balance of the system must be satisfied; therefore, the heat balance constraint is introduced in Equation 1.9.

$$\sum_{u\in\mathbf{U}}\sum_{s\in\mathbf{S}}\left(f_{s,t}\cdot\dot{\mathrm{q}}_{s,t,k}\right)+\dot{R}_{t,k+1}-\dot{R}_{t,k}=0\quad\forall\ t\in\mathbf{TT},\ k\in\mathbf{K} \tag{1.6}$$

$$\dot{R}_{t,k}\geq 0\ \ \forall\ t\in\mathbf{TT},\ k\in\mathbf{K} \tag{1.7}$$

$$f_{s,t}=f_{u,t}^{'}\ \ \forall\ s\in\mathbf{S},\ u\in\mathbf{U},\ t\in\mathbf{TT} \tag{1.8}$$

$$\dot{R}_{t,1}=0,\ \dot{R}_{t,k+1}=0\ \ \forall\ t\in\mathbf{TT} \tag{1.9}$$

Utility selection is determined using binary and continuous variables; the linking constraint is shown in Equations 1.10 and 1.11. Units are restricted to the capacity of the purchased unit in each time step (Equation 1.12) and can be used only if they are purchased (Equation 1.13). The constraints on existence and size of the process units are given in Equations 1.14 and 1.15.

$$\mathrm{F}_{u}^{\min}\cdot y_{u}\leq f_{u}\leq\mathrm{F}_{u}^{\max}\cdot y_{u}\quad\forall\ u\in\mathbf{U} \tag{1.10}$$

$$\mathrm{F}_{u}^{\min}\cdot y_{u,t}^{'}\leq f_{u,t}^{'}\leq\mathrm{F}_{u}^{\max}\cdot y_{u,t}^{'}\quad\forall\ u\in\mathbf{U},\ t\in\mathbf{TT} \tag{1.11}$$

$$f_{u,t}^{'}\leq f_{u}\quad\forall\ u\in\mathbf{U},\ t\in\mathbf{TT} \tag{1.12}$$

$$y'_{u,t} \leq y_u \quad \forall\, u \in \mathbf{U},\ t \in \mathbf{TT} \tag{1.13}$$

$$y'_{u,t} = 1 \quad \forall\, u \in \mathbf{PU},\ t \in \mathbf{TT} \tag{1.14}$$

$$\mathrm{F}_u^{\min}, \mathrm{F}_u^{\max} = 1 \quad \forall\, u \in \mathbf{PU} \tag{1.15}$$

In the classical formulations [25, 35], process streams are always added to the problem. Since the proposed method dictates that processes (i.e. process streams) are defined with multiple interfaces, additional constraints must be introduced. Parent-child relationships are constructed for each stream by introducing a new set of parents ($sp \in \mathbf{SP}$) so that child ($it \in \mathbf{IT}$) of a stream can be assigned to the same parent. The use of an interface is decided based on a new integer variable ($x_{sp,it}$) added in the formulation. The constraint expressed by Equation 1.16 sets the existence of only one interface for units which exist. Since the streams in the process units are defined with multiple interfaces and only one interface is allowed to be used, the sum of the sizing factors of all the interfaces of a parent in a unit is equal to that of the unit. Thus, Equation 1.8 is reformulated as Equation 1.17.

$$\sum_{it \in \mathbf{IT}} x_{sp,it} = y_u \quad \forall\, sp \in \mathbf{SP},\ u \in \mathbf{PU} \tag{1.16}$$

$$\sum_{it \in \mathbf{IT}} f_{sp,it,t} = f'_{u,t} \quad \forall\, sp \in \mathbf{SP},\ u \in \mathbf{PU},\ t \in \mathbf{TT} \tag{1.17}$$

Table 1.2 shows the description of parameters and variables used in the MILP formulation.

1.3.3 HLD Problem Size Reduction

HLD is a subproblem of HEN synthesis where the matches between the hot and cold streams are determined. This problem is commonly formulated using MILP such that binary variables are used to determine the existence of stream matches and continuous variables are used to determine the heat load of those matches. Since the results of optimal interface selection provides insights such as maintaining the current process/utility match (i.e. no interface change) or matching it with a candidate utility (i.e. switch to a candidate interface), they can be used as a problem reduction method for HLD. The interface selection results are translated as forced matches by setting the binary variables to unity, thus constraining the search space for the HLD problem. The details and

Table 1.2 – Description of the parameters in the MILP.

Parameter	Description
$c_{u,t}^{op1}$	Fixed operating cost [€/h]
$c_{u,t}^{op2}$	Variable operating cost [€/h]
c_{u}^{inv1}	Fixed investment cost [€/year]
c_{u}^{inv2}	Variable investment cost [€/year]
$c_{sp,it}^{int}$	Interface cost [€/year]
t^{op}	Operating time [hour]
F_{u}^{min}	Minimum sizing factor [-]
F_{u}^{max}	Maximum sizing factor [-]
y	Integer variable to use the unit or not [-]
$x_{sp,it}$	Integer variable to use the interface or not [-]
f	Sizing factor of the unit/stream/parent [-]
$\dot{R}_{t,k}$	Residual heat in the temperature interval [kW]
$\dot{q}_{s,t,k}$	Heat from/to streams [kW]

the formulation of the HLD method are not given as the contribution of this work is reducing the problem size but not proposing a novel method for solving the HLD. Mathematical formulations for solving the HLD problem can be found in [14, 36].

1.3.4 Case study and utility systems

Two case studies are utilised to exhibit the applications of the method with two different goals. In the first case, a medium-size industrial process unit adapted from [37] is studied with the focus of observing the impact of multiple interfaces in utility integration. In the second case, a larger process unit adapted from [37] is studied to exhibit the impact of optimal interface selection in reducing the problem size for further analysis. The details of the case studies and the utility systems are given in the following subsections.

1.3.5 Case study 1

A process unit composed of 24 streams is studied. The heating requirement of the unit is satisfied by 24 bar and 8 bar steam from the steam network, while the cooling of the processes is carried out by cooling water heat exchangers and overhead aerocoolers. The process flow diagram and the list of streams in the unit can be found in Appendix A.1.

As a preliminary analysis, the grand composite curve of the unit is plotted in Figure 1.3 considering all the streams in current utility interface and process interface. The openings at the top and the bottom of the curve depict the minimum heating and cooling requirements, respectively. The 27% decrease when interface is switched from current utility to process is due to heat recovery

between the hot and cold streams. Moreover, a drastic change in the shape of the curve can be observed, which results in potential integration of lower temperature utilities and hence decrease in the operating cost. However, for the preliminary analysis, the cost of switching interface is not taken into account.

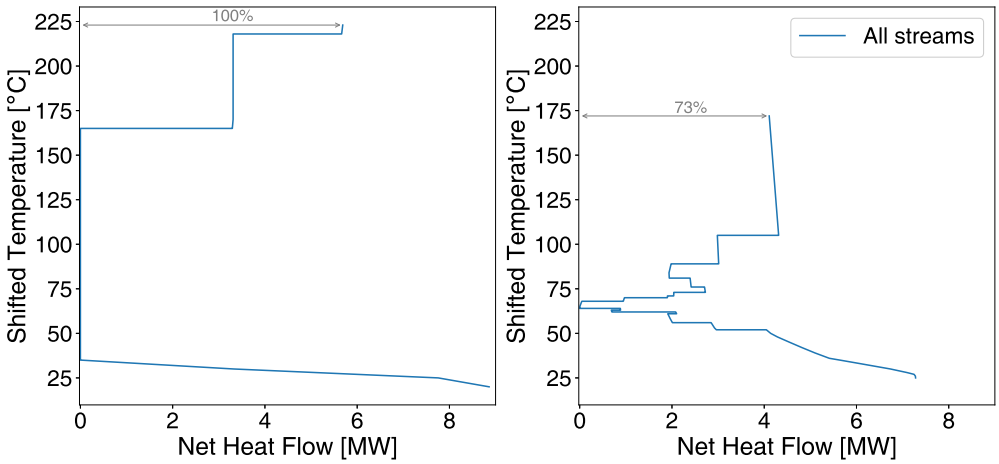

Figure 1.3 – Grand composite curve of case study 1: current utility interface (left), process interface (right).

1.3.6 Case study 2

Since one of the major motivations of the proposed method is reducing the problem size for HEN, a larger production unit is studied for the second case. The unit consists of 51 process thermal streams, composed of 20 cold streams and 31 hot streams. Similar to the unit in Section 1.3.5, the heating requirement of the cold streams is satisfied by the steam network with steam at 24 bar, 8 bar and 2 bar levels. Hot streams are cooled by cooling water heat exchangers and aerocoolers. The process flow diagram and the list of streams in the unit can be found in Appendix A.1. The composite curves of the unit in current utility and process interfaces can be seen in Figure 1.4. As in Section 1.3.5, changing the interfaces of all streams shows that 22% of the total heat can be recovered, representing the MER case.

1.3.7 Utility Systems

The selection of the interface is dependent on the type of utilities, since energy conversion systems define the operating cost. Currently, several energy conversion systems (e.g. boiler, aerocoolers) are already available for both case studies. Additional utilities are also suggested to supplement the utility superstructure by expert insight from analysing the composite curves in Sections 1.3.5 and 1.3.6 according to the methods and rules suggested by [10]. Afterwards, the utilities are added

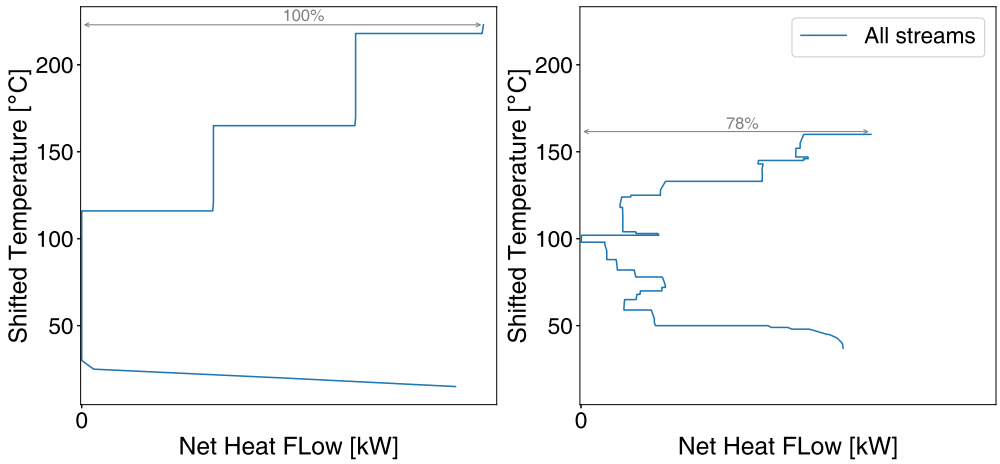

Figure 1.4 – Grand composite curve of case study 2: current utility interface (left), process interface (right).

in the problem superstructure based on [25, 35] and the optimal configuration is selected using optimisation. The details of the utility system models are given in the following sections.

1.3.7.1 Combustion

The generic combustion model represents a boiler which consumes fuel and generates hot gases. As flue gases are not condensed in industrial applications, the lower heating value (LHV) is considered here for calculating the total heat generated by combustion. In a real boiler, heat is transferred simultaneously by means of radiation and convection. Simplifying combustion modelling, it is assumed that radiation and convection occur at different temperature ranges as proposed by [38]. Radiation (Figure 1.5) takes place at a constant temperature (T^{rad}) which corresponds to heat transfer between the adiabatic flame temperature (T^{ad}) and the selected temperature of radiation suggested by [38], while the heat content of the combustion gases between the radiation and the stack temperature (T^{stack}) is transferred by convection.

The adiabatic flame temperature depends on the composition of the fuel and on the air to fuel ratio. For this example, an average composition of natural gas is considered [39] and it is assumed that a stoichiometric reaction takes place in the combustion chamber of the boiler, with 2% excess air. The list of the streams of the combustion model can be seen in Table 1.3.

1.3.7.2 Steam network

Although hot combustion gases can theoretically be used directly to provide heating to processes, secondary utility systems such as steam networks or hot water cycles are typically used to take

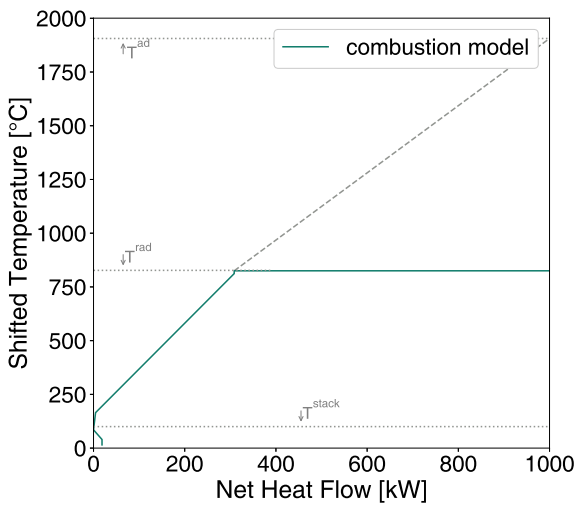

Figure 1.5 – Grand composite curve of the simplified combustion model.

Table 1.3 – Combustion model specifications.

Stream	T^{in} [°C]	T^{out} [°C]	$\dot{q}$[kW]
Fuel	-	-	1031
Radiation	827	827	656
Convection	827	100	324
Air preheating	25	150	-49

heat from the boiler and distribute it throughout the plant. In addition to being an efficient energy carrier, steam has the advantage of potential cogeneration, as mechanical power can be extracted by expanding high pressure steam through turbines to produce electricity.

In steam networks, steam is typically produced at a very high pressure level and distributed to the plant at multiple lower pressure levels. The pressure levels of the steam network model are selected in line with the real pressure levels on the studied plant. It is assumed that steam is superheated by 110°C at the production level and 5-7°C at all the distribution levels. The steam network already exists on the plant, hence no investment cost is associated with it. The summary of the steam network pressure levels can be seen in Table 1.4.

1.3.7.3 Cogeneration engine

An internal combustion engine is considered as an alternative to the currently existing boiler to provide the heating requirement of the system. Heat is supplied by the cogeneration engine with hot exhaust gases and with hot water generated by engine cooling. Although heat is provided at lower temperature compared to the boiler, the cogeneration engine has the advantage of electrical power

Table 1.4 – Pressure and temperature levels of the steam network.

Type	Header Pressure[bara]	Header Temperature[°C]	Turbine
Production	45	367	yes
Distribution	24	228	yes
Distribution	8	175	yes
Distribution	4	150	no
Distribution	2	126	no
Distribution	1	105	no

Table 1.5 – Cogeneration engine specifications.

Stream	T^{in}[°C]	T^{out}[°C]	$\dot{q}$[kW]	$\dot{e}$[kW]
Fuel	-	-	2605	-
Exhaust Gasses	470	120	537	-
Engine Cooling	87	80	653	-
Electricity	-	-	-	1063

generation from the piston work in the engine block. The primary limitation of the cogeneration engine is the temperature level of the engine cooling water. As hot utilities should only be integrated above the pinch point [10], the process pinch point should be lower than the temperature of cooling water of the engine, which is the case for Section 1.3.5. The specifications of the cogeneration engine considered in this work are shown in Table 1.5. The cogeneration engine, if used, must be purchased since it is not available in the current plant layout. The investment cost parameters of the cogeneration engine are provided in Section 1.3.7.6.

1.3.7.4 Heat pumps

From visual inspection of Figures 1.3 and 1.4, a potential for heat pumping is clearly visible for both case studies, transferring heat from below to above the pinch point with small temperature elevation. As heat can be pumped from two temperature levels below the pinch point with low temperature elevation, integration of two ammonia-based heat pumps is considered in both cases. The other specifications of the heat pumps can be seen in Table 1.6. As with all equipment which are not available on the site, there is investment cost associated to the heat pumps. The heat pump investment cost parameters used in MILP are provided in Section 1.3.7.6.

1.3.7.5 Cooling systems

Cooling systems consist of water coolers and aerocoolers. The aerocoolers are mostly used at the top of the distillation columns to condense the product streams first and bring them to ambient

Table 1.6 – Heat pump specifications.

	T^{evap} [°C]	T^{cond} [°C]	$\dot{q}^{evap}$ [kW]	$\dot{q}^{cond}$ [kW]	$\dot{e}^{comp}$ [kW]
$HP1_{case1}$	55	75	1039	1129	90
$HP2_{case1}$	50	75	1024	1150	126
$HP1_{case2}$	93	107	2217	2328	111
$HP2_{case2}$	82	107	2199	2410	211

Table 1.7 – Aerocooler specifications.

	T^{in} [°C]	T^{out} [°C]	$\dot{e}^{fan}$ [kWh/kWh$_{cooling}$]
Aerocoolers	20	30	0.01

temperature before the next processes. The inlet air to the heat exchanger is at ambient conditions, while the outlet temperature is assumed to be 10°C higher than the inlet. (Table 1.7).

Cooling water heat exchangers are used for smaller cooling needs compared to aerocoolers. They are mostly used to drop the temperature of the intermediate product before it is added into a process, or to cool down the final product before storage. Water is at ambient conditions as it enters the heat exchangers and it is assumed that it leaves the heat exchangers with 10°C temperature difference, similar to aerocoolers. The specific water consumption for cooling is calculated using the specific heat and density of water at ambient conditions (Table 1.8).

1.3.7.6 Utility investment cost

The investment cost of the heat pumps is calculated assuming that the main components are two heat exchangers (i.e. evaporator and condenser) and a compressor. The parameters used for the calculation of each component are given in Appendix A.3. For the cogeneration engine a specific investment cost of 1100 €/kW_e is assumed. The values from the cost functions are transformed into c^{inv1} and c^{inv2} to be able to insert them in the MILP formulation by assuming minimum and maximum scaling factors (i.e F^{min} and F^{max}). The resulting list of cost parameters can be seen in Table 1.9

Table 1.8 – Water cooling specifications.

	T^{in} [°C]	T^{out} [°C]	V^{water} [m^3/kWh$_{cooling}$]
Water coolers	15	25	0.086

Table 1.9 – Costing and sizing parameters of the units.

Unit	c^{inv1} [€/year]	c^{inv2} [€/year]	F^{min} [-]	F^{max} [-]
Cogeneration	11910	119096	0.1	1
$HP1_{case1}$	9940	47455	0.1	2.5
$HP2_{case1}$	10981	56940	0.1	1
$HP1_{case2}$	13363	66252	0.1	2
$HP2_{case2}$	16071	97322	0.1	2

1.4 Results and discussion

1.4.1 Optimal interface selection with utility integration

The optimal interface selection and utility integration of case study 1 is carried out in multiple steps, each representing a scenario. The specifications of the scenarios are listed below and visualised in Figure 1.6:

- **scenario 0 (s0):** The current state of the site. In this scenario, the utilities are limited to those already available on site and all processes are represented in their current utility interface. It represents the base case for comparison with the other scenarios;
- **scenario 1 (s1):** Optimal heat transfer interface selection with the existing utilities. In this scenario the selection of the interface (i.e. modifications in the heat exchangers) is allowed, but the integration of new utility systems is not considered;
- **scenario 2 (s2):** Optimal heat transfer interface selection with the existing utilities and cogeneration engine. In this scenario, a cogeneration utility can be integrated in addition to the existing utilities;
- **scenario 3 (s3):** Optimal heat transfer interface selection with the existing utilities, cogeneration engine, and heat pumps. This scenario builds on s1 with the additional possibility of heat pump integration.

The scenarios are selected to assess the selection of interfaces under the current utility system and the improved cases where more efficient utilities are considered in the superstructure. The sequence of scenarios is ordered in a way that the utility superstructure is increasingly large and thus the modifications required on the plant are permitted to be increasingly complex at each step. These scenarios thus yield several investment options depending on the flexibility of the plant to consider more complex modifications.

The comparison of s0 and s1 is shown in Figure 1.7. The CCCs represent the heat exchange between utility and process streams, both in Carnot factor and normal temperature scales as described in Section 1.2. The shift that can be observed in the plot from s0 to s1 is due to heat recovery between hot and cold process streams, which results in lower heating and cooling utility usage. This reduction

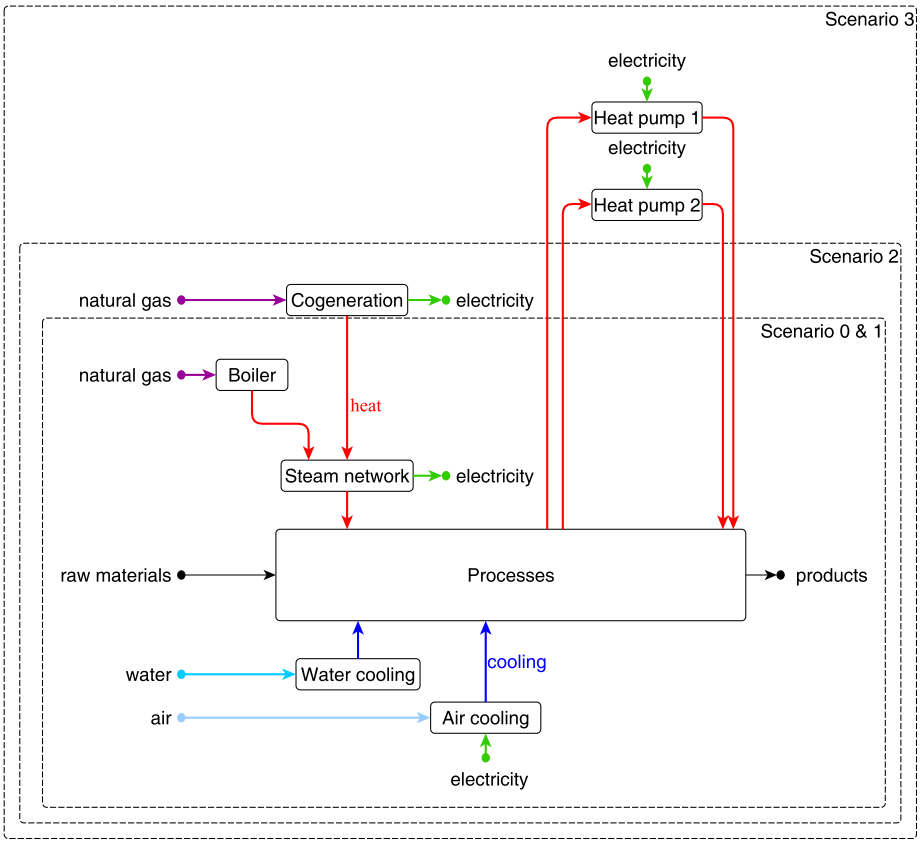

Figure 1.6 – Superstructure of s0, s1, s1 and s3.

is achieved by change of interface in the streams that are in the heat recovery zone of the curve. Moreover, it can be seen that the highest heat recovery that can be obtained from MER analysis is achieved with s1 since the heating and cooling requirements are the same as the MER case. Interface changes outside of the heat recovery zone do not contribute to heat recovery, by definition, but occur as a result of using utilities more efficiently. This is due to higher benefits of turbining steam and using lower pressure steam for heating compared to the investment required to modify the heat exchangers that are currently used with higher pressure steam. The economic differences between s0 and s1 can be seen in Figure 1.7 as well. The operating cost decreases due to reduction in the heating requirement and increase in the electricity production (due to usage of steam at lower pressure levels). Conversely, the interface cost emerges in s1 due to modifications required in the heat exchangers to achieve these operational benefits.

The comparison of s1 and s2 is shown in Figure 1.8. The CCC of the processes changes mainly in the integration zone of the cogeneration engine, more specifically in the region of hot water from the engine. The cogeneration engine has the advantage of electricity production, which, as shown in the results, makes it more cost-effective than the combination of boiler and steam network. It is also

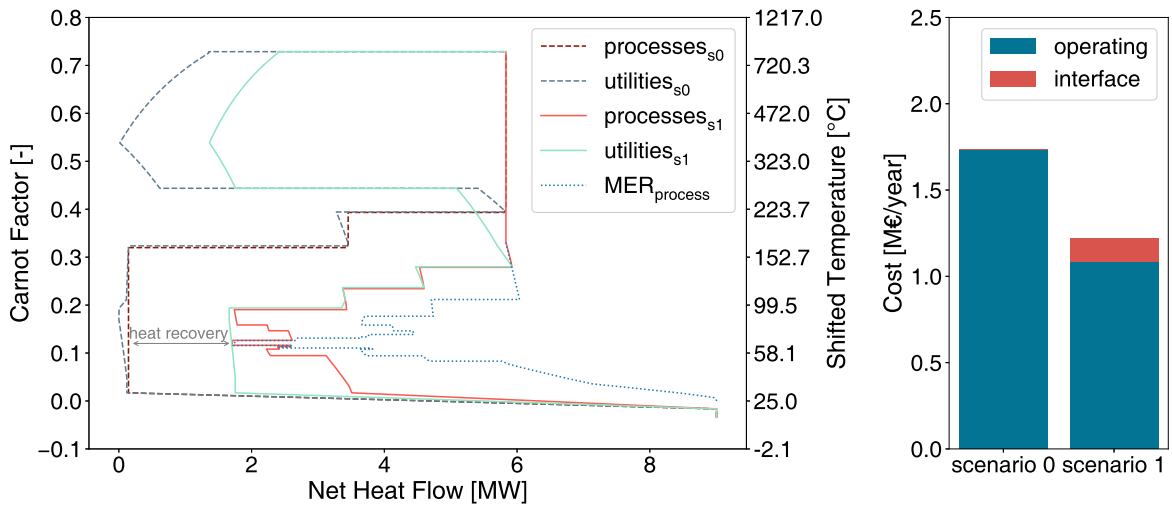

Figure 1.7 – Carnot composite curves (left) and cost comparison (right) of s0 and s1.

evident that the operational benefits of the engine are higher than the cost of required modifications in the heat exchangers to allow such integration. The cost comparison of the results in Figure 1.8 shows that s1 has slightly lower total cost with substantial decrease in the operating cost, despite the fact that the integration of the engine introduces utility investment cost to purchase it and higher interface cost compared to s1.

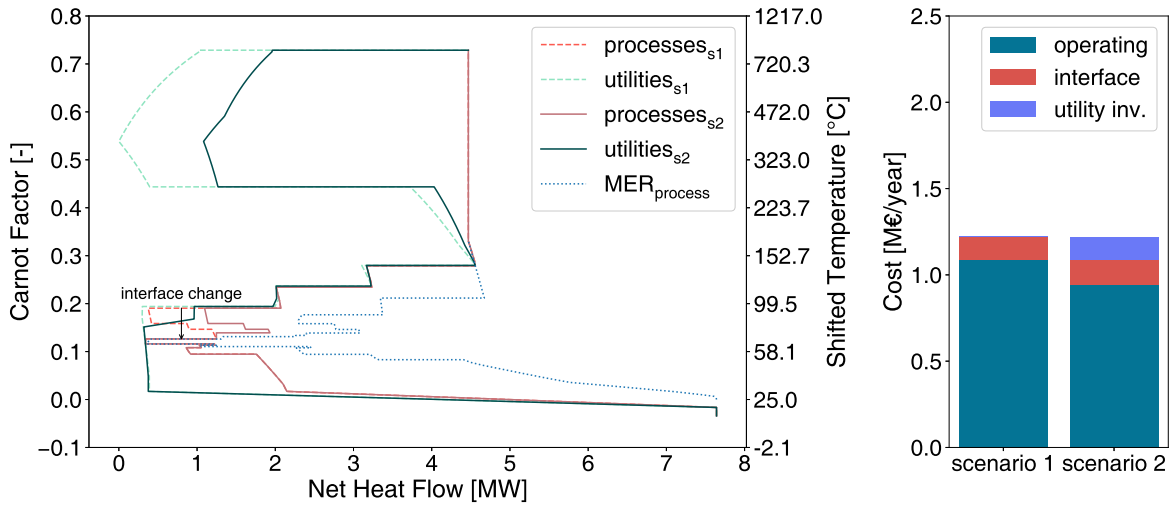

Figure 1.8 – Carnot composite curves (left) and cost comparison (right) of s1 and s2.

Figure 1.9 compares s1 and s3. Since heat pumps supply heat at approximately the same temperature as the hot water from the cogeneration engine, they are in competition with each other. With the introduction of heat pumps, the cogeneration engine is no longer selected for the optimal utility system. Both heat pumps given in Section 1.3.7.4 are selected by the optimiser, due to their ability

to provide heat at lower cost. Interface changes for the streams in the integration zone of the heat pumps can be observed since the decrease in the operating cost is higher than the increase in the interface cost. When the two scenarios are compared economically, there is a substantial decrease in the operating cost due to heat supplied by the heat pumps, while the electricity generated from the steam network is used to supply their electricity requirement. The utility investment cost decreases since the cost of the heat pumps is lower than the one of the engine, while the interface cost increases, as more heat exchangers require modifications.

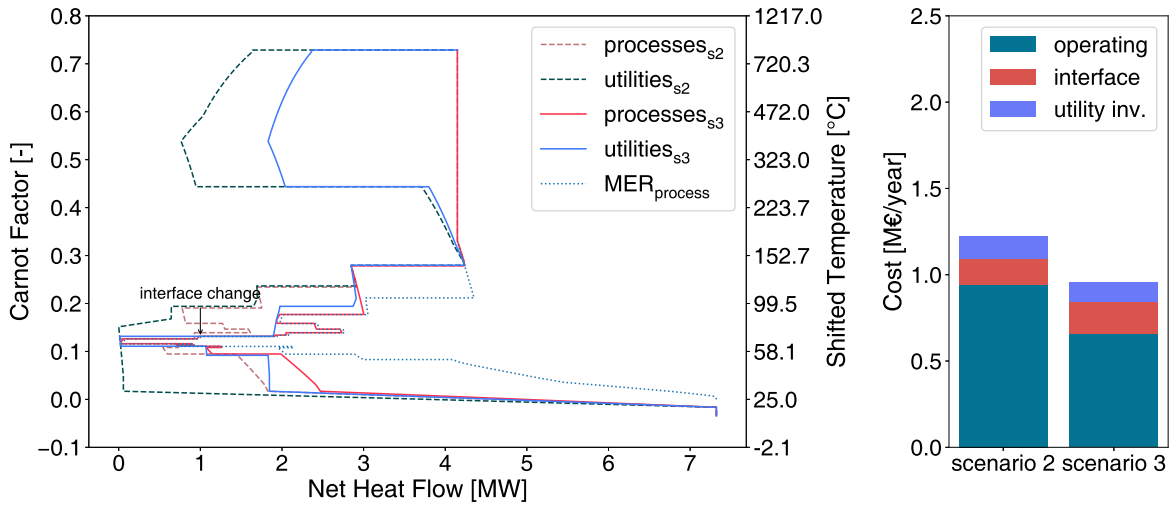

Figure 1.9 – Carnot composite curves (left) and cost comparison (right) of s2 and s3.

In Figure 1.10, the summary of the cost comparison of all the scenarios can be seen. The total cost decreases gradually from the base case (i.e. s0) to the best case (i.e. s3) by 45%. The decrease in the operating cost is due to heat recovery between hot and cold process streams, using the existing utilities more efficiently (e.g. using steam at lower pressure levels) and using more cost-efficient utilities (i.e. heat pumps). For the mentioned cost-saving scenarios, the existing heat exchangers should be modified to allow heat transfer with different fluid or with lower LMTD. As observed in the second y-axis of Figure 1.10, 14 out of 24 heat exchangers need modifications in the last scenario, which reflects 29% of the total cost. In addition, the new utility systems such as cogeneration engine and heat pumps require investment, which contribute 10% of the total cost in the best case scenario.

1.4.2 Problem size reduction using optimal interface selection

As the motivation of the second case study (see Section 1.3.6) is not utility integration, only two scenarios are defined for this case. The definitions of the scenarios are given below:

- **baseline:** The current state of the site without any changes in the site layout;
- **improved:** Optimal heat transfer interface selection with the possibility of integrating heat pumps

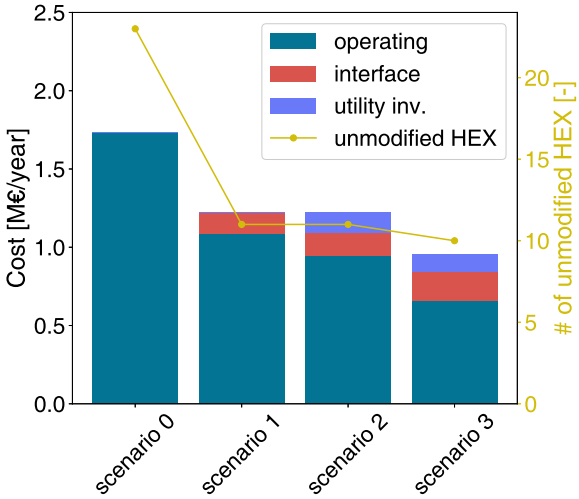

Figure 1.10 – Cost comparison of all scenarios.

and a cogeneration cycle.

Figure 1.11 depicts the comparison of the baseline and improved scenarios. Similar to the results of the first case study, heat recovery reaches its theoretical maximum (i.e. the same value as MER). With heat recovery, integration of heat pumps, and better usage of the steam network, the operating cost of the unit can be decreased by 47%. Integration of new utilities and modifications of heat exchangers introduces investment and interface cost accounting for 9% of the total cost in the improved scenario.

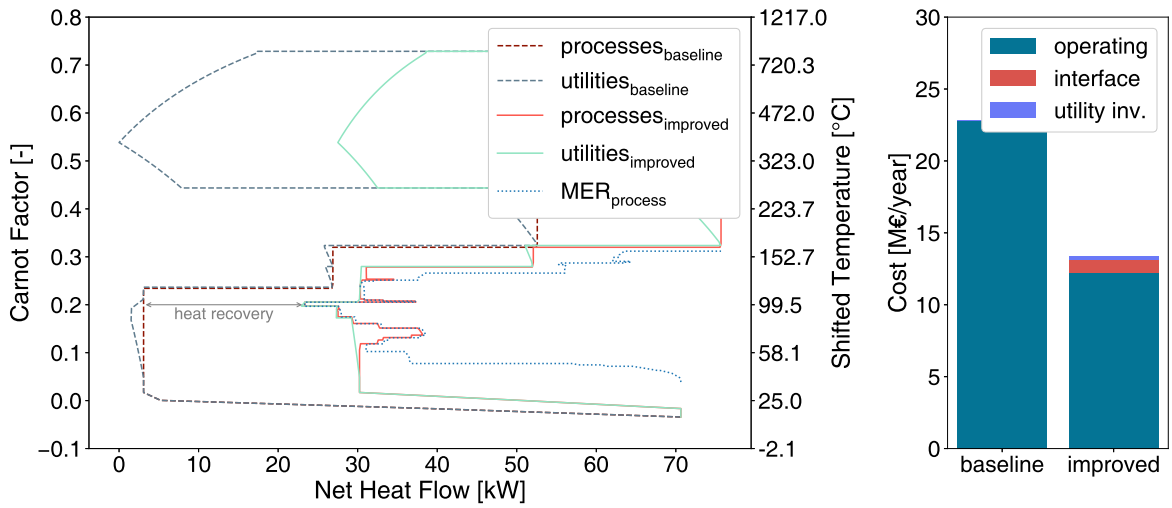

Figure 1.11 – Carnot composite curves (left) and cost comparison (right) of the baseline and improved scenarios.

The HLD problem of case study 2 is solved based on the results of utility integration of the improved

scenario. The sizes of the utilities, variable at the level of utility integration, are hence fixed for solving the HLD. The results of optimal interface selection are used to set forced matches for the HLD problem as explained in Section 1.3.3. The impact of forced matches on reducing computational burden is assessed by evaluating the scenarios depicted in Figure 1.12:

- **heat load distribution scenario 1 (hld1):** Business as usual case without forced matches
- **heat load distribution scenario 2 (hld2):** Heat load distribution with forcing the matches between process streams and their current utility for the streams that remain at current utility interface;
- **heat load distribution scenario 3 (hld3):** Heat load distribution with forcing the matches between process streams and their current utility for the streams that remain at current utility interface and forcing the matches between the process streams and the candidate utility for the streams that switched to one of the candidate interfaces.

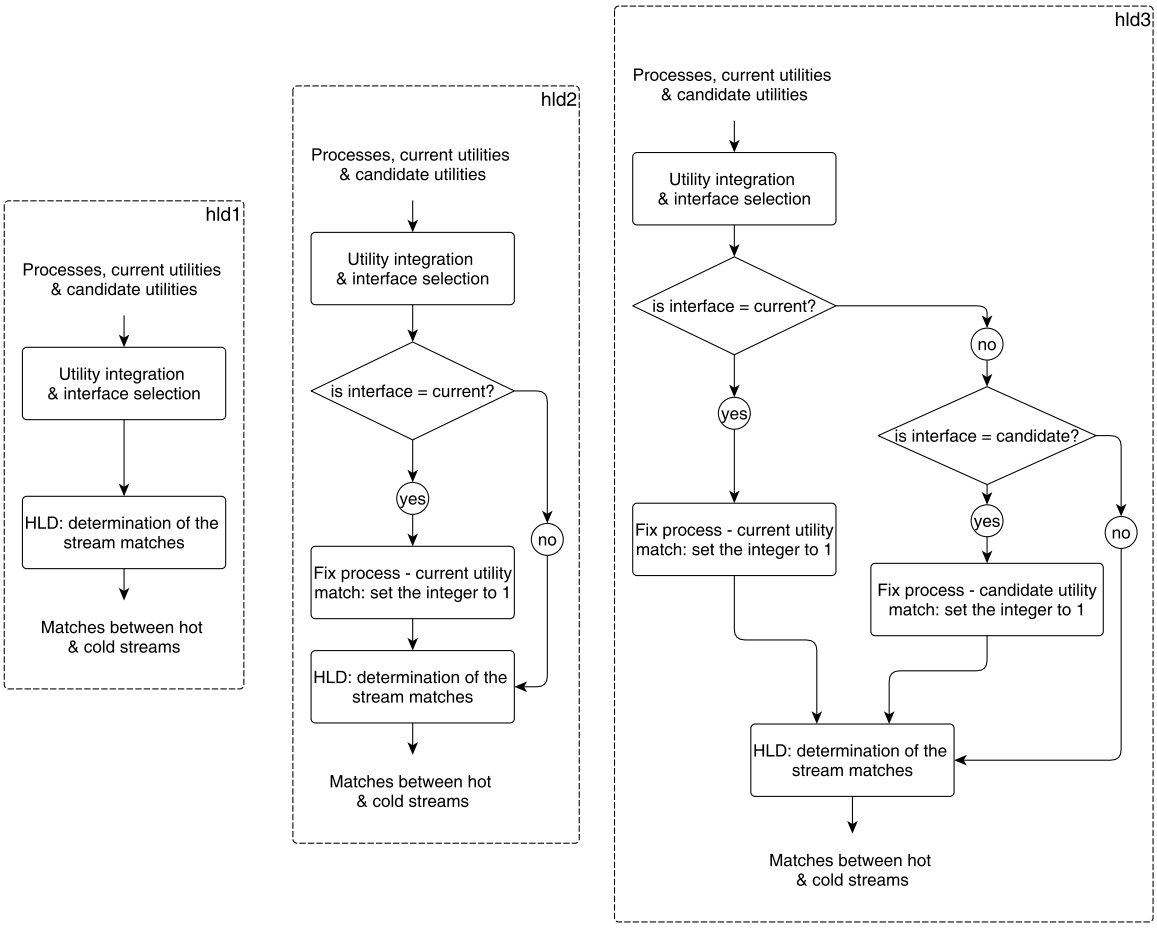

Figure 1.12 – Decision trees of hld1, hld2 and hld3.

Figure 1.13 compares the solution time for the three HLD scenarios described above. With 23 streams

matched with the current utility, the solution time is reduced by 32%. Moreover, with respect to the results of interface selection, forcing 11 streams to match with a candidate utility further reduces the solution time by 78% compared to hld1.

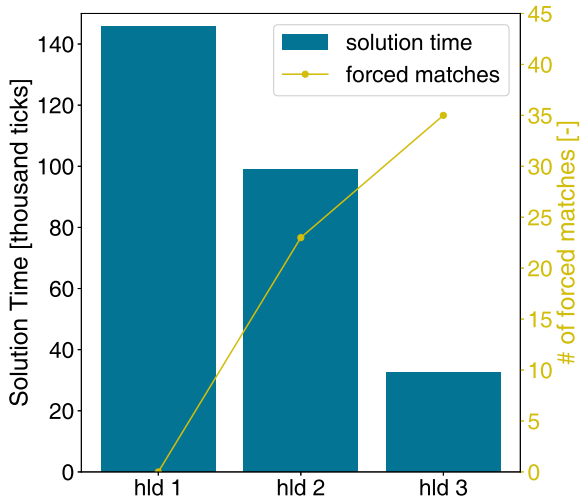

Figure 1.13 – Solution time and forced matches of hld1, hld2 and hld3.

1.4.3 Selection of interface under different economic conditions

The results of optimal interface selection is highly dependent on the cost parameters, since it is formulated as a total cost minimisation problem. To assess the solution sensitivity to costing parameters, optimisation was performed for the second case study using energy prices from 25 organisation for economic co-operation and development (OECD) countries. The specific costs of natural gas and electricity change for each country (see Appendix A.2) while the other parameters are assumed to be stable.

The results comparing the cost distribution of the optimal solution, the number of unmodified heat exchangers and the savings in CO_2 emissions compared to the business as usual operation can be seen in Figure 1.14. The total cost of the system is dominated by the operating cost which, in turn, is driven mostly by natural gas. Thus, the optimal solution in all cases is found to be a combination of interface changes and heat pumping, therefore reducing the operating cost drastically while benefiting from savings in CO_2 emissions up to 37%. When the countries with high and low numbers of unmodified heat exchangers are compared, it is observed that the decision correlates with the ratio of electricity to natural gas prices. In countries with low electricity:natural gas price ratios (e.g. Korea, Switzerland), more heat exchangers remain unmodified. The reason behind this decision is that modifying heat exchangers to use steam at lower pressure and producing electricity becomes less attractive. Conversely, countries where the electricity:natural gas price ratio is high (e.g. Germany, Italy, Canada), the number of streams changing interface increases. However, it should be noted

that interface change becomes less attractive when the utility prices are low, since the benefits of heat recovery are lower relative to the cost of changing interfaces. As a consequence, the number of unmodified heat exchangers is higher in Canada compared to UK, although Canada has higher electricity:natural gas cost ratio. In most cases, the number of unmodified heat exchangers is the same in countries where the cost ratio of electricity to natural gas is similar (e.g. Hungary, Japan, Poland). This result, however, is highly case-dependent. In systems without cogeneration units (e.g. steam network), the decision would be solely dependent on the price of natural gas.

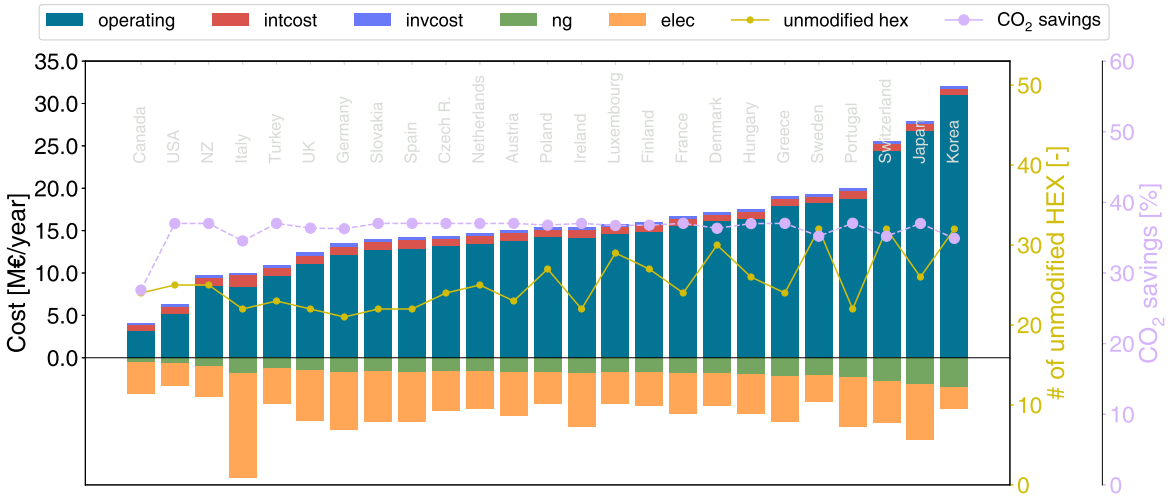

Figure 1.14 – Optimal interface selection under economic conditions of 25 OECD countries.

1.5 Conclusion

This chapter introduced a method which enables definition of the heating and cooling requirement of a process by different heat transfer interfaces. It provides flexibility in defining the desired interfaces compared to the state of the art methods using pre-defined interfaces (e.g. thermodynamic, technology, utility). Changing a process heat transfer interface may yield better heat integration solutions; however, it implies modifications in existing heat exchangers, which is typically neglected in conventional HI problems. A novel MILP formulation based on HI is proposed to enable process definition with multiple heat transfer interfaces and to select the optimal interface for each process, accounting for the cost of interface modifications.

The proposed method is applied to two case studies. In the first case study, heat integration in a plant is improved gradually in four scenarios, starting from the current state of the system. Only allowing interface changes, without integration of new utility systems, yields a 23% decrease in heating demand stemming from heat recovery, 38% decrease in the operating cost and 29% decrease in the total cost including the interface cost. The total cost of the system improves slightly with the integration of a cogeneration engine supplying electricity and heat. Finally, with the integration of

the heat pumps, the total cost of the system is reduced by 45% compared to the base case while the improvements in the system require modifying 14 heat exchangers.

In the second case study, the problem size reduction for HEN analysis is demonstrated, and more specifically for the HLD subproblem. The results of interface selection are used to fix stream matches for HLD *a priori*. The solution time decreases by 32% when streams not changing their interfaces are pre-defined as matching with their current utilities. The solution time further improves when forced matches are extended to streams that change to a candidate utility interface.

The decision of optimal interface selection depends on the cost parameters since the proposed method relies on optimising the total cost objective function. Exploration of solution sensitivity to operating cost parameters in the interface selection, the second case study is carried out using natural gas and electricity cost data from 25 OECD countries. The results depict that the countries which have similar electricity to natural gas cost ratio are likely to have similar solutions for investing in interface changes; however, this conclusion is dependent on the system under consideration as other factors also play a role.

The work presented in this chapter uses deterministic optimisation techniques as opposed to the stochastic and heuristic methods considered as the state of the art. The proposed method provides preliminary retrofit solutions, since it considers the trade-off between the operating cost benefits and the interface cost required to achieve them. In addition, the method identifies the streams that should remain matched with their current utilities and the streams that should match with certain candidate utilities which fixes matches for HEN synthesis, reducing the problem size and thus facilitating its solution.

Incorporating plant layout in heat exchanger network retrofit

Overview

- Considering the plant layout including the locations of the streams and initial heat exchangers;
- A novel MILP formulation for heat load distribution including retrofit actions such as moving heat exchangers, repiping streams, adding area to existing heat exchangers and adding new heat exchangers;
- Piping cost calculation based on the length and diameter;

The content of this chapter is partially published in [40].

2

2.1 Introduction

In Chapter 1, heat exchanger modifications are considered only to the extent of required area addition. This chapter goes deeper in heat exchanger network (HEN) retrofit by incorporating different types of modifications in heat load distribution (HLD). The plant layout is taken into account by defining the initial positions of the streams and heat exchangers and calculating the cost of repiping based on distance. Section 2.2 covers the state of the art in HEN design and retrofit, Section 2.3 outlines the method, Section 2.4 gives the details of the mathematical formulation, Section 2.5 presents the case studies, Section 2.6 analyses the results and Section 2.7 draws the conclusions.

2.2 State of the art

Methods for retrofitting HENs are very similar to those for grass-roots design. In fact, most HEN retrofit methods are derived from grass-roots design methods. Therefore, the state of the art of the two fields can be considered together. Available methods in the literature can be classified into two subgroups; pinch analysis (PA) based methods and mathematical programming (MP) based methods.

The pinch design method was first introduced by Linnhoff and Hindmarsh [10] for grass-roots design and then extended to retrofit by Tjoe and Linnhoff [41]. The overall idea within this method is to maximise heat recovery by preventing heat exchange across the pinch point and modifying the HEN to achieve maximum energy recovery (MER). In PA-based methods, area targeting is carried out by dividing the composite curves into vertical segments and calculating the estimated area for each of those segments [42]. Carlsson et al. proposed a pinch design method which uses criss-cross heat exchange instead of vertical intervals [43] and also accounted for heat exchanger types, space requirements, pressure drop and fouling. In HEN retrofit, modifications might be required for specific heat exchangers rather than the whole network. Van Reisen et al. proposed a method which identifies critical parts of networks and focuses on retrofit in these specific sections [44]. This method, called path analysis, not only reduces the problem size but also results in more realistic retrofit designs. Similarly, Li and Chang [45] proposed a method focusing only on heat exchanges crossing the pinch point, based on [10].

While PA offers clear guidelines for the estimation of capital investment in grass-roots design, methods for retrofit targeting in scientific literature do not provide a systematic approach to determine heat exchanger relocation, repiping, additional area and additional heat exchangers [46]. MP methods have been studied extensively, to overcome the drawbacks of PA-based methods. They can be subdivided into two groups depending on their formulation; simultaneous and sequential. Moreover, another classification can be proposed based on the optimisation method used; deterministic or stochastic. Simultaneous formulation of HENs was first proposed by Yee and Grossmann [15] as SYNHEAT, in the form of an mixed integer non-linear programming (MINLP). Although the formulation had simplifying assumptions, such as isothermal mixing and placing utilities at the top and bottom temperature intervals, many other researchers used it as basis for their work [47–49]. For example, Zamora et al. [50] proposed a method based on the SYNHEAT model. They introduced underestimators for bilinear and linear terms and used simplified assumptions, such as linear cost functions for heat exchangers and arithmetic mean instead of logarithmic mean temperature difference (LMTD) to convexify the MINLP.

One of the first simultaneous methods for HEN retrofitting was also developed by Yee and Grossmann [51]; the method first evaluates the feasibility of the retrofit in the pre-screening stage, and then solves the retrofit HEN superstructure, which is formulated using MINLP. Ciric and Floudas [52] also proposed an MINLP method which simultaneously finds the optimal hot and cold stream matches and HEN retrofit superstructure. However, similarly to SYNHEAT, their method does not include the optimal selection and integration of utilities. Typical HEN synthesis and retrofit methods simplify the problem by assuming that the operating conditions are fixed. However, changing process operating conditions often provides opportunities for improving the design. Ponce-Ortega [53] proposed a retrofit approach based on [51], in which operational and structural modifications were carried out simultaneously. Though, similar to the previous methods, only one hot and one

cold utility were added in the superstructure. Their approach was extended by allowing multiple utilities and isothermal process streams [54].

Superstructure-based MINLP models may be difficult to solve due to local optima and are computationally expensive. A transportation-based mixed integer linear programming (MILP) formulation was developed by Shetna et al. [55] to solve large scale industrial problems. The method considers temperature intervals in small segments, which makes it possible to calculate the LMTD for exchanges between those intervals prior to optimisation. This idea was further pursued by Barbaro and Bagajevicz [56]. Despite the complexities introduced by binary variables linked to temperature intervals, which increases the problem size and solution difficulty, the method has been applied to real industrial case studies, such as crude unit preheating trains [46]. Nguyen et al. [57] proposed a retrofit method based on Barbaro's MILP formulation [56]. While the cost of area addition and reduction was included in the problem, they neglected the cost of topological modifications, such a heat exchanger relocation and repiping. Another effort to reduce the non-linearities was suggested by Pan et al. [58] who initialised the LMTD prior to optimisation, using the temperatures in the heat exchangers from the existing network, while linearising the other non-linear terms using first-order Taylor series expansion. Moreover, the method included heat exchanger details by using correction factors which depend on the number of shell and tube passes. To overcome the computational difficulties, the method was extended in [59], which followed a two-stage iterative procedure. The first stage identified the modifications in the existing HEN, while the second addressed the investment details. Kang and Liu also proposed a HEN retrofit problem with two steps [60]. In the first step, the HEN superstructure is optimised and the required heat exchanger areas are calculated. Afterwards, assignment between the existing heat exchangers and optimal stream matches was carried out, taking into account the additional area and heat exchangers. The computational burden of optimising HENs increases with retrofit decisions. Ayotte-Sauve et al. proposed an MINLP model [61] including retrofit actions, such as adding new heat exchangers and relocating existing ones, and solved it using an iterative procedure to decrease the computational complexity. In each iteration, a new HEN configuration was determined, with the condition of adding at most one new heat exchanger compared to the previous iteration, which reduced the search space significantly. When multiple plants are involved in the problem, the decision of locating heat exchangers between plants becomes crucial. Nair et al. [62] accounted for plant locations in an eco-industrial park and developed a method to obtain the optimal placement of heat exchangers between plants by considering the trade-off between operational benefits and the cost of piping and pumping.

With many retrofit actions considered, the superstructure in simultaneous methods becomes large and difficult to solve. To overcome these difficulties, different strategies are proposed:

- Benders decomposition [63];
- iterations [52];
- simplified assumptions, such as no by-pass or arithmetic mean temperature difference instead of

LMTD [50, 51].

The most common approach in the literature is problem decomposition, which is typically called sequential approach. The problem is divided into three steps; (a) minimum utility consumption (i.e. energy integration (EI)), (b) minimum number of connections (i.e. HLD) and (c) superstructure synthesis. EI was first introduced in the form of an MILP formulation [12] and has been studied and improved by several authors [25, 38]. Although the HEN superstructure is not constructed in EI, it is possible to estimate the total HEN area and the number of heat exchangers based on the composite curves [42]. It is also possible to assess preliminary HEN retrofit decisions by considering the trade-off between additional heat exchanger area required and operational benefits of heat integration [40]. For deeper analysis, HLD is carried out, which was introduced as an MILP formulation [13, 35] aiming to minimise the number of heat exchangers. Yee and Grossmann developed a retrofit HLD method by defining penalty parameters for hot and cold stream matches based on the retrofit action required [64]. For example, stream matches which are already housed in a heat exchanger in the existing network have small penalties compared to the matches which would require repiping, reallocation of heat exchangers, or adding hew heat exchangers. Ciric and Floudas proposed a method which accounts for the cost of modifications in the existing network rather than assigning penalties for the stream matches [65]. Pouransari and Maréchal introduced the impact of stream locations in HLD [66]. Similar to [64], they defined penalty parameters for stream matches; however, the penalty values are selected based on the stream locations. After the stream matches and their corresponding heat loads are determined, the optimal HEN configuration is determined by deciding how the streams are split and mixed [14].

The main advantage of the methods using problem decomposition is that a single step MILP/MINLP problem is divided into smaller MILP and non-linear programming (NLP) problems, which are easier to solve. Conversely, since optimisation is carried out in multiple steps, the solution is likely to be sub-optimal, compared to the simultaneous optimisation methods that obtain the global optimum. To overcome this drawback, decomposition methods are often combined with stochastic methods. Mian et al. proposed a framework combining a sequential approach (slave optimisation) with particle swarm optimisation (master optimisation) [36]. While the parameters that are fixed at the level of HEN synthesis, such as the minimum approach temperature in the heat exchangers are manipulated at the master level, optimal HEN design is determined at the slave optimisation. This approach is extended to multi-objective optimisation by replacing particle swarm optimisation with a genetic algorithm (GA) [67]. Similarly, Rezaei and Shafiei [68] coupled a GA with deterministic methods. The GA was used to generate different network configurations and optimised the structural modifications, while the NLP was used to determine the loads of the heat exchangers, by maximising MER and integer programming (IP) minimised the cost of the modifications. Soltani and Shafiei extended the formulation by taking pressure drop into account [69]. To take advantage of the flexibility of stochastic optimisation, purely stochastic methods have been studied as well. Liu et

al. proposed a method coupling a GA with simulated annealing [70], which was determined to be well-suited for non-differential problems. Sreepathi and Rangaiah [71] used a differential algorithm with different exchanger assignment strategies as well as multi objective optimisation (MOO) with non-dominated sorting genetic algorithm. They concluded that exchanger assignment strategies play an important role in obtaining better results.

Although the simultaneous approach has the advantage of providing global optimality, its computational difficulties have been reported by several studies. Thus, for large problems, the sequential approach presents a good alternative to study HEN retrofit. Since the focus of recent research has been towards the simultaneous approach (see Table 2.1), few methods using problem decomposition are available in the literature on HEN retrofit. Although the cost of piping modifications and civil engineering have significant contributions in the retrofit cost [72], most literature methods either neglect those aspects, or assign a constant cost parameter per piping modification. This work proposes a sequential HEN retrofit method and focusing on the HLD subproblem. The method is based on [65], however it offers improvements by including the plant layout in the analysis which results in more realistic solutions.

Table 2.1 – Literature review on heat exchanger network design and retrofit.

Publication	Year	Method	Strategy	Retrofit	Plant layout	Moving HEX	Adding area	Adding HEX	Repiping
Carlsson et al. [43]	1993	PA-based	heuristic	✖	✖	✖	✖	✖	✖
Van Reisen et al. [44]	1995	PA-based	heuristic	✔	✖	✖	✔	✔	✖
Li and Chang [45]	2010	PA-based	heuristic	✔	✖	✖	✔	✔	✖
Yee and Grossmann [51]	1991	MP-based	simultaneous	✔	✖	✔	✖	✖	✖
Nguyen et al. [57]	2010	MP-based	simultaneous	✔	✖	✖	✔	✖	✖
Kang and Liu [60]	2015	MP-based	simultaneous	✔	✖	✔	✔	✔	✖
Ayotte-Sauve et al. [61]	2017	MP-based	simultaneous	✔	✖	✔	✔	✖	✖
Nair et al. [62]	2018	MP-based	simultaneous	✔	✖	✖	✖	✖	✔
Yee and Grossmann [64]	1987	MP-based	sequential	✔	✔	✖	✖	✖	✖
Ciric and Floudas [65]	1989	MP-based	sequential	✔	✖	✔	✔	✔	✔
Pouransari and Maréchal [66]	2914	MP-based	sequential	✔	✔	✖	✖	✖	✖
This thesis	2019	MP-based	sequential	✔	✔	✔	✔	✔	✔

2.3 Method

The method proposed in this work follows a sequential approach in line with the state of the art, thus the problem is decomposed into multiple steps with optimisation carried out in each. Figure 2.1 depicts the overall framework of the method.

The problem is defined using units ($u \in \mathbf{U}$) characterised by their corresponding material, electricity and heat input and output (i.e. streams) creating a superstructure. The units are classified into two main groups; process units $pu \in \mathbf{PU}$ with fixed size and operation (e.g. production units), representing demands, and utility units $uu \in \mathbf{UU}$ with variable size and operation (e.g. energy conversion systems), representing the supply. To define the characteristics of the units, thermodynamic (e.g.

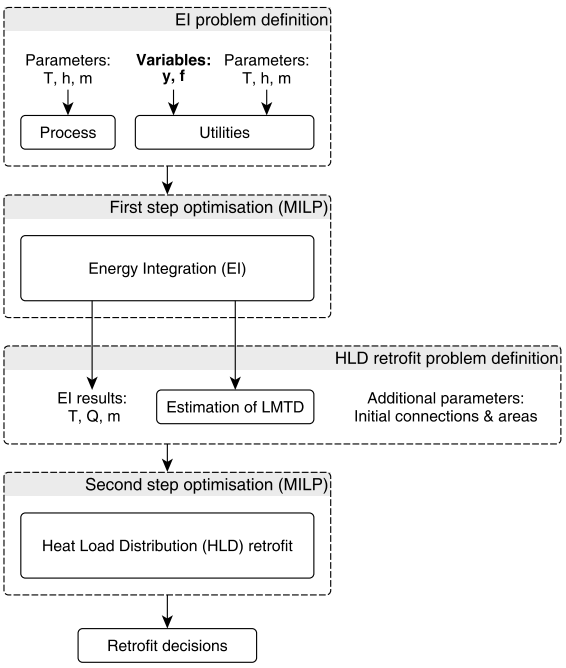

Figure 2.1 – Overall framework of the proposed method.

temperature, enthalpy) and physical (e.g. mass flowrate) parameters of their corresponding input and output must be provided. The operating conditions, and hence the parameters of the units, can vary throughout a defined operating period. Thus, the problem is formulated using time steps $t \in \mathbf{TT}$, which allows consideration of different operating modes.

After the problem superstructure is defined, the EI subproblem is solved using an MILP formulation [38]. The objective function of the first optimisation is minimisation of the total system cost, comprising the operating cost due to consumption of certain resources (e.g. natural gas) and the investment cost for purchasing new energy conversion technologies. The objective function is minimised by varying the scheduling and sizing of utilities respecting the main constraints, such as heat cascade (i.e. heat balance), electricity and mass balances. Further details of the formulation in this step are given in [38].

Once EI is solved, the size of the utility units are fixed according to the optimal solution. In addition to the thermodynamic and physical parameters, LMTD parameters obtained from the results of EI are used to define the HLD retrofit subproblem. Moreover, the initial connections between the hot and cold streams and their current heat exchangers are defined to form the basis for the retrofit. Section 2.4 gives the details and mathematical formulation of the HLD retrofit subproblem.

2.4 Heat load distribution retrofit

2.4.1 Definition of sets

EI closes the heat, electricity and mass balances of the system. Moreover, it selects the optimal combination of utility systems to provide heating, cooling and electricity to the process units. HLD, on the other hand, determines the distribution of heat in the system, which is optimised in terms of sizing and selection of utilities in EI. Since heat is the focus of this step, only units with heat streams are considered. The main sets of the formulation are listed as follows:

- **H**: The set of heat streams comprising hot and cold streams of each unit in the system;
- **SG**: The set of stream groups. The streams with non-linear temperature - enthalpy profiles (e.g streams with phase change) are modelled as piecewise linear streams $s \in \mathbf{H}$. Afterwards, the group of streams representing a non-linear stream are assigned to the same stream group $sg \in \mathbf{SG}$ as suggested by [66]. An example of the relationship between streams and stream groups is depicted in Figure 2.2, where a hot stream group containing two streams exchanges with a cold stream group with three streams. The advantage of using stream groups is not only the capacity to work with streams with non-linear profiles, but also reducing the problem size by allocating variables to stream groups rather than to streams;

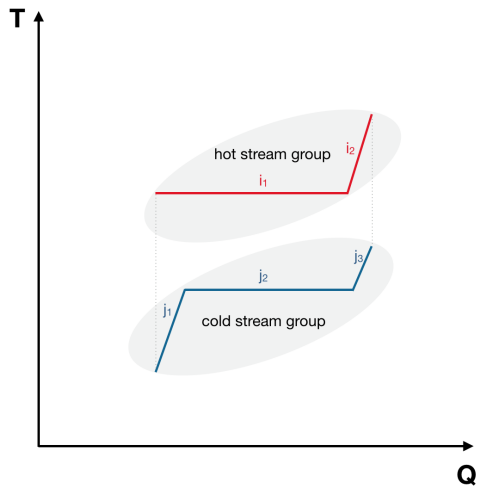

Figure 2.2 – Illustrative example of hot and cold stream groups.

- $\mathbf{SS}_{sg}$: The set of streams of stream groups. This set is used to assign streams to their corresponding stream groups;
- $\mathbf{K}_t$: The set of temperature intervals created by each unique temperature in the system;
- $\mathbf{ZN}_t$: The set of zones. This set divides the system into subsystems that are separated by pinch points;
- **HS**: The set of hot streams. The members of this set are within the set of streams, hence **HS**⊂**H**;

- **CS**: The set of cold streams. The members of this set are within the set of streams, hence **CS**⊂**H**;
- **HG**: The set of hot stream groups. The members of this set are within the set of stream groups, hence **HG**⊂**SG**;
- **CG**: The set of cold stream groups. The members of this set are within the set of stream groups, hence **CG**⊂**SG**;
- **EX**: The set of existing heat exchangers in the initial configuration of the plant;
- **I**: The set of initial matches between hot and cold stream groups;
- **IE**: The set of initial matches between hot stream groups $(ig, jg) \in \mathbf{I}$ and existing heat exchangers $e \in \mathbf{EX}$;

Other sets used in specific parts of the formulation are described in the following subsections.

2.4.2 Objective function

Capturing the main actions, retrofit decisions are classified into the following subgroups, each representing a set in the formulation:

- $\mathbf{R^1}$: Moving an existing heat exchanger. This action is a result of housing a stream group match in an existing heat exchanger $e \in \mathbf{EX}$ which was not the case in the initial network $\therefore (ig, jg, e) \notin \mathbf{IE}$;
- $\mathbf{R^2}$: Adding area to an existing heat exchanger. This occurs when a stream group match is housed in an existing heat exchanger $e \in \mathbf{EX}$ and the area of the heat exchanger is lower than what is required for the match;
- $\mathbf{R^3}$: Repiping a stream group. This action is taken when a new stream group match occurs, which does not exist in the initial connections $\therefore (ig, jg) \notin \mathbf{I}$ and hence one of the streams is repiped;
- $\mathbf{R^4}$: Buying a new heat exchanger. This action occurs when there is a stream group match and that it is not housed in one of the existing heat exchangers.

Although the retrofit actions are divided into subgroups, they do not represent exclusive decisions, i.e. several actions can be taken simultaneously. For example, an existing heat exchanger might be moved to house a new match which requires one of the stream groups to be repiped and adding area to the heat exchanger. The objective function of the proposed HLD method is minimisation of the total cost of retrofit actions required, (see Equation 2.1) based on the initial configuration.

$$\min \left\{ \sum_{(ig,jg,e)\in\mathbf{R^1}} C^{move}_{ig,jg,e} + \sum_{(ig,jg,e)\in\mathbf{R^2}} C^{add}_{ig,jg,e} + \sum_{(ig,jg)\in\mathbf{R^3}} C^{rep}_{ig,jg} + \sum_{(ig,jg)\in\mathbf{R^4}} C^{nh}_{ig,jg} \right\} \tag{2.1}$$

where $C^{move}_{ig,jg,e}$ is the cost of moving an existing heat exchanger to a new stream group match, $C^{add}_{ig,jg,e}$ is the cost of adding area to an existing heat exchanger, $C^{rep}_{ig,jg}$ is the cost of repiping a stream group,

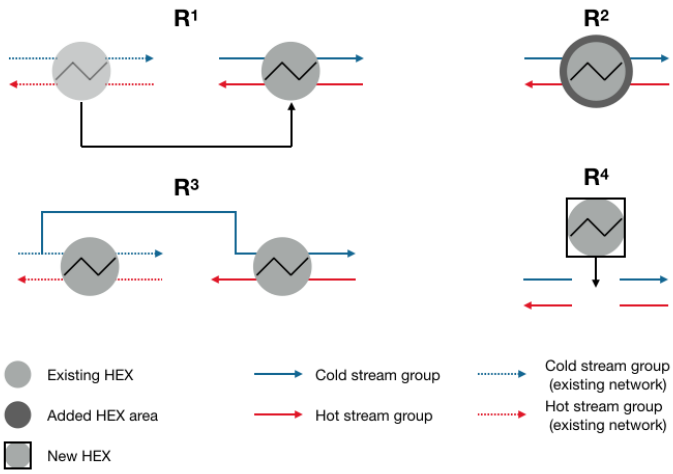

Figure 2.3 – Retrofit actions in the heat exchanger network.

and $C^{nh}_{ig,jg}$ is the cost of purchasing a new heat exchanger for the corresponding match.

2.4.3 Heat flow model

Heat flow model is a set of constraints which ensure that heat flows from hot to cold streams as well as from higher to lower temperature intervals. The heat flow formulation is adapted from [14]. The sets that are introduced to impose the heat flow constraints are as follows:

- $\mathbf{KT}_{t,z}$: The set of top temperature intervals. This set contains the highest temperature interval of each zone $z \in \mathbf{Z}_t$ in each time step $t \in \mathbf{TT}$;
- $\mathbf{KB}_{t,z}$: The set of bottom temperature intervals. This set contains the lowest temperature interval of each zone $z \in \mathbf{Z}_t$ in each time step $t \in \mathbf{TT}$;
- $\mathbf{KZ}_{t,z}$: The set of temperature intervals of each zone $z \in \mathbf{Z}_t$ in each time step $t \in \mathbf{TT}$;
- $\mathbf{HK}_{t,z,k}$: The set of hot streams within and above temperature interval $k \in \mathbf{K}_{t,z}$;
- $\mathbf{CK}_{t,z,k}$: The set of cold streams within temperature interval $k \in \mathbf{K}_{t,z}$;

The heat from the hot streams in the top interval of each zone is either transferred to cold streams within the interval or to lower temperature intervals in the form of residual heat, which is represented by Equation 2.2.

$$\dot{R}_{i,t,z,k} + \sum_{j \in \mathbf{CK}_{t,z,k}} \dot{Q}_{i,j,t,z,k} - \dot{q}_{i,t,k} = 0 \quad \forall\ i \in \mathbf{HK}_{t,z,k}, t \in \mathbf{TT}, z \in \mathbf{ZN}_t, k \in \mathbf{KT}_{t,z} \tag{2.2}$$

where $\dot{R}_{i,t,z,k}$ is the residual heat delivered to the interval below k, $\dot{Q}_{i,j,t,z,k}$ is the heat transfer from

the hot to cold streams and $\dot{q}_{i,t,k}$ is the heat load of the hot streams. In the bottom interval of each zone, residual heat to the lower interval is equal to zero, since there is no lower temperature interval. Therefore, the residual heat received from the interval above and heat in the hot streams within the interval must be transferred to cold streams, which is ensured by Equation 2.3.

$$\dot{R}_{i,t,z,k-1} - \sum_{j \in \mathbf{CK}_{t,z,k}} \dot{Q}_{i,j,t,z,k} + \dot{q}_{i,t,k} = 0 \quad \forall\ i \in \mathbf{HK}_{t,z,k}, t \in \mathbf{TT}, z \in \mathbf{ZN}_t, k \in \mathbf{KB}_{t,z} \tag{2.3}$$

where $\dot{R}_{i,t,z,k-1}$ is the residual heat from the interval above. In all intervals except the top and the bottom, heat from the hot streams and residual heat from the interval above is either delivered to cold streams within the interval or to the interval below as residual heat. This is enforced by Equation 2.4.

$$\dot{R}_{i,t,z,k} - \dot{R}_{i,t,z,k-1} + \sum_{j \in \mathbf{CK}_{t,z,k}} \dot{Q}_{i,j,t,z,k} - \dot{q}_{i,t,k} = 0 \quad \forall\ i \in \mathbf{HK}_{t,z,k}, t \in \mathbf{TT}, z \in \mathbf{ZN}_t, k \in \mathbf{KZ}_{t,z} : k \notin \mathbf{KB} \cup \mathbf{KT} \tag{2.4}$$

Finally, the heat requirement of the cold streams in an interval is equal to the sum of the heat transferred to them by hot streams in the same or higher temperature intervals, which is governed by Equation 2.5.

$$\dot{q}_{j,t,k} - \sum_{i \in \mathbf{HK}_{t,z,k}} \dot{Q}_{i,j,t,z,k} = 0 \quad \forall\ j \in \mathbf{CK}_{t,z,k}, t \in \mathbf{TT}, z \in \mathbf{ZN}_t, k \in \mathbf{KZ}_{t,z} \tag{2.5}$$

where $\dot{q}_{j,t,k}$is the heat required by the cold streams.

2.4.4 Stream matches

A connection (i.e. match) between a hot and cold stream group exists if there is heat exchange between them. A binary variable is allocated to each stream group match to determine its existence. In state of the art methods, all matches between streams [13, 14] or stream groups [66] are considered in the analysis. This includes matches between two process unit streams (i.e. heat recovery), a stream from a process unit and one from a utility unit (i.e. utility heat exchanger), and two utility unit streams (i.e. utility connections). Figure 2.4 illustrates heat recovery between two distillation columns, heat exchange between a steam network and a distillation column, and between a steam network and a boiler as examples for process - process, process - utility and utility - utility matches, respectively.

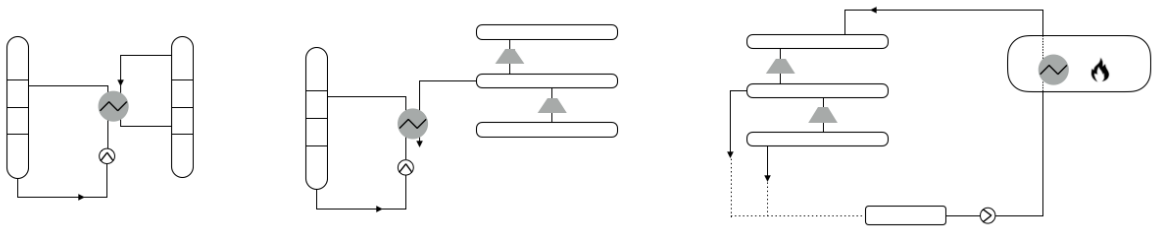

Figure 2.4 – Possible matches in a system: process - process (left), process - utility (centre), utility - utility (right).

In practice, the first two types of matches are housed in heat exchangers, while utility - utility heat exchange occurs inside the utility systems (e.g. boiler) themselves, for which investment cost has already been taken into account in EI. Therefore, including such matches in the analysis would double-count the investment cost for some utilities. In the present work, utility - utility matches are excluded from the analysis by using restricted sets.

The possible matches between hot and cold streams are those which respect temperature constraints. Hence a cold stream $j \in \mathbf{CK}_{t,z,k}$ can only exchange heat with a hot stream $i \in \mathbf{HK}_{t,z,k}$ as long as the temperature of the hot stream is higher than that of the cold. Based on this, the sets for stream matches are defined as follows:

- **MS**: The set of possible stream matches. This set includes all process - process and process - utility stream matches that respect the temperature constraints. Hence, it is a subset of combinations obtained from crossing $j \in \mathbf{CK}_{t,z,k}$ and $i \in \mathbf{HK}_{t,z,k}$;
- **MG**: The set of possible stream group matches. This is a two dimensional set based on **MS** and hence includes matches between stream groups whose streams can potentially exchange heat.

The binary variable allocated for connection, $y_{ig,jg}$, takes the value of 1 if there is heat transfer between the concerned stream groups and 0 otherwise. This is enforced by including 'big-M'-style constraints, as illustrated in Equation 2.6.

$$\frac{y_{ig,jg}}{\text{bigM}} \leq \sum_{(i,j)\in\mathbf{MS}} \sum_{k\in\mathbf{KZ}_{t,z}} \dot{Q}_{i,j,t,z,k} \leq y_{ig,jg} \cdot \text{bigM} \quad \forall\ (ig,jg) \in \mathbf{MG}, t \in \mathbf{TT}, z \in \mathbf{ZN}_t : i \in \mathbf{SS}_{ig}, j \in \mathbf{SS}_{jg} \tag{2.6}$$

where bigM is a parameter which is large enough to not impose real upper and lower bounds but not so large as to cause numerical problems in the optimisation and $y_{ig,jg}$ is a binary variable which decides the existence of stream group match ($ig, jg \in \mathbf{MG}$).

2.4.5 Maximum heat exchange between stream groups

The heat exchange between streams $(i, j) \in \mathbf{MS}$ in each time step, zone and temperature interval is calculated by the heat flow model presented in Section 2.4.3. The heat transfer between stream groups $(ig, jg) \in \mathbf{MG}$ in each time step can then be calculated using Equation 2.7.

$$\sum_{(i,j)\in\mathbf{MS}} \sum_{z\in\mathbf{ZN}_t} \sum_{k\in\mathbf{KZ}_{t,z}} \dot{Q}_{i,j,t,z,k} = \dot{Q}_{ig,jg,t} \quad \forall\ (ig, jg) \in \mathbf{MG}, t \in \mathbf{TT} : i \in \mathbf{SS}_{ig}, j \in \mathbf{SS}_{jg} \tag{2.7}$$

where $\dot{Q}_{ig,jg,t}$ is the heat exchange between stream groups, a time-dependent variable, which can take different values at each time step. However, the maximum heat exchange between stream group matches (see Equation 2.8) is required for sizing certain equipment (e.g. piping).

2

$$\dot{Q}^{max}_{ig,jg} = \max_{t\in\mathbf{TT}}(\dot{Q}_{ig,jg,t}) \quad \forall\ (ig, jg) \in \mathbf{MG} \tag{2.8}$$

Since the maximum function is non-linear, it is replaced by a set of linear constraints (Equations 2.9–2.14) to fit within the MILP framework.

$$\dot{Q}_{ig,jg,t} \leq \dot{Q}^{max}_{ig,jg} \quad \forall\ (ig, jg) \in \mathbf{MG}, t \in \mathbf{TT} \tag{2.9}$$

$$\dot{QT}_{ig,jg,t} \leq \dot{Q}_{ig,jg,t} \quad \forall\ (ig, jg) \in \mathbf{MG}, t \in \mathbf{TT} \tag{2.10}$$

$$\dot{Q}_{ig,jg,t} - (1 - w_{ig,jg,t}) \cdot \text{bigM} \leq \dot{QT}_{ig,jg,t} \quad \forall\ (ig, jg) \in \mathbf{MG}, t \in \mathbf{TT} \tag{2.11}$$

$$\dot{Q}^{max}_{ig,jg} \leq \dot{QT}_{ig,jg,t} + (1 - w_{ig,jg,t}) \cdot \text{bigM} \quad \forall\ (ig, jg) \in \mathbf{MG}, t \in \mathbf{TT} \tag{2.12}$$

$$\dot{QT}_{ig,jg,t} \leq w_{ig,jg,t} \cdot \text{bigM} \quad \forall\ (ig, jg) \in \mathbf{MG}, t \in \mathbf{TT} \tag{2.13}$$

$$\sum_{t\in\mathbf{TT}} w_{ig,jg,t} = 1 \quad \forall\ (ig, jg) \in \mathbf{MG} \tag{2.14}$$

where $\dot{Q}^{max}_{ig,jg}$ is the maximum heat load between stream groups over all time steps, $\dot{QT}_{ig,jg,t}$ is a slack variable which takes the value of $\dot{Q}_{ig,jg,t}$ during the time step of the maximal load and 0 in

the others and $w_{ig,jg,t}$ is a binary variable which takes the value of 1 during the time step of the maximal load and 0 in the others.

2.4.6 LMTD estimation

At the stage of HLD, connections between hot and cold streams as well as their corresponding heat loads are determined; however, the temperatures inside the heat exchangers are not identified at this stage. Thus, the LMTD for heat exchange between hot and cold streams cannot be calculated. Ciric and Floudas [65] estimated the LMTD between the hot and cold streams in each temperature interval based on the inlet and outlet temperatures of streams; however, they did not provide further details on the method used for the calculations and thus it cannot be replicated here.

In the present work, an LMTD estimation method based on EI results is used. The composite curves of the system are created first; then, vertical intervals (i.e. enthalpy intervals) are created based on the inlet and outlet temperatures of the streams, following the area targeting method proposed by [42]. The LMTD of each vertical interval is calculated using the temperature differences on both ends of the interval. The HLD formulation uses temperature intervals (i.e horizontal intervals) rather than vertical ones; therefore, the LMTD from the vertical intervals should be converted to horizontal temperature intervals. One or more vertical intervals might exist in the same temperature interval (see Figure 2.5). Moreover, the number of vertical intervals within the same temperature interval can be different for hot and cold streams. Hence, LMTD is calculated for the hot and cold streams in each temperature interval, by taking the weighted average of the LMTD of the vertical intervals with respect to their heat load, using Equations 2.15 and 2.16.

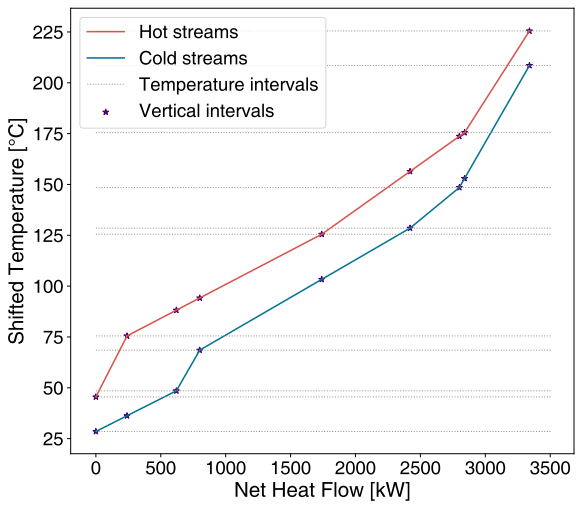

Figure 2.5 – Vertical and horizontal intervals highlighted on a composite curve.

$$\text{LMTD}^{\text{hot}}{}_{t,k} = \frac{\sum_{vi \in VI} \text{LMTD}^{\text{hot}}{}_{vi} \cdot \dot{\text{q}}_{vi}}{\sum_{vi \in VI} \dot{\text{q}}_{vi}} \quad \forall\ t \in \mathbf{TT}, t \in \mathbf{K} \tag{2.15}$$

$$\text{LMTD}^{\text{cold}}{}_{t,k} = \frac{\sum_{vi \in VI} \text{LMTD}^{\text{cold}}{}_{vi} \cdot \dot{\text{q}}_{vi}}{\sum_{vi \in VI} \dot{\text{q}}_{vi}} \quad \forall\ t \in \mathbf{TT}, k \in \mathbf{K} \tag{2.16}$$

where $\text{LMTD}^{\text{hot}}{}_{t,k}$ and $\text{LMTD}^{\text{cold}}{}_{t,k}$ are the LMTD of the hot and cold streams in each interval and time step, respectively, $\text{LMTD}^{\text{hot}}{}_{vi}$, $\text{LMTD}^{\text{cold}}{}_{vi}$ are the LMTD of the vertical intervals on the hot and cold curves, respectively, and $\dot{\text{q}}_{vi}$ is the heat load of the vertical intervals.

2

2.4.7 Area estimation

As discussed in Section 2.4.6, since the superstructure of the HEN is not created in HLD, a rigorous area calculation is not possible. An approximation is carried out instead using the estimated LMTD values and Equation 2.17.

$$A_{i,j,t,z,k} = \dot{Q}_{i,j,t,z,k} \cdot \left(\frac{1}{\text{LMTD}^{\text{hot}}{}_{t,k} \cdot \text{h}_i} + \frac{1}{\text{LMTD}^{\text{cold}}{}_{t,k} \cdot \text{h}_j} \right) \quad \forall\ (i,j) \in \mathbf{MS}, t \in \mathbf{TT}, z \in \mathbf{ZN}_t, k \in \mathbf{KZ}_{t,z} \tag{2.17}$$

where $A_{i,j,t,z,k}$ is the area required for the stream match *(i,j)* to realise $\dot{Q}_{i,j,t,z,k}$ and h_i and h_j are the convective heat transfer coefficients for the hot stream i and cold stream j.

Assuming that a stream group match $(ig, jg) \in \mathbf{MG}$ is housed in a single heat exchanger, their corresponding area requirement in each time step is calculated based on $A_{i,j,t,z,k}$ by Equation 2.18.

$$A_{ig,jg,t} = \sum_{(i,j) \in \mathbf{MS}} \sum_{z \in \mathbf{ZN}_t} \sum_{k \in \mathbf{KZ}_{t,z}} A_{i,j,t,z,k} \quad \forall\ (ig, jg) \in \mathbf{MG} : i \in \mathbf{SS}_{ig}, j \in \mathbf{SS}_{jg} \tag{2.18}$$

where $A_{ig,jg,t}$ is the area required for the stream group match *(ig,jg)*. The area required for the exchange between a stream group match may differ at each time step depending on the variations of the heat load. However, the purchased area of the heat exchanger housing a hot and cold stream group match is fixed and should be sufficient to realise the required heat exchange at any time step. Thus, the area of the exchanger is selected as the maximum area (see Equation 2.19) that would be

required for the corresponding match.

$$A_{ig,jg}^{max} = \max_{t \in \mathbf{TT}}(A_{ig,jg,t}) \quad \forall\ (ig, jg) \in \mathbf{MG} \tag{2.19}$$

A set of constraints similar to those described in Section 2.4.5 are introduced to linearise the maximum area function (see Equations 2.20–2.25)

$$A_{ig,jg,t} \leq A_{ig,jg}^{max} \quad \forall\ (ig, jg) \in \mathbf{MG}, t \in \mathbf{TT} \tag{2.20}$$

$$AT_{ig,jg,t} \leq A_{ig,jg,t} \quad \forall\ (ig, jg) \in \mathbf{MG}, t \in \mathbf{TT} \tag{2.21}$$

$$A_{ig,jg,t} - (1 - u_{ig,jg,t}) \cdot \text{bigM} \leq AT_{ig,jg,t} \quad \forall\ (ig, jg) \in \mathbf{MG}, t \in \mathbf{TT} \tag{2.22}$$

$$A_{ig,jg}^{max} \leq AT_{ig,jg,t} + (1 - u_{ig,jg,t}) \cdot \text{bigM} \quad \forall\ (ig, jg) \in \mathbf{MG}, t \in \mathbf{TT} \tag{2.23}$$

$$AT_{ig,jg,t} \leq u_{ig,jg,t} \cdot \text{bigM} \quad \forall\ (ig, jg) \in \mathbf{MG}, t \in \mathbf{TT} \tag{2.24}$$

$$\sum_{t \in \mathbf{TT}} u_{ig,jg,t} = 1 \quad \forall\ (ig, jg) \in \mathbf{MG} \tag{2.25}$$

where $A_{ig,jg}^{max}$ is the maximum area required for the stream group matches over all time steps, $AT_{ig,jg,t}$ is a slack variable which takes the value of $A_{ig,jg,t}$ during the time step of the maximal area requirement and 0 in the others and $u_{ig,jg,t}$ is a binary variable which takes the value of 1 during the time step of maximal area requirement and 0 in the others.

2.4.8 Retrofit model

The retrofit model consists of a set of constraints governing the retrofit decisions. The retrofit problem is defined with a set of initial connections and their corresponding heat exchangers $(ig, jg, e) \in \mathbf{IE}$. In the optimised system, connections might change to reach the targets set by EI. As a result, the existing heat exchangers are moved to another location or phased out.

An existing heat exchanger housing a connection from the initial network can be used for a match $(ig, jg) \in \mathbf{MG}$ in the retrofitted network. However, this possibility is restricted by the existence of the

new match (ig, jg) using Equation 2.26.

$$ex_{ig,jg,e} \leq y_{ig,jg} \quad \forall\ (ig, jg) \in \mathbf{MG}, e \in \mathbf{EX} \tag{2.26}$$

where $ex_{ig,jg,e}$ is a binary variable related to matches being housed in existing heat exchangers. An existing heat exchanger can be used maximum once in the retrofitted network, which is enforced by Equation 2.27.

$$\sum_{(ig,jg)\in\mathbf{MG}} ex_{ig,jg,e} \leq 1 \quad \forall\ e \in \mathbf{EX} \tag{2.27}$$

A connection that occurs in the retrofitted network has to be housed either in an existing heat exchanger or a new one (see Equation 2.28).

$$\sum_{e\in\mathbf{EX}} ex_{ig,jg,e} + n_{ig,jg} - y_{ig,jg} = 0 \quad \forall\ (ig, jg) \in \mathbf{MG} \tag{2.28}$$

where $n_{ig,jg}$ is a binary variable related to matches which require a new heat exchanger. The area requirement of a match $(ig, jg) \in \mathbf{MG}$ must be satisfied by existing heat exchanger area and/or new area added to the network. This constraint is represented by Equations 2.29 and 2.30.

$$A^{slack}_{ig,jg} \leq \sum_{e\in\mathbf{EX}} ex_{ig,jg,e} \cdot \mathrm{A}^{\mathrm{ex}}{}_{e} \quad \forall\ (ig, jg) \in \mathbf{MG} \tag{2.29}$$

$$A^{slack}_{ig,jg} + A^{extra}_{ig,jg} = A^{max}_{ig,jg} \quad \forall\ (ig, jg) \in \mathbf{MG} \tag{2.30}$$

where $\mathrm{A}^{\mathrm{ex}}{}_{e}$ is the area of the existing heat exchanger, $A^{slack}_{ig,jg}$ is a slack variable that takes the value 0 if no existing heat exchanger is used for the concerned match (i.e. $ex_{ig,jg,e} = 0$) and it can take any value up to $\mathrm{A}^{\mathrm{ex}}{}_{e}$ when the integer variable is 1 and $A^{extra}_{ig,jg}$ is the additional area required for the match. When an existing heat exchanger is used for the match and the required area is smaller than the area of the existing heat exchanger, $A^{slack}_{ig,jg}$ takes the value of the required area and $A^{extra}_{ig,jg}$ becomes 0. On the other hand, if the required area is larger than the area of the existing heat exchanger, the slack variable takes the value of $\mathrm{A}^{\mathrm{ex}}{}_{e}$ and $A^{extra}_{ig,jg}$ becomes equal to the difference between the required and existing areas.

The additional heat exchanger area is included in the system in two forms; as additional area to the existing heat exchangers if the connection is housed in an existing heat exchangers, or as a new heat

exchanger which is enforced by Equation 2.31.

$$A_{ig,jg}^{extra} = \sum_{e \in \mathbf{EX}} A_{ig,jg,e}^{add} + A_{ig,jg}^{nh} \quad \forall\ (ig, jg) \in \mathbf{MG} \tag{2.31}$$

where $A_{ig,jg,e}^{add}$ is area addition to the existing heat exchangers and $A_{ig,jg}^{nh}$ is the area of a new heat exchanger that must be purchased in case the connection is not housed in an existing heat exchanger. The area addition to the existing heat exchangers should be kept within practical limits. Equation 2.32 imposes an upper bound of 15% as suggested by [71].

$$A_{ig,jg,e}^{add} \leq ex_{ig,jg,e} \cdot \mathrm{A}^{\mathrm{ex}}{}_{e} \cdot 0.15 \quad \forall\ (ig, jg) \in \mathbf{MG}, e \in \mathbf{EX} \tag{2.32}$$

The area of a new heat exchanger $A_{ig,jg}^{nh}$ for a given connection $(ig, jg) \in \mathbf{MG}$ is dependent on the value of the binary variable $n_{ig,jg}$ associated with that match. Equation 2.33 ensures this relationship using the continuous and binary variables in the formulation.

$$n_{ig,jg} \cdot \mathrm{A}^{\mathrm{purc,lb}} \leq A_{ig,jg}^{nh} \cdot \leq n_{ig,jg} \cdot \mathrm{A}^{\mathrm{purc,ub}} \quad \forall\ (ig, jg) \in \mathbf{MG} \tag{2.33}$$

where $\mathrm{A}^{\mathrm{purc,lb}}$ and $\mathrm{A}^{\mathrm{purc,ub}}$ are the lower and upper bound of the heat exchanger area that can be purchased, respectively, and fixed to 1 m^2 and 2000 m^2.

2.4.9 Piece-wise linear heat exchanger cost calculation

The heat exchanger cost functions available in the literature are based on statistical data and have non-linear profiles. Since the proposed method is within an MILP framework, it uses a piece-wise linear approximation of a cost function [73]. The parameters of the cost function as well as the comparison of the linear approximation with the real profile are given in Appendix B.1. A new set is defined for the piece-wise linearisation of the cost function as follows:

- **AS**: The set of area segments. This set is used to create the piece-wise linear segments of the area - cost relationship.

If the purchased area of a new heat exchanger falls into a segment of the piece-wise profile, it must be within the boundaries of the segment. This is ensured by Equation 2.34.

$$a_{ig,jg,as} \cdot \mathrm{A}^{\mathrm{seg,lb}}{}_{ig,jg,as} \leq AL_{ig,j,as} \leq a_{ig,jg,as} \cdot \mathrm{A}^{\mathrm{seg,ub}}{}_{ig,jg,as} \quad \forall\ (ig, jg) \in \mathbf{MG}, s \in \mathbf{AS} \tag{2.34}$$

where $a_{ig,jg,as}$ is a binary variable that decides if the area $A^{new}_{ig,jg}$ is in the corresponding segment $as \in \mathbf{AS}$, and $AL_{ig,j,as}$ is a slack variable which takes the value of $A^{new}_{ig,jg}$ if the binary variable $a_{ig,jg,as}$ is 1, otherwise equals to 0. Equation 2.35 enforces equality between the slack variable $AL_{ig,jg,as}$ and $A^{new}_{ig,jg}$.

$$A^{new}_{ig,jg} = \sum_{as \in \mathbf{AS}} AL_{ig,jg,as} \quad \forall\ (ig, jg) \in \mathbf{MG} \tag{2.35}$$

The purchased area can fall only within one segment. Equation 2.36 ensures that the binary variable $a_{ig,jg,as}$ does not take the value 1 in multiple segments.

$$\sum_{as \in \mathbf{AS}} a_{ig,jg,as} \leq n_{ig,jg} \quad \forall\ (ig, jg) \in \mathbf{MG} \tag{2.36}$$

The cost of new heat exchangers is calculated based on binary and continuous variables using Equation 2.37.

$$C^{nh}_{ig,jg} = \sum_{as \in \mathbf{AS}} (a_{ig,jg,as} \cdot \mathrm{c}^{\,\mathrm{nh1}}{}_{as} + AL_{ig,jg,as} \cdot \mathrm{c}^{\,\mathrm{nh2}}{}_{as}) \quad \forall\ (ig, jg) \in \mathbf{MG} \tag{2.37}$$

where $C^{nh}_{ig,jg}$ is the cost of the new heat exchanger housing $(ig, jg) \in \mathbf{MG}$, $\mathrm{c}^{\,\mathrm{nh1}}{}_{as}$ and $\mathrm{c}^{\,\mathrm{nh2}}{}_{as}$ are fixed and variable cost parameters associated with the segment. The lower and upper bound, as well as fixed and variable cost of each segment are shown in Table 2.2.

Table 2.2 – Piece-wise heat exchanger - area linearisation parameters.

Segment	$\mathrm{A}^{\,\mathrm{seg,lb}}{}_{ig,jg,as}$	$\mathrm{A}^{\,\mathrm{seg,ub}}{}_{ig,jg,as}$	$\mathrm{c}^{\,\mathrm{nh1}}{}_{as}$	$\mathrm{c}^{\,\mathrm{nh2}}{}_{as}$
1	0	1	13000	1530
2	1	10	14530	555
3	10	50	19527	287
4	50	100	30990	197
5	100	500	40841	122
6	500	1000	89743	84
7	1000	2000	131765	65

2.4.10 Repiping cost

This work considers the plant layout by identifying the locations of the streams and of the heat exchangers in the initial network. The impact of the locations is taken into account in the calculation of repiping cost. Piping cost is often given as a discrete function, dependent on the pipe diameter (see Appendix B.2). For each stream group in the system, the heat loads corresponding to the standard diameters are calculated, given that the density (ρ), velocity (u) and specific enthalpy difference (Δh) of the fluid are known (see Equation 2.38), which results in a discrete relationship between heat load and specific piping cost.

$$\dot{q}_{sg} = \frac{\pi \cdot d^2 \cdot u_{sg} \cdot \rho_{sg} \cdot \Delta h_{sg}}{4} \quad \forall\ sg \in \mathbf{SG} \tag{2.38}$$

Since the streams have different thermodynamic properties, they require different sizes (i.e. pipe diameters) for the same heat load. For example, Table 2.3 depicts the heat load - piping cost relationship for a stream with a fluid density of 800 kg/m^3, flowing at a velocity of 1.8 m/s in the pipe with a specific enthalpy difference of 150 kJ/kg.

Table 2.3 – Piping cost for standard heat load.

Diameter [mm]	20	40	65	80	100	125
Heat load [kW]	68	271	717	1086	1696	2651
Specific cost [€/m]	96	166	250	312	387	480

Based on the discrete relationship between the heat load and the specific piping cost, the calculation of repiping cost is adapted in the MILP formulation with a set of constraints. The following additional set is used to govern the piping cost calculations.

- **PS**: The set of pipe sizes. This set is used to model the heat load - specific piping cost relationship.

The stream which needs to be repiped is selected depending on the connections. As the utility systems are more flexible, the utility stream is repiped for utility - process matches. However, since utility systems are typically well-distributed throughout the plants, it is assumed that additional utility piping is not required, regardless of their location in the plant. Conversely, for direct connections between processes, the stream that requires smaller piping diameter is repiped. Equations 2.39–2.41 list the constraints determining the piping size required when the hot stream is repiped for the connection $(ig, jg) \in \mathbf{MG}$.

$$p^{ph}_{ig,jg,ps} \cdot \dot{q}^{lb}_{ig,ps} \leq \dot{Q}P^{ph}_{ig,jg,ps} \leq p^{ph}_{ig,jg,ps} \cdot \dot{q}^{ub}_{ig,ps} \quad \forall\ (ig, jg) \in \mathbf{MG}, ps \in \mathbf{PS} \tag{2.39}$$

$$\sum_{ps \in \mathbf{PS}} \dot{Q}P^{ph}_{ig,jg,ps} = \dot{Q}^{max}_{ig,jg} \quad \forall\ (ig, jg) \in \mathbf{MG} \tag{2.40}$$

$$\sum_{ps \in \mathbf{PS}} p^{ph}_{ig,jg,ps} \leq y_{ig,jg} \quad \forall\ (ig, jg) \in \mathbf{MG} \tag{2.41}$$

where $p^{ph}_{ig,jg,ps}$ is a binary variable deciding which pipe size is used, $\dot{Q}P^{ph}_{ig,jg,ps}$ is a slack variable which takes the value of $\dot{Q}^{max}_{ig,jg}$ if the binary variable ($p^{ph}_{ig,jg,ps}$) is 1, and 0 otherwise. $\dot{\mathrm{q}}^{\mathrm{lb}}_{\mathrm{ig,ps}}$ and $\dot{\mathrm{q}}^{\mathrm{ub}}_{\mathrm{ig,ps}}$ are the lower and upper boundaries of the heat load that can be housed with the corresponding piping size. Equivalent constraints apply to the cold streams, expressed in Equations 2.42–2.44.

2

$$p^{pc}_{ig,jg,ps} \cdot \dot{\mathrm{q}}^{\mathrm{lb}}_{\mathrm{jg,ps}} \leq \dot{Q}P^{pc}_{ig,jg,ps} \leq p^{pc}_{ig,jg,ps} \cdot \dot{\mathrm{q}}^{\mathrm{ub}}_{\mathrm{j,ps}} \quad \forall\ (ig, jg) \in \mathbf{MG}, ps \in \mathbf{PS} \tag{2.42}$$

$$\sum_{ps \in \mathbf{PS}} \dot{Q}P^{pc}_{ig,jg,ps} = \dot{Q}^{max}_{ig,jg} \quad \forall\ (ig, jg) \in \mathbf{MG} \tag{2.43}$$

$$\sum_{ps \in \mathbf{PS}} p^{pc}_{ig,jg,ps} \leq y_{ig,jg} \quad \forall\ (ig, jg) \in \mathbf{MG} \tag{2.44}$$

The cost of piping is calculated based on the piping size, specific piping cost and length according to Equations 2.45 and 2.46.

$$C^{pipe}_{ig} = \sum_{ps \in \mathbf{PS}} p^{ph}_{ig,jg,ps} \cdot \mathrm{c}^{\,\mathrm{ps}} \cdot \mathrm{D}_{\mathrm{ig}} \quad \forall\ (ig, jg) \in \mathbf{MG} \tag{2.45}$$

$$C^{pipe}_{jg} = \sum_{ps \in \mathbf{PS}} p^{pc}_{ig,jg,ps} \cdot \mathrm{c}^{\,\mathrm{ps}} \cdot \mathrm{D}_{\mathrm{jg}} \quad \forall\ (ig, jg) \in \mathbf{MG} \tag{2.46}$$

where C^{pipe}_{ig} and C^{pipe}_{jg} are the hot and cold stream repiping cost, and D_{ig} and D_{jg} are the respective piping distances. Repiping is required only when the connection in the retrofitted network does not exist in the initial one. Thus, it is counted only for the connections that are in $\mathbf{R^3}$.

$$C^{rep}_{ig,jg} = C^{pipe}_{ig} + C^{pipe}_{jg} \quad \forall\ (ig, jg) \in \mathbf{R^3} \tag{2.47}$$

2.4.11 Other costs

The cost of moving heat exchangers and adding heat exchanger area to existing heat exchangers are calculated using simple cost functions. The cost of moving heat exchangers is associated mostly to freight within the plant and is independent of the size or location; this is calculated in Equation 2.48.

$$C^{move}_{ig,jg,e} = \mathrm{c}^{\,\mathrm{move}} \cdot ex_{ig,jg,e} \quad \forall\ (ig, jg, e) \in \mathbf{R^1} \tag{2.48}$$

where $C^{move}_{ig,jg,e}$ is the cost of moving heat exchanger $e \in \mathbf{EX}$ to the match $(ig, jg) \in \mathbf{MG}$ and $\mathrm{c}^{\,\mathrm{move}}$ is the unit cost of moving heat exchangers, which is assumed as 250€, according to [68]. Expanding the effective area of heat exchangers is possible with minor modifications and within practical limits, according to [71]. Therefore, Equation 2.49 is used to calculate the cost instead of the heat exchanger cost function presented previously.

$$C^{add}_{ig,jg} = \mathrm{c}^{\,\mathrm{add}} \cdot A^{add}_{ig,jg,e} \quad \forall\ (ig, jg, e) \in \mathbf{R^2} \tag{2.49}$$

where $C^{add}_{ig,jg,e}$ is the cost of adding area to the existing heat exchanger $e \in \mathbf{EX}$ and $\mathrm{c}^{\,\mathrm{add}}$ is the unit cost of adding area, assumed to be 250€/m^2, according to [58].

2.5 Case studies and utility systems

The case studies considered include a small-scale example from the literature and an industrial problem which shows the effectiveness of the proposed method in solving large problems.

2.5.1 Small scale case study

This example is taken from [65] and consists of three hot and cold streams as well as a hot and a cold utility. In the initial HEN, there are seven heat exchangers including one with the hot utility and one with the cold utility. Despite the fact that the system does not require a heating utility according to the MER solution, it currently consumes 360 kW of steam and 800 kW of cooling water, costing ~41000 €annually. Figure 2.6 illustrates the initial configuration of the HEN.

In the original problem, the locations of the initial heat exchangers and streams are not given, as the reference method does not consider this aspect. Since the locations play an important role in the method introduced in this paper, a location is assigned to each heat exchanger and stream in the reference case. Table 2.4 and Table 2.5 depict the properties and locations of the streams and heat exchangers of the case study, respectively.

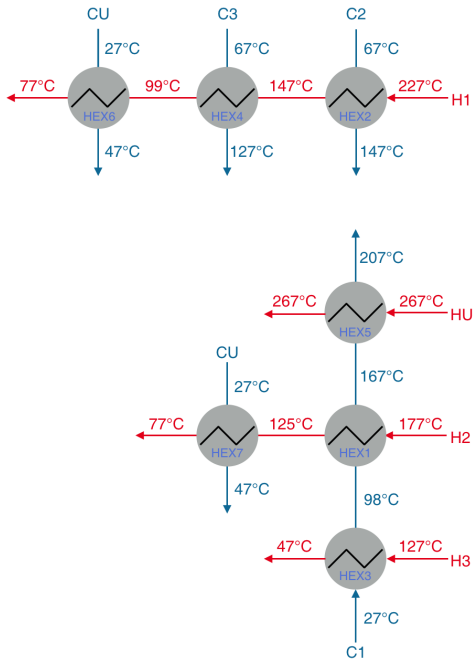

Figure 2.6 – Initial heat exchanger network of the small scale case study, adapted from [65].

Table 2.4 – Small scale case study streams.

Stream	T^{in}[°C]	T^{out}[°C]	$\dot{q}$[kW]	x[m]	y[m]	z[m]
H1	227	77	1500	12	18	0
H2	177	77	1200	23	22	0
H3	127	47	640	35	30	0
C1	27	207	1620	15	23	2
C2	67	147	480	39	14	4
C3	67	127	800	26	20	1
HU	267	267	100	0	0	0
CU	27	47	100	0	0	0

Table 2.5 – Small scale case study heat exchangers.

Heat exchanger	Area[m^2]	Hot stream	Cold stream	x[m]	y[m]	z[m]
HEX1	45.06	H2	C1	23	22	0
HEX2	12.50	H1	C2	12	18	0
HEX3	33.09	H3	C1	15	23	2
HEX4	23.50	H1	C3	12	18	0
HEX5	5.75	HU	C1	15	23	2
HEX6	5.39	H1	CU	12	18	0
HEX7	11.49	H2	CU	23	22	0

2.5.2 Industrial case

The industrial case study is adapted from Chapter 1. In the initial system, heating is provided by natural gas combustion in a boiler and distribution through a steam network, while cooling is supplied via cooling water heat exchangers and aero-coolers. Thus, there is no heat recovery between the process streams. Chapter 1 showed that a 23% reduction in heating requirement is possible by heat recovery among process streams and further operating cost reductions could be achieved by using the existing energy conversion technologies more effectively and integrating more efficient technologies, such as cogeneration engines and heat pumps. In addition to the heating and cooling requirements, an electricity requirement of 3091 kW is also considered in this case. Figure 2.7 illustrates the initial heat exchangers, hot and cold stream matches.

The locations of the heat exchangers and streams are modelled according to the real plant layout. Figure 2.8 depicts the coordinates of the initial heat exchangers, hot and cold process streams. More detailed data, including initial heat exchanger area is given in Appendix B.3.

As this case study is adapted from Chapter 1, the utility systems are the same as in Chapter 1, i.e. the potential integration of a cogeneration engine and two heat pumps operating at different temperature levels is considered to improve the energy efficiency of the system. Further details on existing and additional energy conversion technologies are given in Chapter 1.

2.6 Results and discussion

2.6.1 Retrofit of the small scale case

In the MER solution, the heating utility can be eliminated by recovering heat from process streams; however, this requires modifications in the HEN. Table 2.6 shows the stream matches, allocations of existing heat exchangers and the retrofit actions required in the retrofitted HEN. As opposed to

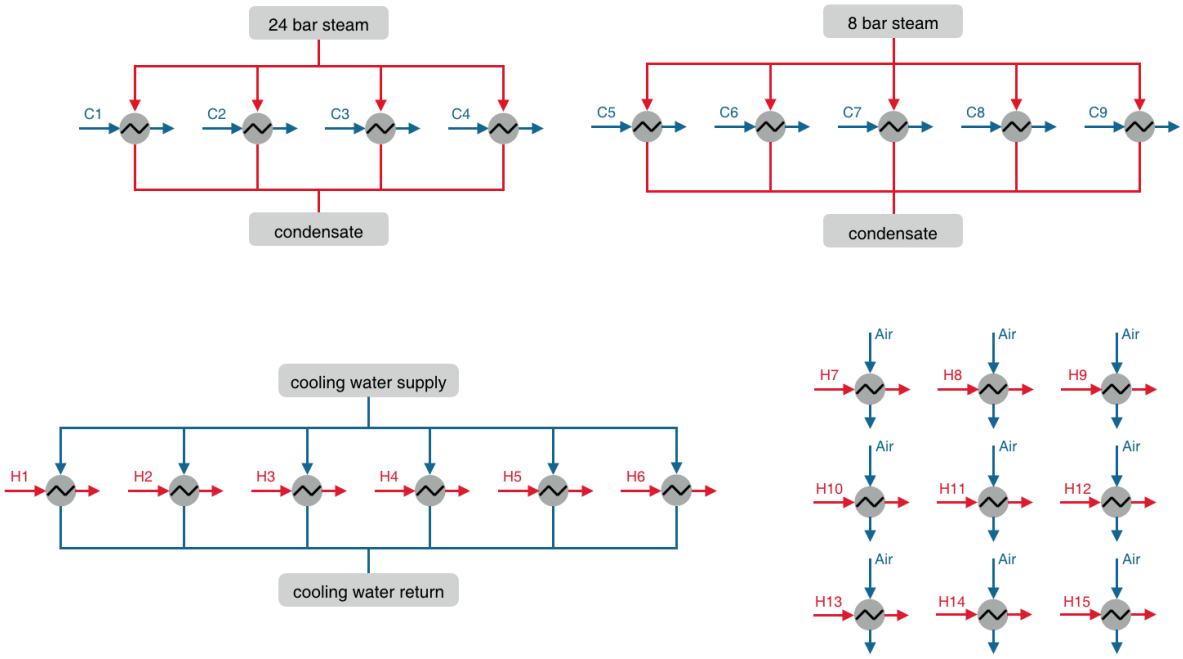

Figure 2.7 – Industrial case study streams and initial connections.

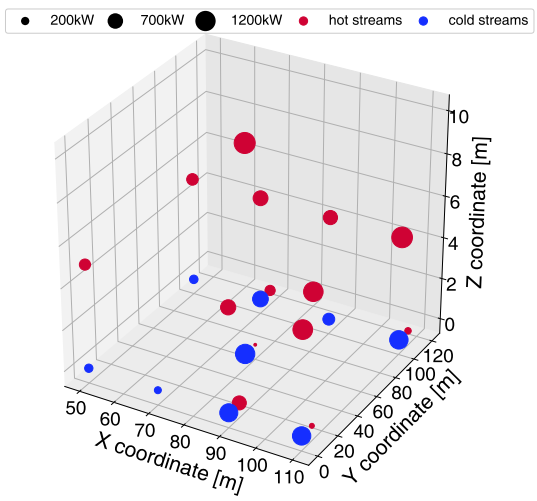

Figure 2.8 – Layout of the initial heat exchanger network in the industrial case study.

the initial network, the retrofitted network requires seven heat exchangers, with the additional heat exchanger housing the H2-C1 stream match. All heat exchangers in the initial network are either used for the same stream matches (i.e. HEX3, HEX6 and HEX7) or assigned to a different location in the plant (i.e. HEX2, HEX4 and HEX5). Additional area is required in HEX2, HEX5 and HEX7, since their heat loads in the retrofitted network are larger than the initial ones.

Table 2.6 – Small scale case study retrofit heat exchanger assignments.

Hot stream	Cold stream	Area[m^2]	Heat exchanger	Retrofit category
H1	C1	23.50	HEX4	R^3
H1	C2	34.44	HEX1	R^1
H1	C3	6.18	HEX5	R^1, R^2
H1	CU	4.45	HEX6	-
H2	C1	22.82	new	R^4
H2	C3	14.38	HEX2	R^1, R^2
H2	CU	12.46	HEX7	R^2
H3	C1	26.56	HEX3	-

Figure 2.9 compares the optimal solutions found for HEN retrofit using [65] and the method proposed in this chapter. The main difference between the two results is that the state-of-the-art method does not require adding a new heat exchanger, since area additions for the existing heat exchangers are unlimited. The previous method also shows that some heat exchangers are re-allocated to new stream matches with more than 100% area addition, while the proposed method limits the additional area to a more realistic value from of 15% as described by [71]. An economic comparison between the two methods is not conducted here, since additional terms are used in the objective function in this work to include the piping cost between locations; therefore, a direct comparison is not possible.

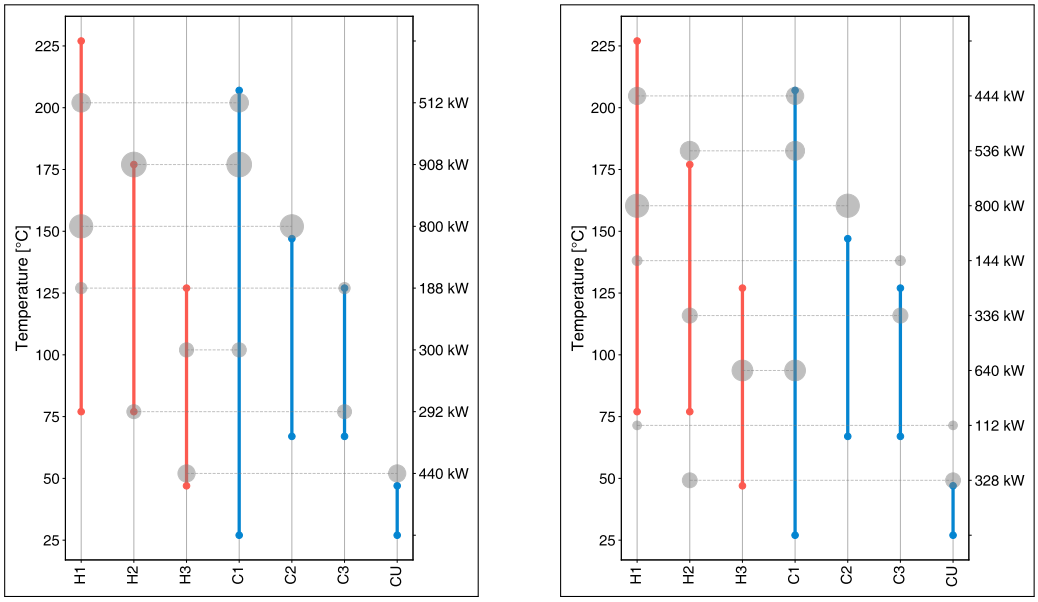

(a) Results from a state-of-the-art method [65]

(b) Results from the proposed method

Figure 2.9 – Heat load distribution for the small scale case study.

2.6.2 Retrofit of the industrial case

Parametric optimisation is carried out on the industrial case study, both at the EI and HLD level, to generate solutions with different utility system configurations and retrofit actions in the HEN. Figure 2.10 depicts the multi-criteria comparison of the generated results using parallel coordinates. The solutions are sorted with respect to their total cost (i.e. lower total cost is depicted by the blue end of the spectrum). Savings in total cost range from 5% - 13% using the existing energy conversion technologies, 15% - 17% when heat pumps are integrated, and 33% - 34% with the integration of the cogeneration engine. Compared to the results in Chapter 1, the solutions with cogeneration engine perform better than those with heat pumps (HPs), since the electricity requirement of the site is taken into account, making the cogeneration engine integration more beneficial. The contribution of operating cost in total cost is large; thus, although integrating new energy conversion systems requires investment in new technologies and modifications in the HEN, they result in lower total cost, due to drastic improvements in operating cost.

Focusing on the cost of the retrofit actions in the HEN reveals that adding heat exchangers and repiping are the major contributors, while the shares of adding area to existing heat exchangers and moving heat exchangers less significant. This can be attributed to the 15% additional area limitation and the low unit cost of moving heat exchangers. Solutions that require integrating new utilities necessitate more new heat exchangers and repiping. In terms of HEN retrofit, the most expensive solutions are those with HP integration, requiring 17 - 22 new heat exchangers. Heat pumps operate

at temperatures very close to the processes and therefore require large heat exchanger areas (i.e. due to low LMTDs). Since the heat exchangers from the initial network do not have sufficient area, new heat exchangers are purchased. The number of new heat exchangers required decreases in the solutions with cogeneration engines (i.e. 12 - 16 new heat exchangers) as they operate at higher temperatures. Even in the business-as-usual utility scenario, a minimum of six additional heat exchangers are required to recover heat between processes while using the existing technology configurations (e.g. different pressure levels).

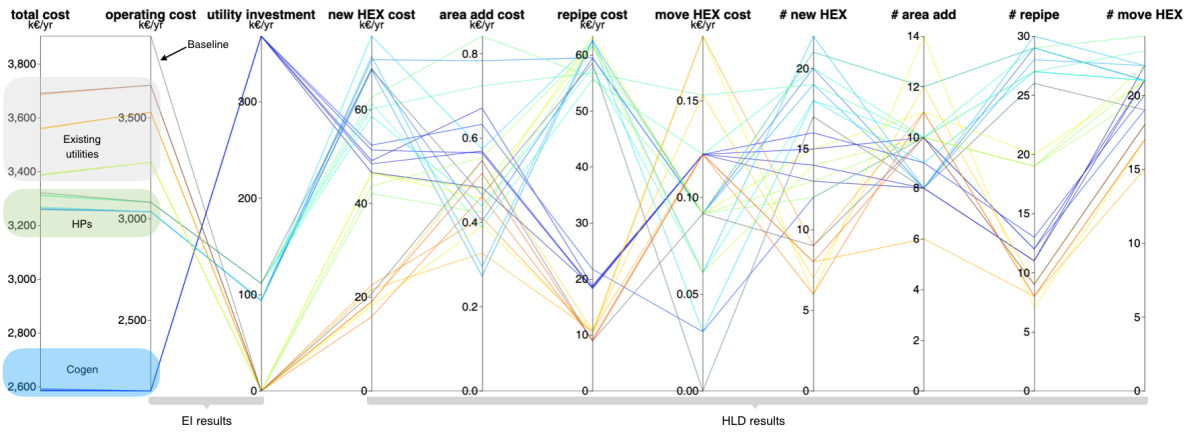

Figure 2.10 – Multiple solutions generated by parametric optimisation; higher total cost moving toward the red side of the colour spectrum.

Four solutions are selected in Figure 2.11 for detailed analysis. Solution 1 represents a case in which the existing energy technologies on the plant are used to deliver heat and electricity. In addition, steam is used at the current pressure levels; 24 bar and 8 bar. Solution 2 also uses the existing utilities; however, the steam network is operated more efficiently, using steam at lower pressure levels. Solutions 3 and 4 use HPs and a cogeneration engine to improve the onsite energy consumption.

Figure 2.12 compares the heat load distribution of the four solutions highlighted in Figure 2.11. Moreover, it illustrates the allocation of existing heat exchangers to the hot and cold stream matches in the optimal retrofit network found in each case. Even in the business-as-usual case (i.e. existing utilities and pressure levels) (Figure 2.12a), six new heat exchangers are required, as some of the existing heat exchangers are allocated for heat recovery between hot and cold process streams, e.g. HEX14 is placed between H1 and C7, with a heat load of 191 kW. The new heat exchangers have heat loads ranging from 20 kW to 390 kW. In Solution 2 (Figure 2.12b), as steam is used at lower pressure levels, higher heat exchanger areas are required for the same heat load; thus, the number of new heat exchangers increases. Compared to Solution 1, significant changes can be observed in the allocation of the heat exchangers. For example, while being used for the C5 - 8 bar steam stream couple, HEX8 is used for heat recovery between H14 and C3. Moreover, the heat load of the heat

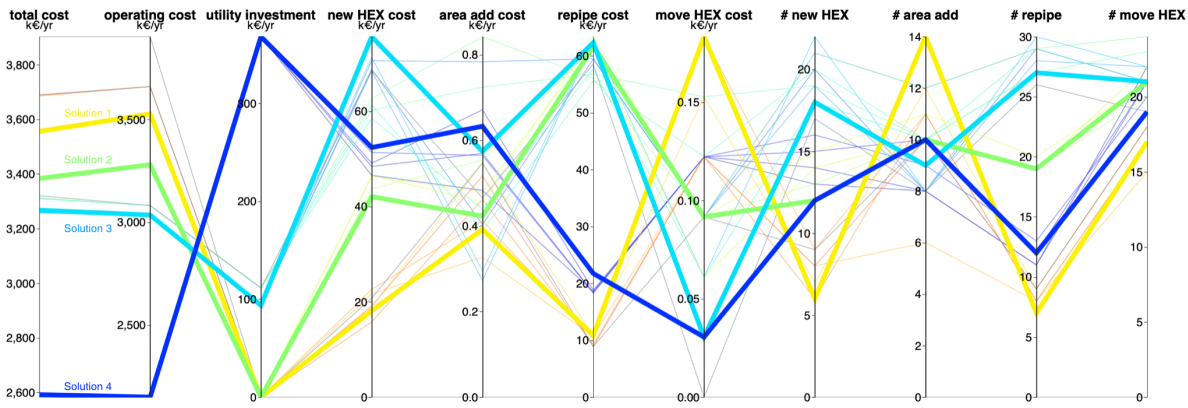

Figure 2.11 – Parallel coordinates with highlighted selected solutions.

2

exchanger decreases from 670 kW to 142 kW since the LMTD is reduced. The integration of heat pumps creates new pinch points in Solution 3 (Figure 2.12c); consequently, as heat should not be transferred across pinch points, the number of connections between the hot and cold streams in the zone of heat pump integration increases. Instead of large heat exchanges in the previous solutions, multiple smaller ones are used instead. For instance, while H12 is connected to air cooling with 910 kW in Solution 2, it exchanges 255 kW and 656 kW with HP evaporation and air cooling, respectively, in Solution 3. In Solution 4 (Figure 2.12d), the number of new heat exchangers decreases compared to Solution 3, as the cogeneration engine streams are at higher temperatures compared to the HP streams. Heat from the cogeneration engine is principally transferred to the process streams through direct exchange, for example C1 receives 980 kW from the cooling water stream of the engine. In addition, 255 kW from the exhaust gases is transferred to C7, though most of the exchange from the cogeneration engine flue gases is through the steam network, thus not illustrated on the heat load distribution diagram. In all solutions, there are exchanges that might not be practically feasible, such as that between hot process streams and boiler air preheating. Such exchanges emerge because EI targets maximum energy recovery; thus, below the process pinch point heating is provided only by heat recovery from the hot processes. To overcome issues related to impractical heat exchanges, the EI subproblem can be constrained so that the optimal solution does not always yield maximum heat recovery.

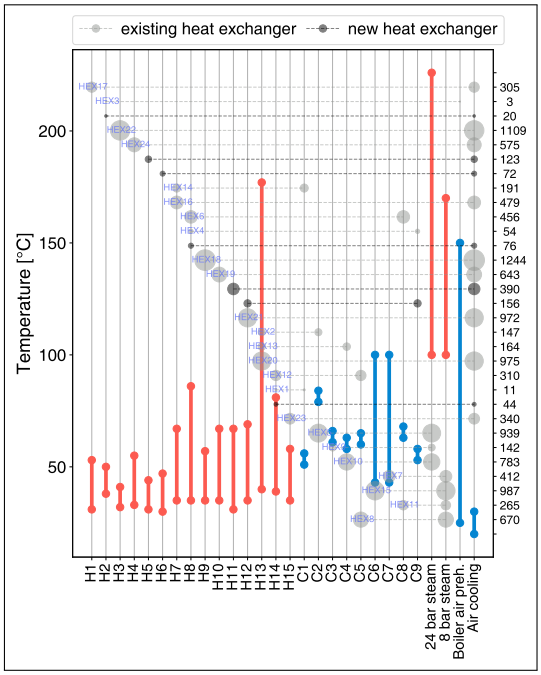

(a) Solution 1

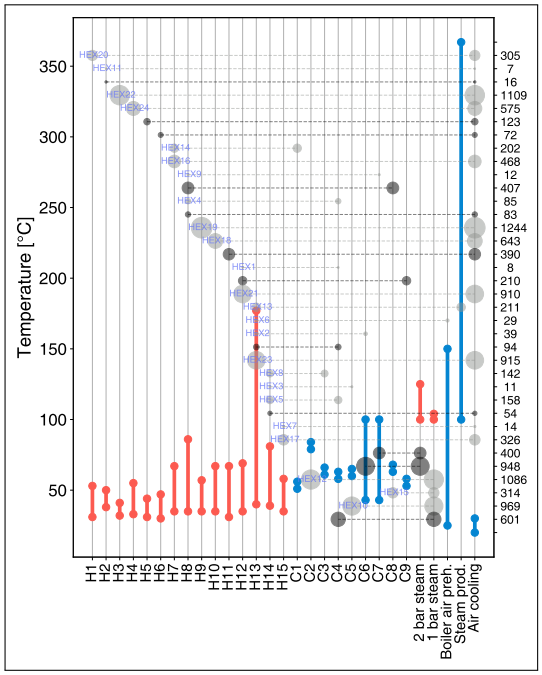

(b) Solution 2

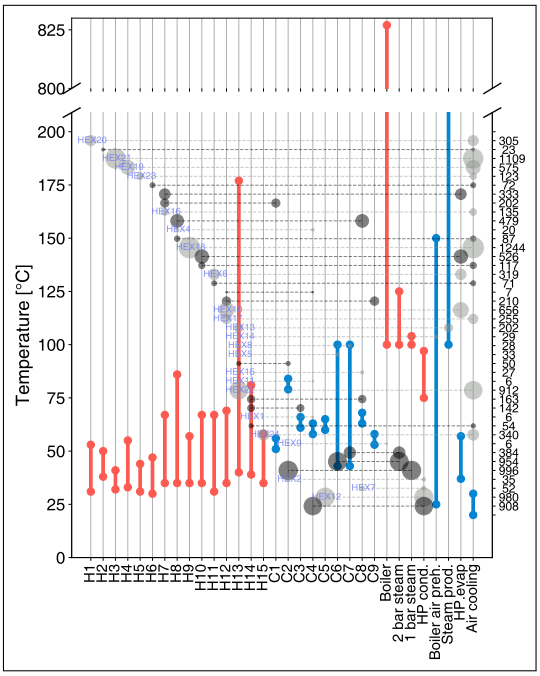

(c) Solution 3

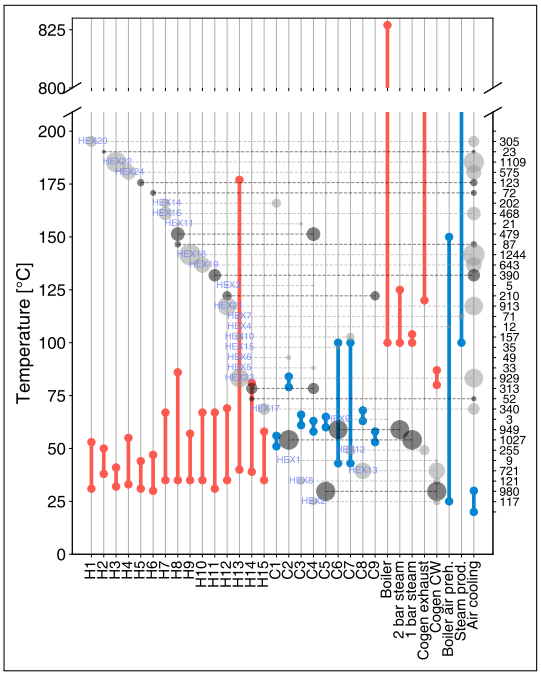

(d) Solution 4

Figure 2.12 – Heat load distribution diagrams of the selected solutions.

2.6.3 Comparison with the state of the art

The improvements in HLD retrofit proposed in this method are integrated in [65] in multiple steps, each representing a scenario to observe their impact in the solution. The specifications of the scenarios are listed below:

- Scenario 1: Using the formulation of [65];
- Scenario 2: Modifying the heat exchanger cost function using the piece-wise linearisation approach as described in Section 2.4.9;
- Scenario 3: Applying constraints on additional heat exchanger area as suggested in Section 2.4.8 in addition to using piece-wise linear heat exchanger cost functions;
- Scenario 4: Using the method proposed in this chapter. This scenario adds location-dependent piping cost in addition to the considerations included in Scenario 3.

Figure 2.13 compares the results of each scenario both in terms of HEN retrofit cost and number of required modifications. Using the piece-wise linear heat exchanger cost function results in a significant decrease in the number of new heat exchangers added in the system. However, the retrofit cost increases as the piece-wise cost function has higher fixed and variable investment cost parameters compared to what was used in [65]. Moreover, the cost of adding area to the existing heat exchangers increases drastically, since the area requirement of the system is satisfied using this approach instead of buying new heat exchangers. When the area additions are restricted in Scenario 3, fewer modifications in this category are suggested. As large area additions are disallowed, the contribution of this cost becomes insignificant. Conversely, although the number of additional heat exchangers does not change compared to Scenario 2, the associated cost associated increases due to purchasing heat exchangers with larger area. Finally, in Scenario 4 with the introduction of stream and heat exchanger locations and with piping cost dependent on topology, repiping requires a higher share in the total cost of HEN retrofit. As repiping modifications are more costly compared to Scenario 3, such actions are discouraged, which results in fewer repiping modifications. In Scenario 4, the total retrofit cost is dominated by the cost of additional heat exchangers and repiping. Comparing all scenarios, the additional features proposed in this chapter result in larger objective values related to the use of improved cost functions and accounting for topological elements. Conversely, fewer modifications are required by applying the suggested strategie,s which increases the likelihood of retrofit solutions to be acted on within industrial plants. Moreover, the solution time is improved as the added features aid in distinguishing solutions.

2.7 Conclusion

This chapter proposes a methodology for introducing the plant layout in retrofit problems and analyse its impact on the resulting solutions. The method proposed in this chapter follows the

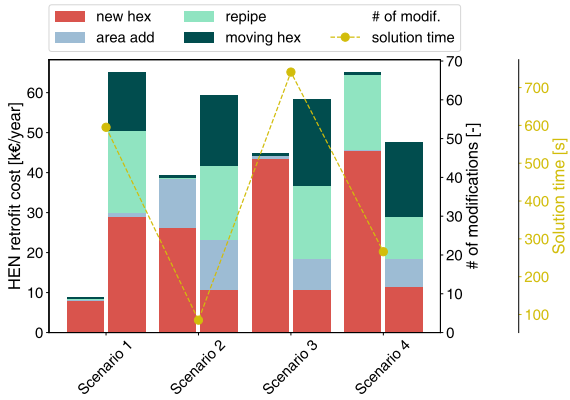

Figure 2.13 – Impact of the additional features of the proposed method.

sequential solution strategy for HEN retrofit and focuses specifically on HLD. The plant layout is defined by assigning coordinates to the streams and to the heat exchangers from the initial network. The formulation of Ciric and Floudas [65] is improved by integrating the impact of the stream locations, considering distance and diameter-dependent piping cost.

A small case study from the literature is used to compare the method with [65]. Although the proposed method results in a solution with an additional heat exchanger compared to the literature method, the results are more realistic, since the area addition to the existing heat exchangers is limited to 15%. A large industrial case from Chapter 1 is also studied, using parametric optimisation to systematically generate multiple results. The reduction in the total cost of the plant ranges from 5% to 34%, depending on the type and configuration of the energy conversion technologies used. As opposed to Chapter 1, the cogeneration engine integration results in a significantly better solution, since the electricity consumption of the site is considered. Heat pump integration led to the highest number of modifications in the HEN, as such solutions require more new heat exchangers and repiping. The cogeneration engine integration also requires a high number of additional heat exchangers; however, the reduction in operating cost compensates the required investment. The heat exchangers from the initial network are assigned to connections with lower heat loads in the retrofitted network, partially due to heat recovery matches with reduced LMTD and partially due to creation of new pinch points, which results from the integration of new energy conversion systems.

Each successive improvement in the existing formulations proposed in this work yields a larger HEN retrofit cost but a reduced number of modifications. This provides a crucial step for methods to provide solutions which include additional practical constraints, which could lead to improved acceptance of the solutions or fewer iterations between preliminary design and detailed design phases. More realistic solutions, provided with reduced computation time, may therefore yield higher success rates for implementation.

With the plant layout embedded in the formulation and limitation of additional area in the existing heat exchangers, the method proposed in this chapter results in more realistic solutions. It enables assessing the impact of utility integration in HEN retrofit; however, the method used to calculate LMTD completely relies on the area estimation approach proposed by Ahmad et al. [42], which might deviate from the real area requirement of the connections. Thus, the results of this work can be used as preliminary design decisions, but for calculating the real heat exchanger area requirements and designing the HEN, HEN synthesis methods should still be applied.

Retrofit considering inter-plant exchanges

Overview

- Introducing locations of the plants in process integration;
- Incorporating heat losses, temperature and pressure drop and piping cost in inter-plant heat and resource sharing;
- A novel MILP formulation for systematic generation of multiple optimal retrofit solutions considering different levels of investment in the infrastructure between industrial plants;
- A large scale industrial problem with cross-sectorial heat and resource sharing potential;
- Considering piping investment from a third party and optimisation taking into account the third party profitability.

The content of this chapter is published in [74, 75].

3

Process integration methods have proven to be effective tools in improving industrial sites while decreasing their resource and energy consumption; however, location aspects and their impact are generally overlooked. This chapter presents a method based on process integration, which considers the location of plants. The impact of the locations is included within the mixed integer linear programming framework in the form of heat losses, temperature and pressure drop, and piping cost. The objective function is selected as minimisation of the total cost of the system excluding piping cost and ϵ-constraints are applied on the piping cost to systematically generate multiple solutions. The method is applied to a case study with industrial plants from different sectors. First, the interaction between two plants and their utility integration are illustrated, depending on the piping cost limit which results in the heat pump and boiler on one site being gradually replaced by excess heat recovered from the other plant. Then, the optimisation of the whole system is carried out, as a large-scale application. At low piping cost allowances, heat is shared through high pressure steam in above-ground pipes, while at higher piping cost limits the system switches toward lower pressure steam sharing in underground pipes. Compared to the business-as-usual operation of the sites, the optimal solution obtained with the proposed method leads to 20% reduction in the overall cost of the system, including the piping cost. Further reduction in the cost is possible using a state

of the art method but the technical and economic feasibility is not guaranteed. Thus, the present work provides a tool to find optimal industrial symbiosis solutions under different investment limits on the infrastructure between plants.

3.1 Introduction

Waste heat in industry is often defined as heat discharged to environment from the cooling systems (e.g. cooling towers) as well as the energy conversion technologies (e.g. boilers) in the form of heat losses. However, according to Bendig et al. [76], this is classified as excess heat and waste heat is only the part which cannot be recovered within the process, by another process or by using an energy conversion system. This convention is used throughout this chapter.

According to [77], industrial excess heat accounts for 5-30% of the industrial energy consumption in different countries, averaging 22% in the EU which corresponds to 5-6% of the overall consumption. There are several options for valorisation of excess heat including direct heat recovery within a process, integration of energy conversion technologies (e.g. organic Rankine cycles) and heat recovery through other processes. Bendig et al. [76] suggested that a hierarchy is required between those options. Direct heat recovery is the most preferable since it typically requires the least investment and yields the largest improvement. Following this, remaining heat can be upgraded by heat pumps (HPs), transferred to another process or converted to another form, for example by using an organic Rankine cycle.

International energy agency (IEA) classifies excess heat potential into theoretical, technical and economic potential [78]. Theoretical potential corresponds to the thermodynamic potential without considering the technologies for heat recovery. Technical potential takes into account the availability of technologies for heat recovery. For example, although the steel industry has large heat losses at high temperatures, the technical potential is low since technologies to recover heat from solids are not well developed. Finally, economic potential, leading to the heat recovery options the industries would be willing to invest in, accounts for the cost of heat recovery. Thus, when energy efficiency improvement options are considered, it is crucial to assess the technical and economic feasibility.

This chapter, motivated by the high excess heat potential in industry and the importance of identifying economically feasible solutions, presents a novel methodology to determine heat and resource recovery within and between industrial processes. Instead of imposing a predefined hierarchy between the heat recovery options, the method introduces location aspects in process integration (PI) to obtain the optimal path for heat recovery under different investment cost limits on piping. Section 3.2 covers the methods available in the literature for improving industrial energy efficiency, Section 3.3 explains the method by going through the formulation in detail, Section 3.4 presents the case study that is used as a proof of concept, Section 3.5 discusses the results and Section 3.6 draws the conclusions of this work.

3.2 State of the art

Graphical methods in PI are based on pinch analysis (PA), which divide the system into hot (i.e. heat source) and cold streams (i.e. heat sink), aiming to maximise the heat exchange between them to minimise the hot and cold utility requirements. Although initially developed for direct heat exchange between the processes by Linnhoff and Hindmarsh [10], considering the potential problems of such exchanges because of plant layouts, PA was extended to total site analysis (TSA) which uses the utility systems for exchanging heat between the processes. The design of utility systems is crucial in TSA as they commonly include centralised supply of heat and power to several plants. Pirmohamadi et al. [79] studied the optimal design of cogeneration systems in total sites. The method was based on site utility grand composite curves and aimed at maximising the exergy efficiency of the overall system. Short-term and seasonal storage play an important role in inter-plant heat recovery in the case of multi-period problems. Liew et al. [80] extended the TSA methodology into seasonal total site heat storage cascade to model energy flows between sites and storage systems to determine the required storage size. Exchange between multiple plants brings about other challenges, such as process control and safety. Song et al. proposed a strategy to divide large-scale TSA problems into smaller sections to cope with these issues [81]. TSA was applied in each section to obtain the total inter-plant heat recovery. In inter-plant heat exchange, connections between plants can be in different configurations such as series, parallel or split. In their TSA-based method, Wang et al. [82] identified the excess heat of the plants and analysed inter-plant recovery using different connection patterns. The parallel pattern yielded higher heat recovery, while coming at a higher investment cost.

When the excess heat from plants is identified manually, it is critical to decide which streams participate in inter-plant transfer. A strategy to select such streams was presented by Song et al. [83]. They also introduced the concept of inter-plant shifted composite curves to maximise heat recovery using minimum heat capacity flowrate intermediate circuits. Hackl et al. [84] studied heat recovery in industrial clusters using TSA and intermediate fluids. The energy consumption of the cluster was reduced by introducing a hot water loop between plants. While TSA helps to identify the targets of energy requirements of multiple processes/plants, it brings about challenges in implementation due to the variety of plants/companies involved in the exchange. A method to overcome such challenges was developed by Hackl and Harvey [85]. In the first step of their method, TSA was used to find the total site targets, while in the second step the number of plants/companies involved in inter-plant heat integration was minimised and the investment required for the integration was split into periods. Industrial excess heat can also be valorised in district heating networks (DHNs) as well as other plants. Morandin et al. [86] considered a case with an industrial cluster and a DHN. They concluded that cluster-wide heat collection yields better integration with the DHNs than connecting each site individually. Although using TSA energy targets for several plants have been identified, most methods ignore the distance between them. Chew et al. [87] listed layout as one of the main

issues in implementing total site heat integration. They also recommended including piping cost for better analysis of inter-plant heat integration [84] and performing heat recovery through DHNs [86]. Liew et al. [88] added layout aspects in TSA by considering heat losses, temperature and pressure drop. First, the heat cascade was constructed using the problem table method of [10]. Afterwards, the corresponding heat losses, pressure and temperature drop were calculated and the streams in the problem table method were corrected accordingly. Finally, the heat cascade re-formulated with the new temperatures and heat loads.

Even though PA-based methods are effective in obtaining targets for total sites, when the number of plants and utility systems increase, they generally fail to obtain optimal solutions [82]. Mathematical programming (MP)-based methods emerged to fill this gap and now dominate the field. Most of the early work focused on utility integration [12] and heat load distribution [13]. As heat integration measures require modifications in the heat exchangers, heat exchanger network (HEN) synthesis was also included in some of the methods [15]. Despite the fact that inter-plant heat transfer directly with process streams is considered impractical in most studies, some methods available in the literature still considered it as an option. Zhang et al. [89] introduced a HEN optimisation method for hot direct discharges/feeds between plants. A larger heat recovery was achieved by using process streams directly instead of intermediate fluids; however, issues regarding the implementation of such exchanges were not addressed. Direct heat exchange between processes requires more piping than using an intermediate fluid and hence a higher piping investment cost. Wang et al. studied the heat integration of direct, indirect and combined methods of multiple plants [90]. They concluded that direct exchange is most beneficial method for short distances while combined methods are best for medium distances and indirect transfer should be used for long distances. However, the conclusion was case-dependent and could not be generalised.

The main focus in inter-plant heat integration is excess heat recovery between plants. Since different processes have different pinch temperatures, the excess heat of one plant can be useful for another one. Based on this phenomenon, Rodera and Bagajewicz developed a method for optimal integration of intermediate fluids in inter-plant heat transfer [91]. First, the targets for inter-plant exchange were identified using linear programming (LP) and source and sink plants were determined. Then, the optimal placement of the intermediate fluid circuit was identified using an mixed integer linear programming (MILP) formulation. Afterwards, the method was extended from two plants to n-plants [92]. When plants with similar pinch points are considered, recovering heat between them using an intermediate fluid might not be feasible. Building on previous work of [92], Bagajewicz and Barbaro developed a method which uses HPs to upgrade the temperature of the excess heat from one plant and use it elsewhere [93].

Stijepovic and Linke also worked on optimal heat recovery in industrial zones focusing on excess heat [94]. They identified the excess heat potential of the plants manually and calculated the maximum heat recovery potential using LP. Finally the optimal heat recovery network was found using an mixed

integer non-linear programming (MINLP) formulation. However, intra-plant process integration and improvements through more efficient energy conversion technologies were not included in the method. The layout constraints or location aspects were considered directly or indirectly in several methods. Kantor et al. [95] formulated the problem as a set of nodes and connections between them. The location aspects were included by adding the cost of resource transportation. Transportation methods were defined for each material sharing potential and an appropriate method for each was established as a result of the optimisation. Becker and Maréchal [96] proposed an MILP method to divide the system into smaller subsystems based on their locations. The subsystems were allowed to exchange heat only using heat transfer systems represented by intermediate fluids. This way, direct heat exchange over long distances was prevented. Pouransari and Maréchal [97] extended the previous problem to a heat load distribution (HLD) formulation. Implementation of sub-systems helped solving large-scale HLD problems, which are often computationally expensive. Bade and Bandyopadhyay [98] worked on a method to minimise the flow of a hot oil circuit between two plants. Although pumping and piping costs were not considered in the objective function, they were indirectly minimised by selecting the lowest possible hot oil flowrate.

HEN synthesis is a difficult problem to solve even for single plants [99]. When multiple plants and inter-plant heat integration are considered, it becomes even more challenging to obtain convergence. Song et al. combined the strengths of PA and MP in their work. In the first step, they divided the problem into smaller sections using an algorithm based on PA [100]. Then they carried out HEN synthesis of each section and finally optimised the inter-plant flows taking into account the pumping and piping costs [101]. Chang et al. [102] also proposed a method to simultaneously optimise the HEN and heat integration between plants. To simplify the problem, they considered a case with only two plants and using only a hot water loop to realise the heat exchange between them. The method was subsequently extended to more than two plants using different options (e.g. steam, hot oil) as intermediate fluids [103]. When a HEN is designed for more than one plant, it is important to determine the locations of the heat exchangers. Nair et al. [62] developed an MINLP method taking into account the locations of the heat exchangers in an eco-industrial park. They assumed that the temperature difference in the heat streams is linearly correlated to the travelled distance. They also considered piping and pumping costs and their trade-off with the operating cost benefits of heat recovery. Kachacha et al. [104] also considered the impact of plant location in the HEN problem by including piping and pumping costs. However, in order to keep the formulation linear, they made simplifying assumptions by using pre-calculated logarithmic mean temperature difference (LMTD) and pipe diameters. Laukkanen and Seppala [105] studied using nano-fluids in inter-plant HEN synthesis. They developed a method to optimise the HEN, taking into account the trade-off between enhanced heat transfer and increased pumping power requirement due to the addition of nano-particles in the heat transfer fluid. Liu et al. [106] combined the efforts in mass integration and HEN synthesis in their heat integrated water allocation network model. Although they considered piping requirements for the water streams, they ignored heat losses and pumping requirements for

transferring heat between the plants.

The literature of PI is rich in methods focused on inter-plant exchanges (see Table 3.1); however, graphical methods often neglect aspects related to plant layout. The most elaborate PA-based methods consider only heat integration using intermediate fluids and calculate heat losses and piping after integration. The MP methods address the location-based issues in inter-plant exchanges more extensively. However, most of the methods simplify the problem by considering the exchange only between two plants [102], identifying the excess heat manually [94] and optimising its valorisation instead of the overall system. Moreover, the integration of new utility systems was not a part of the optimisation [104], which might cause energy efficiency improvement opportunities to be missed. Another aspect overlooked in the literature is the type of the intermediate fluid which is used in inter-plant exchange. Methods have been specifically developed for heat sharing by steam [22], hot water [102] or hot oil [98]. Thus, the gaps in the literature are identified as:

1. not considering the simultaneous integration of energy conversion technologies and inter-plant heat and material exchange infrastructure,
2. only partially accounting for location aspects, and
3. case-specific methods and lack of generalised applicability.

The work presented in this chapter addresses such gaps by formulating the utility integration problem taking into account the location aspects. The method is generic and offers flexibility in integration of new technologies as well as infrastructure for inter-plant heat and material exchange and carries out their optimisation simultaneously.

Table 3.1 – Literature review on inter-plant exchanges.

Publication	Year	Method	Utility integration	Heat sharing	Resource sharing	Fluid	Pressure drop	Heat losses	Piping
Wang et al. [82]	2014	PA-based	✖	✔	✖	direct	✖	✖	✖
Song et al. [83]	2016	PA-based	✖	✔	✖	direct	✖	✖	✖
Hackl et al. [84]	2011	PA-based	✖	✔	✖	hot water	✖	✖	✖
Hackl and Harvey [85]	2015	PA-based	✖	✔	✖	hot water	✖	✖	✖
Liew et al. [88]	2014	PA-based	✔	✔	✖	steam	✔	✔	✔
Zhang et al. [89]	2016	MP-based	✖	✔	✖	direct	✖	✖	✖
Wang et al. [90]	2015	MP-based	✖	✔	✖	direct	✖	✖	✖
Rodera and Bagajewicz et al. [91]	1999	MP-based	✖	✔	✖	hot water	✖	✖	✖
Kantor et al. [95]	2015	MP-based	✔	✔	✔	various	✖	✖	✔
Becker and Maréchal [96]	2012	MP-based	✔	✔	✖	various	✖	✖	✖
Bade and Bandyopadhyay [98]	2014	MP-based	✖	✔	✖	hot oil	✖	✖	✔
Song et al. [101]	2017	MP-based	✖	✔	✖	steam	✔	✖	✔
Chang et al. [103]	2014	MP-based	✖	✔	✖	steam	✔	✖	✔
This thesis	2019	MP-based	✔	✔	✔	various	✔	✔	✔

3.3 Method

The method proposed in this work is a novel MILP formulation based on [25]. The unique aspect that this work introduces is the location of plants and distance between them to understand their impact on PI targets.

3.3.1 Definition of main sets

The basis of the method is modelling a system with mass and energy balances. The following mains sets are therefore defined:

- **TT**: The set of time steps to include the time-dependency of the system;
- **LC**: The set of plant locations in the optimisation problem;
- **U**: The set of units. Units are entities that represent an equipment (e.g. distillation column), a production unit, or an entire plant, depending on its boundaries;
- **S**: The set of streams. Streams represent flows of energy or materials;
- **H**: The set of heat streams $\mathbf{H} \subset \mathbf{S}$. This set is used to create hot and cold streams;
- **Z**: The set of resource streams $\mathbf{Z} \subset \mathbf{S}$. This set is used to model material flows (e.g. water, natural gas);
- **ES**: The set of electricity streams $\mathbf{ES} \subset \mathbf{S}$. This set is used to model the electricity flows;
- **L**: The set of layers. Resource streams are assigned to a member (i.e. layer) in this set where the material is specified;

The problem is defined as a system which has time-dependent behaviour, to be able to capture different operating modes of plants in different time steps ($t \in \mathbf{TT}$). The locations ($lc \in \mathbf{LC}$) divide the system into smaller subsystems, in which the mass and energy balances are closed. The locations can exchange heat and resources with each other using only selected streams (i.e. inter-location streams) while electricity flows freely in the system, without location restrictions. In each location, there can be one or more units ($u \in \mathbf{U}$) that are characterised by streams ($s \in \mathbf{S}$). Streams can represent heat deficit (e.g. cold streams), heat excess (e.g. hot streams), resource deficit/excess and electricity deficit/excess.

Figure 3.1 depicts an illustrative example summarising the method. When a heat stream is used within a location it is not subject to heat losses. Conversely, heat losses apply to use the heat in another location. Streams ($s \in \mathbf{S}$) which are used in a location different from their original one have a pressure drop associated to the transfer and a corresponding pumping requirement. The necessary infrastructure (i.e. piping) which must be installed to realise inter-location exchange is also considered in this work.

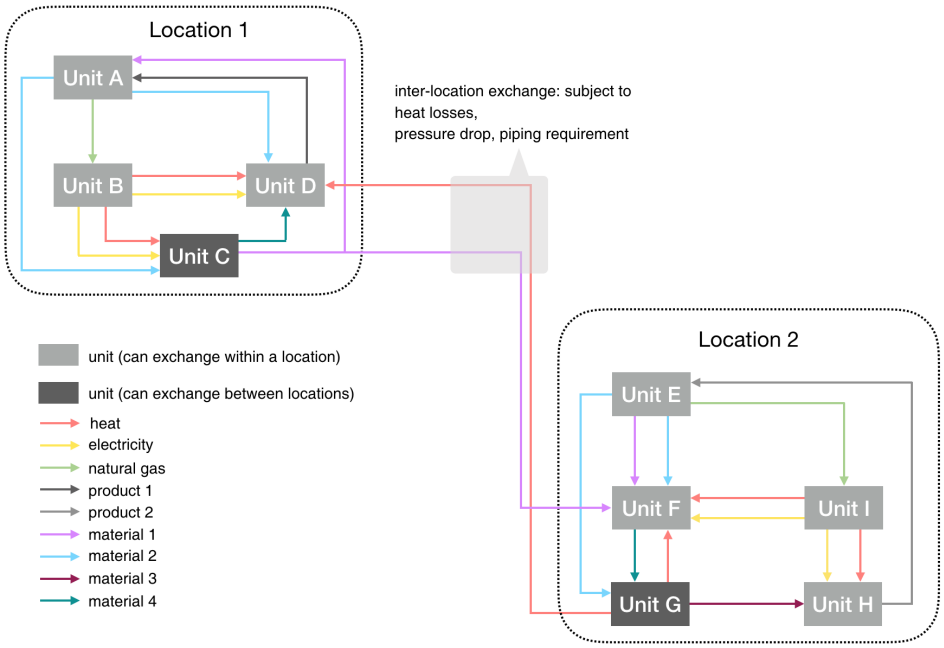

Figure 3.1 – Simple graphical representation of the method.

3.3.2 Objective function

Parametric optimisation is carried out with multiple objectives to generate and evaluate several scenarios. In MILP techniques used in PI, several objective functions are available in the literature. Economic objectives are the most applicable for this work, since the impact of distance can be monetised. Thus, the main objective (Equation 3.1) is selected as the overall cost of the system excluding the investment in pipes for inter-location connections. The piping cost is selected as the second objective and integrated in the MILP framework as an ϵ-constraint (see Equation 3.2).

$$\min \qquad C^{op} + C^{inv} \tag{3.1}$$

$$C^{pipe} \leq \epsilon \tag{3.2}$$

C^{op} represents the operating cost associated with the consumption of resources (Equation 3.3) while C^{inv} is the annual investment cost for integrating new energy conversion technologies (Equation 3.4) and C^{pipe} is the annualised investment cost for piping between locations.

$$C^{op} = \sum_{u \in \mathbf{U}} \left[\sum_{t \in \mathbf{TT}} \left(\mathrm{c}_u^{\mathrm{op1}} \cdot y'_{u,t} + \mathrm{c}_u^{\mathrm{op2}} \cdot f'_{u,t} \right) \cdot \Delta \mathrm{t}_t^{\mathrm{op}} \right] \tag{3.3}$$

$$C^{inv} = \left[\sum_{u \in \mathbf{U}} \left(\mathrm{c}_u^{\mathrm{inv1}} \cdot y_u + \mathrm{c}_u^{\mathrm{inv2}} \cdot f_u \right) \right] \cdot \mathrm{F}^{\mathrm{an}} \tag{3.4}$$

where $\mathrm{c}_u^{\mathrm{op1}}$ and $\mathrm{c}_u^{\mathrm{inv1}}$ are the fixed operating and investment costs of the units associated with their activation, $\mathrm{c}_u^{\mathrm{op2}}$ and $\mathrm{c}_u^{\mathrm{inv2}}$ are the variable operating and investment costs of the units which depend on their size, $\Delta \mathrm{t}_t^{\mathrm{op}}$ is the operating time and F^{an} is the annualisation factor based on interest rate and lifetime of the equipment.

3.3.3 Sizing and scheduling

Sizing and scheduling constraints determine if units are used in a certain time step (i.e. scheduling) as well as the purchased capacity and the utilised capacity in each (i.e. sizing). The units can be divided in two categories based on their behaviour: process units ($pu \in \mathbf{PU} \subset \mathbf{U}$) and utility units ($uu \in \mathbf{UU} \subset \mathbf{U}$). Process units have fixed size and scheduling and represent the production units on industrial plants. The sizing and scheduling constraints for the process units are defined in Equations 3.5–3.8.

$$f'_{u,t} = 1 \quad \forall\, u \in \mathbf{PU},\ t \in \mathbf{TT} \tag{3.5}$$

$$f_u = 1 \quad \forall\, u \in \mathbf{PU} \tag{3.6}$$

$$y'_{u,t} = 1 \quad \forall\, u \in \mathbf{PU},\ t \in \mathbf{TT} \tag{3.7}$$

$$y_u = 1 \quad \forall\, u \in \mathbf{PU} \tag{3.8}$$

where f_u and $f'_{u,t}$ are the overall sizing factor and the sizing factor at time step $t \in \mathbf{TT}$ and y_u and $y'_{u,t}$ are binary variables which decide if a unit is purchased and utilised in time step $t \in \mathbf{TT}$, respectively. Hence although decision variables are defined for process units, they are eliminated by fixing their values.

Utility units are, defined with a certain size (i.e. reference size) but can be used in smaller and larger sizes as they scale with the sizing factor (f) according to the requirements of the process units. The

equations governing the sizing and scheduling of utility units are Equations 3.9–3.12.

$$\mathrm{F}_u^{\min} \cdot y_u \leq f_u \leq \mathrm{F}_u^{\max} \cdot y_u \quad \forall\, u \in \mathbf{UU} \tag{3.9}$$

$$f'_{u,t} \leq f_u \quad \forall\, u \in \mathbf{UU},\ t \in \mathbf{TT} \tag{3.10}$$

$$\mathrm{F}_u^{\min} \cdot y'_{u,t} \leq f'_{u,t} \leq \mathrm{F}_u^{\max} \cdot y'_{u,t} \quad \forall\, u \in \mathbf{UU} \tag{3.11}$$

$$y'_{u,t} \leq y_u \quad \forall\, u \in \mathbf{UU},\ t \in \mathbf{TT} \tag{3.12}$$

where $\mathrm{F}_u^{\min}$ and $\mathrm{F}_u^{\max}$ are the lower and upper bounds of the sizing factor f_u respectively. More detail and explanations on the sizing and scheduling constraints can be found in [25].

3

3.3.4 Resource balance and links

The resource balance is closed for each layer in the overall system as well as in each location. Moreover, resource links are included to observe and limit the flow of resources between units. The following sets are defined for the resource balance constraints:

- $\mathbf{Z}_{u,ly}$: This set consists of resource streams on layer $ly \in \mathbf{L}$ in unit $u \in \mathbf{U}$;
- $\mathbf{U}_{ly}$: The set of units of layer. This set consists of the units which have at least one resource stream on layer $ly \in \mathbf{L}$;
- $\mathbf{U}_{lc}$: The set of units of location. This set comprises of the units in a given location $lc \in \mathbf{LC}$;
- $\mathbf{U}_{ly,lc}$: The set of units of layer and location. This set includes the units in location $lc \in \mathbf{LC}$, which have at least one resource stream on layer $ly \in \mathbf{L} \therefore \mathbf{U}_{ly} \cap \mathbf{U}_{lc}$;
- $\mathbf{OL}_{lc}$: The set of other locations. For a given location $lc \in \mathbf{LC}$ this set includes all the other locations in the system $\therefore o \in \mathbf{OL}_{lc} : o \neq lc$;
- $\mathbf{OL}_u$: The set of other locations of a unit. For a given unit $u \in \mathbf{U}$ this set contains all the locations except for the original location of the unit. It is specifically useful for units which can transfer flows to other locations;
- $\mathbf{RL}_{ly,u}$: The set of resource links of a unit. For a given layer $ly \in \mathbf{L}$ and a unit of that layer $u \in \mathbf{U}_{ly}$ this set consists of the other units on the same layer $\therefore i \in \mathbf{RL}_u : i \neq u$;

A unit can have several resource streams in the same layer; however, when the interactions of the units are considered, the flows in the same layer should be aggregated. This is enforced by

Equation 3.13.

$$\dot{\mathrm{m}}^{\mathrm{in}}_{ly,u,t} = \sum_{z \in \mathbf{Z}_{u,ly}} \dot{\mathrm{m}}^{\mathrm{in}}_{ly,z,t}, \quad \dot{\mathrm{m}}^{\mathrm{out}}_{ly,u,t} = \sum_{z \in \mathbf{Z}_{u,ly}} \dot{\mathrm{m}}^{\mathrm{out}}_{ly,z,t} \quad \forall\, ly \in \mathbf{L},\ u \in \mathbf{U}_{ly},\ t \in \mathbf{TT} \tag{3.13}$$

where $\dot{\mathrm{m}}^{\mathrm{in}}_{ly,u,t}$ and $\dot{\mathrm{m}}^{\mathrm{out}}_{ly,u,t}$ are the in/out reference flows of unit $u \in \mathbf{U}$ and $\dot{\mathrm{m}}^{\mathrm{in}}_{ly,z,t}$ and $\dot{\mathrm{m}}^{\mathrm{out}}_{ly,z,t}$ are the inlet and outlet reference resource stream flows, respectively. Since the unit sizes vary depending on the scaling factor (f), the flows should also be scaled with respect to their units (see Equation 3.14).

$$\dot{M}^{in}_{ly,u,t} = \dot{\mathrm{m}}^{\mathrm{in}}_{ly,u,t} \cdot f'_{u,t}, \quad \dot{M}^{out}_{ly,u,t} = \dot{\mathrm{m}}^{\mathrm{out}}_{ly,u,t} \cdot f'_{u,t} \quad \forall\, ly \in \mathbf{L},\ u \in \mathbf{U}_{ly},\ t \in \mathbf{TT} \tag{3.14}$$

where $\dot{M}^{in}_{ly,u,t}$ and $\dot{M}^{out}_{ly,u,t}$ are scaled flows into/out of the unit, respectively. The overall resource balance (see Equation 3.15) is included such that resource requirements of the units in the system are fulfilled by the other units.

3

$$\sum_{u \in \mathbf{U}_{ly}} \dot{M}^{in}_{ly,u,t} = \sum_{u \in \mathbf{U}_{ly}} \dot{M}^{out}_{ly,u,t} \quad \forall\, ly \in \mathbf{L},\ t \in \mathbf{TT} \tag{3.15}$$

The resource flow from each unit $\mathbf{U}_{ly}$ is transferred to the other units $i \in \mathbf{RL}_{ly,u}$ in the system via resource links. Similarly, the total resource flow into a unit is the sum of the flows from the units $j \in \mathbf{RL}_{ly,u}$ in the resource links. These two conditions are combined in a single constraint (Equation 3.16). The resource flow from a unit to the others is limited to its outflow. This constraint is imposed by Equation 3.17.

$$\dot{M}^{out}_{ly,u,t} + \sum_{i \in \mathbf{RL}_{ly,u}} \dot{M}^{rl}_{ly,i,u,t} = \dot{M}^{in}_{ly,u,t} + \sum_{j \in \mathbf{RL}_{ly,u}} \dot{M}^{rl}_{ly,u,j,t} \quad \forall\, ly \in \mathbf{L},\ u \in \mathbf{U}_{ly},\ t \in \mathbf{TT} \tag{3.16}$$

$$\sum_{j \in \mathbf{RL}_{ly,u}} \dot{M}^{rl}_{ly,u,j,t} \leq \dot{M}^{out}_{ly,u,t} \quad \forall\, ly \in \mathbf{L},\ u \in \mathbf{U}_{ly},\ t \in \mathbf{TT} \tag{3.17}$$

where $\dot{M}^{rl}_{ly,i,u,t}$ and $\dot{M}^{rl}_{ly,u,j,t}$ are positive continuous variables which represent the flows in layer $ly \in \mathbf{L}$ from unit $i \in \mathbf{RL}_u$ to $u \in \mathbf{U}_{ly}$ and from $u \in \mathbf{U}_{ly}$ to $j \in \mathbf{RL}_u$, respectively. Some units can exchange resources only within their origin location while others can have inter-location resource transfer. For units with inter-location resource exchange, a split factor is defined to determine the

magnitude of the resource flow transferred to the other locations as seen in Equation 3.18.

$$\sum_{i \in \mathbf{U}_{ly,o}} \dot{M}^{rl}_{ly,i,u,t} = \dot{\mathrm{m}}^{\mathrm{out}}_{ly,u,t} \cdot a_{ly,lc,o,u,t} \quad \forall\, ly \in \mathbf{L},\ lc \in \mathbf{LC},\ o \in \mathbf{OL}_{lc},\ u \in \mathbf{U}_{ly},\ t \in \mathbf{TT} \tag{3.18}$$

where $a_{ly,lc,o,u,t}$ is the split factor of the flow in layer $ly \in L$ in unit $u \in \mathbf{U}_{ly}$ from location $lc \in \mathbf{LC}$ to the other locations $o \in \mathbf{OL}_{lc}$. The resource balance is closed within locations as well as for the overall system. For a given location $lc \in \mathbf{LC}$ and layer $ly \in \mathbf{L}$, the supply flows are those from the units of that location $u \in \mathbf{U}_{ly,lc}$ and inter-location flows from the other locations. Similarly, the demand flows are those to the units of that location $u \in \mathbf{U}_{ly,lc}$ and the inter-location flows to the other locations. Equation 3.19 ensures that the supply flow in a location is equal to the demand.

$$\begin{aligned} &\sum_{o \in \mathbf{OL}_{lc}} \sum_{u \in \mathbf{U}_{ly,o}} \dot{\mathrm{m}}^{\mathrm{out}}_{ly,u,t} \cdot a_{ly,o,lc,u,t} + \sum_{u \in \mathbf{U}_{ly,lc}} \dot{M}^{out}_{ly,u,t} \\ &= \sum_{o \in \mathbf{OL}_{lc}} \sum_{u \in \mathbf{U}_{ly,o}} \dot{\mathrm{m}}^{\mathrm{out}}_{ly,u,t} \cdot a_{ly,lc,o,u,t} + \sum_{u \in \mathbf{U}_{ly,lc}} \dot{M}^{in}_{ly,u,t} \quad \forall\, ly \in \mathbf{L},\ lc \in \mathbf{LC},\ t \in \mathbf{TT} \end{aligned} \tag{3.19}$$

3

3.3.5 Distribution heat losses

Direct heat exchange between process streams has been considered as an option for heat recovery in several case studies [107]; however, its drawbacks have also been highlighted [22]. Especially when sharing heat over long distances, direct exchange between process streams becomes impractical. Therefore, distribution of heat between locations is carried out by using intermediate heat transfer media (e.g. hot water, steam, etc.).

Conceptually, heat streams that are allowed to exchange between locations are first duplicated and assigned to the other locations in the system. All duplicates as well as the stream itself are then assigned to a stream parent. Stream parents, although possessing no physical correspondence, are entities used to group the streams with their duplicates in different locations. There are two options for the heat streams that could be shared between different locations; to use them in their original location or to use their duplicate in other locations. These actions can be taken mutually; a stream can be used in its original location while its duplicate is used in another location. When the heat streams are used in the location of origin, it is assumed that heat losses do not occur, while heat losses and temperature drop apply for their duplicates in other locations. This is illustrated in Figure 3.2 considering heat distribution by steam and hot water as examples.

In order to transfer heat between locations, pipes should be installed. To transport the fluid in urban areas, underground pipes are preferable because of regulations, but in other settings, above-ground pipes could be a better option since they have lower investment cost. However, as ground acts

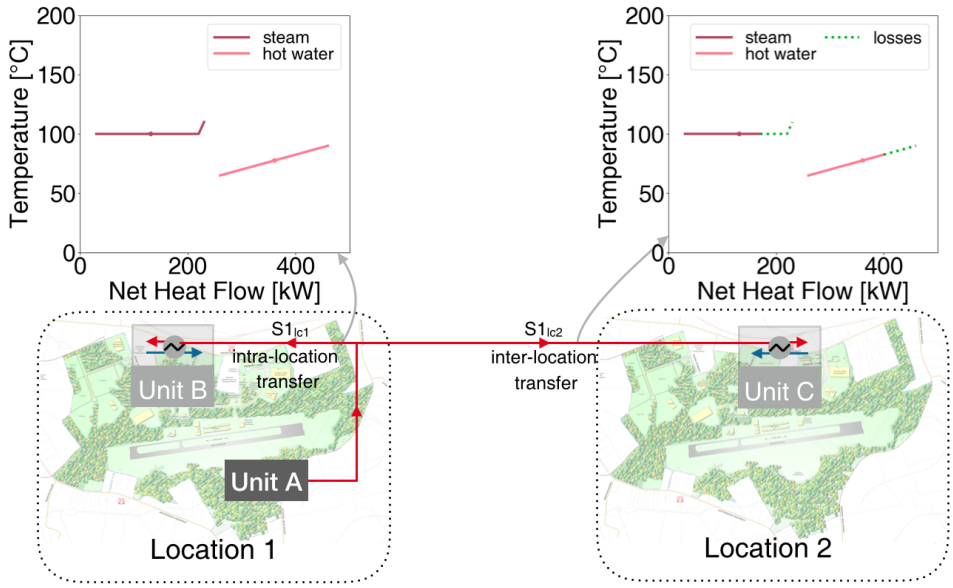

Figure 3.2 – Distribution heat losses and their impact on the temperature-enthalpy profile.

like an additional layer of insulation, heat losses in underground transfers are lower. Since both options are considered, another layer of decision is introduced in the problem, by creating duplicates of the streams for different transfer types (i.e. underground and above-ground). Heat losses in each transfer type are calculated following the methods explained in Sections 3.3.5.1 and 3.3.5.2. Considering the temperature drop associated with the heat losses, the temperature-heat profiles of the duplicate streams are reconstructed.

3.3.5.1 Above-ground heat losses

Heat losses in above-ground pipes occur because of heat transfer to ambient air. Assuming that the inner surface of the pipes is at the same temperature as the fluid flowing through them, the calculation of the heat losses can be simplified. The overall heat transfer coefficient and the surface area of the heat distribution pipes are calculated using Equations 3.20 and 3.21.

$$\frac{1}{\mathrm{V}_s} = \frac{1}{\mathrm{h}^{\,\mathrm{amb}}} + \frac{\mathrm{x}_s^{\mathrm{pipe}}}{\lambda_s^{\mathrm{pipe}}} + \frac{\mathrm{x}_s^{\mathrm{ins}}}{\lambda_s^{\mathrm{ins}}} \quad \forall\, s \in \mathbf{H} \tag{3.20}$$

$$\mathrm{A}_{s,lc,o}^{\mathrm{pipe}} = 2 \cdot \pi \cdot \mathrm{d}_s^{\mathrm{ins}} \cdot \mathrm{D}_{lc,o}^{\mathrm{pipe}} \quad \forall\, s \in \mathbf{H},\ lc \in \mathbf{LC},\ o \in \mathbf{OL}_{lc} \tag{3.21}$$

where V_s is overall heat transfer coefficient, $\mathrm{h}^{\,\mathrm{amb}}$ is the convective heat transfer coefficient of ambient air, $\lambda_s^{\mathrm{pipe}}$ and λ_s^{ins} are the conductive heat transfer coefficients of pipe and insulation,

x_s^{pipe} and x_s^{ins} are the thickness of the pipe and of the insulation material, $D_{lc,o}^{pipe}$, d_s^{ins}, and $A_{s,lc,o}^{pipe}$ are the length, insulated diameter and surface area of the pipe, respectively. The heat losses in the supply and return are then calculated using simple heat transfer equations (Equations 3.22 and 3.23) and the remaining heat content of the stream is obtained by subtracting the distribution losses (Equation 3.24).

$$\dot{q}_{s,lc,o,t}^{sup} = V_s \cdot A_{s,lc,o}^{pipe} \cdot \left(T_{s,t}^{in'} - T_t^{amb}\right) \quad \forall\, s \in \mathbf{H},\ lc \in \mathbf{LC},\ o \in \mathbf{OL}_{lc},\ t \in \mathbf{TT} \tag{3.22}$$

$$\dot{q}_{s,lc,o,t}^{ret} = V_s \cdot A_{s,lc,o}^{pipe} \cdot \left(T_{s,t}^{out'} - T_t^{amb}\right) \quad \forall\, s \in \mathbf{H},\ lc \in \mathbf{LC},\ o \in \mathbf{OL}_{lc},\ t \in \mathbf{TT} \tag{3.23}$$

$$\dot{q}_{s,t} = \dot{q}'_{s,t} - \dot{q}_{s,lc,o,t}^{sup} - \dot{q}_{s,lc,o,t}^{ret} \quad \forall\, s \in \mathbf{H},\ lc \in \mathbf{LC},\ o \in \mathbf{OL}_{lc},\ t \in \mathbf{TT} \tag{3.24}$$

where $\dot{q}_{s,lc,o,t}^{sup}$ and $\dot{q}_{s,lc,o,t}^{ret}$ are the heat losses at supply and return, $T_{s,t}^{in'}$ and $T_{s,t}^{out'}$ are the inlet and the exit temperatures of the stream prior to heat losses, $\dot{q}'_{s,t}$ and $\dot{q}_{s,t}$ are the heat content of the stream prior to and after the heat losses, and T_t^{amb} is the ambient temperature.

3

3.3.5.2 Underground heat losses

The heat loss calculations for heat distribution with underground pipes is adapted from [108]. To simplify the problem, convection at the surface of the ground is converted to an equivalent layer of soil and added to the depth by Equation 3.25.

$$x^{ground} = x^{ground'} + \frac{\lambda^{ground}}{h^{amb}} \tag{3.25}$$

where λ^{ground} is the conductive heat transfer coefficient of ground, $x^{ground'}$ is the real pipe depth and x^{ground} is the corrected pipe depth (i.e. thickness of soil). Heat losses also depend on the thermal resistance. In the case of heat distribution with double pipes (i.e. supply and return) the thermal resistance comes from the mutual interaction of the pipes, the ground, and the insulation material. These parameters are calculated according to Equations 3.26–3.28.

$$X_s^{mut} = \frac{1}{4 \cdot \pi \cdot \lambda^{ground}} \cdot \ln\left[1 + \left(\frac{2 \cdot x^{ground}}{D^{pp}}\right)^2\right] \quad \forall\, s \in \mathbf{H} \tag{3.26}$$

$$X_s^{ground} = \frac{1}{2 \cdot \pi \cdot \lambda^{ground}} \cdot \ln\left(\frac{4 \cdot x^{ground}}{d_s^{ins}}\right) \quad \forall\, s \in \mathbf{H} \tag{3.27}$$

$$X_s^{ins} = \frac{1}{2 \cdot \pi \cdot \lambda_s^{ins}} \cdot \ln\left(\frac{d_s^{ins}}{d_s^{pipe}}\right) \quad \forall\, s \in \mathbf{H} \tag{3.28}$$

where D^{pp} is the distance between the supply and return pipes, d_s^{pipe} is the diameter of the pipe excluding the insulation, and X_s^{mut}, X_s^{ground} and X_s^{ins} are the thermal resistances of the mutual interaction between the pipes, ground and insulation material, respectively. The heat loss coefficients $W_s^{'}$ and $W_s^{''}$ are then calculated using Equation 3.29.

$$W_s^{'} = \frac{X_s^{ground} + X_s^{ins}}{\left(X_s^{ground} + X_s^{ins}\right)^2 - X_s^{mut2}} \quad W_s^{''} = \frac{X_s^{mut} + X_s^{ins}}{\left(X_s^{ground} + X_s^{ins}\right)^2 - X_s^{mut2}} \quad \forall\, s \in \mathbf{H} \tag{3.29}$$

The heat losses at supply and return are calculated using Equations 3.30 and 3.31 and are subtracted from the heat load of the stream (see Equation 3.24).

3

$$\dot{q}_{s,lc,o,t}^{sup} = \left[\left(W_s^{'} - W_s^{''}\right) \cdot \left(T_{s,t}^{in} - T_t^{ground}\right) + W_s^{''} \cdot \left(T_{s,t}^{in} - T_{s,t}^{out}\right)\right] \cdot D_{lc,o}^{pipe} \tag{3.30}$$
$$\forall\, s \in \mathbf{H},\ lc \in \mathbf{LC},\ o \in \mathbf{OL}_{lc},\ t \in \mathbf{TT}$$

$$\dot{q}_{s,lc,o,t}^{ret} = \left[\left(W_s^{'} - W_s^{''}\right) \cdot \left(T_{s,t}^{out} - T_t^{amb}\right) - W_s^{''} \cdot \left(T_{s,t}^{in} - T_{s,t}^{out}\right)\right] \cdot D_{lc,o}^{pipe} \tag{3.31}$$
$$\forall\, s \in \mathbf{H},\ lc \in \mathbf{LC},\ o \in \mathbf{OL}_{lc},\ t \in \mathbf{TT}$$

3.3.5.3 Modified heat cascade

The heat cascade constraints close the heat balance and make sure that heat flows from higher to lower temperatures. In the state-of-the-art targeting formulation [25], the heat balance is closed for the overall system. However, in this work with the introduction of locations, it is closed for each location, including the streams that can exchange between locations. The heat cascade set and parameter definitions are listed as follows:

- $\mathbf{K}_{lc}$: The set of temperature intervals of a location. An interval represents the zone above a certain temperature level (T_k^{lb}). Thus, this set is formed of intervals created by unique temperatures in each location in ascending order;
- T_k^{lb}: Temperature level of the interval $k \in \mathbf{K}_{lc}$. This parameter sets the lower bound of the interval;
- $\mathbf{HS}_{lc}$: The set of hot streams in each location ($lc \in \mathbf{LC}$). It includes the streams that are originally in the location as well as the inter-location streams from the other locations;
- $\mathbf{CS}_{lc}$: The set of cold streams in each location ($lc \in \mathbf{LC}$). It includes the streams that are originally

in the location as well as the inter-location streams from the other locations;

- $\mathbf{HS}_{lc,k}$: The set of hot streams in each location ($lc \in \mathbf{LC}$) and temperature interval ($k \in \mathbf{K}$) $\therefore \mathbf{HS}_{lc,k} \in \mathbf{HS}_{lc}$. A hot stream $i \in \mathbf{HS}_{lc}$ is in a certain interval if its inlet temperature is higher than the temperature level of the interval $\therefore \mathrm{T}_{i,t}^{\mathrm{in}} \geq \mathrm{T}_{k}^{\mathrm{lb}}$
- $\mathbf{CS}_{lc,k}$: The set of cold streams in each location ($lc \in \mathbf{LC}$) and temperature intervals ($k \in \mathbf{K}$) $\therefore \mathbf{CS}_{lc,k} \in \mathbf{CS}_{lc}$. A cold stream $j \in \mathbf{CS}_{lc}$ is in a certain interval if its outlet temperature is higher than the temperature level of the interval $\therefore \mathrm{T}_{j,t}^{\mathrm{out}} \geq \mathrm{T}_{k}^{\mathrm{lb}}$
- $\mathbf{HI}$: The set of heat streams that are allowed to transfer heat between locations (i.e. inter-location streams) $\therefore \mathbf{HI} \subset \mathbf{H}$;
- $\mathbf{HI}_u$: The set of inter-location heat streams in unit $u \in \mathbf{U} \therefore \mathbf{HI}_u \subset \mathbf{HI}$
- $\mathbf{SP}$: The set of heat stream parents. When a stream is allowed to be used in different locations (i.e. $\therefore s \in \mathbf{HI}$), it is duplicated in other locations as explained in Section 3.3.5. Parents are used to assign a stream and its duplicates to the same entity;
- $\mathbf{SP}_u$: The set of stream parents of a unit $\therefore \mathbf{SP}_u \subset \mathbf{SP}$;
- $\mathbf{H}_u$: The set of heat streams of a unit $\therefore \mathbf{H}_u \subset \mathbf{H}$;
- $\mathbf{S}_p$: The set of streams of parents. Streams and their duplicates in other locations are aggregated in this set;
- $\mathbf{OL}_p$: Other locations of a parent. This set contains all the locations in the problem except for the original location of the parent;
- $\mathbf{TR}$: The set of transfer types. The elements of this set are predefined as 'under-ground' and 'above-ground' since those are the transfer types considered for heat streams;
- $\mathbf{S}_{sp,lc,tr}$: The set of streams of parents in each location and for each transfer type $\therefore \mathbf{S}_{sp,lc,tr} \subset \mathbf{HI}$;

In order to be able to calculate the heat loads of the streams in the temperature intervals, their heat capacities are calculated according to Equation 3.32.

$$\dot{\mathrm{m}}\mathrm{c}_{P\,s,t} = \frac{\dot{\mathrm{q}}_{s,t}}{|\mathrm{T}_{s,t}^{\mathrm{in}} - \mathrm{T}_{s,t}^{\mathrm{out}}|} \quad \forall\, s \in \mathbf{H},\ t \in \mathbf{TT} \tag{3.32}$$

where $\dot{\mathrm{q}}_{s,t}$ is the total reference heat load of the stream, $\mathrm{T}_{s,t}^{\mathrm{in}}$ is the inlet temperature, $\mathrm{T}_{s,t}^{\mathrm{out}}$ is the outlet temperature and $\dot{\mathrm{m}}\mathrm{c}_{P\,s,t}$ is the heat capacity. In each interval, heat either flows from hot streams to the cold streams or is transferred to other intervals in the form of residual heat. This is enforced by Equation 3.33.

$$\Big(\sum_{i \in \mathbf{HS}_{lc,k}} \dot{\mathrm{q}}_{i,k,t} \cdot s_{i,t}\Big) - \Big(\sum_{j \in \mathbf{CS}_{lc,k}} \dot{\mathrm{q}}_{j,k,t} \cdot s_{j,t}\Big) - \dot{R}_{lc,k,t} = 0 \quad \forall\, lc \in \mathbf{LC},\ k \in \mathbf{K}_{lc},\ t \in \mathbf{TT} \tag{3.33}$$

where $\dot{R}_{lc,k,t}$ is the continuous positive variable representing the residual heat in the interval, $\dot{\mathrm{q}}_{i,k,t}$

and $\dot{q}_{j,k,t}$ are the reference heat loads of hot and cold streams in interval k, respectively, and $s_{i,t}$ and $s_{j,t}$ are scaling factors of the hot and cold streams, respectively. The reference load of a stream in an interval is equal to its total reference load if it is fully in the interval (Equations 3.34 and 3.35). Otherwise the partial load of the stream in the interval is calculated (Equations 3.36 and 3.37).

$$\dot{q}_{i,k,t} = \dot{m}c_{P\,i,t} \cdot \left(T_{i,t}^{in} - T_{i,t}^{out}\right) \quad \forall\, i \in \mathbf{HS}_{lc,k},\ lc \in \mathbf{LC},\ k \in \mathbf{K}_{lc},\ t \in \mathbf{TT} \tag{3.34}$$

$$\dot{q}_{j,k,t} = \dot{m}c_{P\,j,t} \cdot \left(T_{j,t}^{out} - T_{j,t}^{in}\right) \quad \forall\, j \in \mathbf{CS}_{lc,k},\ lc \in \mathbf{LC},\ k \in \mathbf{K}_{lc},\ t \in \mathbf{TT} \tag{3.35}$$

$$\dot{q}_{i,k,t} = \dot{m}c_{P\,i,t} \cdot \left(T_{i,t}^{in} - T_{k}^{l}\right) \quad \forall\, i \in \mathbf{HS}_{lc,k},\ lc \in \mathbf{LC},\ k \in \mathbf{K}_{lc},\ t \in \mathbf{TT} \tag{3.36}$$

$$\dot{q}_{j,k,t} = \dot{m}c_{P\,j,t} \cdot \left(T_{j,t}^{out} - T_{k}^{l}\right) \quad \forall\, j \in \mathbf{CS}_{lc,k},\ lc \in \mathbf{LC},\ k \in \mathbf{K}_{lc},\ t \in \mathbf{TT} \tag{3.37}$$

3

Abiding by the first law of thermodynamics, since energy cannot be created or destroyed, residual heat at the top and bottom intervals are set to zero (Equation 3.38).

$$\dot{R}_{lc,k,t} = 0 \quad \forall\, lc \in \mathbf{LC}, t \in \mathbf{TT}, k = first(\mathbf{K}_{lc})\ or\ k = last(\mathbf{K}_{lc}) \tag{3.38}$$

The flow of a stream is scaled with its associated unit; hence, the scaling factor of a heat stream is equal to that of its unit (see Equation 3.39). However, this applies only to the streams which cannot exchange between locations.

$$f'_{u,t} = s_{s,t} \quad \forall\, u \in \mathbf{U},\ s \in \mathbf{H}_u,\ t \in \mathbf{TT}:\ s \notin \mathbf{HI} \tag{3.39}$$

For the inter-location streams, splitting is taken into account using stream parents ($sp \in \mathbf{SP}$). A parent of an inter-location stream can be used in its original location as well as other locations. In addition, it can be transferred between locations using different transfer types ($tr \in \mathbf{TR}$). The sum of all splitting factors of a parent is equal to the scaling factor of its unit. This is enforced by Equation 3.40.

$$f'_{u,t} = \sum_{lc \in \mathbf{LC}} \sum_{tr \in \mathbf{TR}} b_{sp,t,lc,tr} \quad \forall\, u \in \mathbf{U},\ sp \in \mathbf{SP}_u,\ t \in \mathbf{TT} \tag{3.40}$$

where $b_{sp,t,lc,tr}$ is the splitting factor of parents in each location, time and for different transfer types. Similar to the relationship between units and streams, the streams of a parent scale together with the parent (Equation 3.41).

$$s_{s,t} = b_{sp,t,lc,tr} \quad \forall\, sp \in \mathbf{SP},\ t \in \mathbf{TT},\ lc \in \mathbf{LC},\ tr \in \mathbf{TR},\ s \in \mathbf{S}_{sp,lc,tr} \tag{3.41}$$

3.3.6 Distribution pump work

Heat and resource flows between locations are subject to pressure drop, which must be compensated by pumping. The pumping power requirement for inter-location exchange is considered by including additional electricity demand in the problem. The friction factor must be calculated first to estimate the pressure drop. Instead of the generic Colebrook equation, an explicit approximation by Haaland [109] is used in this work (see Equation 3.42) as suggested by [110]. The Reynolds number is calculated using stream properties and pipe geometry, according to Equation 3.43.

$$\mathrm{ff}_{s,t} = \left\{ -1.8 \cdot \log_{10} \left[\left(\frac{\varepsilon_s}{3.7} \right)^{1.11} + \frac{6.9}{\mathrm{Re}_{s,t}} \right] \right\}^{-2} \quad \forall\, s \in \mathbf{S},\ t \in \mathbf{TT} \tag{3.42}$$

$$\mathrm{Re}_{s,t} = \frac{\mathrm{u}_s \cdot \mathrm{d}_s}{\nu_{s,t}} \quad \forall\, s \in \mathbf{S},\ t \in \mathbf{TT} \tag{3.43}$$

where $\nu_{s,t}$ is the kinematic viscosity, u_s is the velocity, $\mathrm{Re}_{s,t}$ is the Reynold's number, ε_s is the pipe roughness and $\mathrm{ff}_{s,t}$ is the friction factor. The pressure drop is then calculated using the Darcy-Weisbach equation, Equation 3.44.

$$\Delta \mathrm{P}_{s,t,lc,o} = \mathrm{ff}_{s,t} \cdot \left(\frac{\mathrm{D}_{lc,o}^{\mathrm{pipe}}}{\mathrm{d}_s^{\mathrm{pipe}}} \right) \cdot \left(\frac{\rho_{s,t}}{2} \right) \cdot \mathrm{u}_{s,t}{}^2 \quad \forall\, s \in \mathbf{S},\ t \in \mathbf{TT},\ lc \in \mathbf{LC},\ o \in \mathbf{OL}_{lc} \tag{3.44}$$

where $\rho_{s,t}$ represents the density and $\Delta \mathrm{P}_{s,t,lc,o}$ the pressure drop. Ignoring the mechanical inefficiencies of pumps, the required electricity to drive them is calculated by Equation 3.45.

$$\dot{\mathrm{e}}_{s,t,lc,o}^{\mathrm{pm}} = \Delta \mathrm{P}_{s,t,lc,o} \cdot \mathrm{u}_{s,t} \cdot \frac{\pi \cdot \mathrm{d}_s^{\mathrm{pipe}^2}}{4} \quad \forall\, s \in \mathbf{S},\ t \in \mathbf{TT},\ lc \in \mathbf{LC},\ o \in \mathbf{OL}_{lc} \tag{3.45}$$

where $\dot{\mathrm{e}}_{s,t,lc,o}^{\mathrm{pm}}$ is the reference pumping electricity requirements for the transfer of a stream between two locations. Resource streams require a transfer in only one direction since they are consumed at

the target location. On the other hand, heat streams require bi-directional transfer because they have supply and return pipes. Thus, for heat streams, the pumping requirement is the sum of the electricity required in the supply and return pipes (see Equation 3.46).

$$\dot{e}^{\text{pm}}_{s,t,lc,o} = \dot{e}^{\text{sup}}_{s,t,lc,o} + \dot{e}^{\text{ret}}_{s,t,lc,o} \quad \forall\, s \in \mathbf{H},\ t \in \mathbf{TT},\ lc \in \mathbf{LC},\ o \in \mathbf{OL}_{lc} \tag{3.46}$$

where $\dot{e}^{\text{sup}}_{s,t,lc,o}$ and $\dot{e}^{\text{ret}}_{s,t,lc,o}$ are the reference pumping power requirement at the supply and return respectively. It should be noted that the parameter $\dot{e}^{\text{pm}}_{s,t,lc,o}$ corresponds to a certain flow (e.g. reference flow). Hence, the pumping requirement of a flow scales with it. This is carried out for the resource (Equation 3.47) and heat (Equation 3.48) streams in two separate equations since different scaling factors are defined for different types of streams.

$$\dot{E}^{pm}_{s,t,o} = \dot{e}^{\text{pm}}_{s,t,lc,o} \cdot a_{ly,lc,o,u,t} \quad \forall\, ly \in \mathbf{L},\ u \in \mathbf{U}_{lc},\ t \in \mathbf{TT},\ lc \in \mathbf{LC},\ o \in \mathbf{OL}_{lc}, s \in \mathbf{Z}_{u,ly} \tag{3.47}$$

3

$$\dot{E}^{pm}_{s,t,o} = \dot{e}^{\text{pm}}_{s,t,lc,o} \cdot b_{sp,t,o,tr} \quad \forall\, sp \in \mathbf{SP},\ t \in \mathbf{TT},\ lc \in \mathbf{LC},\ o \in \mathbf{OL}_{lc},\ s \in \mathbf{S}_{sp,lc,tr} \tag{3.48}$$

where $\dot{E}^{pm}_{s,t,o}$ is the pumping electricity requirement

3.3.7 Electricity balance

Contrary to resource and heat streams, location restrictions do not apply to the electricity streams since the losses and infrastructure investment in the transfer of electricity are negligible compared to the others. To define the electricity balance, the following set is defined:

- $\mathbf{ES}_u$: This set consists of electricity streams in unit $u \in \mathbf{U}$;

Similar to resource streams, there might be several electricity streams in a unit. The reference flows of electricity in and out of a unit are calculated as the sum its electricity streams by Equation 3.49.

$$\dot{e}^{\text{in}}_{u,t} = \sum_{es \in \mathbf{ES}_u} \dot{e}^{\text{in}}_{es,t}, \quad \dot{e}^{\text{out}}_{u,t} = \sum_{es \in \mathbf{ES}_u} \dot{e}^{\text{out}}_{es,t} \quad \forall\, u \in \mathbf{U},\ t \in \mathbf{TT} \tag{3.49}$$

where $\dot{e}^{\text{in}}_{u,t}$ is the reference inflow and $\dot{e}^{\text{out}}_{u,t}$ is the reference outflow of electricity of unit $u \in \mathbf{U}$. The electricity flows of a unit, like other flows, scale with the unit itself. To obtain the real electricity generation/demand of a unit, the scaling factor is taken into account in Equations 3.50 and 3.51. In addition to the electricity streams, the demand of a unit includes the electricity for pumping

resources and heat to other locations which is included in Equation 3.51.

$$\dot{E}^{out}_{u,t} = \dot{\mathrm{e}}^{\mathrm{out}}_{u,t} \cdot f'_{u,t} \quad \forall\, u \in \mathbf{U},\ t \in \mathbf{TT} \tag{3.50}$$

$$\dot{E}^{in}_{u,t} = \dot{\mathrm{e}}^{\mathrm{in}}_{u,t} \cdot f'_{u,t} + \Big(\sum_{o \in \mathbf{OL}_{lc}} \sum_{s \in \mathbf{HI}_u} \dot{E}^{pm}_{s,t,o} \Big) + \Big(\sum_{o \in \mathbf{OL}_{lc}} \sum_{ly \in \mathbf{L}} \sum_{s \in \mathbf{Z}_{u,ly}} \dot{E}^{pm}_{s,t,o} \Big) \quad \forall\, lc \in \mathbf{LC},\ u \in \mathbf{U}_{lc},\ t \in \mathbf{TT} \tag{3.51}$$

where $\dot{E}^{out}_{u,t}$ and $\dot{E}^{in}_{u,t}$ are positive continuous variables representing the electricity supply and demand of the units, respectively. Finally, electricity demand of the units in the system is satisfied by the other units, which is imposed by Equation 3.52

$$\sum_{u \in \mathbf{U}} \dot{E}^{in}_{u,t} = \sum_{u \in \mathbf{U}} \dot{E}^{out}_{u,t} \quad \forall\, t \in \mathbf{TT} \tag{3.52}$$

3

3.3.8 Distribution piping cost

To realise heat and resource sharing between locations, the necessary infrastructure (i.e. pipeline) must be installed. Neglecting the investment for piping would result in unrealistically optimistic scenarios; therefore, this work includes the piping cost in the formulation. In multi-time problems, the flow of heat and resources between locations might vary in different time steps. The installed pipes must be capable of handling the flows at any time step; hence, the sizing of the pipes is carried out with respect to the maximum flow over all time steps (see Equations 3.53 and 3.54).

$$\dot{Q}^{max}_{sp,o,tr} = \max(\dot{\mathrm{q}}_{s,t} \cdot b_{sp,t,o,tr}) \quad \forall\, sp \in \mathbf{SP}, t \in \mathbf{TT}, s \in \mathbf{S}_p, o \in \mathbf{OL}_p, tr \in \mathbf{TR}_p \tag{3.53}$$

$$\dot{M}^{max}_{ly,o,u} = \max(\dot{\mathrm{m}}^{\mathrm{out}}_{ly,u,t} \cdot a_{ly,lc,o,u,t}) \quad \forall\, ly \in \mathbf{L},\ lc \in \mathbf{LC},\ o \in \mathbf{OL}_{lc},\ u \in \mathbf{U}_{ly},\ t \in \mathbf{TT} \tag{3.54}$$

The max function is non-linear but can be converted to a set of linear constraints by introducing new continuous and binary variables. Linearisation of $\dot{Q}^{max}_{sp,o,tr}$ is shown in Equations 3.55–3.60. A similar procedure is applied to linearise $\dot{M}^{max}_{ly,o,u}$, but the equations are not included here.

$$\dot{\mathrm{q}}_{s,t} \cdot b_{sp,t,o,tr} \leq \dot{Q}^{max}_{sp,o,tr} \quad \forall\, sp \in \mathbf{SP},\ t \in \mathbf{TT},\ s \in \mathbf{S}_p,\ o \in \mathbf{OL}_p,\ tr \in \mathbf{TR} \tag{3.55}$$

$$\dot{G}_{sp,t,o,tr} \leq \dot{\mathrm{q}}_{s,t} \cdot b_{sp,t,o,tr} \quad \forall\, sp \in \mathbf{SP},\ t \in \mathbf{TT},\ s \in \mathbf{S}_p,\ o \in \mathbf{OL}_p,\ tr \in \mathbf{TR} \tag{3.56}$$

$$\dot{\mathrm{q}}_{s,t} \cdot b_{sp,t,o,tr} - \left(1 - w_{sp,t,o,tr}\right) \cdot \mathrm{bigM} \leq \dot{G}_{sp,t,o,tr} \quad \forall\, sp \in \mathbf{SP},\ t \in \mathbf{TT},\ s \in \mathbf{S}_p,\ o \in \mathbf{OL}_p,\ tr \in \mathbf{TR} \tag{3.57}$$

$$\dot{Q}^{max}_{sp,o,tr} \leq \dot{G}_{sp,t,o,tr} + \left(1 - w_{sp,t,o,tr}\right) \cdot \mathrm{bigM} \quad \forall\, sp \in \mathbf{SP},\ t \in \mathbf{TT},\ o \in \mathbf{OL}_p,\ tr \in \mathbf{TR} \tag{3.58}$$

$$\dot{G}_{sp,t,o,tr} \leq w_{sp,t,o,tr} \cdot \mathrm{bigM} \quad \forall\, sp \in \mathbf{SP},\ t \in \mathbf{TT},\ o \in \mathbf{OL}_p,\ tr \in \mathbf{TR} \tag{3.59}$$

$$\sum_{t \in \mathbf{TT}} w_{sp,t,o,tr} = 1 \quad \forall\, sp \in \mathbf{SP},\ t \in \mathbf{TT},\ o \in \mathbf{OL}_p,\ tr \in \mathbf{TR} \tag{3.60}$$

3

where $\dot{Q}^{max}_{sp,o,tr}$ is the maximum heat load of a stream parent per location and transfer type over time steps, $\dot{G}_{sp,t,o,tr}$ is a slack variable which takes the value of $\dot{\mathrm{q}}_{s,t} \cdot b_{sp,t,o,tr}$ at the time step of the maximal load and 0 in the other time steps, $w_{sp,t,o,tr}$ is a binary variable which takes the value of 1 at the time step of maximal load and 0 in other time steps and bigM is a large number for the big-M constraints [111].

Piping cost can be considered as a discrete function of the pipe diameter since there are standard pipe diameters and specific costs associated to them [112]. Such a relationship (see Table 3.2) is obtained by taking the average of the piping cost functions available in [113], [114], [115], and [116]. This relationship can be converted to flow-cost relationships using the stream properties.

Table 3.2 – Piping cost for standard piping diameters.

Standard pipe size	1	2	3	4	5	6	7	8	9	10	11	12
Diameter [mm]	20	40	65	80	100	125	150	200	250	300	400	450
Specific cost [€/m]	96	166	250	312	387	480	580	775	975	1180	1588	1797

Each standard pipe size ($ps \in \mathbf{PS}$) has an upper bound ($\dot{\mathrm{q}}^{\mathrm{ub}}_{sp,o,tr,ps}$ or $\dot{\mathrm{m}}^{\mathrm{ub}}_{ly,u,o,ps}$) representing the maximum heat/mass that can flow through it as well as a lower bound ($\dot{\mathrm{q}}^{\mathrm{lb}}_{sp,o,tr,ps}$ or $\dot{\mathrm{m}}^{\mathrm{lb}}_{ly,u,o,ps}$). A new binary variable and a set of constraints are defined to determine the standard pipe size required for the flows. The constraints for the heat flow pipes are given in Equations 3.61–3.63.

$$\dot{\mathrm{q}}^{\mathrm{lb}}_{sp,o,tr,ps} \cdot n^{h}_{sp,o,tr,ps} \leq \dot{I}^{p}_{sp,o,tr,ps} \leq \dot{\mathrm{q}}^{\mathrm{ub}}_{sp,o,tr,ps} \cdot n^{h}_{sp,o,tr,ps} \quad \forall\, sp \in \mathbf{SP},\ o \in \mathbf{OL}_p,\ tr \in \mathbf{TR},\ ps \in \mathbf{PS} \tag{3.61}$$

$$\sum_{ps \in \mathbf{PS}} \dot{I}^{p}_{sp,o,tr,ps} = \dot{Q}^{max}_{sp,o,tr} \quad \forall\, sp \in \mathbf{SP},\ o \in \mathbf{OL}_p,\ tr \in \mathbf{TR},\ ps \in \mathbf{PS} \tag{3.62}$$

$$\sum_{ps \in \mathbf{PS}} n^{h}_{sp,o,tr,ps} \leq 1 \quad \forall\, sp \in \mathbf{SP}, o \in \mathbf{OL}_p,\ tr \in \mathbf{TR},\ ps \in \mathbf{PS} \tag{3.63}$$

where $n^{h}_{sp,o,tr,ps}$ is a binary variable which takes the value of 1 if the heat flow is in the corresponding standard piping size and 0 otherwise and $\dot{I}^{p}_{sp,o,tr,ps}$ is the slack variable which takes the value of $\dot{Q}^{max}_{sp,o,tr}$ if $n^{h}_{sp,o,tr,ps}$ is 1 and 0 otherwise. The sizes of the resource pipes are determined similar to the heat pipes according to Equations 3.64–3.66.

$$\dot{\mathrm{m}}^{\mathrm{lb}}_{ly,u,o,ps} \cdot n^{r}_{ly,u,o,ps} \leq \dot{J}_{ly,u,o,ps} \leq \dot{\mathrm{m}}^{\mathrm{ub}}_{ly,u,o,ps} \cdot n^{r}_{ly,u,o,ps} \quad \forall\, ly \in \mathbf{L},\ u \in \mathbf{U}_{ly},\ o \in \mathbf{OL}_u,\ ps \in \mathbf{PS} \tag{3.64}$$

$$\sum_{ps \in \mathbf{PS}} \dot{J}_{ly,u,o,ps} = \dot{M}^{max}_{ly,u,o,ps} \quad \forall\, ly \in \mathbf{L},\ u \in \mathbf{U}_{ly},\ o \in \mathbf{OL}_u \tag{3.65}$$

$$\sum_{ps \in \mathbf{PS}} n^{r}_{ly,u,o,ps} \leq 1 \quad \forall\, ly \in \mathbf{L},\ u \in \mathbf{U}_{ly},\ o \in \mathbf{OL}_u \tag{3.66}$$

where $n^{r}_{ly,u,o,ps}$ is a binary variable which takes the value of 1 if the resource flow uses the corresponding pipe size and 0 otherwise and $\dot{J}_{ly,u,o,ps}$ is the slack variable which takes the value of $\dot{M}^{max}_{ly,u,o,ps}$ if $n^{r}_{ly,u,o,ps}$ is 1 and 0 otherwise.

After determining the piping sizes, their corresponding costs are calculated according to Equations 3.67 and 3.68, respectively. The total piping cost is then calculated by summing the heat and resource piping costs as presented in Equation 3.69.

$$C^{pipe_h}_{sp,o,tr} = \sum_{ps \in \mathbf{PS}} \mathrm{c}^{\mathrm{pipe}}_{ps} \cdot \mathrm{F}^{\mathrm{tc}} \cdot \mathrm{D}^{\mathrm{pipe}}_{lc,o} \cdot n^{h}_{sp,o,tr,ps} \quad \forall\, sp \in \mathbf{SP},\ lc \in \mathbf{LC},\ o \in \mathbf{OL}_{lc},\ tr \in \mathbf{TR} \tag{3.67}$$

$$C^{pipe_r}_{ly,u,o} = \sum_{ps \in \mathbf{PS}} \mathrm{c}^{\mathrm{pipe}}_{ps} \cdot \mathrm{F}^{\mathrm{tc}} \cdot \mathrm{D}^{\mathrm{pipe}}_{lc,o} \cdot n^{r}_{ly,u,o,ps} \quad \forall\, ly \in \mathbf{L},\ u \in \mathbf{U}_{ly},\ lc \in \mathbf{LC},\ o \in \mathbf{OL}_{lc} \tag{3.68}$$

$$C^{pipe} = \Big(\sum_{sp \in \mathbf{SP}} \sum_{o \in \mathbf{OL}_p} \sum_{tr \in \mathbf{TR}} C^{pipe_h}_{sp,o,tr} + \sum_{ly \in \mathbf{L}} \sum_{u \in \mathbf{U}} \sum_{o \in \mathbf{OL}_u} C^{pipe_r}_{ly,u,o} \Big) \cdot \mathrm{F}^{\mathrm{an}} \quad \forall\, ly \in \mathbf{L},\ u \in \mathbf{U}_{ly},\ lc \in \mathbf{LC},\ o \in \mathbf{OL}_{lc} \tag{3.69}$$

where F^{tc} is the trenching cost factor (TCF) which is 1 for above-ground pipes (i.e. no trenching) and 1.3 for underground pipes [117], c_{ps}^{pipe} is the specific piping cost of the corresponding pipe size and C^{pipe} is the total annualised piping cost for heat and resource exchange between the locations.

3.4 Case study

The case study is a fictitious industrial cluster which consists of eight locations, each containing a plant and its associated utilities. The locations are assigned with x and y coordinates to indicate their geographical position. It is assumed that all locations have the same altitude; hence, the distance between locations is calculated according to the Manhattan distance (MD). The locations and their plants are given as follows:

- Site 1: Low-temperature chemicals production plant. The process requires heat for pre-heating the reactants and re-boiling the bottoms streams of distillation columns. The products separated at the distillation columns are cooled by air in overhead coolers first and then by water in shell and tube heat exchangers. Electricity requirement in the site is due to mechanical drives such as pumps and compressors. The site energy profile is adapted from [16];
- Site 2: Medium-temperature chemicals production plant. Similar to the plant at Site 1, this process requires heating by steam and cooling by water and air as well as electricity for the mechanical drives. The only difference is that this site has a higher pinch point and production rate. The site energy profile is adapted from [16];
- Site 3: Brewery plant. Brewery consists of two main processes; beer production and bottling. In beer production the raw materials are mixed, boiled, fermented and pasteurised. Bottling includes several stages of cleaning. The heating requirement is mainly in the brewhouse for heating and boiling the mixture prior to fermentation [118] and electricity demand is mainly due to refrigeration systems. The model of the site is adapted from [119];
- Site 4: Cement plant with dry process. The Cement process is centred around clinker production which requires heat at high temperatures up to (1450 °C) for preheating the raw materials to temperature required for calcination. After the reaction, the product at high temperature is cooled and milled to give its final form. The heating requirement is satisfied by burning coal and alternative fuels in the kiln while cooling is done by air. Electricity is required to drive the mills and other mechanical equipment. The process is modelled according to [120];
- Site 5: Dairy plant. Dairy plants include processes for multiple products. Depending on the product slate, the process characteristics differ significantly. For example, condensed milk production is heating intensive while ice cream production mostly requires refrigeration. The plant in the case study is assumed to produce condensed milk and yogurt. The model is adapted from [120];
- Site 6: Pulp and paper production plant. Pulp and paper plants may utilise different technologies for pulp production whereas paper production is relatively standard. The main energy con-

sumption of the plant is heat for drying paper and pulp. The model of the plant is adapted from [30];

- Site 7: Oil refinery. Refineries rely on distillation to separate different components of crude oil, followed by several chemical reactions to break large hydrocarbon molecules into smaller ones. The core of the plant, as well as the main energy consumer, is the crude oil distillation unit. Similar to the chemical plants, heat is required for the bottom streams of the distillation columns and reactions, while cooling is required to condense the overhead streams of the distillation columns. The refinery model is adapted from [120];
- Site 8: Waste incineration plant. Waste incineration plants are typically located near cities to provide heat to the district heating networks while producing electricity in the steam network. The plant is modelled according to [121].

As the focus of the method is energy consumption, only the flows related to energy (e.g. fuels, heat, electricity) are taken into account. Thus the raw material and intermediate flows within each plant are neglected. The product flowrates are indicated to provide a reference size of the plants. The locations of the plants can be seen in Figure 3.3.

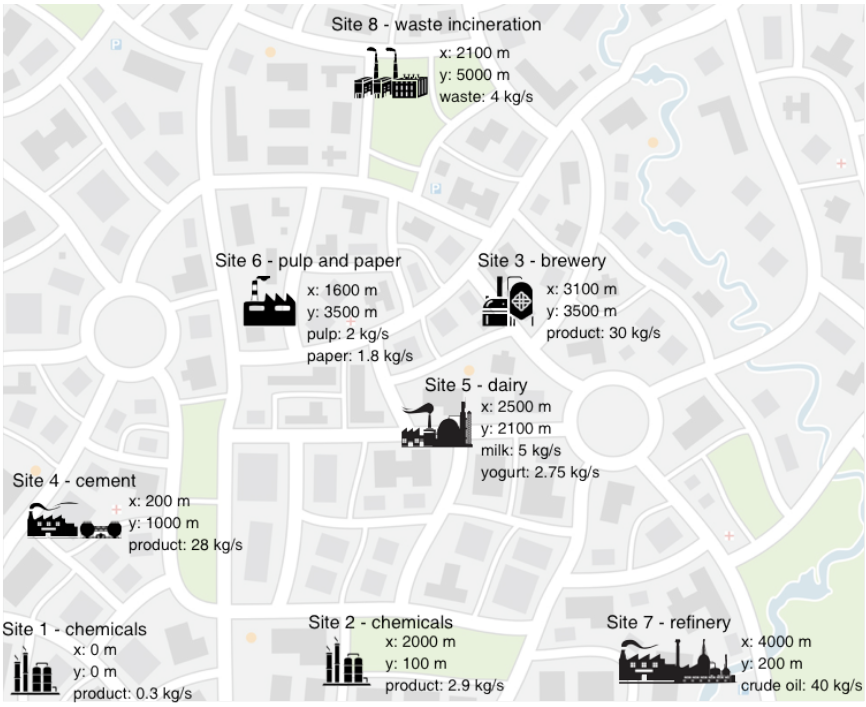

Figure 3.3 – Case study layout.

The grand composite curves (GCCs) of the plants in Figure 3.4 give detailed information about the minimum heating and cooling requirements. The data used to construct the curves are given in Appendix C.1.

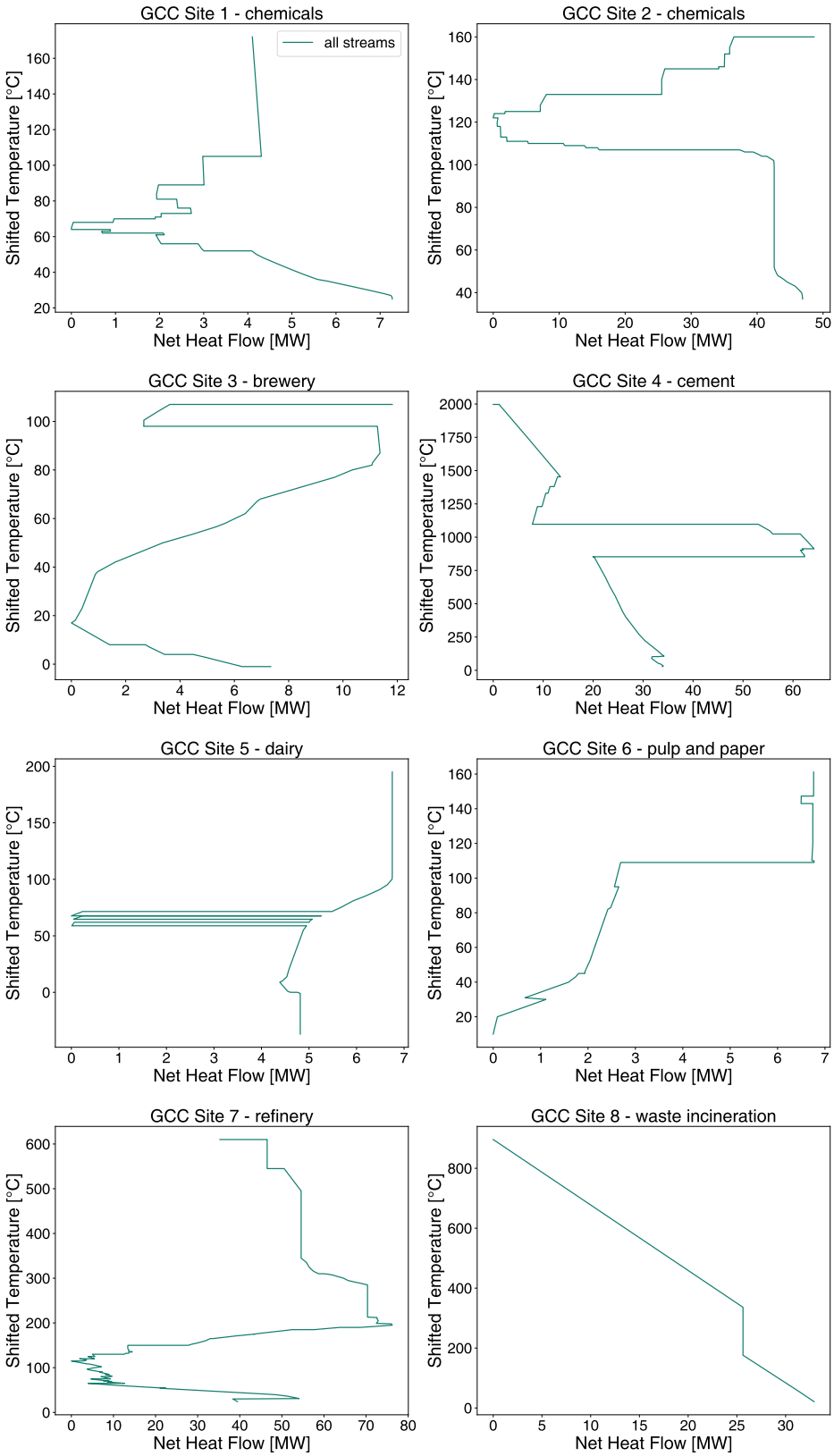

Figure 3.4 – Grand composite curves of the processes in the case study.

3.4.1 Utility systems and resources

3.4.1.1 Existing technologies on the plants

Each plant in the system is considered to operate independently under current conditions. Thus, the sites have their own utility systems to close the energy balance and market access to close the resource balance. The utility systems that already exist on the sites are:

- Boiler: represents a combustion chamber which intakes natural gas and air and outputs heat. The boiler modelling is done according to [38] which assumes that the heat from natural gas consumption is delivered to the steam network by radiation and convection. Table 3.3 depicts the specifications of the boiler model;

Table 3.3 – Boiler model specifications.

Stream	T^{in}[°C]	T^{out}[°C]	$\dot{q}$[kW]
Fuel	-	-	1031
Radiation	827	827	656
Convection	827	100	324
Air preheating	25	150	-49

- Steam network: an intermediate step between the boiler and processes. Heat is delivered to the steam network resulting in steam production. Afterwards, high pressure steam is turbined to cogenerate electricity and low pressure steam which is fed into the processes for heating. The steam network model is adapted from [122]. Table 3.4 illustrates the configuration of the steam network in all locations except for Site 8. The configuration of the waste incineration steam network is adapted from [121];

Table 3.4 – Configuration of the steam network.

Type	Header Pressure[bara]	Header Temperature[°C]	Turbine
Production/Distribution	45	367	yes
Distribution	24	228	yes
Distribution	8	175	yes
Distribution	4	150	no
Production/Distribution	2	126	no
Production/Distribution	1	105	no

- Cooling systems: consist of cooling towers and aerocoolers. Cooling water is used to remove heat from the processes which is then discharged to the environment at the cooling tower. The

cooling tower model (see Table 3.5) is adapted from [123]. Aerocooling is modelled as a simple fan according to [16].

Table 3.5 – Water cooling specifications.

Stream	T^{in}[°C]	T^{out}[°C]	$\dot{q}$[kW]	$\dot{m}$[kg/s]	$\dot{e}$[kW]
Supply	15	25	-1000	-	-
Return	25	15	1000	-	-
Make-up water	-	-	-	0.34	-
Electricity	-	-	-	-	10

- Refrigeration: is needed for the processes requiring sub-atmospheric temperatures (e.g. brewery, dairy). A simple refrigeration cycle model (see Table 3.6) is used which provides the process-specific refrigeration temperature and assuming a coefficient of performance of 3 [121].

Table 3.6 – Refrigeration cycle specifications.

Stream	T^{in}[°C]	T^{out}[°C]	$\dot{q}$[kW]	$\dot{e}$[kW]
Evaporation	-5	-5	-1000	-
Condensation	35	35	1333	-
Electricity	-	-	-	333

3.4.1.2 Additional technologies for improvements

In addition to the existing utility systems, new energy conversion technologies can be purchased and installed to improve the overall energy efficiency and operating cost. The additional utilities considered in the case study are:

- HPs: are ideal in the cases where the pinch temperature is low and heat transfer from below to above the pinch point with low temperature lift is possible. Considering the GCCs presented in Figure 3.4, Site 1, Site 2, Site 5 and Site 7 offer potentials for heat pump integration. The evaporation and condensation temperatures of the HPs are selected manually based on the GCCs. Table 3.7 depicts the specifications of the HPs;

Table 3.7 – Heat pump specifications.

	T^{evap} [°C]	T^{cond} [°C]	$\dot{q}^{evap}$ [kW]	$\dot{q}^{cond}$ [kW]	$\dot{e}^{comp}$ [kW]
HP_{site1}	58	73	-1008	1067	59
HP_{site2}	100	130	-716	797	81
HP_{site5}	82	107	-1035	1131	96
HP_{site7}	100	130	-716	797	81

- Mechanical vapour recompressions (MVRs): similar to HP, but instead of using an intermediate fluid, the vapour is directly compressed to a higher pressure and temperature. Potential MVR integration at Site 3 and Site 6 is considered. Steam can be imported at 1 bar from the other locations and compressed to 2 bar instead of producing it in the boilers.
- Cogeneration Engines: commonly used in industrial sites as they provide both heat and electricity. Similar to HP, pinch point plays an important role in the integration of cogeneration engines. A significant part of the heat comes from the cooling water of the engine. Thus, they are suitable only for the processes with low pinch temperatures such as Site 1, Site 3, Site 5 and Site 6. The specifications of the cogeneration engines (see Table 3.8) are adapted from [16].

Table 3.8 – Cogeneration engine specifications.

Stream	T^{in} [°C]	T^{out} [°C]	$\dot{q}$ [kW]	$\dot{e}$ [kW]
Fuel	-	-	2605	-
Exhaust Gasses	470	120	537	-
Engine Cooling	87	80	653	-
Electricity	-	-	-	1063

- Photo-voltaics (PVs): have the potential to supply the electricity requirement of the industrial processes as well as the utility systems (e.g. HPs). The limitations for PV integration are availability of land and high capital investment. As the industrial plants are generally located outside urban centres, it is assumed that there is enough land and roof surface to install them. The PV model (see Table 3.9) is adapted from [121] for a reference area of 100 m^2.

Table 3.9 – PV specifications.

	T^{in} [°C]	T^{out} [°C]	$\dot{q}$ [kW]	$\dot{e}$ [kW]
PV	-	-	-	16.6

3.4.1.3 Utility and resource costs

Energy conversion technologies not initially available on the sites require investment for the purchase and installation of the equipment. The HPs consist of two heat exchangers (i.e. evaporator and condenser) and a compressor while the MVRs require investment only in a compressor. The cost of the heat exchangers and compressors is calculated according to [34]. The non-linear cost functions are linearised within the range of application [F_u^{min}, F_u^{max}] to be coherent with the MILP framework. The cost parameters are annualised assuming 8% interest rate and a life time of 20 years. The fixed and variable annualised investment cost (c_u^{inv1} and c_u^{inv2}, respectively) of the additional technologies are listed in Table 3.10 and affect the objective function by inclusion in Equation 3.4.

Table 3.10 – Costing and sizing parameters of the additional energy conversion technologies.

Unit	c^{inv1} [€/year]	c^{inv2} [€/year]	F^{min} [-]	F^{max} [-]
HP_{site1}	8774	54521	0.1	5
HP_{site2}	5270	22328	0.1	30
HP_{site5}	8425	46909	0.1	10
HP_{site7}	5270	22328	0.1	10
MVR_{site3}	2265	26950	0.1	4
MVR_{site6}	4595	38142	0.1	2
$Co\text{-}gen_{site1}$	11910	119095	0.1	1
$Co\text{-}gen_{site3}$	11910	119095	0.1	1
$Co\text{-}gen_{site5}$	11910	119095	0.1	1
$Co\text{-}gen_{site6}$	11910	119095	0.1	1
PV	0	70730	0	100

The operating cost of the system is calculated based on the resource and energy consumption. Since raw materials and intermediate products are excluded from the analysis, only the costs of electricity and fuels are considered. Table 3.11 illustrates the specific cost of the main contributors to the operating cost. The specific cost [124], share in the fuel mix [125] and properties [126] of the alternative fuels used in the cement plant are given in Appendix C.2.

Table 3.11 – Specific cost of the main fuels and resources.

Unit	c^{spec}
Natural gas	0.030 [€/kWh]
Coal	0.600 [€/kg]
Electricity purchase	0.092 [€/kWh]
Electricity selling	0.055 [€/kWh]

3.5 Results and discussion

The method is first applied to two of the plants presented in the case study introduced in Section 3.4 to analyse the results in deeper detail. The optimisation of the overall case study is also completed to display the capability and effectiveness of the method in solving large-scale, complex industrial problems.

3.5.1 Symbiosis between two chemical plants

The two chemical plants introduced in the case study represent an opportunity for industrial symbiosis by heat sharing. Site 2 has a higher pinch point than Site 1, thus its excess heat can be recovered and used in Site 1. Figure 3.5 illustrates the results of parametric optimisation in which the sum of the operating and utility investment cost of the plants is minimised while the investment in piping between the plants is constrained with a limit (ϵ). Figure 3.5(a) exhibits the trade-off between the two objectives while the colour indicates the sum of both (i.e. total cost with piping). The minimum total cost with piping is obtained in Solution 6 when a cogeneration engine is installed on Site 1 and a heat pump on Site 2 while heat is shared between the sites with 1 bar steam; however, similar total cost results are obtained with other solutions where investments in piping are between 0 and 0.3 M€. As the investment cost limit for the pipeline between plants is increased, lower piping-exclusive total cost is obtained. This decrease coincides with lower operating cost due to excess heat recovery between the sites. Investment decisions also vary with respect to the limit on the piping investment. For example, investment on Site 1 HP decreases in correlation with piping investments because the imported steam from Site 2 replaces the HP. Conversely, integration of the cogeneration engine on Site 1 is independent of the piping allowance as the decision of installing the cogeneration engine is driven by the electricity generation rather than heat. PV is not integrated in any of the solutions as its capital investment cost is higher than the associated operating cost benefits. Figure 3.5(b) reveals further details about the solutions of parametric optimisation focusing on total investment cost including piping and heat sharing between the sites. When investment on piping between the sites is not allowed (Solution 1, piping cost = 0 M€/year), the optimal solution is investing in HPs on both sites and a cogeneration engine on Site 1. As the limit on piping investment increases, 1 bar steam exchange becomes part of the optimal solution. When 1 bar steam import reaches its limit (solution 6, piping cost = 0.29 M€/year), the investments in exchanging 2 bar steam are made. When heat sharing and losses are considered, a significant decrease in the heat losses in the last solution (solution 10, piping cost = 0.53 M€/year) is observed, although the absolute heat exchanged remains the same as underground pipes are selected given the high allowance on piping cost. The same phenomenon can be observed comparing solutions 8 (piping cost = 0.41 M€/year) and 9 (piping cost = 0.45 M€/year). In the latter solution, more 2 bar steam is shared, but heat losses are lower due to installation of underground pipes.

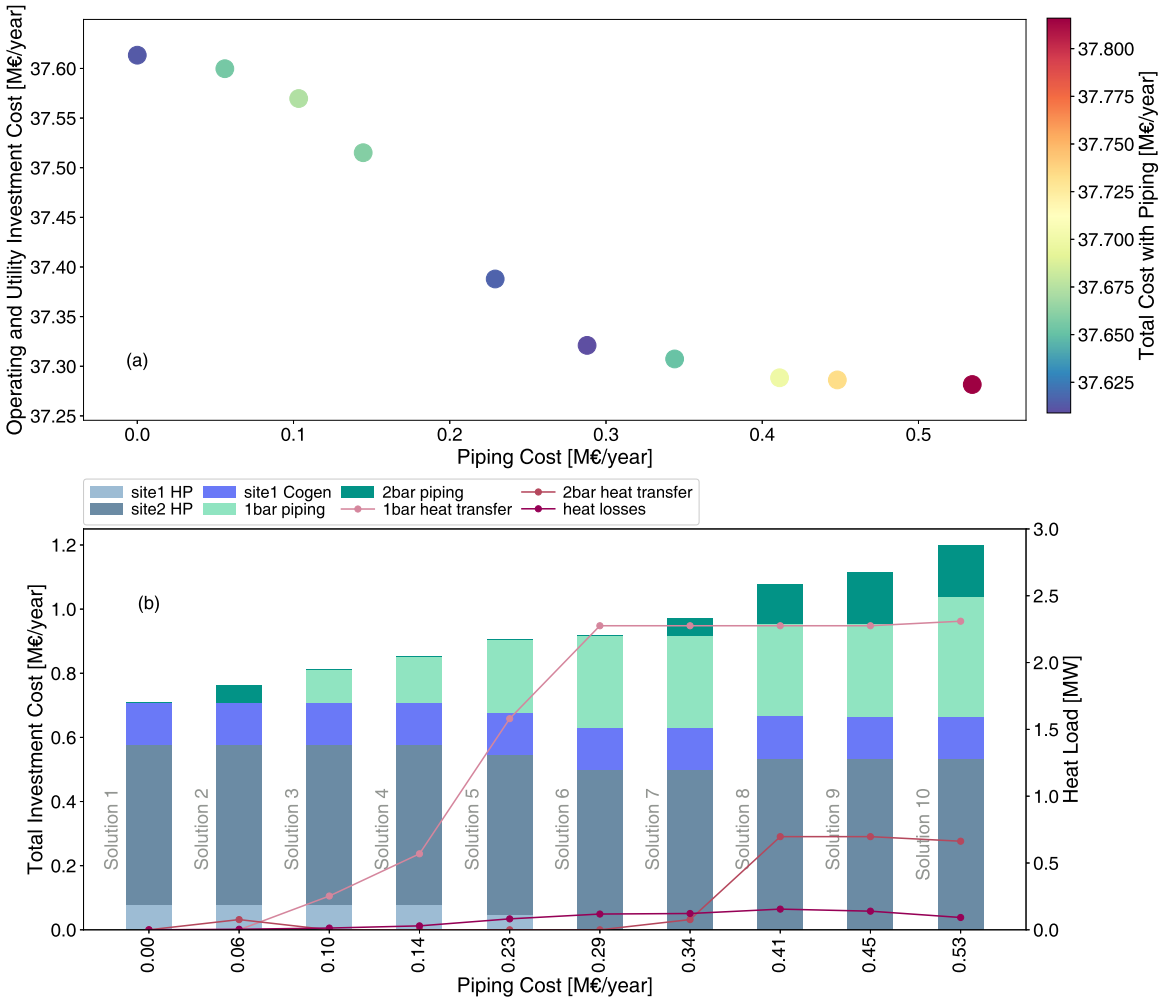

Figure 3.5 – Parametric optimisation with two chemical plants. (a) pareto frontier; (b) investment cost breakdown and heat sharing.

Figure 3.6 depicts the Carnot composite curves (CCCs) of Site 1 and Site 2 which provide more detail about heat integration. HP at Site 1 is partially replaced by 1 bar steam import when solutions 1 and 4 are compared. In solution 7, 1 bar steam import from Site 2 completely replaces the HP at Site 1. Moreover, the size of the HP at Site 2 increases to produce 2 bar steam and export it to Site 1. In solution 10, the boiler at Site 1 is completely substituted by 1 and 2 bar steam imports.

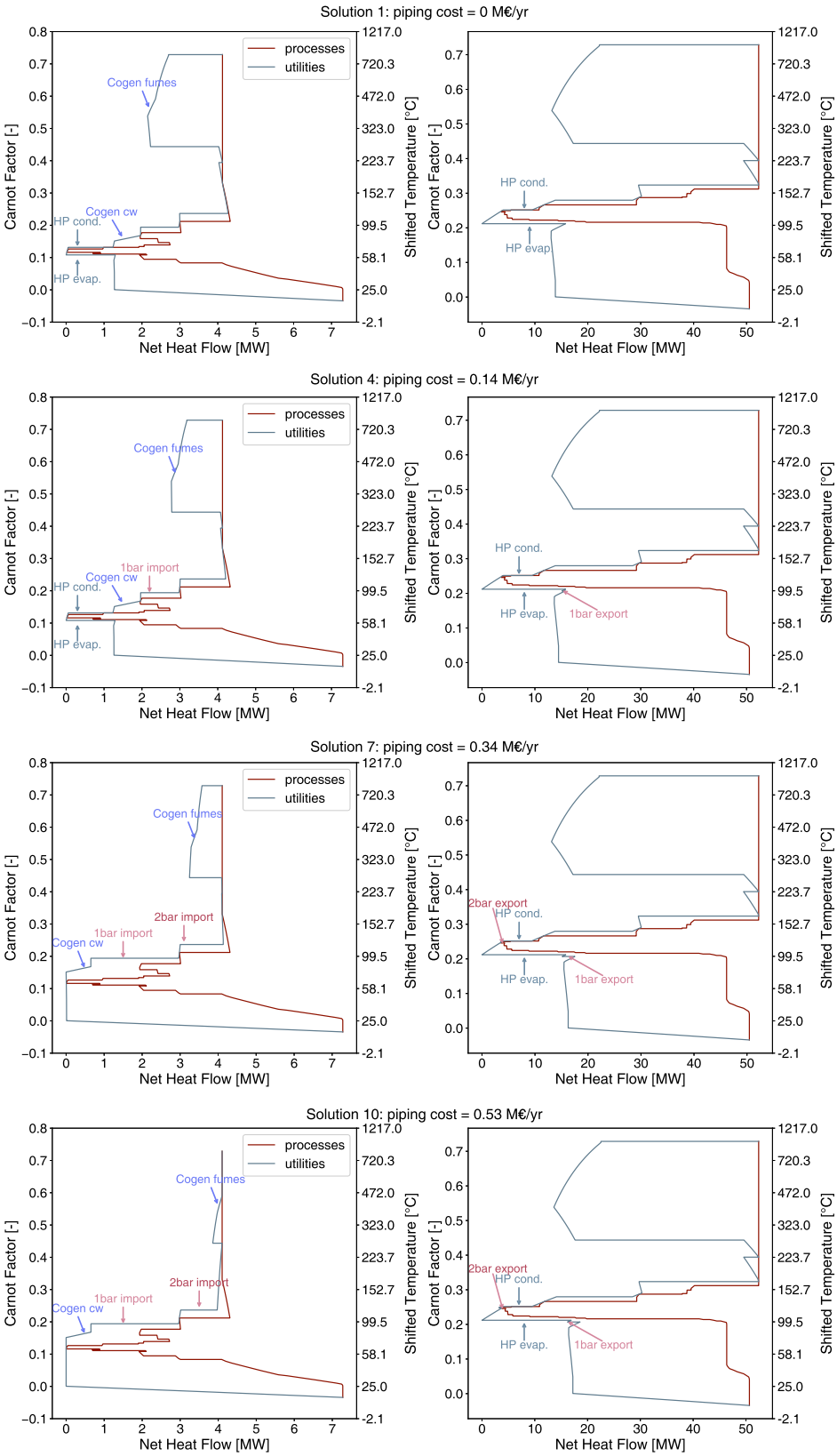

Figure 3.6 – Carnot composite curves of Site 1 (left) and Site 2 (right) with different piping cost investment limits.

3.5.2 Symbiosis between all plants

Optimisation of the case study introduced in Section 3.4 with all plants is completed to exhibit the capability of the method to solve complex, large-scale problems. Sites 2 and 7 have excess heat, while Sites 1, 3, 5 and 6 require heating at relatively low temperatures. In addition, the waste incineration plant at Site 8 can provide steam to the other locations instead of turbining and condensing it at low pressure. Thus, there is a large potential for heat sharing between the locations. The transfer of heat can be done only via utility systems. As there is a steam network in each location except Site 4, steam is considered to be the transfer fluid. In addition to symbiosis by sharing heat, there is a possibility to share material from Site 1 to Site 4, as the cement process can use chemical waste as a fuel. Similar to the case with two chemical plants, the total cost of the system excluding the piping cost is minimised, while constraining the piping investment cost at different limits.

Figure 3.7a depicts the parametric optimisation results. Similar to Section 3.5.1, the operating and utility investment cost decrease as the limit on piping investment is increased. Considering all cost elements, the minimum is obtained when the piping cost is ~2.2M€/year. Other solutions show that the operating and utility cost can be further decreased; however, the additional piping cost is larger than the associated economic benefit. Further than ~6 M€/year investment in piping to connect the sites only results in marginal improvement in the main objective. The breakdown of total investment cost can be seen in Figure 3.7b, as well as the amount of heat sharing and losses. In solutions with a low piping cost limit (similar in magnitude to the utility investment cost), all investments are relatively small. With increasing limits on the piping investment, it quickly dominates the investment cost distribution as heat sharing can be done over long distances and with high flowrates. At low piping investment limits, the investment goes toward sharing high pressure steam since it requires smaller pipe diameter. As the limit on the piping cost increases, heat sharing switches to lower pressure (i.e. lower temperature) steam as lower temperature corresponds to lower heat losses. With increasing allowance, heat losses trend upward until the pipe investment cost reaches ~6.6 M€/year as more heat is shared between the sites. Past this level, despite stable or increased heat sharing, heat losses start decreasing since higher allowance on piping cost permits investment in underground pipes which are naturally more insulated.

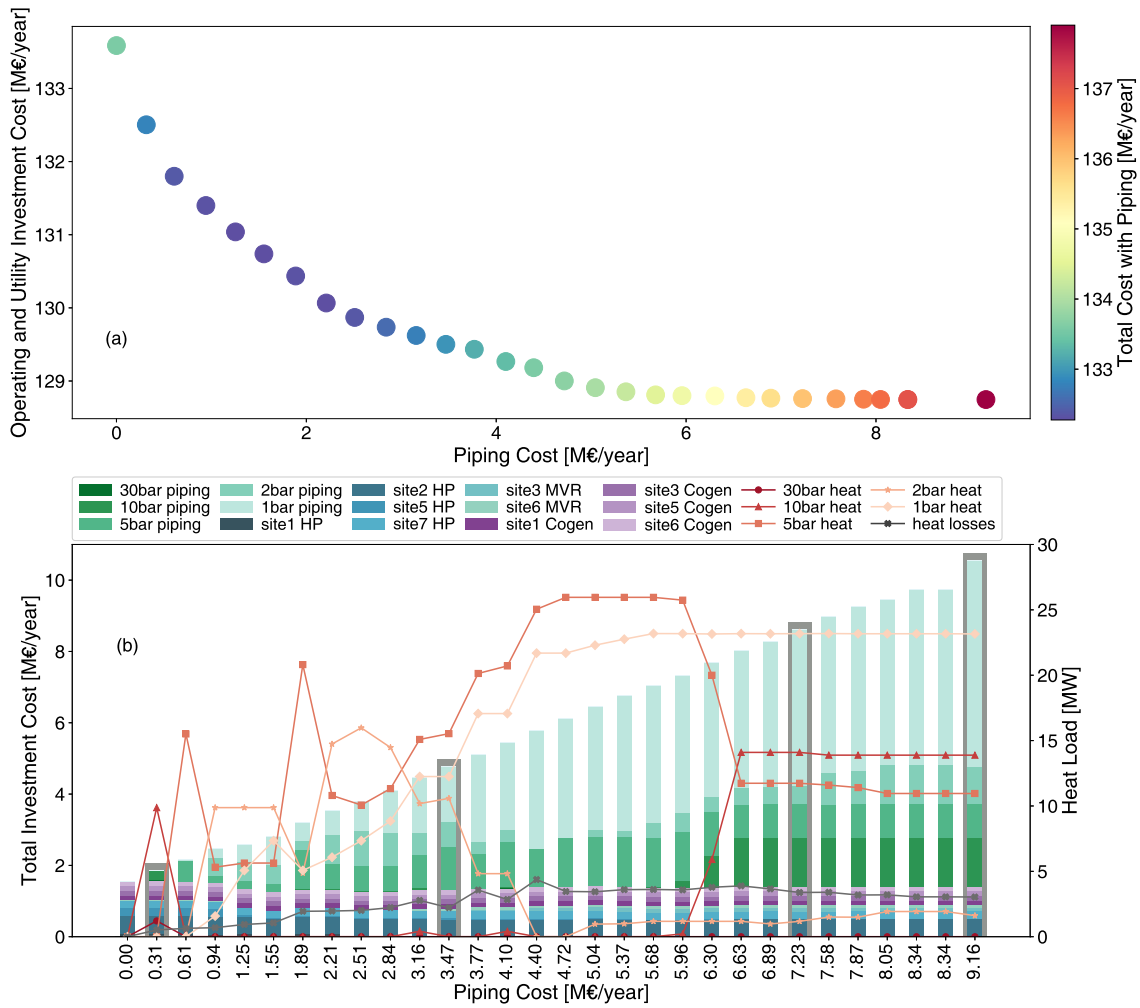

Figure 3.7 – Parametric optimisation results for an industrial complex (a) pareto frontier; (b) investment cost breakdown and heat sharing.

Figure 3.8 illustrates the layout of the plants and their connections for four solutions with different piping investment levels from parametric optimisation (highlighted in Figure 3.7b. The switch from high to low pressure steam sharing can be observed by comparing solutions with lower (e.g. Figure 3.8a) and higher piping investments (e.g. Figure 3.8b). Sharing chemical waste with the cement plant is activated with a low piping investment allowance. Heat sharing is selected using above-ground pipes at low piping investment solutions (e.g. Figure 3.8a), while increasing this allowance first encourages a mixture of above-ground and underground pipes (e.g. Figure 3.8b and Figure 3.8c) and then only underground pipes (e.g. Figure 3.8d). With large piping investment limits, even very small heat sharing options (< 1 MW) are activated which might not be practically feasible.

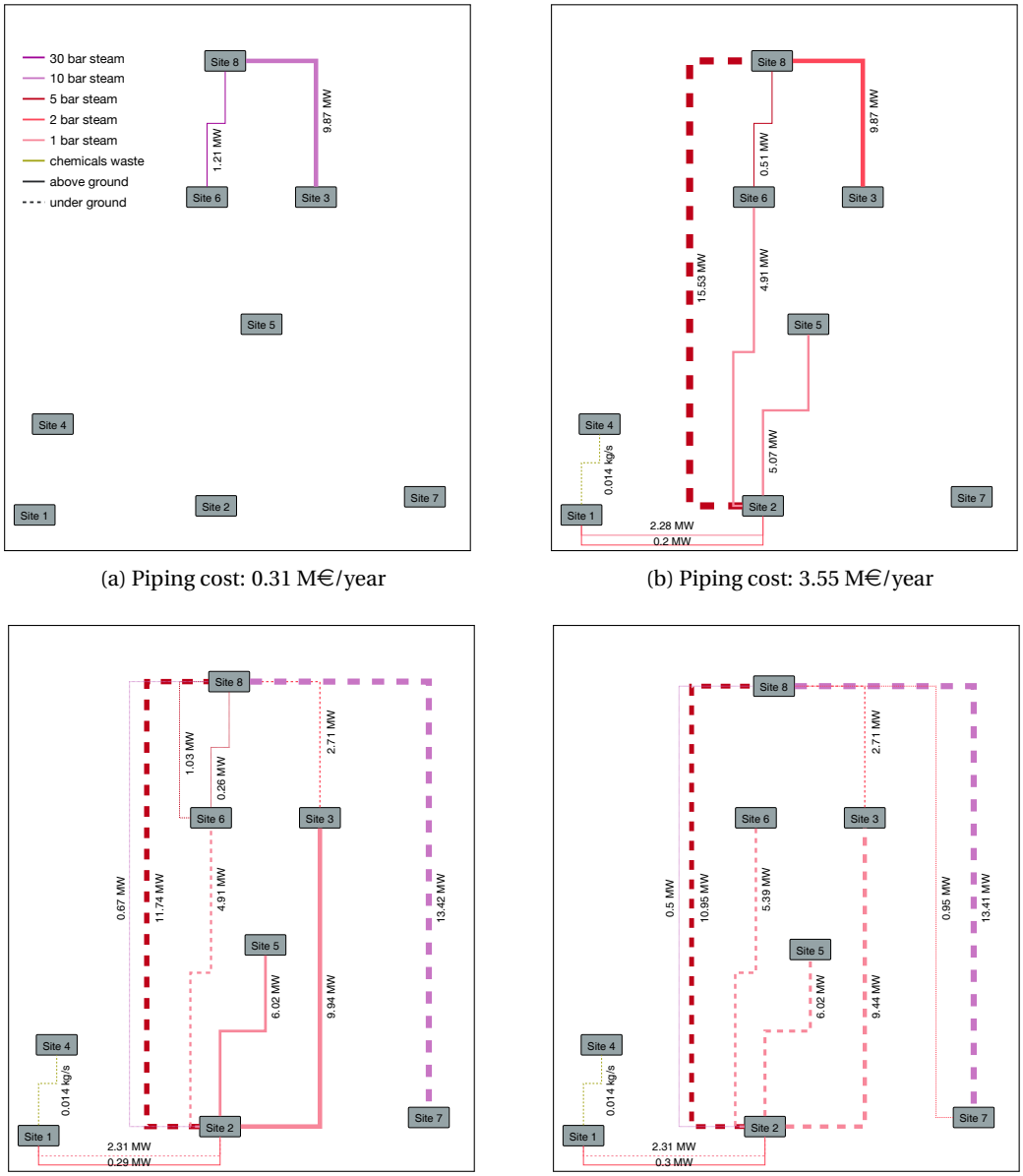

(a) Piping cost: 0.31 M€/year

(b) Piping cost: 3.55 M€/year

(c) Piping cost: 7.48 M€/year

(d) Piping cost: 9.42 M€/year

Figure 3.8 – Optimal piping connections at different investment levels.

3.5.3 Piping investment by a third party

Although investment in inter-plant infrastructure has proven economic benefits, industries are often reluctant to partake in such projects as they include several companies and the payback time may not fit within stringent economic policies. In such cases, the involvement of a third party could be considered. The analysis presented in Section 3.5.2 examines the piping investment to be made by industries, but the same investment could alternatively be made by a third party with

less stringent payback requirements. The investment to be made by such a third party would be recuperated by providing steam at a slight premium compared to the cost of generation. Such a strategy mitigates industrial risk and investment while providing improvements in operating cost and business opportunities for utility providers, which use different business models than the large process industries. The steam price provided to the industries is calculated to recuperate the piping cost over the time horizon of the installation and an additional premium to realise profitability for the third party. The steam premium is varied between 0% – representing a non-profit third party or shared industrial investment – to 20%, providing a business case for the third party to compensate the investment and be profitable. The results are compared in Figure 3.9a based on the overall system profit. The baseline for the profitability analysis is the solution in which piping cost is zero, i.e. there is no sharing between the industries and each plant pays for its own energy technologies. For the other solutions, the system profit is calculated as the difference between the change in operating cost and the annualised investment cost including piping. As the steam price premium increases, the profitable zone narrows and the highest potential profit decreases, since a higher price is paid for the same operating cost savings, due to the profit margin of the third party. The solutions with different steam price premiums selected in Figure 3.9a are compared in terms of steam price in Figure 3.9b. The price of steam is calculated as the ratio between the cost of piping including the profit margin of the third party and the total amount of steam shared between sites. The savings on steam price for the industries (compared to the break-even price) range between 47% and 32%. With increasing third-party profit, the steam price increases; however, it remains well below the break-even price.

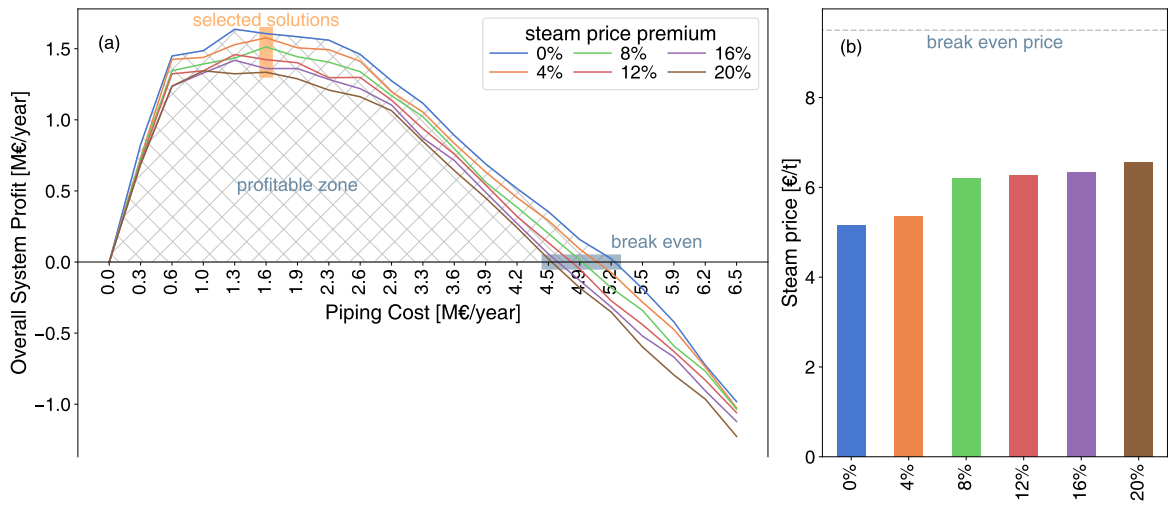

Figure 3.9 – Overall profitability (a) and steam price (b) considering the premium charged by a third party.

3.5.4 Comparison with baseline and state of the art

The baseline operation of the sites represent their current state in which little or no heat is recovered, better performing technologies (e.g. HPs) are not integrated and heat and resources are not shared between locations. The baseline fuel and electricity consumption of the sites is modelled according to [16, 120]. State-of-the-art methods do not consider the location aspects, as discussed in Section 3.2; thus, processes in different locations can exchange heat and resources without any restriction. Table 3.12 compares economic and environmental key performance indicators (KPIs) of the overall system in the baseline state, when a state-of-the-art targeting method [25] is used and when the proposed method is used. The objective function is modified in this case to include the piping cost. Compared to the baseline, the total cost and CO_2 emissions of the system decrease by 21% and 35%, respectively, using the proposed method. This is partially due to the integration of new energy conversion technologies and partially because of heat and resource sharing between the locations as discussed in the previous sections. The reduction in the economic objective function and CO_2 emissions reach 33% and 48%, respectively, using the targeting approach. Although the targeting method offers further reduction in the cost, it represents only the theoretical potential while the proposed method takes the practical constraints of locations and piping investment into account.

Table 3.12 – Comparison of the results of the present work with the baseline and targeting approach.

KPI	Unit	Baseline	State of the art	This work
Operating cost	M€/year	167.8	111.4	128.8
Utility investment cost	M€/year	0	1.1	1.3
Piping cost	M€/year	0	0	2.2
Total	M€/year	167.8	112.6	132.2
CO_2 emissions	Mt/year	867	452	562

3.6 Conclusion

This work proposes a PI method considering location aspects. Consequently, the heat cascade is reformulated to account for heat distribution losses and temperature drops, while the electricity balance is modified to include pumping work required to compensate pressure drops. The cost of the infrastructure between the plants is also considered in the form of piping cost, and the resulting problem is formulated using MILP. Parametric optimisation is employed to systematically generate multiple solutions.

The method is first applied on a scenario with two chemical plants, to study the potential heat sharing between them. The results show that the lowest total cost solution is achieved by sharing

1 bar steam between the plants, with a cogeneration engine installed in one plant and a HP is integrated in each. Other solutions are also found, which prove the possibility of eliminating the main heating utility of one plant by multi-level steam sharing.

As a large-scale application of the method, parametric optimisation on eight industrial plants in geographical proximity is also completed. In this case, with small piping investment budgets, the optimal solutions favour sharing heat via high-pressure steam, since higher pressure levels require smaller pipe diameters. With larger budgets, lower pressure steam sharing options emerge, stemming from reduced heat losses. Following the same trend, above-ground pipes are preferred at low piping cost limits, while underground pipes are selected at high limits, due to the trade-off between heat losses and piping investment.

When process industries are not willing to take the risk of investing in inter-plant infrastructure, involvement of a third party can be beneficial. The third-party, making the initial investment and selling steam between plants, could be a non-profit governmental organisation or a utility company with profitability targets. In either case, solutions resulting in overall system profit are obtained, with lower system profit at higher steam price premiums. Industries benefit from such a strategy by avoiding investment risks while benefiting from a 40% reduction in steam prices (on average) with the third party profiting from a steam price premium of up to 20%.

The optimal results obtained using the proposed method lead to a 21% and 35% reduction in the total cost and CO_2 emissions, respectively, compared to the baseline operation of the sites, resulting from heat and resource sharing between the sites and integrating new energy conversion systems. The theoretical optimum suggested by the targeting approach results in an even lower total cost and environmental impact; however, contrary to the work presented in this chapter, it does not account for technical constraints (e.g. using commercially available technologies), or economic constraints (e.g. including the investment cost of the new technologies or the piping cost).

The present work provides a complete analysis for industrial symbiosis with heat and resource sharing as well as a set of options for investment budgets on inter-plant infrastructure. Heat losses and pumping work requirements are assumed to scale linearly with the flow for inclusion within the MILP framework. Such assumptions simplify the model solution process but may result in missing the global optimum solution. Thus, further analysis should be carried out, studying non-linearity aspects and their impact in the results. Moreover, large industrial retrofit projects, as the one presented in this work, are generally carried out over a long time horizon. Hence, future work should include investment scheduling analysis of the system, which will offer insight into the timeline of the investment in new technologies and piping as well as utility replacement requirements.

Planning investments in long time horizons

Overview

- Introducing a multi-period approach to model long time horizons;
- Considering the existing plant layouts, their age and lifetime;
- A novel MILP formulation for optimal investment planning and its synthesis with process integration;
- Solution strategies to effectively solve large scale problems and generate multiple optimal results;
- Analysis of the investment decisions under different budget constraints.

The content of this chapter is published in [127].

4

Retrofitting existing industrial plants require large investments, which remains the largest barrier to implementing energy saving solutions. Process integration has the strength to identify the best investments to improve the efficiency of plants as illustrated in the previous chapters, yet their timing remains to be answered using an optimisation approach. Even more critically, investment decisions must also account for future investments to avoid stranded or regretted investments. This chapter presents a method incorporating investment planning over long time horizons in the framework of process integration. The time horizon is included by formulating the problem using multiple investment periods, partially decoupled from, but still synchronised with, temporal operating differences. Investment planning is conducted using a superstructure approach which permits both commissioning and decommissioning of units in the beginning of each period. The method is applied to a large case study, with an industrial cluster neighbouring an urban centre to also explore options of heat integration between industries and cities. First, optimal planning without budget constraints is performed, which yields a solution including installing heat pumps and cogeneration engines to improve intra-plant energy efficiency and steam pipelines between industrial sites, as well as the district to valorise excess heat. All investments are suggested in the first year to benefit from operating cost savings as much as possible; however, this requires a large capital expense in a single period which might not be realistically possible. Adapting the problem by

imposing annual investment limits and restricting the investment period to five or ten years, such large investments are no longer feasible. The energy conversion technologies invested in remain the same, but the investment decisions are spread over the defined investment period. Compared to the business-as-usual operation, optimal investment planning improves the operating cost of the system by 27% without budget constraints and 16-26% with constraints on budget and investment period which reflects as increase in the net present value and decrease in the CO_2 emissions. In all cases, the operating cost benefits pay off the investment in less than two years. The work presented in this chapter is efficient in finding energy saving solutions based on the interest of industries. This method adds additional perspectives in the decision-making process and is adaptable to various time horizons, budgets, and economic constraints.

4.1 Introduction

Developing countries account for 49% of the final energy used in industry, followed by developed countries with 40% [128]. This shows that improvements in the industrialised countries are important since they are large contributors to the overall consumption and can change the state of the art for the developing countries. In general terms, the energy efficiency of an existing industrial plant or cluster can be improved following a wide variety of technical actions, including:

- maintaining and/or refurbishing existing equipment to restore their efficiency;
- replacing and retiring obsolete equipment and production processes with the best available techniques;
- using waste management measures such as insulation and sharing excess heat and material from one process to another.

These retrofitting actions come with investment, the biggest barrier to improving energy efficiency [129]. Energy efficiency investments are subject to rigorous criteria such as payback time lower than 12 months, thus they have to compete for capital and short-termism [130]. Conversely, it is often overlooked that current equipment on plants have a limited lifetime and investment would eventually be required, regardless of resistance to capital expenditures. Therefore, considering long time horizons provides investments in energy efficiency improvements better ground for competition over just replacing the equipment which reach their end of lifetime (EoL). Nevertheless, this adds another layer of complexity, as not only the question of 'what to invest in' but also when to make the investment must be answered.

To answer these questions, this chapter presents a novel method for simultaneous optimisation of investment planning and process integration. Section 4.2 covers the investment planning methods available in the literature, Section 4.3 illustrates the formulation and its detailed explanation, Section 4.4 presents the case study, Section 4.5 discusses the results and Section 4.6 draws the conclusions of this work.

4.2 State of the art

Process integration (PI) methods available in the literature can be found in the previous chapters. The literature review in this chapter focuses rather on investment planning.

Investment planning has been applied in different fields, such as energy planning, carbon capture, urban systems planning and production of chemicals and pharmaceuticals. One of the branches of energy planning that has been extensively studied is generation expansion planning (GEP), which determines the type, siting, sizing and timing of new plant additions. Bakirtzis et al. developed an mixed integer linear programming (MILP) GEP model using small periods (i.e. months) which results in better scheduling, as mid-term decisions are permitted [131]. They also included the cost of refurbishment of the existing units which helped with the problem convergence. Pereira et al. incorporated long and short time horizons in GEP [132]. While the investment planning of renewable energy system penetration in electricity generation was carried out for a time horizon of 10 years, every year was evaluated in hourly time steps to investigate the short term impact of the investment decisions. It was concluded that high dependence on renewables increases the system's sensitivity to the seasonality of resources, which is often neglected in methods working only with yearly averages. The main gaps in GEP have been highlighted as not including the transmission system in the analysis and considering only centralised systems [131]. A long term expansion planning method was developed by Zhang et al. [133] to optimise an energy hub, taking into account the transmission system. The objective was to find the system with the lowest cost of satisfying the hub requirements. The units considered for investment included generating units, transmission lines, natural gas furnaces and combined heat and power (CHP) units. Botterud et al. proposed a stochastic dynamic optimisation model for investments in power generation embodying both centralised and decentralised decision making [134]. Instead of minimising the total cost as most methods in literature, they maximised either investor profits or social welfare in the system. Energy planning models can be computationally expensive, especially when detailed time resolution is considered. Bakken et al. treated model complexity by dividing it into operational and investment sub-problems [135]. The operational planning model included alternative supply structures for multiple energy carriers such as electricity, natural gas, liquid natural gas, oil, biomass and district heating and their scheduling using hourly time steps. Afterwards, the planning of investment was carried out for a long time horizon using an investment model, in the form of dynamic programming.

Most of the methods present in literature use an economic objective, as the main focus is the investment. Although decreasing the cost indirectly helps reducing CO_2 emissions, there are a few methods explicitly targeting improvements in environmental impact. Mirzaesmaeeli et al. proposed a method to select the optimal mix of energy supply sources to meet the current and future electricity demand in Ontario, while minimising the cost of electricity [136]. The model also included constraints on CO_2 emissions, so that the selected power generation systems do not

violate the regulations on emissions that are in place. Fripp created a multi-period stochastic linear programming model called Switch to reduce the environmental impact of power generation by choosing optimal portfolios for renewable energy deployment [137]. The model was able to decide how much capacity to build in different load zones, as well as how much power transfer capacity to install between them. Another novelty in the model was the flexibility of using existing systems or turning them off for a period of time, to decrease the operating and maintenance costs. Cristobal et al. studied CO_2 mitigation by CO_2 capture systems [138]. They proposed a stochastic MILP model to retrofit a coal power plant, and choose between buying CO_2 allowance and installing a CO_2 capture system as well as to determine the optimal time for investment. Stochasticity was introduced with the variations in the future CO_2 allowance prices.

Investment planning in urban energy systems is generally carried out at two different scales, namely building and district. Cano et al. developed an energy systems planning model for buildings to decide which technologies to install, as well as the time of the investments [139]. They considered ageing of technologies and its impact on system performance. A time horizon of 15 years with 12 monthly profiles and hourly time steps was considered. This way, variations in the availability of some technologies, such as PV, were taken into account. A district-level, multi-stage stochastic programming model was proposed by Lambert et al. [140] for optimal phasing of district heating networks. In the first step, the optimal selection of pipe diameters was conducted, minimising capital cost and heat losses. In the second step, the optimal deployment of district heating network pipes was determined, over a long time horizon.

Industrial applications of investment planning include areas of waste management, utility systems, process design and capacity expansion. Chakraborty et al. proposed a long term operation and investment planning method for waste management [141]. While the investment decisions were optimised for a five-year period, the optimal operation of the plant was carried out for another 20 years, to correctly asses the long-term impact of investment decisions. The method was extended, by introducing a dynamic view of designing optimal waste management strategies under uncertainty [142]. Wickart and Madlener developed a method to optimally choose between investing in an industrial boiler or a CHP unit and the appropriate investment time [143]. The effect of uncertainty was considered for fuel and electricity prices. It was concluded that if the operational risks are high, investors are likely to prefer a less capital-intensive option, i.e. investing in the steam boiler.

Sahinidis et al. studied a capacity expansion problem consisting of a network of existing and new processes with forecasts for prices and demands within a long range horizon [144]. They formulated the problem as an MILP model to optimise the net present value (NPV), determine how much of each chemical is produced in each period, the capacity expansion and shut-down decisions. This model was extended, by including flexible processes, which could operate in both continuous and batch modes [145]. Norton and Grossmann further extended the method, by adding raw material flexibility on top of product flexibility [146]. Raw material flexibility included using different

chemical feedstocks, as well as supplying them from different sources. Jain and Grossmann worked on long-term scheduling of tests in new product development in the pharmaceutical industry [147]. They proposed a method which considered the trade-off between greater product sales from a shorter-term test in parallel configuration and lower expected value of total cost from longer sequential tests. This was an extension of the work from Schmidt and Grossmann [148], considering resource limitations. Maravelias and Grossmann [149] combined the scheduling [147] and planning [146] efforts in the literature to predict which products should be tested and determine the detailed test schedules, production profiles and design decisions. The selection of the product portfolio was added as an additional decision variable and disjunctive programming was used to solve the problem.

The literature on investment planning has addressed a broad range of issues; however, the focus of research was directed mostly towards energy planning and expansion of electricity generation systems (see Table 4.1). Only a few methods in the literature propose methods for industrial problems, and even those consider processes as simple input-output models, neglecting detailed flows. PI offers an effective approach to such problems, incorporating heat cascade and mass balance constraints. A PI method targeting industrial investment over a long time horizon has not been proposed. The work presented in this paper combines the strength of investment planning and PI. This way, investments in industrial plants and clusters can be optimally planned, without compromising on the level of detail of the processes or energy conversion systems.

Table 4.1 – Literature review on investment planning.

Publication	Year	Method	Sector	Time horizon	Objective	Retrofit	Comissioning	Decommissioning	PI integration
Bakirtzis et al. [131]	2012	MILP	electricity	long	economic	✔	✔	✖	✖
Pereira et al. [132]	2017	MILP	electricity	long/short	economic	✔	✔	✖	✖
Zhang et al. [133]	2015	MILP	electricity	long	economic	✖	✔	✖	✖
Botterud et al. [134]	2005	stochastic	electricity	long	economic	✔	✔	✖	✖
Bakken et al. [135]	2007	MILP	electricity	long	economic	✔	✔	✖	✖
Mirzaesmaeeli et al. [136]	2010	MILP	electricity	long	economic	✔	✔	✖	✖
Fripp [137]	2012	stochastic	electricity	long	environmental	✔	✔	✔	✖
Cristobal [138]	2013	MILP	electricity	long	economic	✔	✔	✖	✖
Cano et al. [139]	2014	MILP	urban	15 years	economic	✖	✔	✔	✖
Lambert et al. [140]	2016	MILP	urban	long	economic	✖	✔	✔	✖
Chakraborty et al. [142]	2004	MILP	industry	20 years	economic	✖	✔	✔	✖
Wickart and Madlener [143]	2007	dynamic programming	industry	long	economic	✖	✔	✔	✖
Sahinidis et al. [144]	1989	MILP	industry	long	economic	✔	✔	✖	✖
Maravelias and Grossmann [149]	2001	MILP	industry	long	economic	✔	✔	✖	✖
This thesis	2019	MILP	industry	long	economic	✔	✔	✔	✔

4.3 Method

The method proposed in this work is an MILP framework for simultaneous optimisation of process integration and long term investment planning (PIIP). Figure 4.1 illustrates a simple graphical overview of the method. The problem consists of multiple investment periods ($p \in \mathbf{P}$), each representing an opportunity to modify plant configuration for the next periods (e.g. One period representing one year in a time horizon of 20 years). Each period consists of a single or multiple time steps ($t \in \mathbf{TT}_p$), which are used to divide their corresponding period into smaller time segments (e.g. seasons, months, days etc.), representing different operational modes. Investment decisions are made at the beginning of each period and the system is operated within the boundaries of those decisions in the time steps of the period.

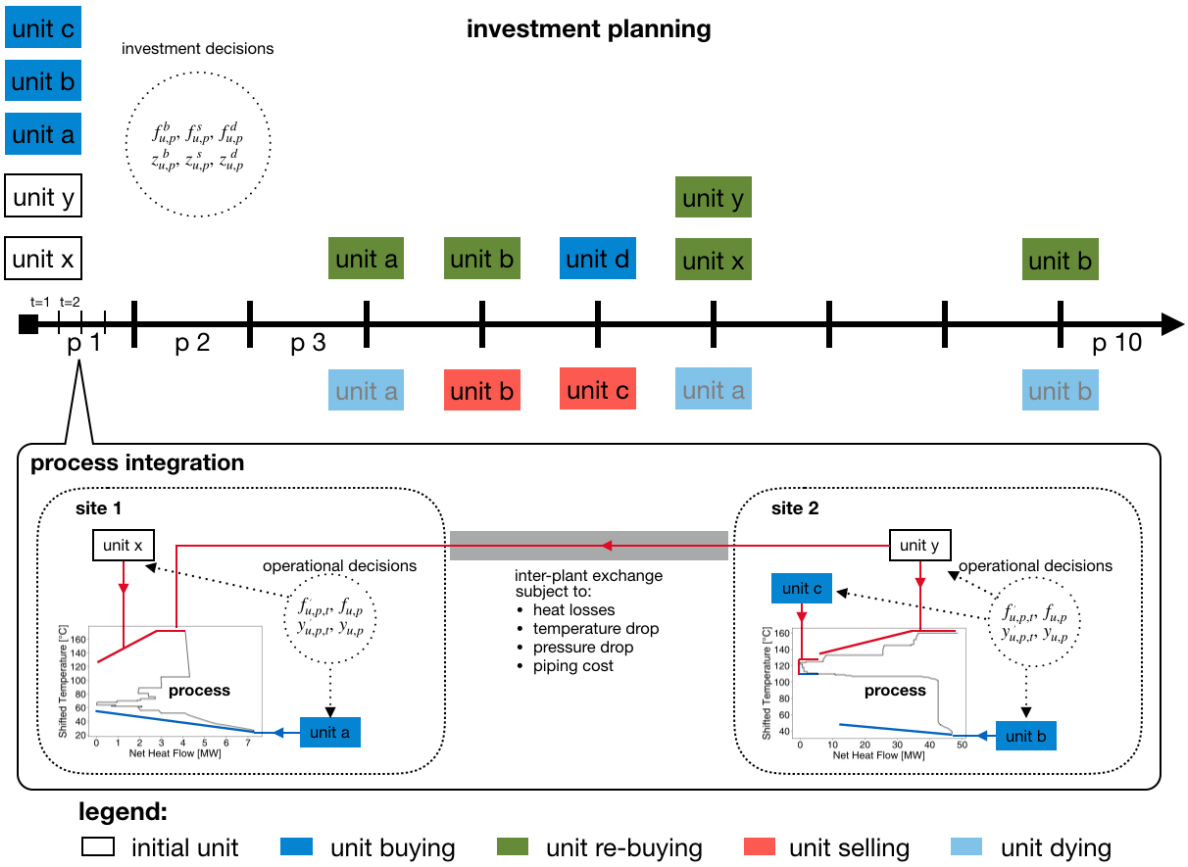

Figure 4.1 – Overview of the PIIP method.

The objective function is selected as the NPV of the system, as given in Equation 4.1. NPV is the sum of the cash flows in the periods, discounted by the expected interest rate. Including the interest rate

in the calculations makes it possible to distinguish investments in different periods.

$$\min NPV \tag{4.1}$$

$$NPV = \sum_{p \in \mathbf{P}} \left[\frac{C_p^{cf}}{(1+\mathrm{i})^p} \right] \tag{4.2}$$

where C_p^{cf} is the cash flow in period $p \in \mathbf{P}$ and i is the expected interest rate. While the PI model is adapted from [74], a novel formulation for investment planning and economic analysis is proposed and integrated to PI. Thus, the main focus in this section is describing the equations governing investment planning and economic analysis. For a clear representation of the method, the PI model is discussed briefly, followed by a detailed description of the investment planning formulation and economic model.

4.3.1 Process integration

The PI model is based on energy and resource balances. Demand and supply of energy and resources are modelled using units. The system includes two types of units in terms of their operation, namely process units ($pu \in \mathbf{PU}$) and utility units ($uu \in \mathbf{UU}$). Process units represent manufacturing of products and hence have fixed size and operation, whereas utility units satisfy demands from process units and have flexible size and operation. The units in the system are clustered with respect to their locations ($lc \in \mathbf{LC}$). The heat balance is closed within each location with hot ($h \in \mathbf{HS}_{lc}$) and cold ($c \in \mathbf{CS}_{lc}$) streams from the units. Heat cascade constraints are added to ensure that heat flows from hot streams to cold streams in each temperature interval ($k \in \mathbf{K}_{lc}$), and from higher to lower temperature. Resource balances are closed within each location and for each layer ($ly \in \mathbf{L}$) representing the resource type. The electricity balance, in contrast, is closed for the overall system — simulating that all units are connected to each other through the electrical grid. Heat and resource exchanges between locations are possible, but subject to heat losses, temperature and pressure drop, and requiring the associated infrastructure. Heat sharing from a location ($lc \in \mathbf{LC}$) to another location ($ol \in \mathbf{OL}_{lc}$) can be via two different transfer types ($tr \in \mathbf{TR}$) (underground or above-ground), while resource sharing is assumed to take place only through underground pipes. Heat and resource stream splitting constraints ensure that heat and resource balances are not violated for inter-location exchanges. Figure 4.2 illustrates the main equations of the PI model. Further details on it can be found in [74];

Sizing and scheduling: process units

$$f'_{u,p,t} = 1 \quad \forall\, u \in \mathbf{PU},\, p \in \mathbf{P},\, t \in \mathbf{TT}_p$$

$$f_u = 1 \quad \forall\, u \in \mathbf{PU},\, p \in \mathbf{P}$$

$$y'_{u,t} = 1 \quad \forall\, u \in \mathbf{PU},\, p \in \mathbf{P},\, t \in \mathbf{TT}_p$$

$$y_{u,p} = 1 \quad \forall\, u \in \mathbf{PU},\, p \in \mathbf{P}$$

Sizing and scheduling: utility units

$$\mathrm{F}^{\min}_{u,p} \cdot y'_{u,p} \leq f'_{u,p} \leq \mathrm{F}^{\max}_{u,p} \cdot y'_{u,p} \quad \forall\, u \in \mathbf{UU},\, p \in \mathbf{P}$$

$$f'_{u,p,t} \leq f'_{u,p} \quad \forall\, u \in \mathbf{UU},\, p \in \mathbf{P},\, t \in \mathbf{TT}_p$$

$$\mathrm{F}^{\min}_{u,p,t} \cdot y'_{u,p,t} \leq f'_{u,p,t} \leq \mathrm{F}^{\max}_{u,p,t} \cdot y'_{u,p,t} \quad \forall\, u \in \mathbf{UU},\, p \in \mathbf{P},\, t \in \mathbf{TT}_p$$

$$y'_{u,p,t} \leq y'_{u,p} \quad \forall\, u \in \mathbf{UU},\, p \in \mathbf{P},\, t \in \mathbf{TT}_p$$

Heat cascade

$$\Big(\sum_{i \in \mathbf{HS}_{lc,k}} \dot{\mathrm{q}}_{i,k,p,t} \cdot s_{i,p,t}\Big) - \Big(\sum_{j \in \mathbf{CS}_{lc,k}} \dot{\mathrm{q}}_{j,k,p,t} \cdot s_{j,p,t}\Big) - \dot{R}_{lc,k,p,t} = 0 \quad \forall\, lc \in \mathbf{LC},\, k \in \mathbf{K}_{lc},\, p \in \mathbf{P},\, t \in \mathbf{TT}_p$$

$$\dot{R}_{lc,k,p,t} = 0 \quad \forall\, lc \in \mathbf{LC},\, p \in \mathbf{P},\, t \in \mathbf{TT}_p,\, k = first(\mathbf{K}_{lc})\ or\ k = last(\mathbf{K}_{lc})$$

$$f'_{u,p,t} = s_{s,p,t} \quad \forall\, u \in \mathbf{U},\, s \in \mathbf{H}_u,\, p \in \mathbf{P},\, t \in \mathbf{TT}_p :\ s \notin \mathbf{HI}$$

Heat stream splitting

$$f'_{u,p,t} = \sum_{lc \in \mathbf{LC}} \sum_{tr \in \mathbf{TR}} b_{sp,lc,tr,p,t} \quad \forall\, u \in \mathbf{U},\, sp \in \mathbf{SP}_u,\, p \in \mathbf{P},\, t \in \mathbf{TT}_p$$

$$s_{s,p,t} = b_{sp,lc,tr,p,t} \quad \forall\, sp \in \mathbf{SP},\, lc \in \mathbf{LC},\, tr \in \mathbf{TR},\, p \in \mathbf{P},\, t \in \mathbf{TT}_p$$

Resource balance

$$\dot{\mathrm{m}}^{\mathrm{in}}_{ly,u,p,t} \cdot f'_{u,p,t} = \dot{M}^{in}_{u,p,t} \quad \forall\, ly \in \mathbf{L},\, u \in \mathbf{U}_{ly},\, p \in \mathbf{P},\, t \in \mathbf{TT}_p$$

$$\dot{\mathrm{m}}^{\mathrm{out}}_{ly,u,p,t} \cdot f'_{u,p,t} = \dot{M}^{out}_{u,p,t} \quad \forall\, ly \in \mathbf{L},\, u \in \mathbf{U}_{ly},\, p \in \mathbf{P},\, t \in \mathbf{TT}_p$$

$$\sum_{u \in \mathbf{U}_{ly}} \dot{M}^{in}_{u,p,t} = \sum_{u \in \mathbf{U}_{ly}} \dot{M}^{out}_{u,p,t} \quad \forall\, ly \in \mathbf{L},\, p \in \mathbf{P},\, t \in \mathbf{TT}_p$$

Resource stream splitting

$$\sum_{ol \in \mathbf{OL}_{lc}} \sum_{u \in \mathbf{U}_{ly,ol}} \dot{\mathrm{m}}^{out}_{u,p,t} \cdot a^{out}_{ly,ol,lc,u,p,t} + \sum_{u \in \mathbf{U}_{ly,lc}} \dot{M}^{out}_{u,p,t} = \sum_{ol \in \mathbf{OL}_{lc}} \sum_{u \in \mathbf{U}_{ly,ol}} \dot{\mathrm{m}}^{out}_{u,p,t} \cdot a^{out}_{ly,lc,ol,u,p,t} + \sum_{u \in \mathbf{U}_{ly,lc}} \dot{M}^{in}_{u,p,t} \quad \forall\, ly \in \mathbf{L},\, lc \in \mathbf{LC},\, p \in \mathbf{P},\, t \in \mathbf{TT}_p$$

Electricity balance

$$\sum_{u \in \mathbf{U}} \dot{E}^{in}_{u,p,t} = \sum_{u \in \mathbf{U}} \dot{E}^{out}_{u,p,t} \quad \forall\, p \in \mathbf{P},\, t \in \mathbf{TT}_p$$

Figure 4.2 – Formulation of the PI problem from [74].

4.3.2 Investment planning model

The investment planning model consists of a set of constraints, which ensure that investment actions are logical. Such actions include commissioning and decommissioning of units as well as installation of pipes for heat and resource sharing between sites. Since process units ($pu \in \mathbf{PU}$) have fixed operation, they cannot be bought or sold, which excludes them from investment analysis. The other units are classified into main groups from the investment perspective, defined as sets in the

formulation:

- **BU**: The set of base case units. These units exist in the initial system in which the plants are operated business as usual. Thus, they do not need to be purchased initially;
- **NU**: The set of new units. This set consists of units that can potentially improve the efficiency of the plants (e.g. heat pumps) but currently do not exist on the sites. Therefore, they must be purchased before using them;
- **IU**: The set of investment units. This set includes base case and new units and it present to simplify the formulation, $\therefore \mathbf{IU} \subset \mathbf{UU} = \mathbf{BU} \cup \mathbf{NU}$.

At the beginning of each period ($p \in \mathbf{P}$), an investment unit $u \in \mathbf{IU}$ can be commissioned or decommissioned. While commissioning refers to the purchase and installation of the unit, decommissioning can either reflect selling the unit or using it until the end of its lifetime. Each of these actions are modelled with binary decision variables $z^b_{u,p}$ for purchasing, $z^s_{u,p}$ for selling and $z^d_{u,p}$ for reaching EoL, respectively. For a given time horizon, these actions can happen more than once. For example, a unit can be re-purchased if it is has been decommissioned at the beginning of the same period or before. It is also possible to take a commissioning and decommissioning action on the same unit in the same period. This gives flexibility to the system to re-purchase units which recently reached EoL or were sold.

4

Investment decisions are chronological and interdependent. For instance, a new unit ($u \in \mathbf{NU}$) has to be commissioned before it is decommissioned. Another binary variable, $z^e_{u,p}$, is introduced to the problem to define units' existence and govern the relationship between the investment decisions. If a unit exists, it cannot be re-purchased before decommissioning it. This also prevents progressive installation and phasing out of a unit.

A new unit ($u \in \mathbf{NU}$) exists (i.e. $z^e_{u,p} = 1$) if it has been purchased and has not yet been decommissioned. The same applies to the base case units ($u \in \mathbf{BU}$) except that they already exist in the beginning of the project. These existence constraints are imposed by Equation 4.3 and Equation 4.4, respectively.

$$z^e_{u,p} = \sum_{pp \in \{1..p\}} (z^b_{u,pp} - z^s_{u,pp} - z^d_{u,pp}) \quad \forall\, u \in \mathbf{NU},\ p \in \mathbf{P} \tag{4.3}$$

$$z^e_{u,p} = 1 + \sum_{pp \in \{1..p\}} (z^b_{u,pp} - z^s_{u,pp} - z^d_{u,pp}) \quad \forall\, u \in \mathbf{BU},\ p \in \mathbf{P} \tag{4.4}$$

An investment unit ($u \in \mathbf{IU}$) in a period ($p \in \mathbf{P}$) can be decommissioned only if it exists in the previous period (see Equation 4.5). This constraint applies to all periods except the first. In the first period, a new unit ($u \in \mathbf{NU}$) cannot be decommissioned (see Equation 4.6) because it either does not exist or

has just been purchased. Conversely, a base case unit can be decommissioned in the first period (see Equation 4.7).

$$z^d_{u,p} + z^s_{u,p} \leq z^e_{u,p-1} \quad \forall\, u \in \mathbf{IU},\ p \in \mathbf{P} : p \neq 1 \tag{4.5}$$

$$z^d_{u,p} + z^s_{u,p} = 0 \quad \forall\, u \in \mathbf{NU},\ p \in \mathbf{P} : p = 1 \tag{4.6}$$

$$z^d_{u,p} + z^s_{u,p} \leq 1 \quad \forall\, u \in \mathbf{BU},\ p \in \mathbf{P} : p = 1 \tag{4.7}$$

In PI, utility units are sized according to the requirements of process units. When a utility unit is defined, it has a reference size (e.g. 100 kW boiler), which is scaled with respect to the demand, using a continuous variable, $f_{u,p}$ [74]. The same method is used to determine the real size of the investment units; they are defined with reference sizes and scaled with continuous variables (f) to determine the size of the equipment that is commissioned or decommissioned. Although f is literally a scaling factor, it is referred to as size in this formulation, for simplicity.

The purchase size of a unit, $f^b_{u,p}$, must be within a logical range, which reflects the minimum and maximum sizes of the technology available in the market. This is enforced by Equation 4.8, which also links the binary and continuous variables unit procurement.

$$z^b_{u,p} \cdot \mathrm{F}^{\min}_u \leq f^b_{u,p} \leq z^b_{u,p} \cdot \mathrm{F}^{\max}_u \quad \forall\, u \in \mathbf{IU},\ p \in \mathbf{P} \tag{4.8}$$

The available size of an investment unit ($u \in \mathbf{IU}$) changes throughout periods because of investment decisions. For example, a unit available with a certain size might be sold in a period and purchased again with a larger size in a subsequent period. A continuous variable, $f^e_{u,p}$, is introduced in the formulation to obtain the existing size of a unit in a given period. The base case units ($u \in \mathbf{BU}$) are defined with an initial size ($\mathrm{F}^{\mathrm{init}}_u$) according to the actual capacity of the equipment on the site, as they exist in the beginning, while the initial size of new units is zero (i.e. $\mathrm{F}^{\mathrm{init}}_u = 0 \quad \forall\, u \in \mathbf{NU}$). In the first period, the existing size is equal to the sum of the initial size and the difference between the commissioned and decommissioned sizes.

$$f^e_{u,p} = \mathrm{F}^{\mathrm{init}}_u + f^b_{u,p} - (f^s_{u,p} + f^d_{u,p}) \quad \forall\, u \in \mathbf{IU},\ p \in \mathbf{P} : p = 1 \tag{4.9}$$

where $f^s_{u,p}$ and $f^d_{u,p}$ are decommissioned sizes for selling and dying, respectively. In the other periods,

the existing size is equal to the sum of what remained from the previous period and the difference between the commissioned and decommissioned sizes (Equation 4.10).

$$f^{e}_{u,p} = f^{e}_{u,p-1} + f^{b}_{u,p} - (f^{s}_{u,p} + f^{d}_{u,p}) \quad \forall\, u \in \mathbf{IU},\ p \in \mathbf{P} : p \neq 1 \tag{4.10}$$

As progressive decommissioning is not allowed, the size that is phased out by decommissioning ($f^{s}_{u,p}$ or $f^{d}_{u,p}$) is equal to the size that existed before. In the first period, only the base case units ($u \in \mathbf{BU}$) can be decommissioned. Equations 4.11 and 4.12 ensure that the decommissioned size takes the value of the initial size if one of the decommissioning actions is taken.

$$f^{s}_{u,p} = \mathrm{F}^{\mathrm{init}}_{u} \cdot z^{s}_{u,p} \quad \forall\, u \in \mathbf{BU},\ p \in \mathbf{P} : p = 1 \tag{4.11}$$

$$f^{d}_{u,p} = \mathrm{F}^{\mathrm{init}}_{u} \cdot z^{d}_{u,p} \quad \forall\, u \in \mathbf{BU},\ p \in \mathbf{P} : p = 1 \tag{4.12}$$

In the other periods, the decommissioned size is equal to the existing size from the previous period. This constraint is expressed in non-linear terms in Equations 4.13 and 4.14 and linearised in Appendix D.1.

4

$$f^{s}_{u,p} = f^{e}_{u,p-1} \cdot z^{s}_{u,p} \quad \forall\, u \in \mathbf{IU},\ p \in \mathbf{P} : p \neq 1 \tag{4.13}$$

$$f^{d}_{u,p} = f^{e}_{u,p-1} \cdot z^{d}_{u,p} \quad \forall\, u \in \mathbf{IU},\ p \in \mathbf{P} : p \neq 1 \tag{4.14}$$

A unit can be used only as long as its lifetime. The remaining life ($l_{u,p}$) is defined as an integer variable which also depends on investment decisions. The constraints given in Equations 4.15–4.21 govern the relationship between the unit life and the rest of the formulation:

- A unit can exist only if it has a remaining life (Equation 4.15);
- Only the existing units have a remaining life (Equation 4.16);
- In the first period, the remaining life is equal to either the life span (for new units) or the difference between the life span and the initial age (base case units) (Equation 4.17);
- In the other periods, the remaining life decreases compared from the previous period by one period. In addition, buying actions increase the remaining lifetime while selling decreases it (Equation 4.18);
- A unit can be purchased again only after it is decommissioned (Equation 4.19);

- A unit dies only if its lifetime in the previous period is one year (Equation 4.20);
- A unit can be sold only if its lifetime in the previous period is two years or more (Equation 4.21);

$$z^e_{u,p} \leq l_{u,p} \quad \forall\, u \in \mathbf{IU},\ p \in \mathbf{P} \tag{4.15}$$

$$l_{u,p} \leq z^e_{u,p} \cdot \mathrm{LI}^{\mathrm{lt}}_u \quad \forall\, u \in \mathbf{IU},\ p \in \mathbf{P} \tag{4.16}$$

$$l_{u,p} = \left(z^b_{u,p} \cdot \mathrm{LI}^{\mathrm{lt}}_u\right) + \left(\mathrm{LI}^{\mathrm{lt}}_u - \mathrm{LI}^{\mathrm{init}}_u\right) \cdot \left(1 - z^s_{u,p} - z^d_{u,p}\right) \quad \forall\, u \in \mathbf{IU},\ p \in \mathbf{P} : p = 1 \tag{4.17}$$

$$l_{u,p} = l_{u,p-1} - z^e_{u,p-1} + \left(\mathrm{LI}^{\mathrm{lt}}_u \cdot z^b_{u,p}\right) - l^s_{u,p} \quad \forall\, u \in \mathbf{IU},\ p \in \mathbf{P} : p \neq 1 \tag{4.18}$$

$$l_{u,p-1} - l^s_{u,p} \leq \left(1 - z^b_{u,p}\right) \cdot \mathrm{LI}^{\mathrm{lt}}_u + 1 \quad \forall\, u \in \mathbf{IU},\ p \in \mathbf{P} : p \neq 1 \tag{4.19}$$

$$l_{u,p-1} \leq \left(1 - z^d_{u,p}\right) \cdot \mathrm{LI}^{\mathrm{lt}}_u + 1 \quad \forall\, u \in \mathbf{IU},\ p \in \mathbf{P} : p \neq 1 \tag{4.20}$$

$$\left(1 - z^e_{u,p-1}\right) \cdot \mathrm{LI}^{\mathrm{lt}}_u + \left(1 - z^s_{u,p-1}\right) \cdot \mathrm{LI}^{\mathrm{lt}}_u + l_{u,p-1} \leq 2 \quad \forall\, u \in \mathbf{IU},\ p \in \mathbf{P} : p \neq 1 \tag{4.21}$$

where $\mathrm{LI}^{\mathrm{lt}}_u$ is the unit life span, $\mathrm{LI}^{\mathrm{init}}_u$ is the initial age and $l^s_{u,p}$ is the life of the unit at the period it is sold. $l^s_{u,p}$ is equal to the remaining life of the unit if it is sold and zero otherwise. This is ensured by Equations 4.22–4.24.

$$l^s_{u,p} \geq l_{u,p-1} - z^e_{u,p-1} - \left(1 - z^s_{u,p-1}\right) \cdot \mathrm{LI}^{\mathrm{lt}}_u \quad \forall\, u \in \mathbf{NU},\ p \in \mathbf{P} : p \neq 1 \tag{4.22}$$

$$l^s_{u,p} \leq l_{u,p-1} - z^e_{u,p-1} \quad \forall\, u \in \mathbf{NU},\ p \in \mathbf{P} : p \neq 1 \tag{4.23}$$

$$l^s_{u,p} \leq z^s_{u,p-1} \cdot \mathrm{LI}^{\mathrm{lt}}_u \quad \forall\, u \in \mathbf{NU},\ p \in \mathbf{P} : p \neq 1 \tag{4.24}$$

A unit can be used only if it exists and as much as its existing size. Equations 4.25 and 4.26 impose

such existence constraints and connect the investment planning model with PI.

$$y_{u,p} \leq z^{e}_{u,p} \quad \forall\, u \in \mathbf{IU},\ p \in \mathbf{P} \tag{4.25}$$

$$f_{u,p} \leq f^{e}_{u,p} \quad \forall\, u \in \mathbf{IU},\ p \in \mathbf{P} \tag{4.26}$$

where $y_{u,p}$ is a binary decision variable for whether a unit is used or not and $f_{u,p}$ is a continuous decision variable reflecting the used capacity. Investment planning constraints for heat and resource sharing pipes are similar to those for units, though with a few added constraints to reflect industrial reality. Pipelines are long-lasting and, once installed, are used until the end of their useful service. The formulation for pipelines therefore eliminates the possibility of decommissioning and the lifetime is considered to extend beyond the planning horizon. Thus, investment decisions on pipes can be reduced to a decision on procurement alone. Detailed equations governing the investment planning for pipes are given in Appendix D.2.

4.3.3 Economic model

The economic model comprises constraints to calculate cash flows and thus serves as a link between the investment planning model and the objective function. At the beginning of each period, investment actions are taken to either commission or decommission units and purchase pipes for heat and resource sharing between sites. Investment in units and pipes is considered as negative cash flow, while decommissioning actions are reflected as positive cash flow, since even at EoL, units retain some monetary value (i.e. scrap value). In addition, units are operated during each period, consuming resources, such as natural gas and electricity, which are reflected as negative cash flow. With retrofit investments within and between sites, the current operating bill is reduced which is considered as a positive cash flow. The net cash flow in a given period is calculated by summing the positive and negative flows as in Equation 4.27.

$$C^{cf}_{p} = \left(C^{s}_{p} + C^{sc}_{p} - C^{inv}_{p}\right) + \left(\mathrm{c}^{\,\mathrm{op_{cur}}} - C^{op}_{p}\right) \quad \forall\, p \in \mathbf{P} \tag{4.27}$$

where C^{s}_{p} and C^{sc}_{p} represent income from selling units and scrap, C^{op}_{p} and C^{inv}_{p} are the investment and operating costs and $\mathrm{c}^{\,\mathrm{op_{cur}}}$ is the current operating bill without any energy efficiency improvement. The operating cost is calculated using Equation 4.28 accounting for fixed cost (e.g. maintenance) associated with the activation of the units and variable cost associated with the unit

sizes.

$$C_p^{op} = \sum_{u \in \mathbf{U}} \left[\sum_{t \in \mathbf{TT}_p} \left(\mathrm{c}_u^{\mathrm{op1}} \cdot y_{u,p} + \mathrm{c}_u^{\mathrm{op2}} \cdot f_{u,p} \right) \cdot \Delta \mathrm{t}_t^{\mathrm{op}} \right] \quad \forall\, u \in \mathbf{U},\ p \in \mathbf{P} \tag{4.28}$$

where $\mathrm{c}_u^{\mathrm{op1}}$ and $\mathrm{c}_u^{\mathrm{op2}}$ are fixed and variable operating costs and $\Delta \mathrm{t}_t^{\mathrm{op}}$ is the operating time. According to the guidelines suggested by [34], the investment cost of a unit corresponds to the bare module cost, which comprises the purchase cost of the equipment, materials (e.g. fittings), labour, freight, overhead and engineering costs. For piping cost, a function including trenching is used [74]. Details of the piping economic calculations are given in Appendix D.3. Equation 4.29 is used to calculate the total investment cost in a given period. The investments are, when applicable, constrained with overall and annual budget limits which is explained in detail in Appendix D.4 as well.

$$C_p^{inv} = \sum_{u \in \mathbf{IU}} \left(C_{u,p}^{b} + C_{u,p}^{mt} + C_{u,p}^{lr} C_{u,p}^{fr} + C_{u,p}^{oh} + C_{u,p}^{en} \right) + C_p^{ph} + C_p^{pr} \quad \forall\, p \in \mathbf{P} \tag{4.29}$$

where $C_{u,p}^{b}$, $C_{u,p}^{mt}$, $C_{u,p}^{lr}$, $C_{u,p}^{fr}$, $C_{u,p}^{oh}$, $C_{u,p}^{en}$ are the purchasing, materials, labour, freight, overhead and engineering costs of the units and C_p^{ph} and C_p^{pr} are heat and resource piping costs. Purchase cost is calculated based on the investment decisions $z_{u,p}^{b}$ and $f_{u,p}^{b}$ in Equation 4.30. All the other components of the bare module cost are calculated as a fraction of the purchase cost in Equations 4.31–4.35. In the case of re-buying a unit, although investment on the equipment itself, labour, freight and overhead is required again, re-investing in materials and engineering can be avoided. Thus, materials and engineering costs apply only to new units $u \in \mathbf{NU}$, when they are purchased for the first time.

$$C_{u,p}^{b} = \mathrm{c}_u^{\mathrm{inv1}} \cdot z_{u,p}^{b} + \mathrm{c}_u^{\mathrm{inv2}} \cdot f_{u,p}^{b} \quad \forall\, u \in \mathbf{IU},\ p \in \mathbf{P} \tag{4.30}$$

$$C_{u,p}^{mt} = C_{u,p}^{b} \cdot \mathrm{F}_u^{\mathrm{mt}} \cdot \left(1 - z_{u,p}^{bb} \right) \quad \forall\, u \in \mathbf{NU},\ p \in \mathbf{P} \tag{4.31}$$

$$C_{u,p}^{lr} = C_{u,p}^{b} \cdot \mathrm{F}_u^{\mathrm{lr}} \quad \forall\, u \in \mathbf{IU},\ p \in \mathbf{P} \tag{4.32}$$

$$C_{u,p}^{fr} = C_{u,p}^{b} \cdot \mathrm{F}_u^{\mathrm{fr}} \quad \forall\, u \in \mathbf{IU},\ p \in \mathbf{P} \tag{4.33}$$

$$C_{u,p}^{oh} = C_{u,p}^{b} \cdot \mathrm{F}_u^{\mathrm{oh}} \quad \forall\, u \in \mathbf{IU},\ p \in \mathbf{P} \tag{4.34}$$

$$C^{en}_{u,p} = C^{b}_{u,p} \cdot \mathrm{F}^{\mathrm{en}}_{u} \cdot \left(1 - z^{bb}_{u,p}\right) \quad \forall\, u \in \mathbf{NU},\ p \in \mathbf{P} \tag{4.35}$$

where $\mathrm{F}^{\mathrm{mt}}_{u}$, $\mathrm{F}^{\mathrm{lr}}_{u}$, $\mathrm{F}^{\mathrm{fr}}_{u}$, $\mathrm{F}^{\mathrm{oh}}_{u}$, $\mathrm{F}^{\mathrm{en}}_{u}$ are cost factors for materials, labour, freight, overhead and engineering, $\mathrm{c}^{\mathrm{inv1}}_{u}$ and $\mathrm{c}^{\mathrm{inv2}}_{u}$ are fixed and variable investment cost parameters related to the existence and size of the units, respectively, and $z^{bb}_{u,p}$ is a binary variable which is activated if a unit has been previously purchased. While the cost factors are adapted from [34], the investment cost parameters are derived using equipment cost functions. Equations 4.31 and 4.35 are non-linear equations, replaced by a set of linear constraints, the details of which are given in Appendix D.5. The binary variable $z^{bb}_{u,p}$ takes the value 1 if its corresponding unit has been purchased in one of the previous periods and 0 otherwise. This is ensured by Equations 4.36–4.38.

$$z^{bb}_{u,p} = 0 \quad \forall\, u \in \mathbf{NU},\ p \in \mathbf{P} : p = 1 \tag{4.36}$$

$$z^{bb}_{u,p} \leq \sum_{pp \in \{1..p-1\}} z^{b}_{u,pp} \quad \forall\, u \in \mathbf{NU},\ p \in \mathbf{P} : p \neq 1 \tag{4.37}$$

4

$$z^{bb}_{u,p} \geq z^{b}_{u,pp} \quad \forall\, u \in \mathbf{NU},\ p \in \mathbf{P}, pp \in \{1..p-1\} : p \neq 1 \tag{4.38}$$

After a unit is purchased, it starts to lose its economic value. A double declining depreciation method is used in this work, as it is more realistic compared to straight line depreciation [34]. In the first period, only the base case units have remaining value, while this value is zero for new units (Equations 4.39 and 4.40). In the other periods, remaining value and depreciation are calculated with respect to each other and the investment decisions (see Equations 4.41 and 4.42).

$$C^{rv}_{u,p} = \mathrm{c}^{\mathrm{b}}_{u} \cdot \left(1 - 2 \cdot \mathrm{r}^{\mathrm{dep}}_{u}\right)^{\mathrm{LI}^{\mathrm{init}}_{u}} \quad \forall\, u \in \mathbf{BU},\ p \in \mathbf{P} : p = 1 \tag{4.39}$$

$$C^{rv}_{u,p} = 0 \quad \forall\, u \in \mathbf{NU},\ p \in \mathbf{P} : p = 1 \tag{4.40}$$

$$C^{rv}_{u,p} = \left(C^{b}_{u,p-1} - C^{sv}_{u,p-1} - C^{dv}_{u,p-1}\right) + C^{rv}_{u,p-1} - C^{dep}_{u,p-1} \quad \forall\, u \in \mathbf{IU},\ p \in \mathbf{P} : p \neq 1 \tag{4.41}$$

$$C^{dep}_{u,p} = \left[\left(C^{b}_{u,p} - C^{sv}_{u,p} - C^{dv}_{u,p}\right) + C^{rv}_{u,p}\right] \cdot \mathrm{r}^{\mathrm{dep}}_{u} \quad \forall\, u \in \mathbf{IU},\ p \in \mathbf{P} \tag{4.42}$$

$C^{rv}_{u,p}$, $C^{dep}_{u,p}$, $C^{sv}_{u,p}$ and $C^{dv}_{u,p}$ are remaining, depreciated, sold, and EoL values, c^{b}_{u} is the purchase cost of the base case units and r^{dep}_{u} is the depreciation rate. $C^{dv}_{u,p}$ and $C^{sv}_{u,p}$ are continuous variables that take the remaining value of the unit if it reaches EoL or is sold, respectively. The relationship between them and the remaining value is enforced by Equations 4.43 and 4.44. The conversion of these non-linear equations into a set of linear constraints is explained in Appendix D.6.

$$C^{sv}_{u,p} = C^{rv}_{u,p} \cdot z^{s}_{u,p} \quad \forall\, u \in \mathbf{IU},\ p \in \mathbf{P} \tag{4.43}$$

$$C^{dv}_{u,p} = C^{rv}_{u,p} \cdot z^{d}_{u,p} \quad \forall\, u \in \mathbf{IU},\ p \in \mathbf{P} \tag{4.44}$$

It is assumed that if a unit reaches EoL it retains its salvage value (c^{sal}_{u}), which is typically a small fraction of the initial investment (see Equation 4.45). Conversely, if it is sold before reaching EoL, the remaining value is the maximum of $C^{sv}_{u,p}$ and the salvage value, as given in Equation 4.46. The maximum function is non-linear; however, it can be converted to a set of linear equations is explained in Appendix D.7.

$$C^{sc}_{u,p} = c^{sal}_{u} \cdot z^{d}_{u,p} \quad \forall\, u \in \mathbf{IU},\ p \in \mathbf{P} \tag{4.45}$$

$$C^{s}_{u,p} = \max\left(C^{sv}_{u,p}, c^{sal}_{u}\right) \quad \forall\, u \in \mathbf{IU},\ p \in \mathbf{P} \tag{4.46}$$

4.3.4 Solution strategy

The MILP model presented in this work can be solved by commercial solvers such as Gurobi [150] or Cplex [151], using a linear programming-based branch and bound algorithm. However, if a large industrial case study with several plants is considered, the problem size increases drastically. This increase is related to the large number of units and to the number of potential connections between plants for heat and resource sharing purposes. Taking into account these aspects within a multi-period formulation considering a long time horizon makes the model computationally expensive, even simply for finding an integer feasible solution. To solve large scale problems without compromising model complexity, a solution strategy is proposed. Model testing identified piping between the plants to be the bottleneck. This can be explained due to the variety of heat and resource sharing media (e.g. steam at different pressure levels), directions (i.e. several candidates for excess heat) and modes (i.e. underground and above-ground). The suggested solution strategy solves the problem by initially neglecting plant connections, which provides a feasible integer solution. With this incumbent solution, the larger problem becomes tractable and can be solved to optimality

within a shorter time frame, as a result of reduced computational burden. Figure 4.3 schematically illustrates the solution strategy.

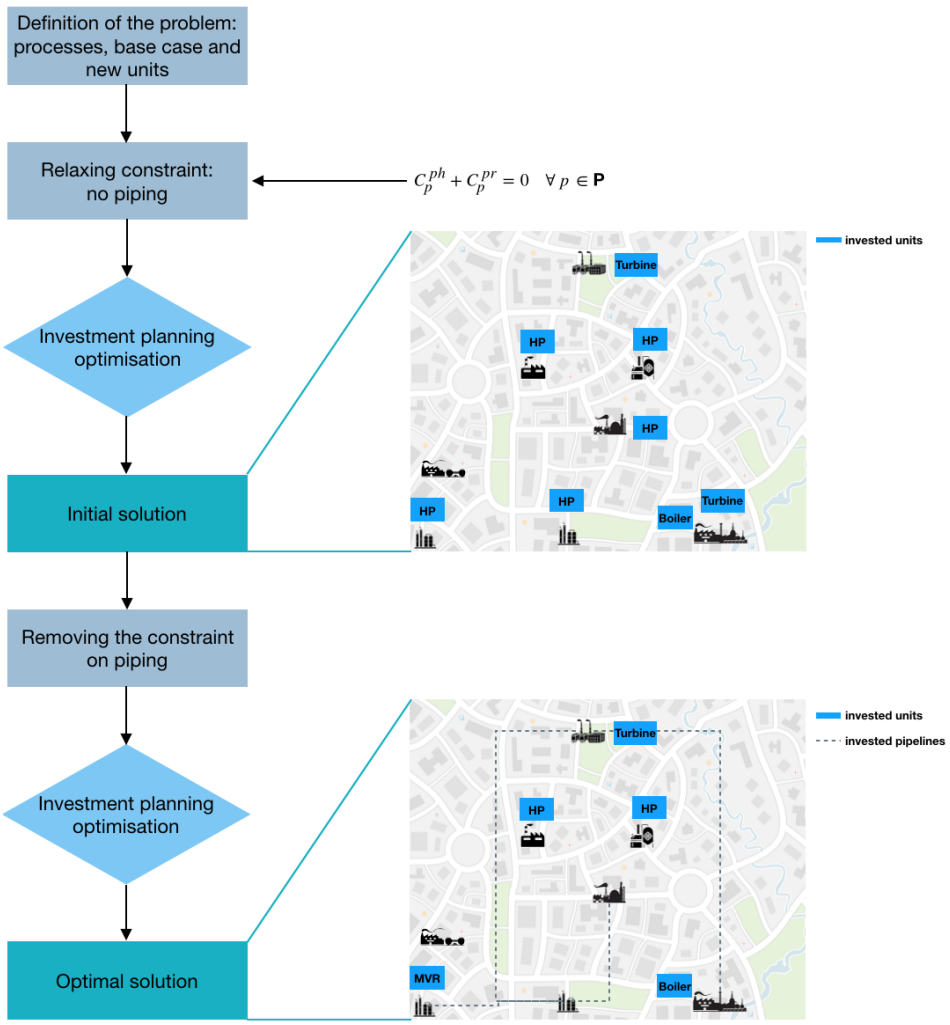

Figure 4.3 – Strategy for solving the problem in two steps; initialisation and optimisation.

4.3.5 Systematic generation of multiple solutions

Finding a single optimal solution in real industrial problems may be problematic as there are often practical constraints that cannot be accounted for in the mathematical programming framework. In such cases, it is beneficial to provide multiple solutions for industries to select that which best fits their interest. Parametric optimisation is a technique used to generate multiple solutions in a

systematic way aiming at optimising more than one objective function (see Equation 4.47) [152].

$$\min\ f(x,y), g(x,y) \tag{4.47}$$

The multi-objective optimisation problem is reformulated such that one of the objective function is optimised while the other one is constrained (see Equations 4.48 and 4.49) above or below certain parameters (i.e. ϵ) which are increased or decreased systematically resulting in a pool of optimal solutions.

$$\min\ f(x,y) \tag{4.48}$$

$$g(x,y) \leq \epsilon \tag{4.49}$$

Although the solution strategy presented in Section 4.3.4 decreases the computation time, it is not sufficient for parametric optimisation in which several optimisation runs are carried out. To solve the problem effectively and generate multiple interesting solutions, a different strategy is followed. First, the parametric optimisation problem is solved using [74], without considering investment planning, setting the objective as the sum of the annual operating and annualised utility investment costs while annualised piping cost is constrained with ϵ. This results in an initial solution pool with investment targets on piping between the plants as well as energy conversion technologies. Based on those targets, the binary variables to invest in pipes and units are fixed as well as the sizes of the pipes and PIIP is solved for each solution in the initial pool to determine the optimal timing for investments considering yearly and overall investment budgets. Figure 4.4 depicts the parametric optimisation solution strategy.

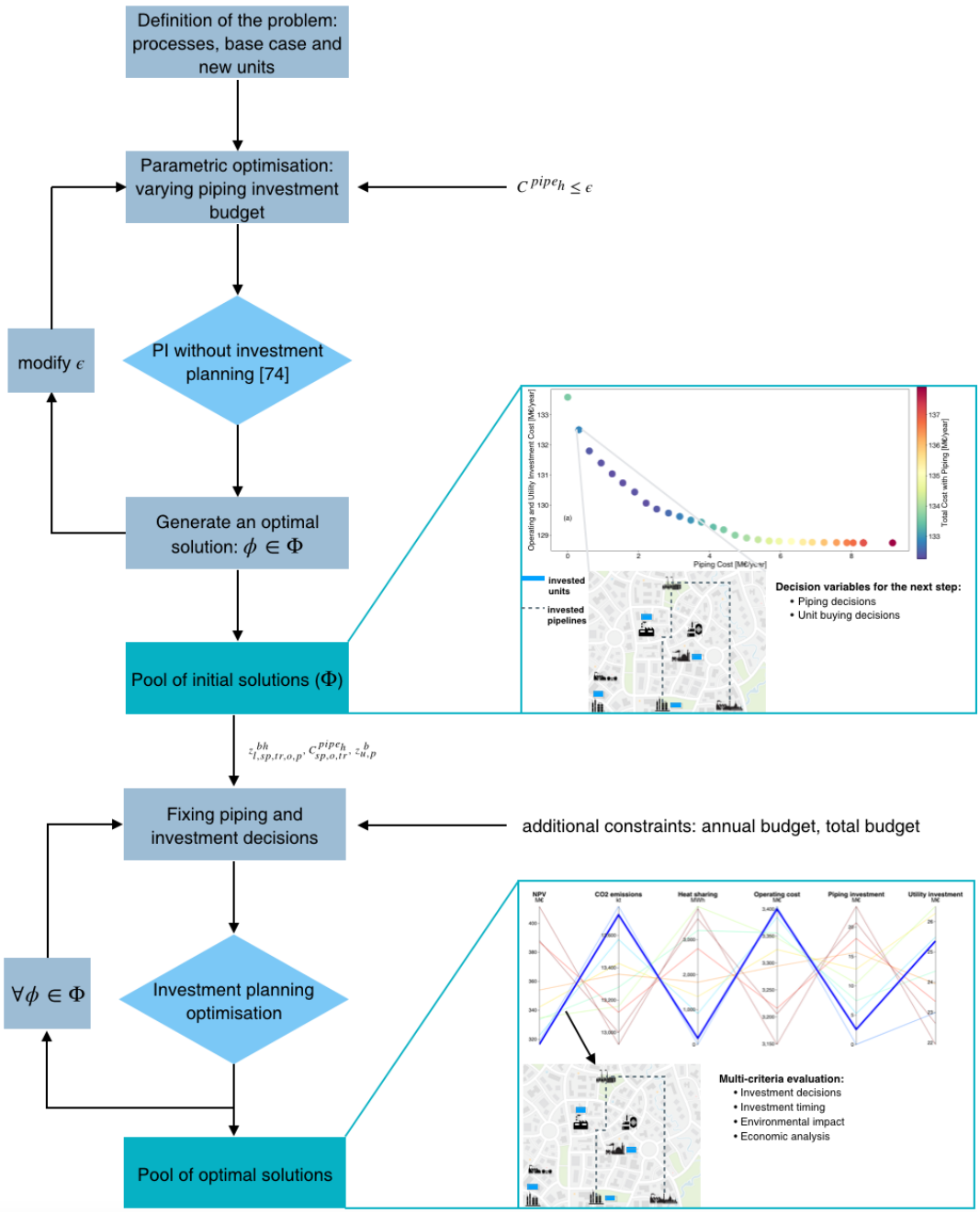

Figure 4.4 – Parametric optimisation solution strategy; targeting and optimising.

4.4 Case studies and utility systems

The case study is adapted from [74] and consists of nine locations. In eight of the locations there are industrial plants operating at their business as usual state, while a district is placed in one of

the locations, representing part of a city close to the corresponding industrial cluster. Energy and resource balances are closed within each location at the current state. Thus, all locations have access to the resources required for their operations (e.g. natural gas, electricity) as well as energy conversion systems (e.g. boiler) to provide the required services. As the focus of this work is energy consumption, the industrial plants and the district are modelled only using their energy flows, i.e. their electricity, hot and cold streams. The resources considered are, therefore, linked to provision of energy services, such as natural gas, electricity and water.

The models of the industrial plants are adapted from [16, 120] and scaled with the flowrate of the main product. The district model includes the demand for district services such as space heating, domestic hot water, cooling, refrigeration and electricity, representing a potential symbiosis with the industry by heat sharing. This model is adapted from [153] and scaled with a population of 50000 people, representing a typical medium-sized district. Figure 4.5 illustrates the overview of the case study with the locations and sizes of the sites.

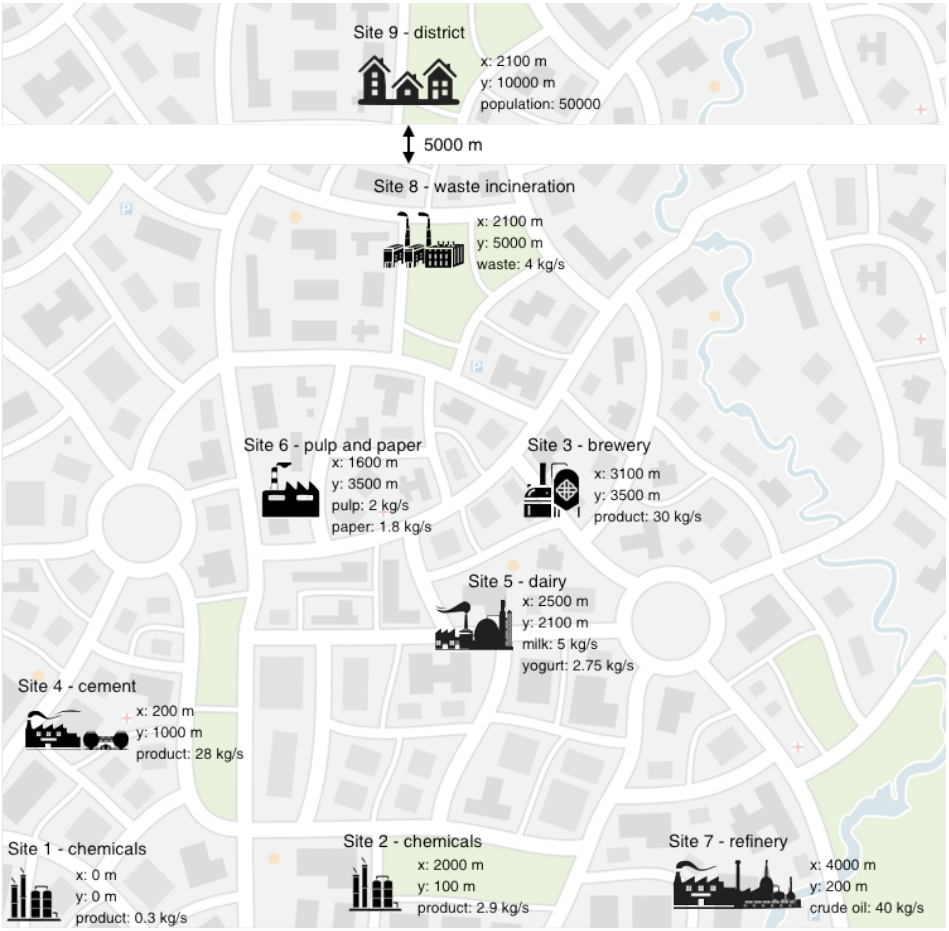

Figure 4.5 – Layout of the industrial cluster neighbouring a district.

Assuming consistent industrial production, the industrial plants are modelled with fixed production rates. In addition, production capacity expansion throughout the studied time horizon is not considered. Seasonal variations are considered in the district model, as the demand for the district services change drastically throughout a year. The population of the district is assumed to remain constant during the evaluated project time. A time horizon of 20 years is evaluated, each year corresponding to a period in the mathematical formulation.

4.4.1 Utility systems and resources

Utility systems include energy conversion technologies that currently exist on the sites, $u \in \mathbf{BU}$, and the ones which can be integrated to improve the system, $u \in \mathbf{NU}$. The utility systems of all the sites are included in the mass and energy balance analysis, but several are excluded from investment planning, namely:

- Site 4: The heating utility of the cement site is kiln, while cooling is carried out by air. Recovering the excess heat from the cement site and using it in other sites is not considered, as the technologies required are not mature enough. Thus, improvements in the utility system of the cement plant is not included in investment planning;
- Site 8: The waste incineration plant has a symbiosis potential by heat sharing with the other sites; however, improving the plant itself by integrating more efficient technologies is not studied in this work;
- Site 9: The district model is added in the case study to extend the potential of symbiosis. Except for sharing industrial excess heat with the district using a pipeline, improvements in the district utility system are not examined.

4.4.1.1 Existing technologies on the plants

Each plant is currently operated with conventional energy conversion technologies, such as boilers, steam networks, cooling circuits and towers. The existing technologies have the advantage that the investment has already been made, and hence do not require an initial investment. However, they are aged equipment and are often less efficient than the competitors available in the market (alternative technologies or more efficient, modern replacements).

Boilers

Boilers are the most common technology used in industrial plants to convert chemical energy into heat by combustion. All industrial plants in the case study, except for cement, have boilers, which currently supply their heating requirements. The boilers in this case study are modelled according to the guidelines suggested by [38]. Table 4.2 depicts the investment parameters (c^{inv1}, c^{inv2}) as well

as the initial size (F^{init}) and age (LI^{init}) of the boilers. The fixed and variable investment costs are calculated according to [154] and the life span is considered as 20 years, according to [155].

Table 4.2 – Existing boilers and their investment parameters.

Location	F^{init} [-]	c^{inv1} [k€]	c^{inv2} [k€]	LI^{init} [years]
Site 1	7	388	13	16
Site 2	62	388	13	12
Site 3	30	388	13	11
Site 5	19	388	13	9
Site 6	11	388	13	6
Site 7	190	388	13	8

Steam networks

Steam networks are used to distribute high temperature heat generated in boilers to the processes on site. Distributing heat using a steam network is advantageous, not only because steam is a good heat transfer fluid but also since electricity is co-generated by expanding high pressure steam through turbines. The steam network model of each site is built as a super-structure, following the method of [122].

Steam networks consist of turbines and steam production and distribution levels, called headers, which are simply pipelines. As the pipelines are already installed on the sites and have a long lifetime, it is assumed that only the turbines are involved in the investment planning decisions. The existing turbines and their investment parameters are depicted in Table 4.3. The investment cost parameters are calculated according to [34] and linearised to fit the MILP framework. The life span of turbines is assumed to be 20 years [155].

Table 4.3 – Existing steam network turbines and their investment parameters.

Location	Inlet [bar]	Outlet [bar]	F^{init}[-]	c^{inv1}[k€]	c^{inv2}[k€]	LI^{init}[years]
Site 1	45	24	1.3	64	22	16
Site 1	45	8	1.6	153	19	16
Site 2	45	24	12.2	64	22	12
Site 2	45	8	12.4	153	19	12
Site 3	45	2	13	232	16	11
Site 5	45	2	8	232	16	9
Site 6	45	4	5	195	18	6
Site 7	45	24	24	64	22	8
Site 7	45	8	14	153	19	8
Site 7	45	4	50	195	18	8

Cooling towers

The main cooling media in industrial plants are air and water. While heat from processes is discharged to the environment directly from aero-coolers, cooling water circuits first collect the excess heat in water and then release it to the environment via cooling towers. The cooling tower model in this work is adapted from [123]. Table 4.4 outlines the investment parameters of the cooling towers in the system. The life span of cooling towers is estimated to be 25 years [155] and the investment cost parameters are calculated according to [154].

Table 4.4 – Existing cooling and their investment parameters.

Location	F^{init}[-]	c^{inv1}[k€]	c^{inv2}[k€]	LI^{init}[years]
Site 1	9	82	13	15
Site 2	57	82	13	10
Site 3	22	82	13	3
Site 5	5	82	13	14
Site 6	2	82	13	6
Site 7	150	82	13	4

4.4.1.2 Additional technologies

Energy conversion technologies that can potentially improve the efficiency and operating cost of the system are considered as additional technologies. Although they are more efficient than the technologies already installed on the plants, they require investment, which might pose a barrier

to their purchase and installation. Appropriate additional technologies are selected based on the grand composite curves (GCCs) of the plants given in Section 3.4 and Appendix D.8.

Heat pumps

Heat pumps (HPs) are used to recover low temperature excess heat and upgrade it to a higher temperature. Site 1, 2, 5 and 7 have a potential for HP integration, as they have a pinch temperature at which HPs can operate and heat recovery is possible with a small temperature lift. The investment cost of HPs is calculated according to [34], considering that the main contributors are two heat exchangers (i.e. evaporator and condenser) and a compressor. The life span of the HPs is estimated as 15 years, according to [155]. Table 4.5 summarises the investment parameters of the HPs.

Table 4.5 – Potential heat pumps and their investment parameters.

Location	c^{inv1} [k€]	c^{inv2} [k€]	LI^{lt} [years]
Site 1	26	52	15
Site 2	556	216	15
Site 5	270	454	15
Site 7	305	217	15

Mechanical vapor recompression

Mechanical vapour recompression (MVR) works using a similar principle to HPs, but instead of using an intermediate fluid, vapor is compressed to a higher pressure and temperature. In this case study, sites 1, 3, and 6 have a potential for MVR integration, when importing 1 bar steam from the other sites and upgrading it to 2 bar steam. The investment parameters of the MVRs are calculated according to [34] and the life span is estimated as 15 years [155]. Table 4.6 shows the investment parameters of the MVRs.

Table 4.6 – Potential mechanical vapour recompression and their investment parameters.

Location	c^{inv1} [k€]	c^{inv2} [k€]	LI^{lt} [years]
Site 1	36	317	15
Site 3	151	261	15
Site 6	9	38	15

Internal combustion engines

Internal combustion engines (ICEs) are alternatives to industrial boilers. They have the advantage of co-generating heat and electricity. However, because of engine cooling water, they are applicable only for processes with low pinch point. In addition, they are not used for large scale applications. Hence, they can only partially replace boilers. Based on the preliminary analysis of the GCCs, sites 1, 3, 5 and 6 have a potential for ICE integration. The investment cost parameters of the engines are adapted from [16] as 117 k€ and 1169 k€ for the fixed and variable cost, respectively. The life span is estimated as 20 years [155].

4.5 Results and discussion

The method is applied to the case study following several scenarios and solution strategies. Section 4.5.1 determines investment planning without limitation on the budget, Section 4.5.2 studies the impact of seasonality in the investment decisions, Section 4.5.3 considers restricting the investment budget as well as the investment period, and Section 4.5.4 considers parametric optimisation to obtain multiple investment scenarios. Section 4.5.5 compares the solutions in Section 4.5.1 and Section 4.5.3, with the business as usual operations and investments of the industrial cluster.

4.5.1 Optimal investment decisions without budget constraints

Optimal investment planning for the system introduced in Section 4.4 is determined for a horizon of 20 years, without any budget constraints. The optimal NPV is obtained as 463 M€, considering operating and investment costs resulting in 7748 kt savings on CO_2 emissions. The investment decisions can be grouped in two; within the plants on energy conversion systems and between the plants on piping. The investment cost in the optimal solution totals 107 M€, dominated by investments in infrastructure within the plants, which represent 79%. Figure 4.6 depicts the results in terms of investment cost and the year of investment. To maintain simplicity and clarity, decommissioning is not included in the figure.

Cogeneration engines are installed in Site 1, 3, 5 and 6 as these sites have relatively low pinch points and thus allow such integration. In addition, heat pumps are integrated in Site 1, 2 and 7, taking advantage of transferring heat across the pinch point with a small temperature lift. Since heat pumps have a life span of 15 years, they reach their EoL before the end of the evaluated project period. For this reason, recurring investment is be observed; this also implies that their payback time is less than five years.

In addition to the integration of more efficient energy conversion technologies, the system is improved by installing steam pipes between the sites. Heat is shared using high-pressure steam (e.g.

10 bar) from Site 8 to 7 and low-pressure steam (e.g. 2 bar) from Site 8 to 6 and Site 2 to 9. Although Site 9 represents a heat sharing option with a longer distance compared to the other plants, it is still selected in the optimal solution, as the energy prices are higher for the district compared to the industries. Thus, replacing a district boiler with excess heat from the industry is more profitable than replacing an industrial boiler. Site 2 is selected as the main source to provide heat to Site 9, even though the distance is greater than to Site 8, due to economies of scale (i.e. more heat is available at Site 2 compared to Site 8) and since the heat from Site 8 is at higher temperature and can be used for other plants. A Similar phenomenon is observed in the distribution of heat from Site 8 to the other industrial sites; instead of multiple neighbouring sites (e.g. Site 3 and 5), heat is shared with Site 7, as it requires a higher amount, but installing only one pipeline.

Chronology of investments show that most occur in the first period. This is logical since investments yielding economic benefits should be made as soon as possible to take full advantage over the planning horizon. The few investments made in subsequent periods are replacements for equipment reaching their EoL. Investment in boilers in Site 1 and 2 are examples of such decisions. However, the boilers in Site 3 and 7 are repurchased in the first period, which might be related to the age and size of the equipment, i.e. as they are currently oversized, selling them before further ageing is more profitable for the system. However, since the plants would still need heating utilities after the existing boilers are sold, new ones are purchased in the first period. The piping investment decisions, similar to the equipment investment, are taken as early as possible, to benefit from corresponding operational savings.

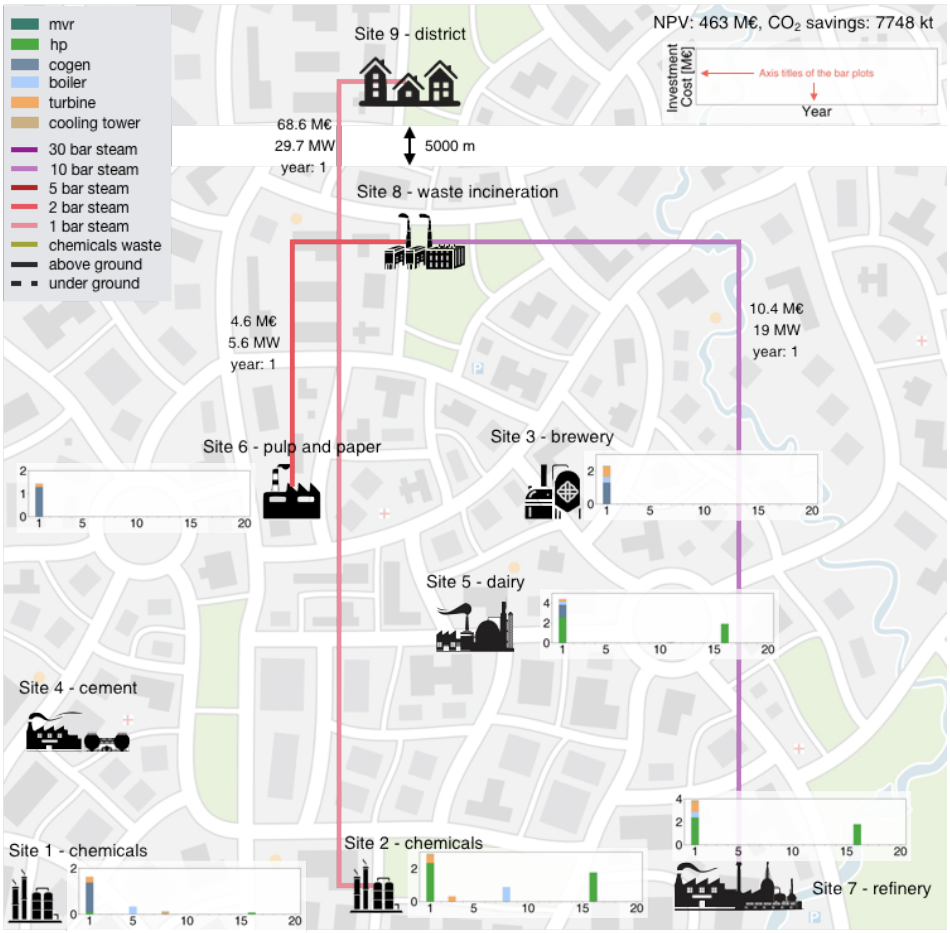

Figure 4.6 – Optimal investment planning without budget constraints.

4.5.2 Impact of seasonality in the investment decisions

The impact of seasonality in investment planning is studied by considering four seasons (i.e. time steps) in a 20-year time horizon (i.e. periods), as seen in Figure 4.7. As stated in Section 4.4, only the district demand changes seasonally, which is reflected as a slight decrease in NPV. The most drastic change occurs in the piping investment decisions. As the district has higher demand in winter compared to the annual average considered in Section 4.5.1, the amount of steam transferred from Site 2 increases even though the piping investment stays the same as the pipe size is large enough to handle a higher flowrate. In addition, all excess heat available on Site 8 is transferred to Site 9 and Site 2. In winter, the heat is wholly transferred to the district in the form of low pressure steam, while in summer it is shared with Site 2 as high pressure steam since the district heating demand is very small in summer and the chemical site has a constant demand throughout the year. In the other seasons, the excess heat from Site 8 is shared between the district and the chemical site, giving priority to the district.

The impact of seasonality can also be observed in the investments in energy conversion technologies. Transferring most of the excess heat below the pinch point to the district, Site 2 has a lower potential for heat pump integration. Moreover, larger investment on boilers occur on Site 6 and 7 as they no longer receive excess heat from Site 8. In terms of investment timing, results are similar to Section 4.5.1; most of the investments occur in the first year and the rest are for repurchasing of equipment which reach the end of their life span.

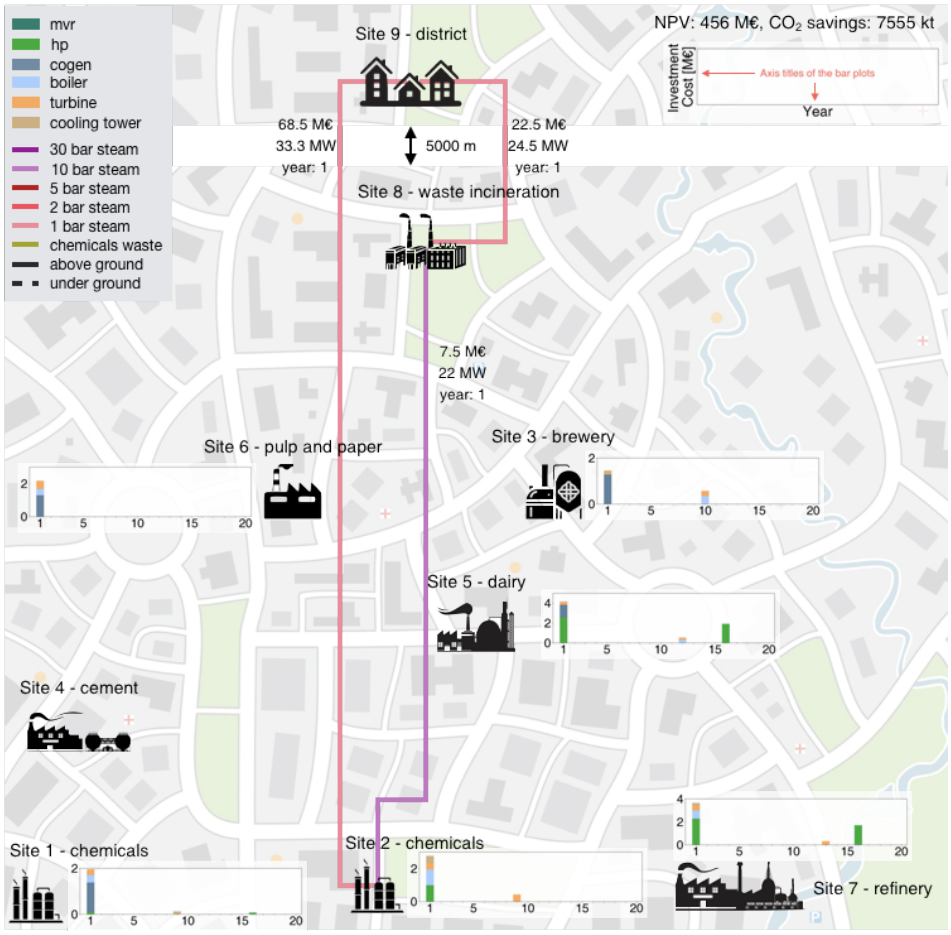

Figure 4.7 – Optimal investment planning considering seasonality in district energy demand.

4.5.3 Budget and investment constraints

In real industrial retrofit projects, there is always a limitation on the budget, as the companies involved do not have unlimited resources. In such cases, it is important to spot the investments that are the most profitable under the project budget. The budget limitation is studied by introducing a constraint which limits the investments to 75% of the total investment cost of the optimal solution obtained in Section 4.5.1 (i.e. 80 M€). In addition, further constraints are applied to limit the yearly

investment.

As a first case, an investment period of five years is considered. This means that all the investment decisions are taken in the first five years and the system is operated for the rest of the time given those decisions. It is assumed that the budget is evenly distributed within the investment period (i.e. 16 M€/year), under the condition that if it is not completely spent in a year, it can be transferred to the following one. With the investment constraints, NPV and CO_2 savings of the system decrease by 5% and 9% respectively compared to the optimal solution in Figure 4.6. Figure 4.8 illustrates the investment decisions and their corresponding year for the optimal solution with five-year investment horizon. Compared to Figure 4.6, the type of the technologies and equipment invested in are similar; cogeneration engines are installed in sites 1, 3, 5 and 6, heat pumps are installed in sites 2 and 7, boilers and turbines are replaced in almost all sites, and steam pipes are installed between sites 1, 5, 8 and 9. The impact of the budget restrictions can be seen in the timing of the investments as well as the size of some of the equipment; instead of purchasing most of the equipment in the first year, investments are spread over five years. In some of the years (e.g. year 1), the budget allowance is not fully used, either to be able to transfer some of it to the following year or because it is not sufficient enough for further investment. This way, large investments, such as piping between Site 8 and 9, which require larger investments than the yearly allowance are still possible. However, very large investments, e.g. 68.6 M€ piping between Site 2 and 9 (see Figure 4.6) are not selected, as other options lead to more beneficial results for the objective function.

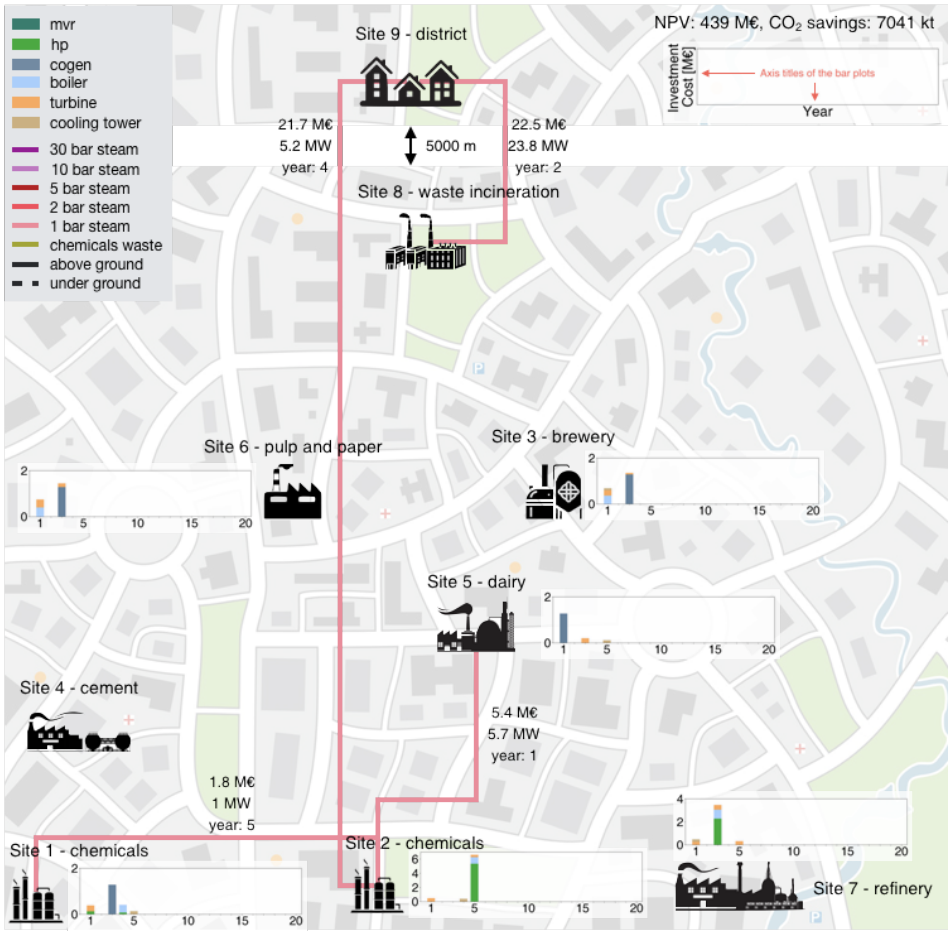

Figure 4.8 – Optimal investment decisions with 5 years of investment and 16 M€ annual budget.

As a more conservative investment strategy, a case with a ten-year investment period is evaluated in Figure 4.9. Since the investment period is broader, the yearly budget reduces to 8 M€, which results in a 13% lower NPV and 12% lower CO_2 reduction compared to the optimal solution in Figure 4.6. Similar to the previous case, it is assumed that the yearly investment budget, if unused, can be transferred to the following years. Since the annual budget is reduced, the number of simultaneous investments decreases. The energy conversion system investments are prioritised over piping as they are smaller and can therefore be be completed earlier. Most of the intra-plant improvements via investing on better energy conversion systems are carried out in the first year. In the second year, the largest investment is in the pipeline between site 2 and 5, as it is within the yearly budget. Following this, large investments are avoided for two years, to accumulate sufficient budget for piping between site 8 and 9 (taking place in year five). Similarly, between year six and eight, investments are not made so as to accumulate sufficient budget for the large piping investment between site 2 and 9 in year nine.

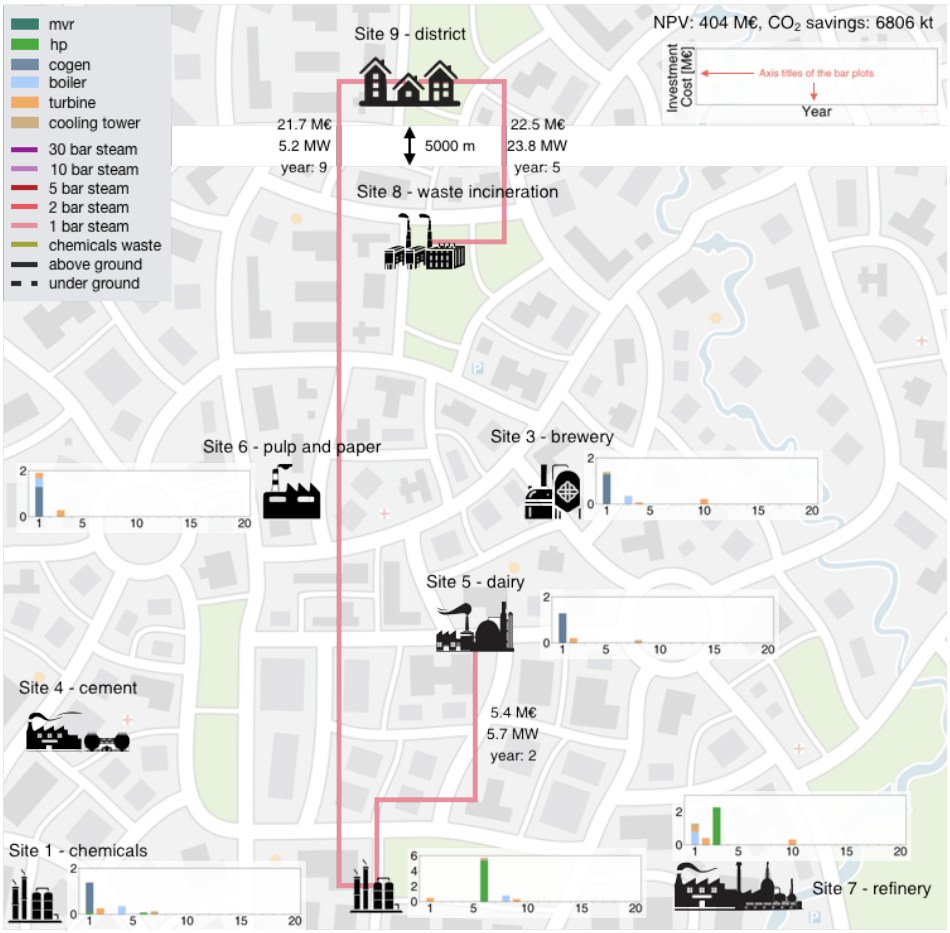

Figure 4.9 – Optimal investment decisions with 10 years of investment and 8 M€ annual budget.

4.5.4 Multiple scenarios for investment

The parametric optimisation strategy described in Section 4.3.5 is utilised to obtain 30 solutions with different limits on the piping cost, representing multiple scenarios for investment. Figure 4.10 depicts the multi-criteria comparison of the solutions from parametric optimisation as well as the one from Figure 4.9, all with 80M€overall investment budget and investment period of first ten years. The solutions are sorted with respect to NPV, which is the main objective and the solution from Figure 4.9 is highlighted with a bold line.

The solutions with high NPV also yield high CO_2 savings, taking the advantage of reduced operating cost (i.e. natural gas and electricity consumption). The solutions with low limit on piping investment budget rank the worst in NPV, CO_2 savings, operating cost and utility system investment. Conversely, piping investment does not always bring operational benefits which results in the solutions at the upper end of 'Piping investment' axis having lower NPV than the ones below them. Heat shared with

the district and industries have an inverse relationship, as the quantity of heat is limited and only its distribution varies between solutions. The solutions in which industrial excess heat is shared with the district yield better results in terms of NPV as natural gas and electricity prices are higher for the residential users compared to industries. The solution from Figure 4.9 ranks worse than half of the solutions obtained with parametric optimisation in both economic and environmental key performance indicators (KPIs). This can be explained by the use of a larger optimality gap (i.e. 5%) as the solution time is longer, thus the solver does not try to explore better solutions. Despite having a higher optimality gap, the solution from Figure 4.9 requires computation time more than ten times that of the solutions from parametric optimisation.

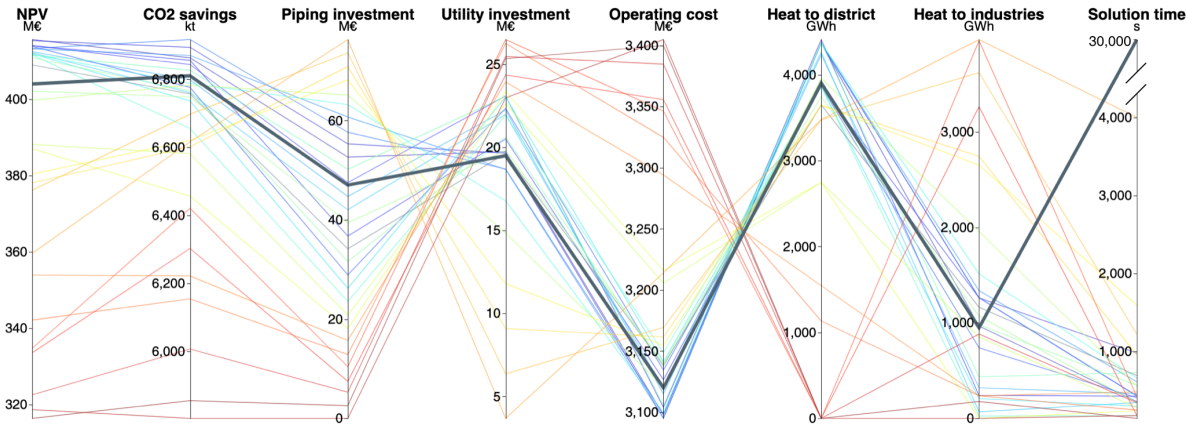

Figure 4.10 – Multiple solutions generated by parametric optimisation; the higher the NPV, the colder the line colour.

4.5.5 Comparison with baseline

Comparison of the baseline of the system with the optimal solutions identified (i.e. with and without budget constraints) is depicted in Figure 4.11. Baseline represents the current state of the system when the plants are operated with the energy conversion technologies that already exist on the sites. The investment cost in this case is required for the equipment reaching the end of their life span, to be able to continue the plant operation. Therefore, the operating cost remains constant throughout the twenty years, as nothing is done to improve the system efficiency. Similarly, in the optimal solution without budget constraints, the operating cost is the same for the span of the project, due to the fact that all the investments improving the system are carried out at the beginning of the first year. This also explains the large investment and 27% reduction in the operating cost in the first year compared to the baseline. When investments are limited to the first five years, the operating cost gradually improves 16-26% with the investments performed each year and then stabilises at the fifth year until the rest of the project. The same phenomenon happens for the case with ten years of investment; the operating cost improves by 16-24% in the investment period and

then stays constant for the last ten years. Considering NPV and environmental impact, optimal investment planning without budget constraints improves the system by ~463M€ and 7748 kt CO_2 in twenty years horizon, while investment budget constraints of five and ten years result in 5% and 13% lower NPV, and 9% and 12 % lower CO_2 savings, respectively, when compared to the unconstrained solution. Although the investment planning strategy requires large investments, totalling 107 M€, yearly operating cost savings surpass 50 M€, resulting in a simple payback time of slightly greater than two years.

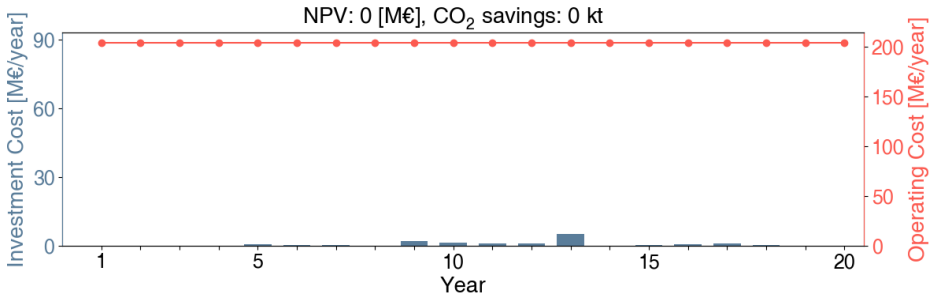

(a) Business as usual operation and investments

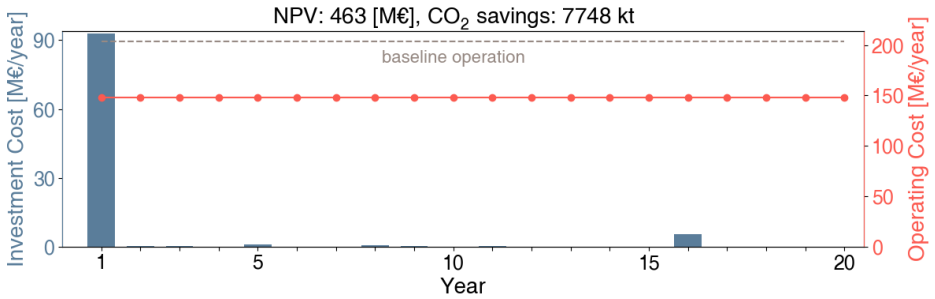

(b) Optimal solution without budget constraints

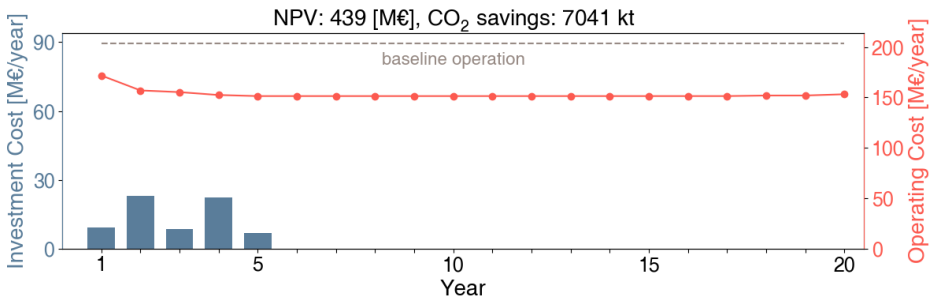

(c) Optimal solution with 5 years of investment and 16 M€/year budget

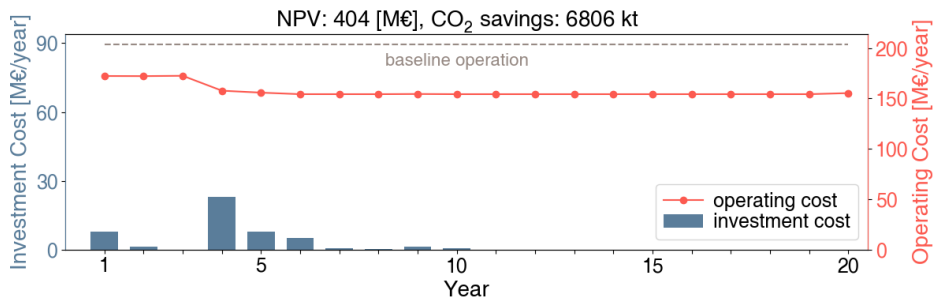

(d) Optimal solution with 10 years of investment and 8 M€/year budget

Figure 4.11 – Comparison of operating and investment costs of the optimal solutions with the baseline.

4.6 Conclusion

This work proposes an MILP framework, PIIP, which combines the efforts in process integration and long-term investment planning. The method takes advantage of PI, by modelling the energy and resource flows in detail, including heat cascade, mass and energy balances. A novel investment planning formulation is proposed and integrated with PI, capturing all investment actions, such as commissioning and decommissioning of utility systems, while considering external exchanges via pipeline.

The method is applied to a large case study, with eight industrial plants from different sectors and a district neighbouring an industrial cluster, for a time horizon of twenty years. When the investment budget and period are not limited, all investments improving the operating cost are made in the first year, to maximise benefits from the operating cost savings as long as possible. Heat pumps and cogeneration engines are preferred over industrial boilers in all sites where their integration is possible. In inter-plant exchanges, priority is given to heat sharing with the district, since this option is more profitable because of lower industrial energy prices relative to residential ones. In addition, heat sharing over long distances with a single pipeline is preferred over investing in multiple pipelines connecting smaller nearby sites. When seasonality is taken into account, given the variations in the district demand, the investment decisions change drastically. A larger amount of heat is shared between the industrial cluster and the district resulting in less heat sharing between the industrial plants. Based on interactions between plants, different investment options become favourable. Thus, in the cases where energy demand varies greatly throughout a year, it is crucial to consider seasonality, to obtain the optimal selection and planning of the investments.

To simulate a more industrially-realistic scenario (i.e. refurbishment planning of plant infrastructure), an investment budget is imposed and the investment period is restricted to the first five or ten years, with the possibility of transferring budget from one year to the next. Since the yearly budget does not allow for large early investments, they occur over the whole investment period. Some large investments found in the optimal solution without budget restrictions no longer appear, since annual budgets would need to accumulate for several years, making other solutions more attractive. As the investment strategy becomes more conservative (i.e. lower annual budget in a longer investment period), competition between investment in energy conversion technologies and inter-plant steam pipes increases, since parallel investments are not feasible. Although in the studied case, investment in energy conversion technologies receives priority over pipelines, the solution is dependent on the case study, energy profiles, prices and distances.

A strategy is proposed to generate multiple investment options using parametric optimisation by setting an upper limit for piping investment and varying it, and the results are compared with a single optimal solution. The parametric optimisation strategy not only generates 30 solutions in shorter time, but also finds solutions with better economic and environmental KPIs. Thus, in the

case of industrial applications, it is better to generate multiple optimal solutions instead of trying to reach the global optimum. In all solutions ranking highly in economic and environmental KPIs, industrial excess heat is shared with the district. Thus, it is crucial to consider symbiosis options with a nearby heat consumers in industrial retrofit applications, which is often overlooked.

The optimal solution using the proposed method without investment restrictions leads to a ~463M€ increase in the NPV of the system and 7748 kt CO_2 savings compared to the baseline, owing to operating cost benefits of investment decisions. Applying a budget limit on the investment cost with an investment period of five and ten years results in 5% and 13% decrease in NPV and 9% and 12% decrease in CO_2 savings compared to the solution without any budget limitation but they still provide significant improvement compared to the baseline. Although more conservative investment planning strategies result in slightly lower savings in the operating cost, they still lead to reductions of ~50 M€, or in other words a payback time of less than two years for the investments.

The method presented in this work provides a holistic strategy for investment planning of large industrial cases in long time horizons. Additional constraints can easily be integrated to customise it according to the limitations of the industrial clusters on the investment budget and periods. Future work includes adding stochasticity in the energy prices and cost of energy conversion technologies, as well as in the production capacity of plants and population of districts nearby. In addition, the objective function can be modified to optimise for an environmental objective instead of using a purely economic one.

Conclusions

"Don't adventures ever have an end? I suppose not. Someone else always has to carry on the story."
J.R.R. Tolkien

Overview

- Main results and contributions
- Future perspectives

This thesis presents methods to retrofit industrial plants and clusters as well as plan required investments towards industrial energy and resource efficiency. Four main research questions are identified and answered throughout the chapters of the thesis. This chapter recaps the research questions, main findings and conclusions, followed by future perspectives.

Main results and contributions

Chapter 1: Targeting retrofit at early design stages

"How do we take the cost of heat integration into account at early design stages?"

This chapter proposes the concept of heat exchange interfaces, which are used to represent the heating and cooling requirement of the processes. Switching from one interface to another might bring operational benefits through better heat integration; however requires modifications in the heat exchangers by area addition, thus the additional area cost is calculated and associated to changing interfaces. A novel mixed integer linear programming (MILP) method is developed to simultaneously optimise the utility systems and the selection of heat transfer interfaces.

Different functions of the proposed method are illustrated carrying out two case studies, comprising of chemical plants and their utility systems. The first case study employs four scenarios to simulate the business as usual operation of a plant and gradually improve the total cost. Allowing heat recovery by changing heat transfer interfaces and using the existing utilities more efficiently results in 23% decrease in heating demand, 38% decrease in operating cost and 29% decrease in total cost,

including the cost of modifications in the heat exchangers due to switching interfaces. Further improvements by integrating a cogeneration engine and heat pumps total up to 45% reduction in the total cost and requires modifications in 14 out of 23 heat exchangers.

The other function of the proposed method is identifying the heat exchangers that do not require modifications (i.e. streams that do not need to switch their current interface) and relax the heat exchanger network (HEN) design problem, by fixing stream matches at the level of heat load distribution (HLD). A larger case study is carried out to observe the impact of fixing the stream matches, which results in a 32% reduction in the solution time.

This chapter provides a decision aid tool for the industries to evaluate retrofit in early design stages, by identifying the heat exchangers that should be targeted for better heat integration, using the concept of heat transfer interfaces.

Chapter 2: Incorporating plant layout in heat exchanger network retrofit

"What is the impact of plant layout in heat exchanger retrofit?"

This chapter takes the retrofit analysis further, by studying it at the stage of HLD. Instead of considering retrofit in the HEN only as additional area, the proposed method captures the main retrofit actions, including moving heat exchangers, adding new heat exchangers, adding area to existing heat exchangers and repiping streams. The plant layout is included in the method by defining the coordinates of the streams and of the heat exchangers from the initial network and using a repiping cost function based on the piping length.

The proposed method is applied to a case study and compared with the state of the art. Since practical constraints, such as maximum 15% increase in the area of existing heat exchangers are introduced, the optimal solution yields more additional heat exchangers. In addition, as a large scale application, a case study from Chapter 1 is carried out, using parametric optimisation. The total cost of the system including the retrofit cost of the HEN reduces by 5% to 34%, depending primarily on the type of energy conversion technologies integrated. The best performing system is the one with a cogeneration engine, which takes advantage of supplying both heat and electricity. Integration of both heat pumps and the cogeneration engine requires a high number of additional heat exchangers as well as repiping streams, but the associated operational benefits are larger than the investment cost.

The method presented in this chapter results in smaller number of modifications in the HEN compared to the state of the art as the plant layout and practical constraints are taken into account. It can be used by the industries for assessment of HEN retrofit before a more detailed analysis is carried out.

Chapter 3: Retrofit considering inter-plant exchanges

"How do we determine the optimal interactions between industrial plants, taking their locations into account?"

This chapter expands the boundaries of the retrofit problem, by considering industrial clusters and interactions between plants for sharing excess heat and resources. A comprehensive method is proposed to incorporate location aspects in process integration (PI), by considering heat distribution losses, temperature and pressure drops as well as piping cost, in inter-plant exchanges. The problem is formulated using MILP and parametric optimisation is used to generate multiple retrofit scenarios, by applying ϵ-constraints on the piping cost.

A large case study with eight neighbouring plants from different industrial sectors is studied to determine the optimal retrofit, simultaneously considering intra-plant improvements by heat recovery and integrating more efficient energy conversion systems and inter-plant exchanges by sharing waste resources and excess heat (in the form of steam at different pressure levels). At low piping investment budgets, the optimal solutions lead to excess heat sharing between the plants via high pressure steam, as it requires smaller pipe diameters; while, as the piping allowance increases, lower pressure steam becomes more beneficial, since it has lower heat losses. Similarly, above-ground pipes are used at lower piping investment budgets, but underground pipes are more favourable at higher piping allowances due to the trade off between piping cost and heat losses.

As inter-plant exchanges present risks and most of the time include more than one company, industries might not be willing to invest in the infrastructure between plants, despite proven benefits. The involvement of a third party, either a non-profit governmental organisation or a utility company with profitability targets, is considered to simulate such cases, in which the third party invests on the steam pipes between the plants. Regardless of the nature of the third party, overall, the cluster benefits from the interactions of the plants, however a higher third party turnout results in a lower system profit. Although the benefit of the industries decreases with the involvement of a profit-oriented third party, they can still take advantage of a 40% reduction in steam prices while avoiding investment risks and the third party can charge a steam price premium of up to 20%.

Compared to the business as usual operation of the industrial cluster, using the proposed method prompts up to a 21% and 35% reduction in total cost and energy related CO_2 emissions, respectively. These benefits are stemming from heat recovery within plants, integration of efficient energy conversion systems, as well as sharing excess heat and resources between the plants. The results yield lower economic and environmental savings compared to the targeting methods available in the literature; however, accounting for technical and economic feasibility, they are more likely to be implemented.

Chapter 4: Planning investments in long time horizons

"What is the optimal time for energy efficiency investments?"

This chapter combines the efforts in PI with a novel investment planning formulation to identify the optimal retrofit investment decisions in long time horizons. The method benefits from PI in modelling energy and resource flows in detail, applying heat cascade and mass balance constraints, at the same time, capturing the main investment actions, such as commissioning and decommissioning energy conversion technologies and pipelines between plants.

The case study from Chapter 3 is extended by adding a residential district, to increase the superstructure for industrial excess heat valorisation and evaluating a 20-year horizon. When the investment budget is not limited, all the major investments are carried out in the first year, to benefit from their corresponding operating cost savings throughout the evaluated period. Cogeneration engines and heat pumps integrate as utility systems in the plants, replacing industrial boilers where possible. In addition, the optimal solution includes investments in pipelines for heat sharing between industries, as well as heat transfer from the industries to the district. Despite the fact that the piping distance to the district is longer compared to the distance to other industries and that it requires a higher investment, the optimal solution favours sharing industrial excess heat with the district, as residential energy prices are higher than industrial ones. When the seasonality in the heating demand of the district is taken into account, the results change drastically, as a larger investment in the pipeline to the district is required to provide more heat, which has an impact on the investment decisions on other pipelines between the plants as well as on the energy conversion technology selection, since all the plants are interconnected.

To simulate industrially-realistic scenarios, overall and annual investment budgets are imposed, with the possibility of transferring budget from one year to the following one and the investment period is limited to the first five or ten years. With these constraints, the investments are spread over the defined investment period, as they can no longer be carried out at once, in the first year. Moreover, very large investments (well above the annual investment budget) disappear, since the system has to save from the investment budget for several years, to be able to afford them. The priority is given to investments in energy conversion technologies, as they cost less than new piping between the sites; however, the results are dependent on the case study, the cost of energy and the prices of energy conversion technologies.

The optimal solution without budget constraints yields a 27% decrease in the operating cost, which results in a 463 M€ increase in net present value (NPV) and 7748 kt CO_2 savings throughout 20 years. Applying budget limits decreases the NPV by 5-13% and CO_2 savings by 9-12% compared to the solution without budget restrictions, but still leads to significant improvements compared to the baseline.

A parametric optimisation strategy is used to generate multiple solutions and the results are compared to the single objective optimisation ones. The strategy proposed solves 30 optimisation problems faster than one single objective solution. Additionally, if obtains solutions ranking better both from and economic and environmental perspective. This proves that, trying to reach the global optimum solution does not always bring better results and global optimality can be traded with several suboptimal solutions, to provide alternative investment options for industrial parties.

Future perspectives

The method presented in Chapter 1 **identifies promising retrofit options at early design stages, using the concept of heat exchange interfaces**. Further improvements could include:

- more detailed heat transfer and additional area calculations (e.g. considering two phase flow);
- increasing the superstructure by adding energy conversion technologies, that could potentially further improve the case studies considered;
- refining the time resolution to consider multiple time steps and variation in heating and cooling demands.

Chapter 2 proposes a method for **retrofitting heat exchanger networks, by taking into account the plant layout**. Further investigations could include:

- validating the logarithmic mean temperature difference (LMTD) and heat exchanger area estimations. This could be done by carrying out a detailed heat exchanger network design and cross-checking the results;
- refining the cost functions for moving heat exchangers and adding area to existing heat exchangers;
- constraining the problem to take the type of heat exchangers into account.

The method to **account for location aspects in PI** presented in Chapter 3 determines how to optimally share waste resources and excess heat between industries. The limitations of the method, which could be addressed in future work, include:

- better assessing the heat losses and pumping work without the simplifying assumptions which keep the problem in the MILP domain;
- validating the heat distribution losses calculation;
- extending the method by including different means of transportation (e.g. railway, road, etc.) for resource sharing between industrial plants;
- expanding the heat sharing superstructure by adding other fluids, such as hot water and oil loops.

The optimisation approach for **planning retrofit investments in industry for long time horizons**, presented in Chapter 4 could be enhanced by:

- considering stochasticity in the energy prices and in the investment cost of energy conversion technologies;
- taking into account variations in the production capacity of plants and population of districts nearby in a given time horizon;
- using environmental objective functions instead of purely economic ones;
- adding policy constraints, to guide the industries in reaching ambitious targets;
- extending the evaluated time to longer periods.

Appendix

(Chapter 1)

A.1 Details of the case studies

The process streams of case study 1 and 2 are listed in Tables A.1 and A.2 respectively. The stream information includes inlet and outlet temperatures, heating/cooling requirement, convective heat transfer coefficient, saturation temperature (if it is the case) and the utility that is currently consumed.

Table A.1 – Case 1 streams.

Stream	T^{in} [°C]	T^{out} [°C]	$\Delta \dot{Q}$ [kW]	ΔT^{min} [°C]	α [kW/m^{2}K]	$T^{phase\ change}$ [°C]	Current Utility
HEX1	51	56	202	10	0.25	56	24bar Steam
HEX2	79	84	1086	10	0.25	84	24bar Steam
HEX3	61	66	142	10	0.25	66	24bar Steam
HEX4	58	63	947	10	0.25	63	24bar Steam
HEX5	60	65	980	10	0.25	65	8bar Steam
HEX6	43	100	987	10	0.25	100	8bar Steam
HEX7	43	100	412	10	0.25	100	8bar Steam
HEX8	63	68	721	10	0.25	68	8bar Steam
HEX9	63	68	210	10	0.25	68	8bar Steam
HEX10	53	31	305	10	0.25	-	Water Cooling
HEX11	50	38	23	10	0.25	-	Water Cooling
HEX12	41	32	1109	10	0.25	-	Water Cooling
HEX13	55	33	575	10	0.25	-	Water Cooling
HEX14	44	31	123	10	0.25	-	Water Cooling
HEX15	47	30	72	10	0.25	-	Water Cooling
HEX16	67	35	670	10	0.25	67	Air Cooling
HEX17	86	35	586	10	0.25	86	Air Cooling
HEX18	57	35	1244	10	0.25	57	Air Cooling
HEX19	67	35	643	10	0.25	67	Air Cooling
HEX20	67	31	390	10	0.25	67	Air Cooling
HEX21	69	35	1128	10	0.25	67	Air Cooling
HEX22	117	40	1287	10	0.25	61	Air Cooling
HEX23	81	39	365	10	0.25	81	Air Cooling
HEX24	58	35	340	10	0.25	-	Air Cooling

A

The process flow diagram of case study 1 and 2 can be seen in Figures A.1 and A.2 respectively. The process flow diagrams represent the streams that are listed in Tables A.1 and A.2 and their current utility usage.

Table A.2 – Case 2 streams.

Stream	T^{in} [°C]	T^{out} [°C]	$\Delta \dot{Q}$ [kW]	ΔT^{min} [°C]	α [kW/m^{2}K]	$T^{phase\ change}$ [°C]	Current Utility
HEX1	135	140	1900	10	0.25	140	24bar Steam
HEX2	135	140	5800	10	0.25	140	24bar Steam
HEX3	150	155	12800	10	0.25	155	24bar Steam
HEX4	142	147	800	10	0.25	147	24bar Steam
HEX5	131	136	900	10	0.25	136	24bar Steam
HEX6	135	140	100	10	0.25	140	24bar Steam
HEX7	135	140	800	10	0.25	140	24bar Steam
HEX8	123	128	18400	10	0.25	128	8bar Steam
HEX9	114	119	1700	10	0.25	119	8bar Steam
HEX10	115	120	200	10	0.25	120	8bar Steam
HEX11	115	120	900	10	0.25	120	8bar Steam
HEX12	115	120	4200	10	0.25	120	8bar Steam
HEX13	115	120	300	10	0.25	120	8bar Steam
HEX14	92	97	14700	10	0.25	97	2bar Steam
HEX15	58	63	600	10	0.25	63	2bar Steam
HEX16	62	67	2200	10	0.25	67	2bar Steam
HEX17	55	60	2200	10	0.25	60	2bar Steam
HEX18	60	65	400	10	0.25	65	2bar Steam
HEX19	60	65	1200	10	0.25	65	2bar Steam
HEX20	60	65	2500	10	0.25	65	2bar Steam
HEX21	49	44	200	10	0.25	-	Water Cooling
HEX22	50	45	100	10	0.25	-	Water Cooling
HEX23	51	46	100	10	0.25	-	Water Cooling
HEX24	53	48	1100	10	0.25	-	Water Cooling
HEX25	50	45	900	10	0.25	-	Water Cooling
HEX26	53	48	500	10	0.25	-	Water Cooling
HEX27	56	51	200	10	0.25	-	Water Cooling
HEX28	52	47	100	10	0.25	-	Water Cooling
HEX29	49	44	100	10	0.25	-	Water Cooling
HEX30	57	52	400	10	0.25	-	Water Cooling
HEX31	47	42	100	10	0.25	-	Water Cooling
HEX32	56	51	100	10	0.25	-	Water Cooling
HEX33	54	49	300	10	0.25	-	Water Cooling
HEX34	48	43	100	10	0.25	-	Water Cooling
HEX35	64	59	5500	10	0.25	64	Air Cooling
HEX36	55	50	21200	10	0.25	55	Air Cooling
HEX37	50	45	400	10	0.25	50	Air Cooling
HEX38	55	50	1400	10	0.25	55	Air Cooling
HEX39	123	118	500	10	0.25	123	Air Cooling
HEX40	148	143	1000	10	0.25	148	Air Cooling
HEX41	152	147	2450	10	0.25	152	Air Cooling
HEX42	93	88	1900	10	0.25	93	Air Cooling
HEX43	55	49	3300	10	0.25	55	Air Cooling
HEX44	53	48	3500	10	0.25	53	Air Cooling
HEX45	77	72	800	10	0.25	77	Air Cooling
HEX46	77	72	800	10	0.25	77	Air Cooling
HEX47	83	78	5300	10	0.25	83	Air Cooling
HEX48	87	82	3400	10	0.25	87	Air Cooling
HEX49	108	103	4400	10	0.25	108	Air Cooling
HEX50	109	104	2600	10	0.25	109	Air Cooling
HEX51	103	98	24800	10	0.25	103	Air Cooling

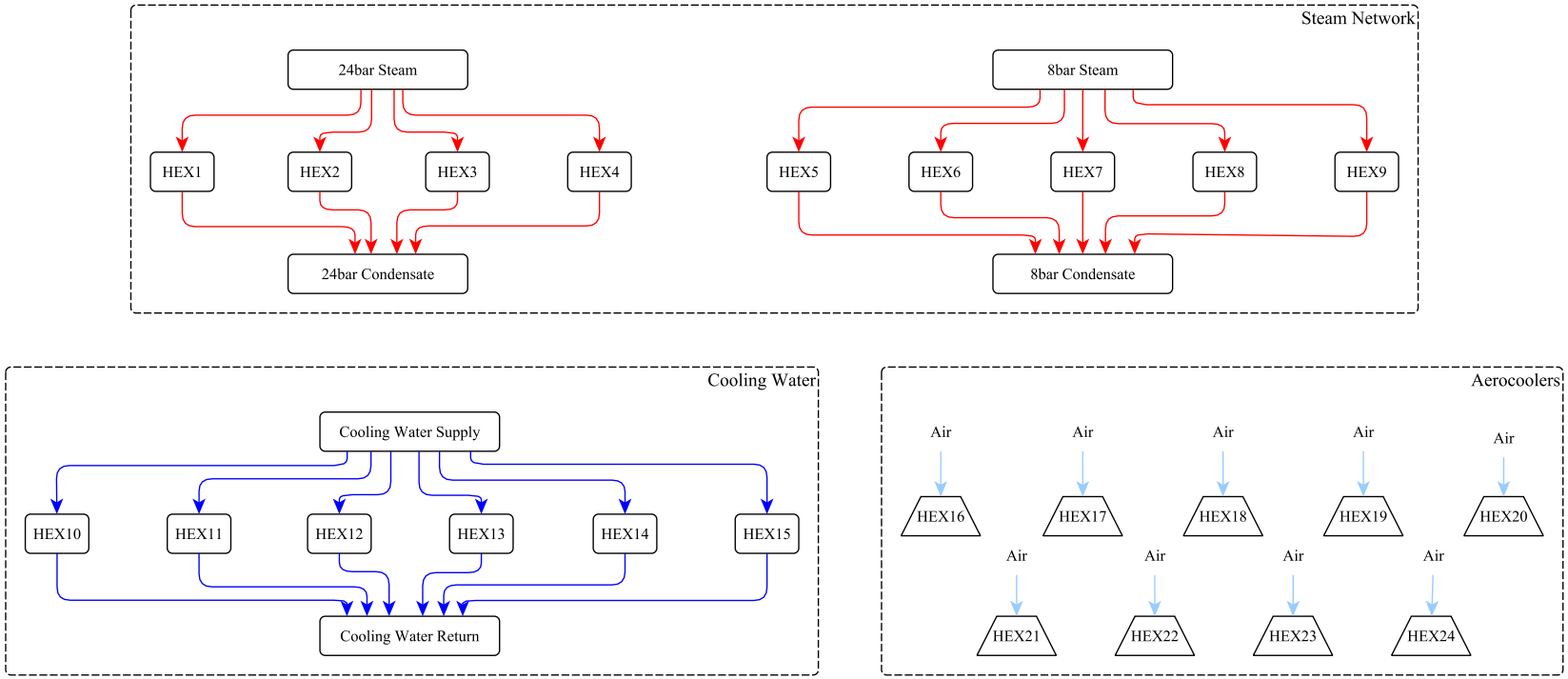

Figure A.1 – Case study 1 process flow diagram.

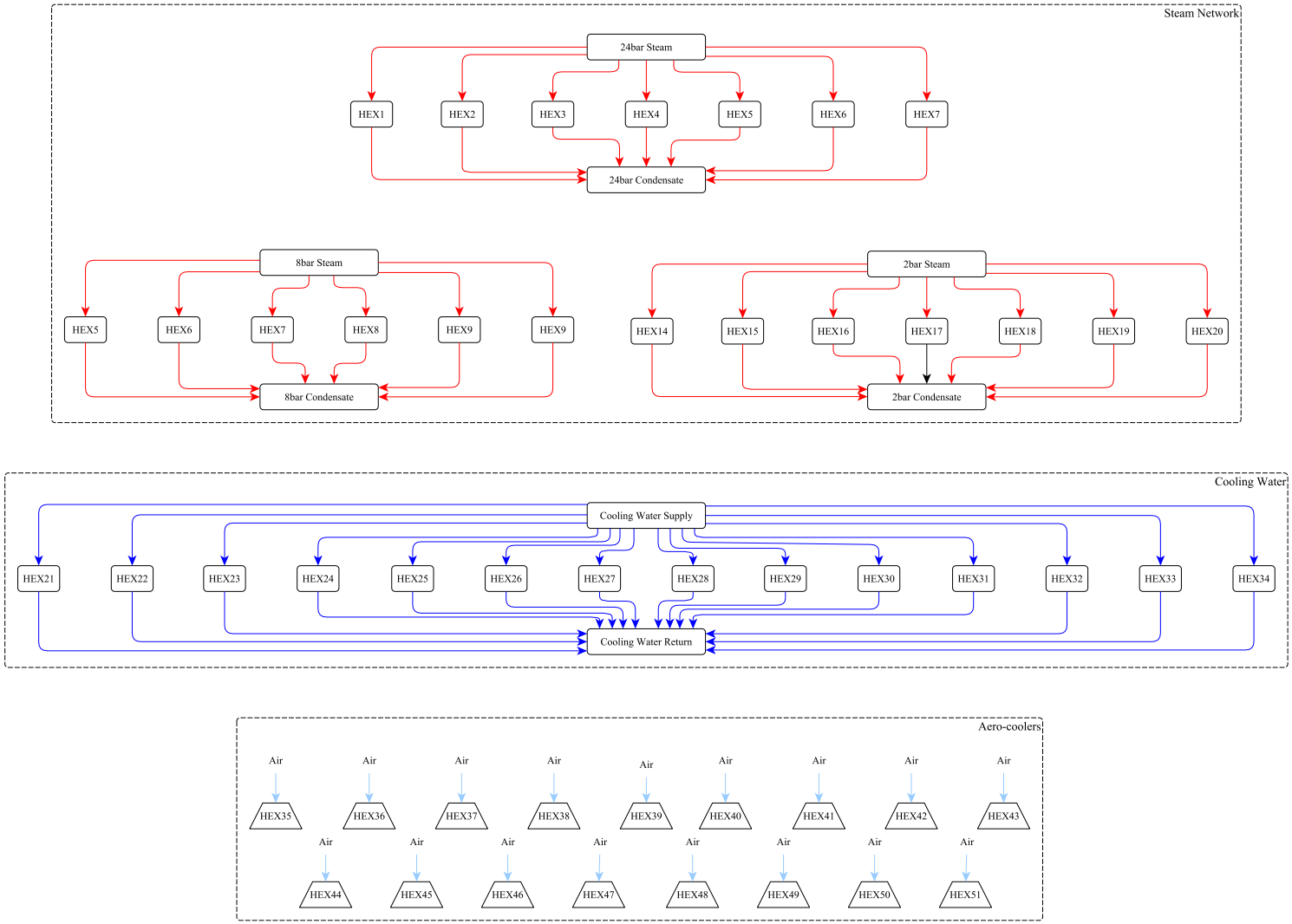

Figure A.2 – Case study 2 process flow diagram.

A.2 Operating cost parameters

The operating cost is dependent on the type of utilities that are used in the system and eventually on the type of resources (e.g. electricity, natural gas, gasoline) used by the utility systems. The cost of the resources used in MILP are taken as reported by Eurostat [156]. The cost of selling electricity to the grid is assumed as 60% of the cost of buying it from the grid. The costs of the resources are listed in Table A.3.

Table A.3 – Resource cost for operating cost calculations.

c^{natgas} [€/kWh]	0.0303
c^{elec} [€/kWh]	0.0916
$c^{elecsell}$ [€/kWh]	0.0549
c^{water} [€/m^3]	0.07

The cost of natural gas and electricity in 25 OECD countries reported in [157] are converted to € using the exchange rate of the corresponding year, and listed in Table A.4

Table A.4 – Resource cost by country.

Country	c^{natgas} [€/kWh]	c^{elec} [€/kWh]
Austria	0.03409	0.10165
Denmark	0.03688	0.07662
Finland	0.03444	0.07864
France	0.03698	0.09477
Germany	0.03356	0.13486
Greece	0.04253	0.10741
Ireland	0.03658	0.12518
Italy	0.03618	0.24662
Luxembourg	0.03373	0.07437
Netherlands	0.03249	0.08884
Portugal	0.04497	0.11734
Spain	0.03344	0.11600
Sweden	0.04134	0.06151
UK	0.03017	0.11843
Canada	0.01145	0.07443
Czech R.	0.03222	0.09246
Hungary	0.03851	0.09280
Japan	0.06152	0.13200
Korea	0.07054	0.05077
NZ	0.02154	0.07109
Poland	0.03299	0.07523
Slovakia	0.03323	0.11809
Switzerland	0.05536	0.09690
Turkey	0.02471	0.08344
USA	0.01375	0.05279

A.3 Investment cost parameters

The investment cost of the equipment is estimated using Equations 1.2 and 1.3 given in Section 1.3.1 and Equations A.1 and A.2. The cost estimation parameters adapted from [33, 34] are listed in Table A.5. The plant cost indexes and assumed cost parameters are given in Table A.6.

$$F^{P} = 10^{c1+c2\cdot log\mathrm{Pres}+c3\cdot(log\mathrm{Pres})^{2}} \tag{A.1}$$

$$F_{BM} = B1 + B2 \cdot F^{P} \cdot F^{M} \tag{A.2}$$

Table A.5 – Equipment cost parameters.

Equipment	k1 [-]	k2 [-]	k3 [-]	c1 [-]	c2 [-]	c3 [-]	F^{M}	$Year^{ref}$
Shell&tube HEX	3.224	0.242	0.091	0	0	0	1	2004
Centrifugal Comp.	2.995	0.954	0	0	0	0	2.5	1996

Table A.6 – Generic cost parameters.

Interest rate [-]	0.08
Equipment life [years]	20
$CEPCI^{t}$ (2014) [-]	576.1
$CEPCI^{ref}$ (2004) [-]	444.2
$CEPCI^{ref}$ (1996) [-]	318.7

A

A

(Chapter 2)

B.1 Linear approximation of the heat exchanger cost function

Figure B.1 illustrates the heat exchanger cost function and its linear approximation.

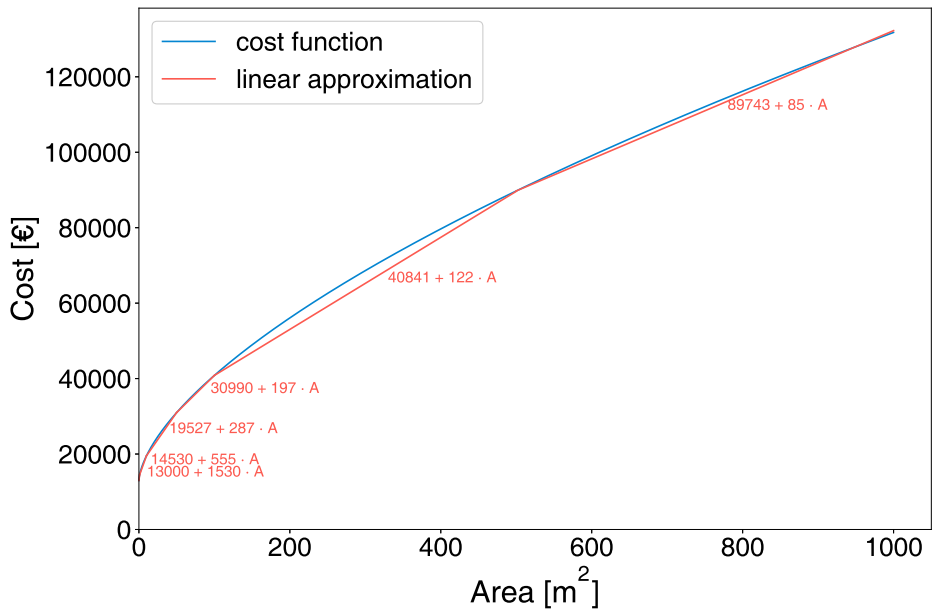

Figure B.1 – Linear approximation of the heat exchanger cost function.

B

B.2 Standard piping sizes

Table B.1 depicts the standard piping sizes and their associated cost.

Table B.1 – Piping cost for standard piping diameters.

Standard pipe size	1	2	3	4	5	6	7	8	9	10	11	12	13	14	15	16
Diameter [mm]	20	40	65	80	100	125	150	200	250	300	400	450	500	550	600	650
Specific cost [€/m]	96	166	250	312	387	480	580	775	975	1180	1588	1797	1900	2000	2090	2170

B.3 Initial heat exchangers

Initial heat exchanger area of the industrial case study and their coordinates are listed in Table B.2.

Table B.2 – Initial heat exchanger areas and coordinates.

Heat exchanger	Area[m^2]	x[m]	y[m]	z[m]
HEX1	2.8	52	0	0
HEX2	18.4	78	52	0
HEX3	2.1	69	0	0
HEX4	13.9	93	1	0
HEX5	21.7	108	2	0
HEX6	31.9	113	103	0
HEX7	13.3	89	102	0
HEX8	16.4	69	102	0
HEX9	4.4	50	97	0
HEX10	70.4	70	111	0
HEX11	4.7	77	57	0
HEX12	332.8	81	122	0
HEX13	121.2	92	12	0
HEX14	34.9	109	111	0
HEX15	19.5	108	13	0
HEX16	233.7	91	0	5
HEX17	152.9	93	102	5
HEX18	524.3	113	100	5
HEX19	221.3	69	99	5
HEX20	139.5	48	100	5
HEX21	385.3	109	0	5
HEX22	780.2	77	47	10
HEX23	95.8	49	3	5
HEX24	251.5	70	0	5

(Chapter 3)

C.1 Heat stream data of the processes

The heat streams of the plants in the case study are listed in Tables C.1–C.7 respectively. The stream information includes inlet and outlet temperatures and inlet and outlet enthalpies.

Table C.1 – Site 1 heat streams.

Stream	T^{in} [°C]	T^{out} [°C]	H^{in} [kW]	H^{out} [kW]
s1p1	51	56	0	10
s1p2	56	56	0	192
s2p1	79	84	0	54
s2p2	84	84	0	1032
s3p1	61	66	0	7
s3p2	66	66	0	135
s4p1	58	63	0	47
s4p2	63	63	0	900
s5p1	60	65	0	49
s5p2	65	65	0	931
s6p1	43	100	0	49
s6p2	100	100	0	938
s7p1	43	100	0	21
s7p2	100	100	0	391
s8p1	63	68	0	36
s8p2	68	68	0	685
s9p1	53	58	0	11
s9p2	58	58	0	200
s10	53	31	305	0
s11	50	38	23	0
s12	41	32	1109	0

Table C.1 – Site 1 heat streams cont.

Stream	T^{in} [°C]	T^{out} [°C]	H^{in} [kW]	H^{out} [kW]
s13	55	33	575	0
s14	44	31	123	0
s15	47	30	72	0
s16p1	67	67	538	0
s16p2	67	40	132	0
s17p1	86	86	452	0
s17p2	86	40	134	0
s18p1	57	57	1084	0
s18p2	57	35	160	0
s19p1	67	67	526	0
s19p2	67	40	117	0
s20p1	67	67	319	0
s20p2	67	40	71	0
s21p1	69	69	881	0
s21p2	69	40	247	0
s22p1	177	61	354	0
s22p2	61	61	840	0
s22p3	61	40	93	0
s23p1	81	81	290	0
s23p2	81	40	75	0
s24	58	40	340	0

Table C.2 – Site 2 heat streams.

Stream	T^{in} [°C]	T^{out} [°C]	H^{in} [kW]	H^{out} [kW]
s1p1	135	140	0	95
s1p2	140	140	0	1805
s2p1	135	140	0	290
s2p2	140	140	0	5510
s3p1	150	155	0	640
s3p2	155	155	0	12160
s4p1	142	147	0	40
s4p2	147	147	0	760
s5p1	136	141	0	45
s5p2	141	141	0	855

Table C.2 – *Site 2 heat streams cont.*

Stream	**T^{in} [°C]**	**T^{out} [°C]**	**H^{in} [kW]**	**H^{out} [kW]**
s6p1	135	140	0	5
s6p2	140	140	0	95
s7p1	135	140	0	40
s7p2	140	140	0	760
s8p1	123	128	0	920
s8p2	128	128	0	17480
s9p1	114	119	0	85
s9p2	119	119	0	1615
s10p1	115	120	0	10
s10p2	120	120	0	190
s11p1	115	120	0	45
s11p2	120	120	0	855
s12p1	115	120	0	210
s12p2	120	120	0	3990
s13p1	115	120	0	15
s13p2	120	120	0	285
s28	49	44	200	0
s29	50	45	100	0
s30	51	46	100	0
s31	53	48	1100	0
s32	50	45	900	0
s33	53	48	500	0
s34	56	51	200	0
s35	52	47	100	0
s36	49	44	100	0
s37	57	52	400	0
s38	47	42	100	0
s39	56	51	100	0
s40	54	49	300	0
s41	48	43	100	0
s42p1	115	115	4950	0
s42p2	115	110	550	0
s43p1	112	112	19080	0
s43p2	112	107	2120	0
s44p1	115	115	360	0

Table C.2 – *Site 2 heat streams cont.*

Stream	T^{in} [°C]	T^{out} [°C]	H^{in} [kW]	H^{out} [kW]
s44p2	115	110	40	0
s45p1	111	111	1260	0
s45p2	111	106	140	0
s46p1	123	123	450	0
s46p2	123	118	50	0
s47p1	118	118	900	0
s47p2	118	113	100	0
s48p1	112	112	2205	0
s48p2	112	107	245	0
s49p1	113	113	1710	0
s49p2	113	108	190	0
s50p1	114	114	2970	0
s50p2	114	109	330	0
s51p1	116	116	3150	0
s51p2	116	111	350	0
s52p1	127	127	720	0
s52p2	127	122	80	0
s53p1	109	109	720	0
s53p2	109	104	80	0

Table C.3 – Site 3 heat streams.

Stream	T^{in} [°C]	T^{out} [°C]	H^{in} [kW]	H^{out} [kW]
s1	65	85	0	396
s2	85	60	742	0
s3	40	60	0	743
s4	40	20	1121	0
s5	15	85	0	63
s6	15	60	0	46
s7	15	85	0	2022
s8	35	60	0	627
s9	1	1	672	0
s10	6	1	1122	0
s11	1	15	0	1291
s12	70	5	7631	0

Table C.3 – *Site 3 heat streams cont.*

Stream	**T^{in} [°C]**	**T^{out} [°C]**	**H^{in} [kW]**	**H^{out} [kW]**
s13	15	80	0	7624
s14	48	65	0	296
s15	48	65	0	660
s16	15	52	0	581
s17	15	55	0	1294
s18	65	75	0	579
s19	105	100	27	0
s20	100	100	5478	0
s21	100	25	758	0
s22	15	80	0	5419
s23	78	105	0	2612
s24	105	105	0	5214
s25	5	80	0	1347
s26	103	10	8536	0
s27	10	10	840	0
s28	10	6	367	0
s29	6	6	668	0

Table C.4 – Site 4 heat streams.

Stream	**T^{in} [°C]**	**T^{out} [°C]**	**H^{in} [kW]**	**H^{out} [kW]**
s1	1450	650	37	0
s2	650	250	37	0
s3	250	100	37	0
s4	860	850	348	0
s5	890	880	668	0
s6	1531	1504	268	0
s7	860	700	1268	0
s8	1719	1531	328	0
s9	880	860	133	0
s10	560	390	1468	0
s11	104	50	2115	0
s12	250	100	37	0
s13	1822	1719	387	0
s14	1222	1177	89	0

Table C.4 – *Site 4 heat streams cont.*

Stream	**T^{in} [°C]**	**T^{out} [°C]**	**H^{in} [kW]**	**H^{out} [kW]**
s15	1177	1050	30	0
s16	390	104	1597	0
s17	104	45	9	0
s18	650	250	37	0
s19	700	560	1166	0
s20	1000	1000	37	0
s21	2000	2000	566	0
s22	1504	1222	357	0
s23	1450	650	37	0
s24	2000	1822	953	0
s25	25	104	0	113
s26	25	56	0	1255
s27	85	100	0	1255
s28	390	104	2652	0
s29	100	100	0	1255
s30	56	85	0	1255
s31	390	104	2477	0
s32	100	104	0	1255
s33	560	390	9018	0
s34	700	560	7807	0
s35	880	860	1200	0
s36	860	700	9297	0
s37	1177	1050	2710	0
s38	2000	1822	3124	0
s39	1719	1531	3882	0
s40	1504	1222	5864	0
s41	1531	1504	338	0
s42	1222	1177	895	0
s43	2000	2000	606	0
s44	1822	1719	1954	0
s45	25	40	0	62
s46	25	60	0	26
s47	626	850	0	11514
s48	850	850	0	39975
s49	850	860	0	348

Table C.4 – *Site 4 heat streams cont.*

Stream	**T^{in} [°C]**	**T^{out} [°C]**	**H^{in} [kW]**	**H^{out} [kW]**
s50	850	890	0	541
s51	1100	1100	45208	0
s52	1100	890	11358	0
s53	25	400	0	37
s54	25	1000	0	37
s55	25	225	0	37
s56	150	35	3613	0
s57	225	35	1598	0
s58	104	35	1300	0
s59	115	35	1287	0
s60	400	35	3126	0
s61	390	150	8202	0
s62	50	268	0	9018
s63	268	437	0	7807
s64	437	626	0	9297
s65	850	850	0	1200
s66	850	850	1	0
s67	910	910	0	2401
s68	910	1027	0	3609
s69	850	900	0	1651
s70	1377	1450	0	2281
s71	1027	910	146	0
s72	1227	1227	0	921
s73	910	900	25	0
s74	900	850	153	0
s75	1327	1377	0	1509
s76	900	910	0	324
s77	900	900	0	596
s78	1377	1377	0	843
s79	1227	1027	85	0
s80	850	850	0	1212
s81	1027	1027	5525	0
s82	1327	1327	0	445
s83	1450	1450	0	606
s84	1027	1227	0	5948

Table C.4 – *Site 4 heat streams cont.*

Stream	T^{in} [°C]	T^{out} [°C]	H^{in} [kW]	H^{out} [kW]
s85	1227	1327	0	2961

Table C.5 – Site 5 heat streams.

Stream	T^{in} [°C]	T^{out} [°C]	H^{in} [kW]	H^{out} [kW]
s1	66	98	0	12
s2	98	4	35	0
s3	86	4	277	0
s4	4	66	0	236
s5	66	86	0	68
s6	6	4	8	0
s7	69	69	0	-1051
s8	61	61	0	988
s9	66	15	94	0
s10	4	66	0	236
s11	70	70	0	1051
s12	66	66	0	-1005
s13	60	60	0	-988
s14	66	66	0	1005
s15	60	15	81	0
s16	69	15	102	0
s17	98	4	35	0
s18	20	10	73	0
s19	6	4	8	0
s20	4	20	0	118
s21	-21	-25	11	0
s22	7	-21	67	0
s23	-21	-21	0	-60
s24	4	95	0	342
s25	6	4	8	0
s26	83	3	254	0
s27	20	73	0	166
s28	-6	-6	1	0
s29	73	83	0	32
s30	3	-6	26	0

Table C.5 – *Site 5 heat streams cont.*

Stream	**T^{in} [°C]**	**T^{out} [°C]**	**H^{in} [kW]**	**H^{out} [kW]**
s31	-6	-6	0	-197
s32	-6	-35	80	0
s33	75	15	13	0
s34	5	5	30	0
s35	15	55	0	17
s36	67	80	0	21
s37	65	15	10	0
s38	59	70	0	19
s39	69	15	102	0
s40	4	90	0	327
s41	66	15	94	0
s42	100	170	0	447
s43	100	170	0	165
s44	170	170	0	3057
s45	35	35	0	122
s46	0	-3	205	0
s47	5	1	1105	0
s48	69	75	0	116
s49	105	105	0	472
s50	170	170	0	1132
s51	44	25	713	0
s52	9	26	0	300
s53	170	190	0	73
s54	78	78	0	179
s55	44	44	0	-2260
s56	35	35	0	551
s57	79	85	0	18
s58	6	28	0	1110
s59	95	95	0	179
s60	48	75	0	1238
s61	75	4	3257	0
s62	6	48	0	2046
s63	66	76	0	195
s64	85	85	0	857
s65	54	4	151	0

Table C.5 – *Site 5 heat streams cont.*

Stream	T^{in} [°C]	T^{out} [°C]	H^{in} [kW]	H^{out} [kW]
s66	44	5	118	0
s67	170	190	0	27
s68	70	70	0	225
s69	15	55	0	145
s70	74	80	0	303
s71	32	25	632	0
s72	86	4	277	0
s73	66	86	0	68

Table C.6 – Site 6 heat streams.

Stream	T^{in} [°C]	T^{out} [°C]	H^{in} [kW]	H^{out} [kW]
s1	5	35	0.00	36.88
s2	15	35	0.00	1064.17
s3	36	35	0.00	-305.55
s4	36	100	0.00	273.15
s5	100	100	0.00	2297.70
s6	36	90	0.00	115.90
s7	148	25	0.00	-883.18
s8	115	115	0.00	-391.55
s9	148	148	0.00	-3622.26
s10	115	25	0.00	-66.94
s11	100	25	0.00	-106.43
s12	100	100	0.00	-767.76
s13	50	138	0.00	270.27
s14	138	144	0.00	9.35
s15	138	138	0.00	1560.40
s16	77	78	0.00	391.25
s17	5	89	0.00	599.10
s18	5	78	0.00	67.25
s19	78	115	0.00	574.64
s20	5	48	0.00	1571.10
s21	5	78	0.00	134.49
s22	51	48	0.00	-397.36
s23	51	89	0.00	140.60

Table C.6 – *Site 6 heat streams cont.*

Stream	**T^{in} [°C]**	**T^{out} [°C]**	**H^{in} [kW]**	**H^{out} [kW]**
s24	5	48	0.00	85.59
s25	40	40	0.00	76.23
s26	5	138	0.00	38.88
s27	35	40	0.00	114.35
s28	5	40	0.00	11.43
s29	138	138	0.00	151.70
s30	70	99	0.00	0.59
s31	52	20	0.00	-0.42
s32	51	20	0.00	-0.07
s33	20	51	0.00	0.07
s34	20	99	0.00	0.77
s35	99	130	0.00	2.45
s36	51	59	0.00	0.15
s37	49	20	0.00	-0.55
s38	51	59	0.00	0.15
s39	49	20	0.00	-0.55
s40	20	100	0.00	0.13
s41	20	49	0.00	0.55
s42	20	50	0.00	0.04
s43	20	50	0.00	0.04
s44	20	59	0.00	0.01
s45	20	59	0.00	0.01
s46	51	20	0.00	-0.07
s47	50	20	0.00	-0.04
s48	50	20	0.00	-0.04
s49	20	49	0.00	0.55
s50	20	51	0.00	0.07
s51	85	85	2.27	0.00
s52	88	88	0.57	0.00
s53	88	20	0.05	0.00
s54	84	20	0.05	0.00
s55	54	54	0.00	1.77
s56	54	54	0.00	0.46
s57	108	108	0.00	0.49
s58	103	103	0.00	2.30

Table C.6 – *Site 6 heat streams cont.*

Stream	T^{in} [°C]	T^{out} [°C]	H^{in} [kW]	H^{out} [kW]
s59	99	20	0.34	0.00
s60	71	20	0.05	0.00
s61	69	20	0.04	0.00
s62	79	20	0.08	0.00
s63	54	20	0.11	0.00
s64	54	20	0.03	0.00
s65	85	85	0.00	2.34
s66	88	88	0.00	0.54
s67	70	70	1.76	0.00
s68	70	20	0.16	0.00
s69	71	71	0.00	0.75
s70	70	70	0.00	2.03
s71	62	62	0.66	0.00
s72	84	84	0.00	0.45
s73	88	88	0.39	0.00
s74	62	62	0.00	0.54
s75	69	69	0.47	0.00
s76	71	71	0.59	0.00
s77	99	99	2.30	0.00
s78	88	20	0.07	0.00
s79	84	84	0.44	0.00
s80	69	69	0.00	0.50
s81	54	54	1.81	0.00
s82	88	88	0.00	0.54
s83	79	79	0.00	0.91
s84	62	20	0.05	0.00
s85	108	108	0.48	0.00
s86	79	79	0.79	0.00
s87	108	20	0.08	0.00
s88	54	54	0.43	0.00
s89	85	20	0.27	0.00
s90	100	100	1.72	0.00
s91	58	90	0.00	0.11
s92	100	100	0.00	1.61
s93	20	61	0.00	0.02

Table C.6 – *Site 6 heat streams cont.*

Stream	T^{in} [°C]	T^{out} [°C]	H^{in} [kW]	H^{out} [kW]
s94	20	69	0.00	0.02
s95	47	61	0.00	0.31
s96	53	69	0.00	0.26
s97	20	160	0.00	0.29

Table C.7 – Site 7 heat streams.

Stream	T^{in} [°C]	T^{out} [°C]	H^{in} [kW]	H^{out} [kW]
s1	25	110	0	72.53
s2	145	145	0	359.51
s3	180	180	0	28.07
s4	160	180	0	141.91
s5	110	150	0	97.76
s6	70	70	0	116.68
s7	180	190	0	141.91
s8	66	64	3.15	0
s9	141	141	0	-6.31
s10	58	55	3.15	0
s11	86	75	15.77	0
s12	132	123	15.77	0
s13	65	65	0	34.69
s14	189	160	12.61	0
s15	25	26	0	9.46
s16	139	133	12.61	0
s17	108	99	15.77	0
s18	62	59	3.15	0
s19	99	95	15.77	0
s20	93	77	12.61	0
s21	139	138	6.31	0
s22	178	175	9.46	0
s23	153	132	15.77	0
s24	118	114	15.77	0
s25	59	58	3.15	0
s26	181	178	9.46	0
s27	146	139	12.61	0

Table C.7 – *Cont.*

Stream	**T^{in}** [°C]	**T^{out}** [°C]	**H^{in} [kW]**	**H^{out} [kW]**
s28	63	63	0	25.23
s29	69	66	3.15	0
s30	112	106	12.61	0
s31	152	130	15.77	0
s32	145	143	6.31	0
s33	120	114	15.77	0
s34	180	180	0	44.15
s35	140	139	6.31	0
s36	140	140	0	-6.31
s37	125	112	12.61	0
s38	175	167	9.46	0
s39	78	54	12.61	0
s40	55	52	3.15	0
s41	148	138	12.61	0
s42	75	53	15.77	0
s43	128	124	12.61	0
s44	113	104	15.77	0
s45	110	110	0	15.77
s46	95	86	15.77	0
s47	160	146	12.61	0
s48	25	26	0	18.92
s49	178	152	15.77	0
s50	52	45	3.15	0
s51	77	46	12.61	0
s52	134	128	12.61	0
s53	84	61	15.77	0
s54	114	108	15.77	0
s55	123	118	15.77	0
s56	119	114	12.61	0
s57	63	110	0	25.23
s58	114	104	12.61	0
s59	142	141	6.31	0
s60	143	142	6.31	0
s61	138	134	12.61	0
s62	130	120	15.77	0

Table C.7 – *Cont.*

Stream	T^{in} [°C]	T^{out} [°C]	H^{in} [kW]	H^{out} [kW]
s63	104	100	15.77	0
s64	100	93	15.77	0
s65	93	84	15.77	0
s66	110	112	0	47.3
s67	64	63	3.15	0
s68	114	113	15.77	0
s69	133	125	12.61	0
s70	104	94	12.61	0
s71	106	93	12.61	0
s72	141	140	6.31	0
s73	141	141	0	-6.31
s74	75	69	3.15	0
s75	124	119	12.61	0
s76	94	78	12.61	0
s77	63	62	3.15	0
s78	141	141	0	-6.31
s79	25	26	0	132.45
s80	25	26	0	91.45
s81	550	500	100.91	0
s82	350	340	31.54	0
s83	75	75	0	56.76
s84	80	80	0	22.08
s85	80	115	0	22.08
s86	150	160	0	72.53
s87	170	180	0	72.53
s88	190	200	0	37.84
s89	160	170	0	72.53
s90	120	29	126.14	0
s91	305	300	9.46	0
s92	320	310	50.46	0
s93	25	26	0	15.77
s94	79	50	97.76	0
s95	75	80	0	12.61
s96	120	120	0	41
s97	25	26	0	22.08

Table C.7 – *Cont.*

Stream	**T^{in} [°C]**	**T^{out} [°C]**	**H^{in} [kW]**	**H^{out} [kW]**
s98	340	330	15.77	0
s99	550	550	0	-100.91
s100	157	120	167.14	0
s101	214	140	135.6	0
s102	50	41	63.07	0
s103	168	120	69.38	0
s104	180	190	0	110.38
s105	140	94	75.69	0
s106	120	33	25.23	0
s107	330	320	25.23	0
s108	310	305	31.54	0
s109	150	155	0	25.23
s110	160	185	0	18.92
s111	120	125	0	25.23
s112	166	170	0	37.84
s113	185	190	0	28.38
s114	135	145	0	28.38
s115	110	110	0	56.76
s116	97	100	0	9.46
s117	93	95	0	53.61
s118	185	185	0	47.3
s119	125	130	0	47.3
s120	155	166	0	12.61
s121	130	135	0	37.84
s122	25	26	0	22.08
s123	90	92	0	18.92
s124	145	150	0	31.54
s125	110	45	47.3	0
s126	95	97	0	63.07
s127	92	93	0	34.69
s128	65	35	227.06	0
s129	25	26	0	15.77
s130	114	45	72.53	0
s131	180	190	0	28.38
s132	160	180	0	28.38

Table C.7 – *Cont.*

Stream	**T^{in}** [°C]	**T^{out}** [°C]	**H^{in} [kW]**	**H^{out} [kW]**
s133	60	60	0	217.6
s134	130	130	0	25.23
s135	25	26	0	22.08
s136	118	129	0	31.54
s137	185	190	0	34.69
s138	129	134	0	12.61
s139	25	26	0	15.77
s140	93	29	47.3	0
s141	73	44	230.21	0
s142	160	185	0	34.69
s143	295	295	0	-3.15
s144	116	118	0	18.92
s145	104	48	85.15	0
s146	185	185	0	72.53
s147	218	217	56.76	0
s148	325	315	6.31	0
s149	99	35	28.38	0
s150	315	315	0	-31.54
s151	180	180	0	56.76
s152	165	170	0	28.38
s153	295	290	56.76	0
s154	204	203	91.45	0
s155	25	26	0	6.31
s156	80	85	0	12.61
s157	79	45	258.59	0
s158	615	615	0	-280.67
s159	50	29	25.23	0
s160	135	145	0	56.76
s161	312	300	37.84	0
s162	203	197	22.08	0
s163	49	49	0	34.69
s164	125	125	0	189.21
s165	171	130	37.84	0
s166	138	60	88.3	0
s167	130	135	0	28.38

Table C.7 – *Cont.*

Stream	**T^{in}** [°C]	**T^{out}** [°C]	**H^{in} [kW]**	**H^{out} [kW]**
s168	130	45	69.38	0
s169	150	160	0	28.38
s170	125	130	0	28.38
s171	170	180	0	28.38
s172	25	26	0	9.46
s173	145	150	0	44.15
s174	300	295	56.76	0
s175	180	180	0	-31.54
s176	160	165	0	44.15
s177	315	314	18.92	0
s178	60	70	0	12.61
s179	70	80	0	15.77
s180	127	127	0	15.77
s181	75	76	0	18.92
s182	314	312	18.92	0
s183	59	45	56.76	0
s184	160	160	0	15.77
s185	115	125	0	22.08
s186	170	180	0	47.3
s187	115	115	0	88.3
s188	180	190	0	18.92
s189	78	45	113.53	0
s190	25	26	0	9.46
s191	170	170	0	28.38
s192	85	85	0	15.77
s193	25	26	0	15.77
s194	70	45	59.92	0
s195	94	34	85.15	0
s196	120	29	81.99	0
s197	180	60	5695.03	0
s198	60	25	1601.73	0
s199	900	340	25627.65	0

C.2 Cement fuel properties

Table C.8 depicts the LHV, share in the fuel mix and price of the fuels used in cement production.

Table C.8 – Cement fuel properties, shares and prices.

Fuel	**LHV [kJ/kg]**	**Share [%]**	**Price [€/kg]**
Coal	28066	10.5	60
Lignite	9500	23.8	11
Petcoke	32701	3.4	83
Fuel oil	40800	0.3	413
Tyres	30000	9.2	10
Waste oil	35000	2.5	10
Waste paper	17000	1.1	20
Waste plastic	20000	10.1	20
Waste textile	35000	0.4	20
Other waste	6000	18.7	20
Animal meal	20000	4	5
Sewage	15000	12.3	10
Scrap wood	17000	0.1	20
Solvents	25000	2.8	20

C

(Chapter 4)

D.1 Decommissioning size linearisation

Decommissioning size is the product of binary and continuous variables as given in Equations 4.13 and 4.14 which are linearised with a set of constraints in Equations D.1–D.3 for selling and Equations D.4–D.6.

$$f^{s}_{u,p} \geq f^{e}_{u,p-1} - (1 - z^{s}_{u,p}) \cdot \mathrm{F}^{\max}_{u} \quad \forall\, u \in \mathbf{IU},\ p \in \mathbf{P} : p \neq 1 \tag{D.1}$$

$$f^{s}_{u,p} \leq f^{e}_{u,p-1} \quad \forall\, u \in \mathbf{IU},\ p \in \mathbf{P} : p \neq 1 \tag{D.2}$$

$$f^{s}_{u,p} \leq z^{s}_{u,p} \cdot \mathrm{F}^{\max}_{u} \quad \forall\, u \in \mathbf{IU},\ p \in \mathbf{P} : p \neq 1 \tag{D.3}$$

$$f^{d}_{u,p} \geq f^{e}_{u,p-1} - (1 - z^{d}_{u,p}) \cdot \mathrm{F}^{\max}_{u} \quad \forall\, u \in \mathbf{IU},\ p \in \mathbf{P} : p \neq 1 \tag{D.4}$$

$$f^{d}_{u,p} \leq f^{e}_{u,p-1} \quad \forall\, u \in \mathbf{IU},\ p \in \mathbf{P} : p \neq 1 \tag{D.5}$$

$$f^{d}_{u,p} \leq z^{d}_{u,p} \cdot \mathrm{F}^{\max}_{u} \quad \forall\, u \in \mathbf{IU},\ p \in \mathbf{P} : p \neq 1 \tag{D.6}$$

D.2 Piping investment planning model

As pipes cannot be sold and have a longer life span than the other equipment, the investment decisions for them reduce to buying them or not in a given period $p \in \mathbf{P}$. Thus compared to the units, the investment planning model of pipes is simplified to the following set of rules:

D

- A pipe exists only if it has been purchased. See Equation D.7 for heat pipes and Equation D.11 for resource pipes;
- A pipe can be purchased only once. See Equation D.8 for heat pipes and Equation D.12 for resource pipes;
- A pipe can be used as long as its life span. See Equation D.9 for heat pipes and Equation D.13 for resource pipes;
- A pipe can be used only if it exists. See Equation D.10 for heat pipes and Equation D.14 for resource pipes;

$$z^{eh}_{ly,sp,tr,o,p} = \sum_{pp=1..p-1} z^{bh}_{ly,sp,tr,o,pp} \quad \forall\, ly \in \mathbf{L},\ sp \in \mathbf{SP},\ tr \in \mathbf{TR},\ o \in \mathbf{OL},\ p \in \mathbf{P} \tag{D.7}$$

$$\sum_{p \in \mathbf{P}} z^{bh}_{ly,sp,tr,o,p} \leq 1 \quad \forall\, ly \in \mathbf{L},\ sp \in \mathbf{SP},\ tr \in \mathbf{TR},\ o \in \mathbf{OL} \tag{D.8}$$

$$\sum_{p \in \mathbf{P}} y^{ph}_{ly,sp,tr,o,p} \leq 50 \quad \forall\, ly \in \mathbf{L},\ sp \in \mathbf{SP},\ tr \in \mathbf{TR},\ o \in \mathbf{OL} \tag{D.9}$$

$$y^{ph}_{ly,sp,tr,o,p} \leq z^{eh}_{ly,sp,tr,o,p} \quad \forall\, ly \in \mathbf{L},\ sp \in \mathbf{SP},\ tr \in \mathbf{TR},\ o \in \mathbf{OL},\ p \in \mathbf{P} \tag{D.10}$$

$$z^{er}_{ly,lc,o,u,p} = \sum_{pp=1..p-1} z^{br}_{ly,lc,o,u,pp} \quad \forall\, ly \in \mathbf{L},\ lc \in \mathbf{LC},\ o \in \mathbf{OL},\ u \in \mathbf{U}_{l,lc},\ p \in \mathbf{P} \tag{D.11}$$

$$\sum_{p \in \mathbf{P}} z^{br}_{ly,lc,o,u,pp} \leq 1 \quad \forall\, ly \in \mathbf{L},\ lc \in \mathbf{LC},\ o \in \mathbf{OL},\ u \in \mathbf{U}_{l,lc} \tag{D.12}$$

$$\sum_{p \in \mathbf{P}} y^{pr}_{ly,lc,o,u,pp} \leq 50 \quad \forall\, ly \in \mathbf{L},\ lc \in \mathbf{LC},\ o \in \mathbf{OL},\ u \in \mathbf{U}_{l,lc} \tag{D.13}$$

$$y^{pr}_{ly,lc,o,u,pp} \leq z^{er}_{ly,lc,o,u,p} \quad \forall\, ly \in \mathbf{L},\ lc \in \mathbf{LC},\ o \in \mathbf{OL},\ u \in \mathbf{U}_{l,lc},\ p \in \mathbf{P} \tag{D.14}$$

D

D.3 Piping cost calculations

The cost of the pipes for heat ($C^{pipe_h}_{p,o,tr}$) and resource sharing ($C^{pipe_r}_{l,u,o}$) is calculated according to Equation D.15 and Equation D.16.

$$C^{pipe_h}_{sp,o,tr} = \sum_{ps \in \mathbf{PS}} \mathrm{c}^{\mathrm{pipe}}_{ps} \cdot \mathrm{F}^{\mathrm{tc}} \cdot \mathrm{l}^{\mathrm{pipe}}_{lc,o} \cdot n^{h}_{sp,o,tr,ps} \quad \forall\, sp \in \mathbf{SP},\ lc \in \mathbf{LC},\ o \in \mathbf{OL}_{lc},\ tr \in \mathbf{TR} \tag{D.15}$$

$$C^{pipe_r}_{ly,u,o} = \sum_{ps \in \mathbf{PS}} \mathrm{c}^{\mathrm{pipe}}_{ps} \cdot \mathrm{F}^{\mathrm{tc}} \cdot \mathrm{l}^{\mathrm{pipe}}_{lc,o} \cdot n^{r}_{ly,u,o,ps} \quad \forall\, ly \in \mathbf{L},\ u \in \mathbf{U}_l,\ lc \in \mathbf{LC},\ o \in \mathbf{OL}_{lc} \tag{D.16}$$

where $n^{h}_{p,o,tr,ps}$ and $n^{r}_{l,u,o,ps}$ are binary variables deciding what size of pipe is used for heat and resource sharing respectively, F^{tc} is the trenching cost factor which is 1 for above-ground pipes (i.e. no trenching) and 1.3 for under-ground pipes [117] and $\mathrm{c}^{\mathrm{pipe}}_{ps}$ is the specific piping cost of the corresponding pipe size. Further details on piping cost calculations can be found in [74].

The specific piping cost is calculated based on the piping cost functions available in the literature [113–116]. Standard piping diameters and their corresponding cost are depicted in Table D.1.

Table D.1 – Piping cost for standard piping diameters.

Standard pipe size	1	2	3	4	5	6	7	8	9	10	11	12
Diameter [mm]	20	40	80	100	200	300	400	500	600	800	1000	1500
Specific cost [€/m]	96	166	312	387	775	1180	1588	2008	2434	3304	4192	6474

D.4 Budget constraints

Equations D.17 and D.18 constraint the overall and annual investment costs according to available budget.

$$\sum_{p \in \mathbf{P}} C^{inv}_{p} \leq \mathrm{c}^{\mathrm{ob}} \tag{D.17}$$

$$C^{inv}_{p} \leq \mathrm{c}^{\mathrm{ab}} \quad \forall\, p \in \mathbf{P} \tag{D.18}$$

where c^{ob} and c^{ab} are overall and annual investment budgets respectively. When transferring the investment budget to the following year is allowed, Equation D.18 is replaced with Equations D.19–

D

D.21.

$$C_p^{tb} \leq \mathrm{c}^{\mathrm{ab}} \quad \forall\, p \in \mathbf{P} : p = 1 \tag{D.19}$$

$$C_p^{tb} = \mathrm{c}^{\mathrm{ab}} + C_{p-1}^{tb} - C_{p-1}^{inv} \quad \forall\, p \in \mathbf{P} : p \neq 1 \tag{D.20}$$

$$C_p^{inv} = C_p^{tb} \quad \forall\, p \in \mathbf{P} \tag{D.21}$$

where C_p^{tb} is a continuous variable which decides how much of a yearly budget is transferred to the following year.

D.5 Materials and engineering cost linearisation

The products of binary and continuous variables in Equations 4.31 and 4.35 are linearised in Equations D.22–D.24 for materials cost and Equations D.25–D.27 for engineering cost.

$$C_{u,p}^{mt} \geq C_{u,p}^{b} \cdot \mathrm{F}_u^{\mathrm{mt}} - z_{u,p}^{bb} \cdot \mathrm{c}_u^{\max} \quad \forall\, u \in \mathbf{NU},\ p \in \mathbf{P} \tag{D.22}$$

$$C_{u,p}^{mt} \leq C_{u,p}^{b} \cdot \mathrm{F}_u^{\mathrm{mt}} \quad \forall\, u \in \mathbf{NU},\ p \in \mathbf{P} \tag{D.23}$$

$$C_{u,p}^{mt} \leq \left(1 - z_{u,p}^{bb}\right) \cdot \mathrm{c}_u^{\max} \quad \forall\, u \in \mathbf{NU},\ p \in \mathbf{P} \tag{D.24}$$

$$C_{u,p}^{en} \geq C_{u,p}^{b} \cdot \mathrm{F}_u^{\mathrm{en}} - z_{u,p}^{bb} \cdot \mathrm{c}_u^{\max} \quad \forall\, u \in \mathbf{NU},\ p \in \mathbf{P} \tag{D.25}$$

$$C_{u,p}^{en} \leq C_{u,p}^{b} \cdot \mathrm{F}_u^{\mathrm{en}} \quad \forall\, u \in \mathbf{NU},\ p \in \mathbf{P} \tag{D.26}$$

$$C_{u,p}^{en} \leq \left(1 - z_{u,p}^{bb}\right) \cdot \mathrm{c}_u^{\max} \quad \forall\, u \in \mathbf{NU},\ p \in \mathbf{P} \tag{D.27}$$

D

where $\mathrm{c}_u^{\max}$ is the maximum purchase cost of a unit which is used as a big M in the equations.

D.6 Selling and dying value linearisation

The product of binary and continuous variables in Equations 4.43 and 4.44 is linearised in Equations D.28–D.30 for selling value and Equations D.31–D.33 for dying value.

$$C^{s}_{u,p} \geq C^{rv}_{u,p} - \left(1 - z^{s}_{u,p}\right) \cdot \mathrm{c}^{\max}_{u} \quad \forall\, u \in \mathbf{IU},\ p \in \mathbf{P} \tag{D.28}$$

$$C^{s}_{u,p} \leq C^{rv}_{u,p} \quad \forall\, u \in \mathbf{IU},\ p \in \mathbf{P} \tag{D.29}$$

$$C^{s}_{u,p} \leq z^{s}_{u,p} \cdot \mathrm{c}^{\max}_{u} \quad \forall\, u \in \mathbf{IU},\ p \in \mathbf{P} \tag{D.30}$$

$$C^{d}_{u,p} \geq C^{rv}_{u,p} - \left(1 - z^{d}_{u,p}\right) \cdot \mathrm{c}^{\max}_{u} \quad \forall\, u \in \mathbf{IU},\ p \in \mathbf{P} \tag{D.31}$$

$$C^{d}_{u,p} \leq C^{rv}_{u,p} \quad \forall\, u \in \mathbf{IU},\ p \in \mathbf{P} \tag{D.32}$$

$$C^{d}_{u,p} \leq z^{d}_{u,p} \cdot \mathrm{c}^{\max}_{u} \quad \forall\, u \in \mathbf{IU},\ p \in \mathbf{P} \tag{D.33}$$

D.7 Linearisation of the max function

The max function in Equation 4.46 is linearised in Equations D.34–D.38.

$$C^{s}_{u,p} \geq C^{sv}_{u,p} \quad \forall\, u \in \mathbf{IU},\ p \in \mathbf{P} \tag{D.34}$$

$$C^{s}_{u,p} \geq z^{e}_{u,p-1} \cdot \mathrm{c}^{\mathrm{sal}}_{u} \quad \forall\, u \in \mathbf{IU},\ p \in \mathbf{P} : p \neq 1 \tag{D.35}$$

$$C^{s}_{u,p} \leq C^{sv}_{u,p} + \left(1 - n^{rem}_{u,p}\right) \cdot \mathrm{c}^{\max}_{u} \quad \forall\, u \in \mathbf{IU},\ p \in \mathbf{P} \tag{D.36}$$

$$C^{s}_{u,p} \leq z^{e}_{u,p-1} \cdot \mathrm{c}^{\mathrm{sal}}_{u} + \left(1 - n^{sal}_{u,p}\right) \cdot \mathrm{c}^{\max}_{u} \quad \forall\, u \in \mathbf{IU},\ p \in \mathbf{P} \tag{D.37}$$

D

$$n_{u,p}^{rem} + n_{u,p}^{sal} = 1 \quad \forall\, u \in \mathbf{IU},\ p \in \mathbf{P} \tag{D.38}$$

where $n_{u,p}^{rem}$ is a binary variable which takes the value of 1 if $C_{u,p}^{sv}$ is greater than c_u^{sal} and $n_{u,p}^{sal}$ is binary variables which takes the value of 1 otherwise.

D.8 Grand composite curves of the sites

The thermal profile of the district is depicted in Figure D.1 in the form of grand composite curves (GCCs).

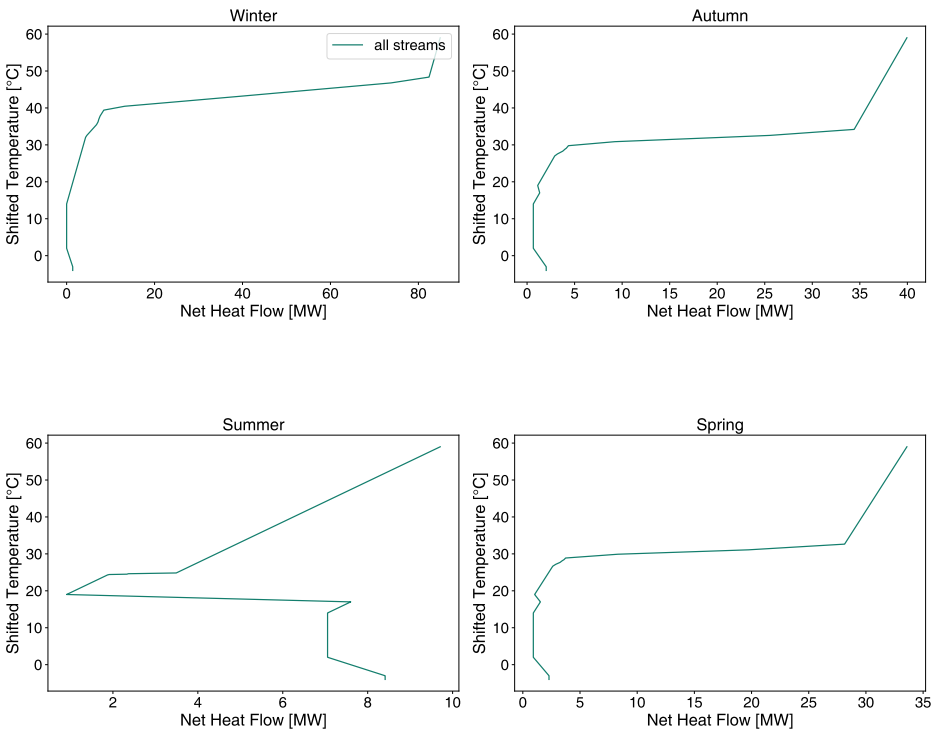

Figure D.1 – Grand composite curves of the district in four seasons.

D

Bibliography

[1] United Nations Department For Economic and Social Affairs. *World Population Prospects 2019*. English. OCLC: 1110488911. New York, USA: United Nations, 2019.

[2] IEA - International Energy Agency. *World Energy Balances 2019*. English. OCLC: 1013820838. Paris, France: OECD Publishing, Aug. 2019.

[3] IEA - International Energy Agency. *Energy Technology Perspectives 2017*. English. Paris, France: OECD Publishing, June 2017.

[4] European Comission. *Europe 2020*. en. Tech. rep. Brussels, Belgium, Mar. 2010.

[5] IEA - International Energy Agency. *CO2 Emissions from Fuel Combustion 2018*. English. OCLC: 1013820838. Paris, France: OECD Publishing, Oct. 2018.

[6] IEA - International Energy Agency. *Key World Statistics 2018*. English. Tech. rep. Paris, France: Organisation for Economic Co-operation and Development, Sept. 2018.

[7] K Tanaka. "Review of policies and measures for energy efficiency in industry sector". en. In: *Energy Policy* 39.10 (Oct. 2011), pp. 6532–6550.

[8] IEA - International Energy Agency. *Energy Efficiency 2018*. English. Tech. rep. Paris, France: Organisation for Economic Co-operation and Development, Oct. 2018.

[9] J Fresner, F Morea, C Krenn, J Aranda Uson, and F Tomasi. "Energy efficiency in small and medium enterprises: Lessons learned from 280 energy audits across Europe". en. In: *Journal of Cleaner Production* 142 (Jan. 2017), pp. 1650–1660.

[10] B Linnhoff and E Hindmarsh. "The pinch design method for heat exchanger networks". en. In: *Chemical Engineering Science* 38.5 (1983), pp. 745–763.

[11] VR Dhole and B Linnhoff. "Total site targets for fuel, co-generation, emissions, and cooling". en. In: *Computers & Chemical Engineering* 17 (Jan. 1993), S101–S109.

[12] SA Papoulias and IE Grossmann. "A structural optimization approach in process synthesis—II". en. In: *Computers & Chemical Engineering* 7.6 (Jan. 1983), pp. 707–721.

[13] J Cerda and AW Westerburg. “Synthesizing Heat Exchanger Networks Having Restricted Stream/Stream Matches Using a Transportation Problem Formulation”. en. In: *Chemical Engineering Science* 38.10 (1983), pp. 1723–1740.

[14] CA Floudas and IE Grossmann. “Synthesis of flexible heat exchanger networks for multiperiod operation”. en. In: *Computers & Chemical Engineering* 10.2 (Jan. 1986), pp. 153–168.

[15] T Yee and I Grossmann. “Simultaneous optimization models for heat integration—II. Heat exchanger network synthesis”. en. In: *Computers & Chemical Engineering* 14.10 (Oct. 1990), pp. 1165–1184.

[16] H Bütün, I Kantor, and F Maréchal. “A heat integration method with multiple heat exchange interfaces”. en. In: *Energy* 152 (June 2018), pp. 476–488.

[17] HE Bütün, ID Kantor, and F Maréchal. “A process integration method with multiple heat exchange interfaces”. In: *Proceedings of ECOS 2017 - The 30th International Conference on Efficiency, Cost, Optimization, Simulation and Environmental Impact of Energy Systems* (2017), pp. 1447–1460.

[18] IC Kemp. *Pinch analysis and process integration: a user guide on process integration for the efficient use of energy*. 2nd ed. OCLC: ocm74969693. Amsterdam ; Boston: Butterworth-Heinemann, 2007.

[19] MM El-Halwagi. *Process integration*. 1st ed. Process systems engineering v. 7. OCLC: ocm65165491. Amsterdam ; Boston: Elsevier Academic Press, 2006.

[20] UV Shenoy. *Heat exchanger network synthesis: process optimization by energy and resource analysis*. English. OCLC: 31865764. Houston: Gulf Pub., 1995.

[21] S Bungener, R Hackl, G Van Eetvelde, S Harvey, and F Marechal. “Multi-period analysis of heat integration measures in industrial clusters”. en. In: *Energy* 93 (Dec. 2015), pp. 220–234.

[22] C Hu and S Ahmad. “Total site heat integration using the utility system”. en. In: *Computers & Chemical Engineering* 18.8 (Aug. 1994), pp. 729–742.

[23] K Raissi. “Total site integration”. PhD thesis. The University of Manchester, 1994.

[24] M François and B Irsia. “Synep1 : A methodology for energy integration and optimal heat exchanger network synthesis”. en. In: *Computers & Chemical Engineering* 13.4-5 (Apr. 1989), pp. 603–610.

[25] F Marechal and B Kalitventzeff. “Targeting the integration of multi-period utility systems for site scale process integration”. en. In: *Applied Thermal Engineering* 23.14 (Oct. 2003), pp. 1763–1784.

[26] F Marechal and D Favrat. “Combined exergy and pinch analysis for the optimal integration of energy conversion technologies”. In: *18th International conference on efficiency, cost, optimization, simulation and environmental impact of energy systems*. 2005, pp. 177–184.

[27] X Feng and X Zhu. “Combining pinch and exergy analysis for process modifications”. en. In: *Applied Thermal Engineering* 17.3 (Mar. 1997), pp. 249–261.

[28] F Staine and D Favrat. “Energy integration of industrial processes based on the pinch analysis method extended to include exergy factors”. en. In: *Applied Thermal Engineering* 16.6 (June 1996), pp. 497–507.

[29] F Maréchal and B Kalitventzeff. “Effect modelling and optimization, a new methodology for combined energy and environment synthesis of industrial processes”. en. In: *Applied Thermal Engineering* 17.8-10 (Aug. 1997), pp. 981–992.

[30] D Brown, F Maréchal, and J Paris. “A dual representation for targeting process retrofit, application to a pulp and paper process”. en. In: *Applied Thermal Engineering* 25.7 (May 2005), pp. 1067–1082.

[31] N Pouransari, G Bocquenet, and F Maréchal. “Site-scale process integration and utility optimization with multi-level energy requirement definition”. en. In: *Energy Conversion and Management* 85 (Sept. 2014), pp. 774–783.

[32] D Muller. “Web-based tools for energy management in large companies applied to food industry”. eng. In: *Lausanne, EPFL* (2007).

[33] VW Uhl. “A guide to chemical engineering process design and economics, by Gail D. Ulrich, John Wiley & Sons, New York, Chichester, Brisbane, Toronto, Singapore“1984” 472 pages.$35.95”. en. In: *AIChE Journal* 30.6 (Nov. 1984), pp. 1036–1036.

[34] R Turton, RC Bailie, WB Whiting, JA Shaeiwitz, and D Bhattacharya. *Analysis, synthesis, and design of chemical processes*. 4th ed. Upper Saddle River, USA: Prentice Hall, 2012.

[35] SA Papoulias and IE Grossmann. “A structural optimization approach in process synthesis—I”. en. In: *Computers & Chemical Engineering* 7.6 (Jan. 1983), pp. 695–706.

[36] A Mian, E Martelli, and F Maréchal. “Framework for the Multiperiod Sequential Synthesis of Heat Exchanger Networks with Selection, Design, and Scheduling of Multiple Utilities”. en. In: *Industrial & Engineering Chemistry Research* 55.1 (Jan. 2016), pp. 168–186.

[37] N Pouransari. “Towards practical solutions for energy efficiency of large-scale industrial sites”. eng. In: *Lausanne, EPFL* (2015).

[38] F Maréchal and B Kalitventzeff. “Process integration: Selection of the optimal utility system”. en. In: *Computers & Chemical Engineering* 22 (Mar. 1998), S149–S156.

[39] M Ferrera and S Zandiri. *Deliverable Report INGAS*. Tech. rep. Mar. 2011.

[40] H Bütün, I Kantor, A Mian, and F Maréchal. “A Heat Load Distribution Method for Retrofitting Heat Exchanger Networks”. en. In: *Computer Aided Chemical Engineering*. Vol. 43. Elsevier, 2018, pp. 1395–1400.

[41] TN Tjoe and B Linnhoff. “Using pinch technology for process retrofit”. In: *Chemical Engineering* 93.8 (1986), pp. 47–60.

[42] S Ahmad, B Linnhoff, and R Smith. “Cost optimum heat exchanger networks—2. targets and design for detailed capital cost models”. en. In: *Computers & Chemical Engineering* 14.7 (July 1990), pp. 751–767.

[43] A Carlsson, PA Franck, and T Bertnsson. “Design better heat exchanger network retrofits”. In: *Chemical Engineering Progress* 89.3 (1993).

[44] JL van Reisen, J Grievink, GT Polley, and PJ Verheijen. “The placement of two-stream and multi-stream heat-exchangers in an existing network through path analysis”. en. In: *Computers & Chemical Engineering* 19 (June 1995), pp. 143–148.

[45] BH Li and CT Chang. “Retrofitting Heat Exchanger Networks Based on Simple Pinch Analysis”. en. In: *Industrial & Engineering Chemistry Research* 49.8 (Apr. 2010), pp. 3967–3971.

[46] M Bagajewicz, G Valtinson, and D Nguyen Thanh. “Retrofit of Crude Units Preheating Trains: Mathematical Programming versus Pinch Technology”. en. In: *Industrial & Engineering Chemistry Research* 52.42 (Oct. 2013), pp. 14913–14926.

[47] KM Björk and R Nordman. “Solving large-scale retrofit heat exchanger network synthesis problems with mathematical optimization methods”. en. In: *Chemical Engineering and Processing: Process Intensification* 44.8 (Aug. 2005), pp. 869–876.

[48] AEŞ Konukman, MC Çamurdan, and U Akman. “Simultaneous flexibility targeting and synthesis of minimum-utility heat-exchanger networks with superstructure-based MILP formulation”. en. In: *Chemical Engineering and Processing: Process Intensification* 41.6 (July 2002), pp. 501–518.

[49] J Aaltola. “Simultaneous synthesis of flexible heat exchanger network”. en. In: *Applied Thermal Engineering* 22.8 (June 2002), pp. 907–918.

[50] JM Zamora and IE Grossmann. “A global MINLP optimization algorithm for the synthesis of heat exchanger networks with no stream splits”. en. In: *Computers & Chemical Engineering* 22.3 (Feb. 1998), pp. 367–384.

[51] TF Yee and IE Grossmann. “A screening and optimization approach for the retrofit of heat-exchanger networks”. en. In: *Industrial & Engineering Chemistry Research* 30.1 (Jan. 1991), pp. 146–162.

[52] AR Ciric and CA Floudas. “A mixed integer nonlinear programming model for retrofitting heat-exchanger networks”. en. In: *Industrial & Engineering Chemistry Research* 29.2 (Feb. 1990), pp. 239–251.

[53] JM Ponce-Ortega, A Jiménez-Gutiérrez, and IE Grossmann. “Simultaneous Retrofit and Heat Integration of Chemical Processes”. In: *Industrial & Engineering Chemistry Research* 47.15 (2008), pp. 5512–5528.

[54] JM Ponce-Ortega, M Serna-González, and A Jiménez-Gutiérrez. “Synthesis of Heat Exchanger Networks with Optimal Placement of Multiple Utilities”. en. In: *Industrial & Engineering Chemistry Research* 49.6 (Mar. 2010), pp. 2849–2856.

[55] HK Shethna, J Jezowski, and F Castillo. “A new methodology for simultaneous optimization of capital and operating cost targets in heat exchanger network design”. en. In: *Applied Thermal Engineering* 20.15-16 (Oct. 2000), pp. 1577–1587.

[56] A Barbaro and MJ Bagajewicz. “New rigorous one-step MILP formulation for heat exchanger network synthesis”. en. In: *Computers & Chemical Engineering* 29.9 (Aug. 2005), pp. 1945–1976.

[57] DQ Nguyen, A Barbaro, N Vipanurat, and MJ Bagajewicz. “All-At-Once and Step-Wise Detailed Retrofit of Heat Exchanger Networks Using an MILP Model”. en. In: *Industrial & Engineering Chemistry Research* 49.13 (July 2010), pp. 6080–6103.

[58] M Pan, R Smith, and I Bulatov. “A novel optimization approach of improving energy recovery in retrofitting heat exchanger network with exchanger details”. en. In: *Energy* 57 (Aug. 2013), pp. 188–200.

[59] M Pan, I Bulatov, and R Smith. “New MILP-based iterative approach for retrofitting heat exchanger networks with conventional network structure modifications”. en. In: *Chemical Engineering Science* 104 (Dec. 2013), pp. 498–524.

[60] L Kang and Y Liu. “Minimizing investment cost for multi-period heat exchanger network retrofit by matching heat transfer areas with different strategies”. en. In: *Chinese Journal of Chemical Engineering* 23.7 (July 2015), pp. 1153–1160.

[61] E Ayotte-Sauvé, O Ashrafi, S Bédard, and N Rohani. “Optimal retrofit of heat exchanger networks: A stepwise approach”. en. In: *Computers & Chemical Engineering* 106 (Nov. 2017), pp. 243–268.

[62] SK Nair, M Soon, and I Karimi. “Locating exchangers in an EIP-wide heat integration network”. en. In: *Computers & Chemical Engineering* 108 (Jan. 2018), pp. 57–73.

[63] AM Geoffrion. “Generalized Benders decomposition”. en. In: *Journal of Optimization Theory and Applications* 10.4 (Oct. 1972), pp. 237–260.

[64] T Yee and IE Grossmann. “Optimisation model for structural modifications in the retrofit of heat exchanger network”. In: *Engineering Design Center* (July 1987), pp. 653–663.

[65] A Ciric and C Floudas. “A retrofit approach for heat exchanger networks”. en. In: *Computers & Chemical Engineering* 13.6 (June 1989), pp. 703–715.

[66] N Pouransari and F Maréchal. “Heat exchanger network design of large-scale industrial site with layout inspired constraints”. en. In: *Computers & Chemical Engineering* 71 (Dec. 2014), pp. 426–445.

[67] A Mian, AV Ensinas, E Martelli, and F Maréchal. “Multi-objective optimization of utility systems and heat exchanger networks: method and application to the solar assisted hydrothermal gasification case”. en. In: *Computer Aided Chemical Engineering*. Vol. 40. Elsevier, 2017, pp. 781–786.

[68] E Rezaei and S Shafiei. “Heat exchanger networks retrofit by coupling genetic algorithm with NLP and ILP methods”. en. In: *Computers & Chemical Engineering* 33.9 (Sept. 2009), pp. 1451–1459.

[69] H Soltani and S Shafiei. “Heat exchanger networks retrofit with considering pressure drop by coupling genetic algorithm with LP (linear programming) and ILP (integer linear programming) methods”. en. In: *Energy* 36.5 (May 2011), pp. 2381–2391.

[70] XW Liu, X Luo, and HG Ma. “Retrofit of Heat Exchanger Networks by a Hybrid Genetic Algorithm with the Full Application of Existing Heat Exchangers and Structures”. en. In: *Industrial & Engineering Chemistry Research* 53.38 (Sept. 2014), pp. 14712–14720.

[71] BK Sreepathi and G Rangaiah. “Improved heat exchanger network retrofitting using exchanger reassignment strategies and multi-objective optimization”. en. In: *Energy* 67 (Apr. 2014), pp. 584–594.

[72] L Čuček, S Boldyryev, JJ Klemeš, Z Kravanja, G Krajačić, PS Varbanov, and N Duić. “Approaches for retrofitting heat exchanger networks within processes and Total Sites”. en. In: *Journal of Cleaner Production* 211 (Feb. 2019), pp. 884–894.

[73] V Enríquez-Gutiérrez, M Jobson, L Ochoa-Estopier, and R Smith. “Retrofit of heat-integrated crude oil distillation columns”. en. In: *Chemical Engineering Research and Design* 99 (July 2015), pp. 185–198.

[74] H Bütün, I Kantor, and F Maréchal. “Incorporating Location Aspects in Process Integration Methodology”. en. In: *Energies* 12.17 (Aug. 2019), p. 3338.

[75] H Bütün, I Kantor, and F Maréchal. “A heat integration method with location-dependent heat distribution losses”. en. In: *Computer Aided Chemical Engineering*. Vol. 44. Elsevier, 2018, pp. 1195–1200.

[76] M Bendig, F Maréchal, and D Favrat. “Defining “Waste Heat” for industrial processes”. en. In: *Applied Thermal Engineering* 61.1 (Oct. 2013), pp. 134–142.

[77] L Miró, S Brückner, and LF Cabeza. “Mapping and discussing Industrial Waste Heat (IWH) potentials for different countries”. en. In: *Renewable and Sustainable Energy Reviews* 51 (Nov. 2015), pp. 847–855.

[78] T Bertnsson and A Asblad. *Industrial Excess Heat Recovery - Technologies and Applications*. en. Tech. rep. Denmark: IEA - International Energy Agency, May 2015.

[79] A Pirmohamadi, M Ghazi, and M Nikian. “Optimal design of cogeneration systems in total site using exergy approach”. en. In: *Energy* 166 (Jan. 2019), pp. 1291–1302.

[80] PY Liew, SR Wan Alwi, WS Ho, Z Abdul Manan, PS Varbanov, and JJ Klemeš. “Multi-period energy targeting for Total Site and Locally Integrated Energy Sectors with cascade Pinch Analysis”. en. In: *Energy* 155 (July 2018), pp. 370–380.

[81] R Song, Y Wang, M Panu, MM El-Halwagi, and X Feng. “Improved Targeting Procedure To Determine the Indirect Interplant Heat Integration with Parallel Connection Pattern among Three Plants”. en. In: *Industrial & Engineering Chemistry Research* 57.5 (Feb. 2018), pp. 1569–1580.

[82] Y Wang, X Feng, and KH Chu. “Trade-off between energy and distance related costs for different connection patterns in heat integration across plants”. en. In: *Applied Thermal Engineering* 70.1 (Sept. 2014), pp. 857–866.

[83] R Song, X Feng, and Y Wang. “Feasible heat recovery of interplant heat integration between two plants via an intermediate medium analyzed by Interplant Shifted Composite Curves”. en. In: *Applied Thermal Engineering* 94 (Feb. 2016), pp. 90–98.

[84] R Hackl, E Andersson, and S Harvey. “Targeting for energy efficiency and improved energy collaboration between different companies using total site analysis (TSA)”. en. In: *Energy* 36.8 (Aug. 2011), pp. 4609–4615.

[85] R Hackl and S Harvey. “From heat integration targets toward implementation – A TSA (total site analysis)-based design approach for heat recovery systems in industrial clusters”. en. In: *Energy* 90 (Oct. 2015), pp. 163–172.

[86] M Morandin, R Hackl, and S Harvey. “Economic feasibility of district heating delivery from industrial excess heat: A case study of a Swedish petrochemical cluster”. en. In: *Energy* 65 (Feb. 2014), pp. 209–220.

[87] KH Chew, JJ Klemeš, SR Wan Alwi, and Z Abdul Manan. “Industrial implementation issues of Total Site Heat Integration”. en. In: *Applied Thermal Engineering* 61.1 (Oct. 2013), pp. 17–25.

[88] PY Liew, SR Wan Alwi, and JJ Klemeš. “Total Site Heat Integration Targeting Algorithm Incorporating Plant Layout Issues”. en. In: *Computer Aided Chemical Engineering*. Vol. 33. Elsevier, 2014, pp. 1801–1806.

[89] B Zhang, J Li, Z Zhang, K Wang, and Q Chen. “Simultaneous design of heat exchanger network for heat integration using hot direct discharges/feeds between process plants”. en. In: *Energy* 109 (Aug. 2016), pp. 400–411.

[90] Y Wang, C Chang, and X Feng. “A systematic framework for multi-plants Heat Integration combining Direct and Indirect Heat Integration methods”. en. In: *Energy* 90 (Oct. 2015), pp. 56–67.

[91] H Rodera and MJ Bagajewicz. “Targeting procedures for energy savings by heat integration across plants”. en. In: *AIChE Journal* 45.8 (Aug. 1999), pp. 1721–1742.

[92] M Bagajewicz and H Rodera. “Energy savings in the total site heat integration across many plants”. en. In: *Computers & Chemical Engineering* 24.2-7 (July 2000), pp. 1237–1242.

[93] MJ Bagajewicz and AF Barbaro. “On the use of heat pumps in total site heat integration”. en. In: *Computers & Chemical Engineering* 27.11 (Nov. 2003), pp. 1707–1719.

[94] MZ Stijepovic and P Linke. “Optimal waste heat recovery and reuse in industrial zones”. en. In: *Energy* (June 2011).

[95] I Kantor, A Betancourt, A Elkamel, M Fowler, and A Almansoori. “Generalized mixed-integer nonlinear programming modeling of eco-industrial networks to reduce cost and emissions”. en. In: *Journal of Cleaner Production* 99 (July 2015), pp. 160–176.

[96] H Becker and F Maréchal. “Energy integration of industrial sites with heat exchange restrictions”. en. In: *Computers & Chemical Engineering* 37 (Feb. 2012), pp. 104–118.

[97] N Pouransari and F Maréchal. “Heat recovery networks synthesis of large-scale industrial sites: Heat load distribution problem with virtual process subsystems”. en. In: *Energy Conversion and Management* 89 (Jan. 2015), pp. 985–1000.

[98] MH Bade and S Bandyopadhyay. “Minimization of Thermal Oil Flow Rate for Indirect Integration of Multiple Plants”. en. In: *Industrial & Engineering Chemistry Research* 53.33 (Aug. 2014), pp. 13146–13156.

[99] KC Furman and NV Sahinidis. “A Critical Review and Annotated Bibliography for Heat Exchanger Network Synthesis in the 20th Century”. en. In: *Industrial & Engineering Chemistry Research* 41.10 (May 2002), pp. 2335–2370.

[100] R Song, Q Tang, Y Wang, X Feng, and MM El-Halwagi. “The implementation of inter-plant heat integration among multiple plants. Part I: A novel screening algorithm”. en. In: *Energy* 140 (Dec. 2017), pp. 1018–1029.

[101] R Song, C Chang, Q Tang, Y Wang, X Feng, and MM El-Halwagi. “The implementation of inter-plant heat integration among multiple plants. Part II: The mathematical model”. en. In: *Energy* 135 (Sept. 2017), pp. 382–393.

[102] C Chang, X Chen, Y Wang, and X Feng. “An efficient optimization algorithm for waste Heat Integration using a heat recovery loop between two plants”. en. In: *Applied Thermal Engineering* 105 (July 2016), pp. 799–806.

[103] C Chang, X Chen, Y Wang, and X Feng. “Simultaneous optimization of multi-plant heat integration using intermediate fluid circles”. en. In: *Energy* 121 (Feb. 2017), pp. 306–317.

[104] C Kachacha, A Farhat, A Zoughaib, and CT Tran. “Site wide heat integration in eco-industrial parks considering variable operating conditions”. en. In: *Computers & Chemical Engineering* 126 (July 2019), pp. 304–320.

[105] T Laukkanen and A Seppälä. “Interplant heat exchanger network synthesis using nanofluids for interplant heat exchange”. en. In: *Applied Thermal Engineering* 135 (May 2018), pp. 133–144.

[106] L Liu, H Song, L Zhang, and J Du. “Heat-integrated water allocation network synthesis for industrial parks with sequential and simultaneous design”. en. In: *Computers & Chemical Engineering* 108 (Jan. 2018), pp. 408–424.

[107] C Chang, Y Wang, J Ma, X Chen, and X Feng. “An energy hub approach for direct interplant heat integration”. en. In: *Energy* 159 (Sept. 2018), pp. 878–890.

[108] B Bohm. “On transient heat losses from buried district heating pipes”. en. In: *International Journal of Energy Research* 24.15 (Dec. 2000), pp. 1311–1334.

[109] SE Haaland. “Simple and Explicit Formulas for the Friction Factor in Turbulent Pipe Flow”. en. In: *Journal of Fluids Engineering* 105.1 (1983), p. 89.

[110] S Genic, I Arandelovic, P Kolendic, M Jaric, N Budimir, and V Genic. “A review of explicit approximations of Colebrook’s equation”. en. In: *FME Transactions* 39.2 (2011), pp. 67–71.

[111] I Nowak. *Relaxation and decomposition methods for mixed integer nonlinear programming*. International series of numerical mathematics v. 152. OCLC: ocm61228819. Boston, USA: Birkhäuser, 2005.

[112] N Yildirim, M Toksoy, and G Gokcen. “Piping network design of geothermal district heating systems: Case study for a university campus”. en. In: *Energy* 35.8 (Aug. 2010), pp. 3256–3262.

[113] DH Kwak, M Binns, and JK Kim. “Integrated design and optimization of technologies for utilizing low grade heat in process industries”. en. In: *Applied Energy* 131 (Oct. 2014), pp. 307–322.

[114] A Alva-Argáez, AC Kokossis, and R Smith. “The design of water-using systems in petroleum refining using a water-pinch decomposition”. en. In: *Chemical Engineering Journal* 128.1 (Mar. 2007), pp. 33–46.

[115] R Nordman and T Berntsson. “Use of advanced composite curves for assessing cost-effective HEN retrofit II. Case studies”. en. In: *Applied Thermal Engineering* 29.2-3 (Feb. 2009), pp. 282–289.

[116] J Persson and T Berntsson. “Influence of short-term variations on energy-saving opportunities in a pulp mill”. en. In: *Journal of Cleaner Production* 18.9 (June 2010), pp. 935–943.

[117] T Nussbaumer and S Thalmann. “Influence of system design on heat distribution costs in district heating”. en. In: *Energy* 101 (Apr. 2016), pp. 496–505.

[118] C Galitsky, N Martin, E Worrell, and B Lehman. *Energy Efficiency Improvement and Cost Saving Opportunities for Breweries: An ENERGY STAR® Guide for Energy and Plant Managers*. en. Tech. rep. Berkeley, USA, 2003.

[119] F Marechal, AK Sachan, and L Salgueiro. “Application of Process Integration Methodologies in the Brewing Industry”. en. In: *Handbook of Process Integration (PI)*. Cambridge, UK: Elsevier, 2013, pp. 820–863.

[120] I Kantor, AS Wallerand, M Kermani, H Bütün, A Santecchia, R Norbert, H Cervo, S Arias, F Wolf, G Van Eetvelde, and F Marechal. “Thermal profile construction for energy-intensive industrial sectors”. en. In: *Proceedings of ECOS 2018 - The 31st International Conference on Efficiency, Cost, Optimization, Simulation and Environmental Impact of Energy Systems*. 2018.

[121] R Suciu, L Girardin, and F Maréchal. “Energy integration of CO 2 networks and power to gas for emerging energy autonomous cities in Europe”. en. In: *Energy* 157 (Aug. 2018), pp. 830–842.

[122] F Maréchal and B Kalitventzeff. “Targeting the optimal integration of steam networks: Mathematical tools and methodology”. en. In: *Computers & Chemical Engineering* 23 (June 1999), S133–S136.

[123] JM Ponce-Ortega, M Serna-González, and A Jiménez-Gutiérrez. “Optimization model for re-circulating cooling water systems”. en. In: *Computers & Chemical Engineering* 34.2 (Feb. 2010), pp. 177–195.

[124] D Bernard, D Lemarchand, N Tétreault, and C Theévenet. *Increasing the use of alternative fuels at cement plants: international best practice*. en. Tech. rep. Washington, USA: International Finance Corporation, 2017.

[125] Verein Deutscher Zementwerke. *Environmental Data of the Germand Cement Industry*. Tech. rep. Düsseldorf, Germany, Dec. 2013.

[126] Office of Energy Efficiency Industrial, Commercial and Institutional Programs. *Energy Consumption Benchmark Guide: Cement Clinker Production*. Tech. rep. Ottawa, Canada, 2001.

[127] H Bütün, I Kantor, and F Maréchal. “An Optimisation Approach for Long-Term Industrial Investment Planning”. en. In: *Energies* 12.21 (Oct. 2019), p. 4076.

[128] E Worrell, L Bernstein, J Roy, L Price, and J Harnisch. “Industrial energy efficiency and climate change mitigation”. en. In: *Energy Efficiency* 2.2 (May 2009), pp. 109–123.

[129] C Walsh and P Thornley. “Barriers to improving energy efficiency within the process industries with a focus on low grade heat utilisation”. en. In: *Journal of Cleaner Production* 23.1 (Mar. 2012), pp. 138–146.

[130] T Napp, A Gambhir, T Hills, N Florin, and P Fennell. “A review of the technologies, economics and policy instruments for decarbonising energy-intensive manufacturing industries”. en. In: *Renewable and Sustainable Energy Reviews* 30 (Feb. 2014), pp. 616–640.

[131] GA Bakirtzis, PN Biskas, and V Chatziathanasiou. “Generation Expansion Planning by MILP considering mid-term scheduling decisions”. en. In: *Electric Power Systems Research* 86 (May 2012), pp. 98–112.

[132] S Pereira, P Ferreira, and A Vaz. “Generation expansion planning with high share of renewables of variable output”. en. In: *Applied Energy* 190 (Mar. 2017), pp. 1275–1288.

[133] X Zhang, M Shahidehpour, A Alabdulwahab, and A Abusorrah. “Optimal Expansion Planning of Energy Hub With Multiple Energy Infrastructures”. In: *IEEE Transactions on Smart Grid* 6.5 (Sept. 2015), pp. 2302–2311.

[134] A Botterud, M Ilic, and I Wangensteen. “Optimal Investments in Power Generation Under Centralized and Decentralized Decision Making”. en. In: *IEEE Transactions on Power Systems* 20.1 (Feb. 2005), pp. 254–263.

[135] BH Bakken, HI Skjelbred, and O Wolfgang. “eTransport: Investment planning in energy supply systems with multiple energy carriers”. en. In: *Energy* 32.9 (Sept. 2007), pp. 1676–1689.

[136] H Mirzaesmaeeli, A Elkamel, P Douglas, E Croiset, and M Gupta. “A multi-period optimization model for energy planning with CO2 emission consideration”. en. In: *Journal of Environmental Management* 91.5 (May 2010), pp. 1063–1070.

[137] M Fripp. “Switch: A Planning Tool for Power Systems with Large Shares of Intermittent Renewable Energy”. en. In: *Environmental Science & Technology* 46.11 (June 2012), pp. 6371–6378.

[138] J Cristóbal, G Guillén-Gosálbez, A Kraslawski, and A Irabien. “Stochastic MILP model for optimal timing of investments in CO2 capture technologies under uncertainty in prices”. en. In: *Energy* 54 (June 2013), pp. 343–351.

[139] EL Cano, M Groissböck, JM Moguerza, and M Stadler. “A strategic optimization model for energy systems planning”. en. In: *Energy and Buildings* 81 (Oct. 2014), pp. 416–423.

[140] RSC Lambert, S Maier, N Shah, and JW Polak. “Optimal phasing of district heating network investments using multi-stage stochastic programming”. en. In: *International Journal of Sustainable Energy Planning and Management* (Mar. 2016), Vol 9 (2016)–-.

[141] A Chakraborty, RD Colberg, and AA Linninger. “Plant-Wide Waste Management. 3. Long-Term Operation and Investment Planning under Uncertainty”. en. In: *Industrial & Engineering Chemistry Research* 42.20 (Oct. 2003), pp. 4772–4788.

[142] A Chakraborty, A Malcolm, RD Colberg, and AA Linninger. “Optimal waste reduction and investment planning under uncertainty”. en. In: *Computers & Chemical Engineering* 28.6-7 (June 2004), pp. 1145–1156.

[143] M Wickart and R Madlener. “Optimal technology choice and investment timing: A stochastic model of industrial cogeneration vs. heat-only production”. en. In: *Energy Economics* 29.4 (July 2007), pp. 934–952.

[144] N Sahinidis, I Grossmann, R Fornari, and M Chathrathi. “Optimization model for long range planning in the chemical industry”. en. In: *Computers & Chemical Engineering* 13.9 (Sept. 1989), pp. 1049–1063.

[145] NV Sahinidis and IE Grossmann. “Multiperiod investment model for processing networks with dedicated and flexible plants”. en. In: *Industrial & Engineering Chemistry Research* 30.6 (June 1991), pp. 1165–1171.

[146] LC Norton and IE Grossmann. “Strategic planning model for complete process flexibility”. en. In: *Industrial & Engineering Chemistry Research* 33.1 (Jan. 1994), pp. 69–76.

[147] V Jain and IE Grossmann. “Resource-Constrained Scheduling of Tests in New Product Development”. en. In: *Industrial & Engineering Chemistry Research* 38.8 (Aug. 1999), pp. 3013–3026.

[148] CW Schmidt and IE Grossmann. “Optimization Models for the Scheduling of Testing Tasks in New Product Development”. en. In: *Industrial & Engineering Chemistry Research* 35.10 (Jan. 1996), pp. 3498–3510.

[149] CT Maravelias and IE Grossmann. “Simultaneous Planning for New Product Development and Batch Manufacturing Facilities”. en. In: *Industrial & Engineering Chemistry Research* 40.26 (Dec. 2001), pp. 6147–6164.

[150] Gurobi Optimization, LLC. *Gurobi Optimizer Reference Manual*. 2019.

[151] CPLEX IBM ILOG. *User’s Manual for CPLEX*. 2016.

[152] YY Haimes, LS Lasdon, and DA Wismer. “On a Bicriterion Formulation of the Problems of Integrated System Identification and System Optimization”. In: *IEEE Transactions on Systems, Man, and Cybernetics* SMC-1.3 (July 1971), pp. 296–297.

[153] R Suciu, I Kantor, H Bütün, and F Maréchal. “Geographically Parameterized Residential Sector Energy and Service Profile”. In: *Frontiers in Energy Research* 7 (July 2019).

[154] H Loh. *Process Equipment Cost Estimation Final Report*. English. OCLC: 1096648453. National Energy Technology Lab. (NETL), Jan. 2002.

[155] C Temple-Bird, W Kawohl, A Lenel, and M Kaur. *How to Plan and Budget for your Healthcate Technology*. English. OCLC: 1096648453. 2005.

[156] Eurostat. *Energy price statistics*. Tech. rep. European Comission, 2015.

[157] Organisation for Economic Co-operation and Development and Organisation for Economic Co-operation and Development. *Key world energy statistics 2014*. English. OCLC: 1010640741. 2014.

Hür BÜTÜN

Rue de Pré-Fleuri 4, 1950 Sion - Switzerland
+41789255184
hur.butun@gmail.com
hurbutun
linkedin.com/in/hur-butun

PROFESSIONAL SUMMARY

- Specialist in thermo-economic modelling, analysis and optimisation of complex energy systems
- Experience with modelling and flow sheeting using Belsim-Vali and TRNSYS
- Knowledge in petro-chemicals, minerals, steel and cement industries as well as fossil based and renewable energy systems

EDUCATION

École Polytechnique Fédérale de Lausanne (EPFL) – Switzerland 2019
PhD: Energy

Focus on industrial energy and resource efficiency

École Polytechnique Fédérale de Lausanne (EPFL) – Switzerland 2014
Master of Science: Energy Engineering

Received excellence scholarship
Minor in Management of Technology

Orta Dogu Teknik Üniversitesi – Ankara, Turkey 2012
Bachelor of Science: Mechanical Engineering

Graduated as a honour student

CORE EXPERIENCE

Industrial Process and Energy Systems Engineering, EPFL

Researcher | Sion - Switzerland | May 2015 - Present

Involved in a European project with 4 major process industries. Development of a toolbox to identify and optimise industrial symbiosis, providing efficient use of energy within and between plants. Combining the strength of programming (Lua), mathematical programming (AMPL) and thermo-economics, my work addressed critical issues in the industry.

INEOS

Energy Consultant | Antwerp - Belgium | February - August 2014

Deep analysis of the energy consumption of a petrochemical site. Modelling on-site energy consumption using a flow-sheeting software, focusing on the steam network. Determining the inefficiencies in the system using Pinch Analysis. Thermo-economic analysis of energy saving scenarios totalling up to >10% of the energy consumption.

CSEM

Renewable Energy Based Cooling System Design | Ras Al Khaimah - UAE | June - August 2013

Modelling of a solar absorption cooling system for a single house and a cluster of houses located in the UAE. Dynamic simulation with punctual climate data using TRNSYS. Based on the conclusions of my work, the system has proven to be technically feasible, however significant reduction in the investment cost is required for economic feasibility.

ADDITIONAL EXPERIENCE

General Electric

Power Plant Construction Management | Samsun - Turkey | August - September 2012

Supervision of the assembly of a combined cycle power plant. Inspection of operations on-site which would influence the efficiency of the power plant. Weekly reporting to the site manager.

Arcelik

R&D Engineer | Ankara - Turkey | September 2011 - January 2012

Design, analysis, manufacture and assembly of an ice cube delivery system for a refrigerator. The design is patented by the funding company

TUSAS Engine Industries

Quality Control Engineer | Eskisehir - Turkey | August - September 2011

Inspection of operation sheets according to technical drawings.

Erkunt Group

Manufacturing Engineer | Ankara - Turkey | June - July 2010

Acquiring knowledge in manufacturing techniques. Technical drawing of engine components using CAD.

TECHNICAL SKILLS

- Modelling and data reconciliation: Belsim Vali, TRNSYS
- Thermal design, techno-economic analysis, environmental impact analysis
- Optimisation: Mixed-integer linear programming, mathematical programming, AMPL, Cplex, Gurobi, genetic algorithm
- Mechanical design: stress analysis, technical drawing, CAD
- Programming languages: Python, Lua, Matlab, C
- Other IT: Git, Mathcad, Microsoft Office (Word, Excel, PowerPoint)
- Strong verbal communication, report writing

PATENTS

A refrigerator comprising an ice cube tray (PCT/EP2013/060621), issued December 2013

The patent is based on my bachelor thesis. Took part in CAD, mechanical and thermal design of the system, as well as manufacturing and assembling it for a prototype demonstration.

LANGUAGES

- English: Fluent spoken and written (C1)
- French: Beginner level spoken (A2) and intermediate level written (B1)
- Turkish: Native language

EXTRA-CURRICULAR ACTIVITIES

- Half and full marathon running
- Team running: Titze de Noel
- Voluntary work for the organisation of Matterhorn Ultraks

PERSONAL

28, single, Swiss B permit, no military obligations

PUBLICATIONS

Energy

152 | June 2018

Bütün H., Kantor I., Maréchal F. A heat integration method with multiple heat exchange interfaces.

Energies

12(17), 3338 | August 2019

Bütün H., Kantor I., Maréchal F. Incorporating Location Aspects in Process Integration Methodology.

Energies

12(21), 4076 | October 2019

Bütün H., Kantor I., Maréchal F. An Optimisation Approach for Long-Term Industrial Investment Planning.

Frontiers in Energy Research

7(69) | August 2019

Suciu R., Kantor I., Bütün H., Maréchal F. Geographically parametrized residential sector energy and service profile.

PSE, Computer Aided Chemical Engineering

44, 1195-1200 | San Diego 2018

Bütün H., Kantor I., and Maréchal F., 2018. A heat integration method with location-dependent heat distribution losses.

ESCAPE, Computer Aided Chemical Engineering

43, 1395-1400 | Graz 2018

Bütün H., Kantor I., Mian A., Maréchal F. A Heat Load Distribution Method for Retrofitting Heat Exchanger Networks.

ECOS, Proceedings of ECOS 2017

- | San Diego 2018

Bütün H., Kantor I., Maréchal F. A process integration method with multiple heat exchange interfaces.

PSE Asia, AIP Conference Proceedings

- | Bangkok 2019

Suciu R., Kantor I., Bütün H., Maréchal F. Exergy-based method for determining heat pricing.

PRES, Chemical Engineering Transactions

70, 709-714 | Prague 2018

Suciu R., Kantor I., Bütün H., Girardin L., Maréchal F. Geographically Parameterized Residential Sector Energy and Service Profile.

ECOS, Proceedings of ECOS 2018

- | Guimaraes 2018

Kantor I., Wallerand A.S., Kermani M., Bütün H., Santecchia A., Wolf F., Van Eetvelde G.M., Maréchal F. Thermal profile construction for energy-intensive industrial sectors.